# INVESTIGATION OF MOLECULAR REGULATORS IN OSTEOBLAST DIFFERENTIATION

Thesis submitted in accordance with the requirements of the University of Liverpool for the degree of Doctor in Philosophy

By

**Mohd Azuraidi Bin Osman**

January 2017

## Abstract

Bones provide mechanical support for movement and normal daily functions, which can only be provided when healthy. Bone diseases such as osteoporosis and cancer are a worldwide problem affecting millions of people and causing significant financial impact. This study should indicate possible solutions that might contribute to combatting bone diseases by understanding the expression of bone markers that are known to be expressed differentially at different stages of osteoblastic differentiation. Thus a reliable, easily available and easy to maintain bone cell model was selected using osteosarcoma cell lines (MG-63, TE-85 and SaOS-2). The effect of ATP and PTH treatments on the expression of these markers was also tested to determine differences with primary osteoblasts (HOBs). We also determined the differential expression of miRNAs between the cell lines and HOBs and identified miRNAs involved in regulating expression of sclerostin, examining also their effect on the properties of trabecular bone in a mouse model. We hypothesized that these models were appropriate for studying the biology of osteoblastic cells and that miRNAs could control bone cell phenotype.

In the first objective of this study, the expression of seven bone markers actively involved in bone development (OPG, ALP, COL1A2, COL6A3, SOST, OSX and RANKL) were investigated. The expression of OPG, COL1A2 and COL6A3 were significantly higher in the least differentiated cell line, MG-63, while expression of ALP, SOST, OSX and RANKL were highest in SaOS-2, the most differentiated. ATP and PTH exerted the expected inhibitory or inductive effects on the cells at the osteoblastic maturation stage confirming that the cell lines were a suitable model for the study of osteoblasts.

MicroRNA profiling of cell lines and HOBs revealed hundreds of differentially expressed miRNAs. Six that were predicted to target the regulation of SOST were chosen for further validation. Mimics and antagomirs of these were transfected into TE-85 and SaOS-2 cells to confirm their involvement in SOST expression regulation. SOST gene expression and protein production were quantified by qPCR and ELISA, revealing that miR-1231, miR-1254 and miR-1914 decreased SOST protein expression in TE-85 and SaOS-2 cells and miR-378a-3p in just TE-85 cells, but these effects were not reversed by the corresponding antagomir. Adult and elderly mice were treated with miR-378a-3p mimic and antagomir by injection into the tail vein. Few differences could be observed in trabecular bone three weeks following treatment, except for significantly increased trabecular pattern factor and decreased trabecular separation in elderly mice treated with miR-378a-3p mimic.

In conclusion, this thesis demonstrates that ATP and PTH regulate osteosarcoma cell lines similarly to HOBs and that miRNAs can be used to control SOST protein expression. Potential future studies should investigate miRNAs as novel therapies for bone diseases.

**Acknowledgements**

I would like to thank my supervisors, Dr. Nick Rhodes and Prof James A. Gallagher for their support and motivation in this project. I would also like to thank Prof. Rob van ‘t Hof for his assistance and support with the processing and analysis of micro-CT samples; Dr. Kasia Whysall for her help and advice on microRNA related work; Dr. Peter Wilson for his support from the first day I start working in the lab until I finished my project; Dr. Hazel and Dr. Craig Keenan for their help, especially with all the lab related works; Jane Dillon who helped me a lot throughout my years in Liverpool University and everyone in the Institute of Ageing and Chronic Disease for being very supportive. I would also like to thank the Ministry of Higher Education Malaysia and Universiti Putra Malaysia for funding my project and to give me the opportunity to further my study at Liverpool University. I have met some lovely people in Liverpool that made my life as a PhD student more exciting. I am very grateful to all my friends, Brendan, Leah, Alessandro Riccio, Mikele, Mattia, Wasu, Francesca, Marc, Ana, Panos, Lorenzo, Corrado, Effy and everyone for their amazing support and company (great conversation, laughs, food, lamb keema etc…). Last but not least I would like to show my gratitude to my parents and my family members for their continuous support, love and encouragement.

## Table of contents

**CHAPTER 5 IDENTIFICATION OF miRNAs INVOLVED IN THE REGULATION OF SCLEROSTIN EXPRESSION**

## Abbreviations

| | |
|---|---|
| % | Percent |
| °C | Degree Celsius |
| µg/mL | Microgram per mililiter |
| µm | Micrometer |
| AC | Adenylate cyclase |
| Ago2 | Argonaute 2 |
| ALP | Alkaline phosphatase |
| ATP | Adenosine 5’-triphosphate |
| BMD | Bone mineral density |
| BMP2 | Bone morphogenetic protein-2 |
| CCND1 | Cyclin D1 |
| cm | Centimetre |
| CO2 | Carbon dioxide |
| COL1A2 | Collagen 1A2 |
| COL1A2 | Collagen 1a2 |
| COL6A3 | Collagen 6A3 |
| DAAM2 | Dishevelled associated activator of morphogenesis 2 |
| DAG | Diacylglycerol |
| Dlx5 | Distal-less homeobox 5 |
| DMEM | Dulbecco’s modified eagle medium |
| DNA | Deoxyribonucleic acid |
| FCS | Fetal calf serum |
| g | Gram |
| IGF | Insulin-like growth factor |
| Igf1 | Insulin like growth factor 1 |
| IP3 | Inositol trisphosphate |

| | |
|---|---|
| LRP5/6 | Low-density lipoprotein receptor-related protein 5/6 |
| MAPK | Mitogen-activated protein kinase |
| miRNA | Micro RNA |
| mL | Mililiter |
| mM | Milimolar |
| mm | Milimeter |
| mRNA | Messenger RNA |
| OBF | Osteoblast binding factor |
| OCIF | Osteoclastogenesis inhibitory factor |
| ODF | Osteoclast differentiation factor |
| OI | Osteogenesis imperfecta |
| OPG | Osteoprotegerin |
| OPGL | Osteoprotegerin ligand |
| PACT | Protein kinase RNA activator |
| PBS | Phosphate-buffered saline |
| PKA | Protein-kinase A |
| PKC | Protein-kinase C |
| PLC | Phospholipase |
| PPi | Pyrophosphate |
| pre-miRNA | Precursor miRNA |
| pri-miRNA | Primary miRNA |
| PTH | Parathyroid hormone |
| RANK | Receptor Activator of Nuclear Factor K B |
| RANKL | Receptor Activator of Nuclear Factor Kappa-B Ligand |
| RISC | RNA-induced silencing complex |
| RNA | Ribonucleic acid |
| RUNX2 | Runt-related transcription factor 2 |

| | |
|---|---|
| Scl-Ab | Sclerostin antibody |
| SMAD4 | SMAD family member 4 |
| SOST | Sclerostin gene |
| TNF | Tumor necrosis factor |
| TNFRSF11B | Tumor necrosis factor receptor superfamily member 11B |
| TNRC6A | Trinucleotide repeat-containing gene 6A |
| TP53 | Tumor protein p53 |
| TRANCE | TNF-related activation-induced cytokine |
| TRBP | Transactivation response RNA binding protein |
| U/mL | Unit per milliliter |
| UTR | Untranslated region |

## List of figures

**Chapter 4**

**Chapter 6**

## List of tables

# CHAPTER 1:

# INTRODUCTION

## 1.0 Overview

Osteoporosis is the commonest metabolic skeletal disease, affecting more than 200 million individuals worldwide (Pesce *et al.*, 2009). The estimated annual cost of treatment for osteoporosis in the US alone is more than $22 billion (Blume & Curtis, 2011). Osteoporosis is characterized by low bone mass and altered bone quality, which causes fragility and fractures.

Bone health is maintained by two major cell types in a delicate balance of active bone remodelling through bone resorption by osteoclasts and bone formation by osteoblasts. The activities of these bone cells are regulated through dynamic and complex genomic and biological functional networks (Krampera *et al.*, 2006; Matsuo & Irie, 2008). Therefore, understanding the molecular regulators of these networks is essential for developing novel agents to allow early diagnosis and an effective therapy for metabolic bone disorders such as osteoporosis.

This research project was directed towards understanding the molecular mechanisms regulating the development of bone and differentiation of osteoblasts. This provided some understanding of underlying age-related metabolic bone disorders such as osteoporosis using modern cellular and molecular biology approaches which in the future could provide strategies for enhancing bone regeneration in sufferers of metabolic bone disorders.

## 1.1 HUMAN BONE BIOLOGY

### 1.1.1 Overview

Bone is a highly specialised connective tissue which performs many important functions. Human bone serves numerous critical roles for the body such as protection of the inner body vital organs and tissue, support, movement, housing of bone marrow and the major reserve for calcium and phosphorus (Chan & Duque, 2002; Kini & Nandeesh, 2012; Raisz, 1999). Human bone tissue is composed of bone matrix and bone cells. Almost 90% of bone matrix comprises type 1 collagen, the remaining 10% being composed of a large number of non-collagenous proteins such as osteocalcin, osteonectin, bone sialoproteins and various proteoglycans (Arvidson *et al.,* 2011). Osteoblasts, osteoclasts and osteocytes are the three main types of bone cell which play the major role in the bone formation process.

### 1.1.2 Bone cells

There are three types of bone cells: osteoclasts, osteoblasts and osteocytes. Osteoclasts are responsible for bone resorption while osteoblasts are cells that form new bone and osteocytes maintain bone and the lining cells that cover the surface of bone.

#### 1.1.2.1 Osteoclasts

Osteoclasts are highly specialized, multinucleated cells that originate from mononuclear macrophage/monocyte-lineage haematopoietic precursor cells which are formed in the bone marrow (Boyce, 2013; Kikuta & Ishii, 2013). Mature osteoclasts are very large (50-100 μm in diameter), containing 2 – 100 nuclei, although normally in the range 10 – 20 (Huijing & Baan, 2003; Duce, 2010;

Roodman, 1991). However, Henriksen *et al.* (2011) and Cheung *et al.* (2009) reported that the size of osteoclasts is increased in Paget's disease and in osteogenesis imperfecta patients. On the other hand, a significant reduction in the size of osteoclasts (18 ± 3 μm diameter) and number of nuclei (2 – 3 in each cell) have been reported in osteopetrosis patients (Madyastha *et al.*, 2000).

The main ultrastructural characteristics of osteoclasts include an abundance of pleomorphic mitochondria, numerous lysosomes, free ribosomes and cytoplasm which contains large quantities of granules (Huijing & Baan, 2003; Roodman, 1991). Mature osteoclasts are short-lived cells (approximately 2 weeks) and can be found on the surface of trabecular and endosteal cortical bone (Edwards & Mundy, 2011).

The main function of mature osteoclasts is to resorb bone via a highly controlled process. Mature osteoclasts are the only known cells in the body that are capable of removing old and damaged bone (Edwards & Mundy, 2011). Development and survival of osteoclasts are controlled and influenced by several hormones (such as parathyroid hormone, calcitonin, interleukin 6 and estrogen), osteoprotegerin (OPG) and receptor activator of nuclear factor kappa-B ligand (RANKL). Over-expression of osteoclasts results in the formation of various bone diseases such as osteoporosis, while defective osteoclast formation can culminates in osteopetrosis (Boyce, 2013).

In the past, it was problematic studying osteoblasts due to their low availability and labile nature when isolated from bone. However, new techniques have been developed, which have contributed to an improved understanding of osteoclast biology. Nowadays, increased research effort is being conducted to identify other functions of these fascinating cells. A growing number of research studies focus of the function of osteoclasts as immune cells. Our understanding of differentiation,

fusion, survival, function and apoptosis of osteoclasts in normal and pathological conditions may contribute to new findings of better therapies for bone metabolic disorders.

#### 1.1.2.2 Osteoblasts

Osteoblasts are mononucleated cells which develop from bone marrow mesenchymal stem cells via the canonical Wnt signalling pathway (Logan & Nusse, 2004). Osteoblasts are single layer cuboidal cells located on periosteal or endosteal bone surfaces (Mackie, 2003). Osteoblasts are responsible for the regulation of bone formation and indirectly control bone resorption via the secretion of RANKL (Logan & Nusse, 2004; Mackie, 2003). Osteoblasts deposit the organic bone matrix of osteoid, which mainly comprises type I collagen and then contributes to its mineralisation. An osteoid seam, a thin layer of unmineralised bone matrix, separates osteoblasts from mineralised bone matrix (Mackie, 2003). However, some osteoblasts which are trapped in the bone matrix become osteocytes which later gradually stop secreting osteoid.

Other osteoblasts which are not trapped in the bone matrix undergo apoptosis or become the lining cells on the surface of the bones (Jilka *et al.*, 1999). Other factors, such as hormones, transcription factors and growth factors also have regulatory effects on osteoblasts which determine bone growth (Harada & Rodan, 2003). However, the number of osteoblasts decreases over the years which results in the loss of balance between bone formation and bone resorption. Deterioration of bone formation activity by osteoblast leads to osteoporosis (D'Ippolito *et al.*, 1999).

#### 1.1.2.3 Osteocytes

Osteocytes are the most abundant cells in bone comprising 95% of bone cells (Dallas & Bonewald, 2010; Kini & Nandeesh, 2012; Mackie, 2003). Osteocytes are mature osteoblastic cells that lies within a lacuna, a small pit in the calcified matrix of fully formed bone (Manolagas, 2000) which acts as a mechanosensor detecting environmental changes that affect bone such as an increase or decrease in workload. Osteocytes send signals to osteoblasts and osteoclasts informing them where and when to reabsorb or form new bone. Osteoblasts, which are embedded in bone matrix, differentiate into osteocytes (Divieti Pajevic, 2013). They survive in the bone matrix they occupy as long as the bone exists. Osteocytes communicate with nearby cells and even distant tissues and organs through small channels that penetrate the surrounding bone called canaliculi. Osteocytes secrete substances through tentacle-like dendrites within the canaliculi and influence the activity of osteoclasts and osteoblasts (Dallas *et al.*, 2013). Osteocytes are also capable of sensing mechanical stress and the daily wear-and-tear that occurs in healthy bone. Osteocytes then communicates with other osteoblastic cells to undertake the necessary repairs or adaptation (Pajevic, 2013).

Mature osteocytes are the only cells that produce sclerostin (SOST), a protein that plays a vital role in new bone formation by blocking the Wnt signalling pathway (Bonewald, 2011; Brunkow *et al.*, 2001). Thus, when sclerostin secretion from osteocytes increases, the production of new bone slows down. Following a bone fracture, osteocytes secrete insulin-like growth factor (IGF) that stimulates osteoblast activity which accelerates the formation of new bone (Sheng *et al*., 2014).

#### 1.1.2.4 Lining cells

Bone lining cells are a relatively inactive form of osteoblasts that cover the surface of bone. Lining cells are thinly extended over bone surfaces and contain few cytoplasmic organelles (Nakamura, 2007). The precise function of bone lining cells is still not well understood. However they seem to be involved in the maintenance of bone fluid, responsible for the immediate release of calcium from bone when the calcium levels in blood are low and for protecting bone from factors which could degrade bone structure. Bone resorption by osteoclasts is not complete as they leave some demineralized non-digested bone collagen. Bone lining cells enter the resorption pit and digest the remnants of collagen left by osteoclasts, forming a cement line and depositing a thin layer of fibrillar collagen on the cleaned surface (Everts *et al.*, 2002).

#### 1.1.2.5 Osteosarcoma cell lines

Osteosarcoma (also called osteogenic sarcoma) is the most common type of primary bone malignancy derived from primitive mesenchymal cells (Ritter and Bielack, 2010). Osteosarcoma can occur at any age but mostly occurs in children and young adults when bone growth is rapid. Osteosarcoma normally occurs in the metaphyseal area of long bones with approximately 75% of all cases take place in the proximal tibia and distal femur (Longhi *et al*., 2006). Tumor or sarcoma cell lines has been considered as a good *in vitro* models for studying general cell biology, malignancies, drug discovery, the functional characteristics of genes and many more. Studies have shown that cell lines adequately represent the tumors they are originating from and considered as a good model to study the cell biology as long as they are cultured in controlled culture conditions (Drexler *et al*., 2003). In this study, we used 3 osteosarcoma cell lines, MG-63, TE-85 and SaOS-2 as the bone model. These three cell lines have been shown to represent different stages of osteoblastic

differentiation; MG-63 has been shown to represent osteoblastic cell at the early stage of differentiation, TE-85 represent the intermediate differentiation stage and SaOS-2 represent the most differentiated cell. These cell lines provide a robust model to study bone biology at different stages of osteoblastic differentiation (Pacheco-Pantoja *et al*., 2011).

### 1.1.3 Bone Formation

There are two processes comprising bone formation: bone remodelling and bone modelling. Both processes are highly regulated. Bone remodelling is a continuous process which involves bone resorption by multinucleated osteoclasts followed by bone formation by osteoblasts. In healthy individuals, a balance in the activity of osteoclasts and osteoblasts results in the maintenance of healthy bone mass.

#### 1.1.3.1 Bone modelling

Bone modelling differs from bone remodelling. Bone modelling is a process where osteoblasts deposit new bone matrix without prior bone resorption by osteoclasts. This process occurs mainly during the growth phase, especially during the early developmental stages, before the age of 20 years in humans. Bone modelling increases bone size, its strength and modifies bone shape. Bone modelling is an adaptive response to the biomechanical force experienced by the bone to prevent the occurrence of injury to the bone (Crockett *et al.*, 2011; Martin & Seeman, 2008). This explains why the dominant arm of a tennis player has a thicker cortex and a larger external diameter than the contralateral radius. However, bone modelling normally is less frequent compared to bone remodelling (Brandi, 2009).

### 1.1.3.2 Bone Remodelling

Bone remodelling is a complex continuous process which involves a series of highly regulated sequential steps (Raisz, 1999). Bone remodelling allows the bone to grow, repair itself and adapt to environmental signals such as an increase or decrease in workload (Orriss *et al.*, 2010). Rapid skeletal growth during the early stages of bone development and stable maintenance of bone mass during adult life is the result of a careful balance between bone formation by osteoblasts and bone resorption by osteoclasts (Bielby *et al.*, 2007). In humans, this process peaks around 20 years of age when bone formation exceeds bone resorption. For the next 40 years, human bone mass remains relatively stable. However, with ageing, the stable process of bone formation and resorption is affected by a reduction in osteoblast differentiation activity resulting in loss of bone mass (Horowitz *et al.*, 2001).

The bone remodelling process starts when lining cells on the bone surface move apart to expose the bone surface. These lining cells then develop into osteoblasts and begin to secrete RANKL, which binds to RANK on the surface of osteoclast precursor cells, initiating their fusion and development into mature osteoclasts. Osteoblasts continuously secrete RANKL which is essential for the formation, function and survival of the osteoclasts. Osteoclasts attach to the bone surface creating an acidic seal zone which dissolves bone mineral content. Osteoblasts then release matrix-degrading enzymes, hydrogen ions and chloride ions to remove the remaining collagen of the bone matrix to complete the bone resorption process (Edwards & Mundy, 2011).

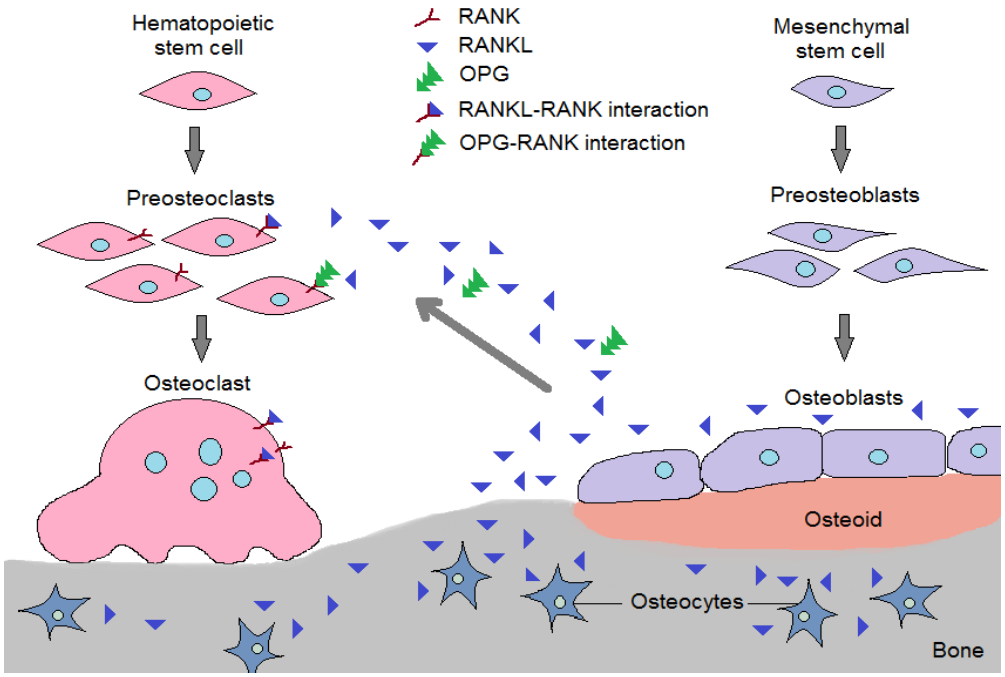


Figure 1.1: Bone remodelling involves solubilisation of bone mineral and degradation of bone matrix by osteoclasts followed by a bone formation phase by osteoblasts which produce osteoid matrix

Following resorption, osteoblasts move to the resorption space and deposit an organic matrix known as osteoid which mainly comprises collagen. Minerals such as calcium and phosphate begin to crystallize around the collagen scaffold and provide a strong framework for the bone (Fig. 1.1).

#### 1.1.3.3 Bone repair

Bone repair is a complex process which involves four overlapping stages; inflammatory response, soft callus formation, hard callus formation and bone remodelling. Inflammatory process starts immediately after bone injury or fracture happens and lasts until bone formation starts. The bleeding at the fracture site is contained by the surrounding tissues and develops into a hematoma. Degranulating platelets, macrophages and inflammatory cells such as lymphocytes, monocytes and granulocytes enter the hematoma to prevent the infection and secrete growth

factors and cytokines (Gerstenfeld *et al*., 2003). In stage 2, pain and swelling start to decrease and soft callus is formed. This semi-rigid soft callus provides mechanical support to the fracture and act as a template for the growth of the new bone. Stage 3 is also known as primary bone formation. At this stage, osteoblast activity and the mineralization of bone matrix are at the highest level. The soft callus is gradually removed and replaced with new bone known as hard callus. Hard callus is normally irregular, woven and under-remodeled. In the final stage, which is the bone remodelling stage also known as secondary bone formation, the bone remodelling process starts when the fracture has solidly fused with woven bone. Lamella bone then slowly replaces the woven bone through the remodelling process which involves bone resorption followed by the formation of lamellar bone. This process lasts until the bone has completely returned to its original morphology and might takes anything from a few months to several years (Gerstenfeld *et al*., 2003; Mulari *et al.,* 2004).

### 1.1.4 Bone diseases

The maintenance of healthy bone is a result of a delicate balance between bone resorption and bone formation (Calvo *et al.*, 1996). However, as age increases and after the menopause in women, the balance of this complex process is disturbed by a few factors such as changes in the production of hormones and growth factors (Silva-Fernandez *et al.*, 2013). After the age of 30, bone resorption increases while bone formation starts to slow down. At this stage, bone resorption slightly exceeds bone formation leading to a slow but continuous loss of bone. Loss of bone mass density reduces bone strength and increases the risk of bone fracture, a condition known as osteoporosis (Li *et al.*, 2013). Currently, osteoporosis is the most common bone metabolic disorder and is considered a major global health problem (Arvidson *et al.*, 2011; Pesce *et al.*, 2009). Osteoporosis is also characterised by a

deterioration in microarchitectural bone tissue and the degradation of matrix protein. Its incidence increases with age in both women and men and is usually clinically symptomless until the occurrence of the first fracture (Stromsoe, 2004). Fractures most commonly occur in the hip, ankle, proximal humerus, vertebrae and wrist, causing disability to patients and a heavy economic burden for many countries (Pesce *et al.*, 2009). Today, bisphosphonates are the most common class of antiresorptive medications used for the treatment of osteoporosis. Bisphosphonates efficiently inhibit osteoclastogenesis in bone marrow, supressing osteoclast activity on the surface of bone and reducing osteoclast life span by the induction of apoptosis (Rodan & Fleisch, 1996).

Osteogenesis imperfecta (OI) is another type of bone disease which is characterized by bones that break easily. The term “osteogenesis imperfecta” means imperfect bone formation. This disease is a rare, inherited skeletal disorder which is caused by the mutation involving multiple genes, especially COL1A1 and COL1A2 which are responsible for the synthesis of collagen type 1, the most abundant protein in the human body that is crucial for the formation of strong bone (Pillion *et al*., 2011). The most distinctive sign of OI is the occurrence of fractures even with very minor accident which might happen just a few or as many as hundreds of fractures in a lifetime. OI patients can also suffer other symptoms including brittle teeth, a curved spine, weak muscles and hearing loss (Cundy, 2012). Until today, there is no cure for OI. Patients are treated with pain medicine, physical therapy, braces, exercise and surgery.

Multiple myeloma is a cancer of the malignant plasma cells in the bone marrow. When the cancerous plasma cells grow out of control, a tumor called a plasmacytoma is formed which normally develop in a bone, rarely in other tissue (Blade *et al*., 2012). If there is only a single plasma cell tumor, it is called isolated or

solitary plasmacytoma. However, when there are more than one plasmacytoma, it is called multiple myeloma. Multiple myeloma represents one percent of human cancers and contribute to almost two percent of total cancer death (Palumbo and Anderson, 2011). Multiple myeloma is normally characterized by low blood counts, kidney damage, bone pain, infections and high calcium levels in the blood but the bones are weak due to increase in bone break-down by osteoclasts but bone repair and growth by osteoblast is suppressed (Khan *et al*., 2015; Palumbo and Anderson 2011).

The balance between the activity of osteoblasts and osteoclasts is essential for the maintenance of healthy bone mass. Too much bone resorption by osteoclasts leads to a weakening of bone. However, if the bone resorption process is too low, bone overgrowth is another serious health concern. Osteopetrosis is an inherited genetic bone disease where the bone density increases significantly due to failure of bone resorption by osteoclasts or a reduced number of osteoclasts, characterised by osteosclerosis, obliteration of the medullary canal, calcified cartilage and brittle bone (Xie *et al.*, 2015). There are three main types of osteopetrosis, based on clinical forms and genetic transmission: infantile malignant (an autosomal recessive form) which is early onset and normally causes lethal outcome in the first decade of life if no treatment is given; intermediate (another autosomal recessive form) which occurs in the first decade of life but with an expectation of a normal life span and benign (an autosomal dominant form) which is milder and is late onset (Mikami *et al.*, 2016; Palagano *et al.*, 2015; Ye *et al.*, 2013).

Bone cancer is one of the most studied bone diseases. There are two types of bone cancer; primary bone cancer and secondary bone cancer. Primary bone cancer begins in the bones while secondary bone cancer is the cancer that spreads to the bones after developing in another part of the body such as the breast, lung or

prostate (Paley *et al*., 2011). Bone cancers normally develop in the long bones of the upper arms and the legs and rarely affect other types of bone. Persistent bone pain, noticeable lump over a bone, bone that fractures easily and inflammation over a bone are among the main symptoms of bone cancer. Until today, in most cases, the reason why a person develops bone cancer is still unknown. However, researchers have found that we are more at risk of getting bone cancer if we exposed to radiation such as during radiotherapy (Wong *et al*., 1997). Treatment for bone cancer depends on how serious or how far it has spread and the type of the bone cancer the person has. Most patients are treated with surgery to remove the section of the cancerous bone, chemotherapy and/or radiotherapy where the cancerous cells are destroyed using radiation. A study has shown that bisphosphonates effectively provide pain relief from pain for bone cancer patients even though it can cause side effects such as nausea and vomiting (Wong and Wiffen, 2002).

### 1.1.5 Current treatments of bone diseases

In recent years, there have been important advance achievements and abilities to treat and prevent bone related diseases, especially in those suffering fragile bones such as osteoporosis, multiple myeloma and osteogenesis imperfecta. Today, bisphosphonates are the most commonly used agents for both treatment and prevention of these fragile bone diseases. Bisphosphonates, such as alendronate, risedronate and ibandronate normally come in tablet form which is taken daily, weekly or monthly (Bock and Felsenberg, 2008). Denosumab, another current treatment which is widely used is a humanized monoclonal antibody which is given to the patients through injection in every 6 months. Compared to bisphosphonate, denosumab works differently but has the same effect of slowing the rate of bone loss by inhibiting osteoclast activity (McClung, 2017). Other treatments includes

strontium ranelate to enhance pre-osteoblastic cells replication (Reginster, 2002), hormone replacement therapy using estrogen or progestogen (Shulman, 2008) and teriparatide (recombinant human parathyroid hormone (1-34)(PTH[1-34]) that acts as an anabolic agent) (Lindsay *et al*., 2016).

## 1.2 Bone markers

### 1.2.1 Overview

Studies of the cellular and extracellular components of skeletal matrix have resulted in the development of bone markers that provide information on bone dynamics. These bone markers are categorised as either markers of bone formation or resorption (Wheater *et al.*, 2013). Bone markers have been used as an early diagnosis of bone lesions and for predicting the rate of bone loss in postmenopausal woman and evaluation of the risk of future fractures (Terpos *et al.*, 2010). The advantage of analysing bone markers is their cost effectiveness, the speed and non-invasiveness and the significant help they provide in assessing disturbances in bone metabolism. In this study, we examined the expression of seven bone markers (osteoprotegerin (OPG), alkaline phosphatase (ALP), collagen 1a2 (COL1A2), collagen 6a3 (COL6A3), receptor activator of nuclear factor Kappa-B Ligand (RANKL), osterix (OSX) and sclerostin (SOST)) in human osteosarcoma cell lines.

### 1.2.2 Bone markers used in this study

#### 1.2.2.1 Osteoprotegerin

Osteoprotegerin (OPG) is a dimeric glycoprotein belonging to the tumour necrosis factor (TNF) receptor superfamily. OPG is also known as osteoblast binding factor (OBF), tumour necrosis factor receptor superfamily member 11B (TNFRSF11B) and osteoclastogenesis inhibitory factor (OCIF) (Kini & Nandeesh, 2012; Kwon *et al.*, 1998; Leibbrandt & Penninger, 2008; Perlot & Penninger, 2012). OPG is extensively expressed as a soluble protein by osteoblasts and other cells from the spleen, heart, liver, kidney and bone marrow (Leibbrandt & Penninger, 2008; Wada *et al.*, 2006). OPG plays an important role in inhibiting the recruitment, differentiation and activation of osteoclasts by inhibiting the binding of RANKL to RANK, thereby reducing the bone resorption process by mature osteoclasts and protecting bone from excessive bone loss. Imbalance in OPG expression can lead to an increase in bone resorption which then results in osteoporosis or other bone metabolic disorders (Kini & Nandeesh, 2012).

#### 1.2.2.2 Alkaline phosphatase

Alkaline phosphatase (ALP) is a metalloenzyme present in serum in as different isoenzymes in different tissues, such as liver, kidney, placenta, intestine and bone (Gomez *et al.*, 1995). However, most ALP isoenzymes derive from the bone and liver (Mukaiyama *et al.*, 2015). ALP is expressed in many species (plants, bacteria and animals) and functions differently in different organisms and tissues (Golub & Boesze-Battaglia, 2007). In this study, we will focus only on bone ALP to investigate its role in mineralisation. Bone ALP is one of the most commonly used bone formation markers for the study of bone development because of easy measurability and its potential use as identifiers for prediction of the potential risk of bone

fractures associated with bone metabolism disorders (Havill *et al.*, 2006). Bone ALP is a non-collagenous protein secreted by osteoblasts and vital for bone mineralisation, which defines ALP as a highly specific marker of osteoblast function (Rey *et al.*, 2007). In bone and calcifying cartilage, ALP expression is highest during the early stage of development. In the later stages, the expression of ALP declines while other genes such as osteocalcin are upregulated, clearly demonstrating that ALP fulfils its role during the initial phases of hard tissue formation (Golub & Boesze-Battaglia, 2007).

#### 1.2.2.3 Collagen 1A2

Type 1 collagen is the most abundant protein in the skeleton, composed of two α1 chains and one α2 chain (Phillips *et al.*, 2000). Any mutation in genes encoding type 1 collagen can cause various bone, cartilage and blood vessel diseases ranging from mild to life threatening (Forlino & Marini, 2016). Collagen type 1 α-2 chain is a protein that is encoded by the COL1A2 gene and a crucial component of bone matrix as it plays a vital role in bone formation and architecture. Mutations in the COL1A2 gene are known to cause the autosomal dominant disorder osteogenesis imperfecta (OI) characterized by fragile and brittle bones from early childhood and low bone mineral density (BMD) (Forlino & Marini, 2016; Styrkarsdottir *et al.*, 2016).

#### 1.2.2.4 Collagen 6A3

Collagen 6 is a microfibrillar protein widely expressed in all connective tissues. It is composed of three genetically different subunits or isoforms, α1(VI), α2(VI) and α3(VI) encoded by COL6A1, COL6A2 and COL6A3, respectively. Each isoform contains a relatively short triple helix structure, about 335 amino acids long (Lamande *et al.*, 2006). COL6A3 is known to be involved in fibrosis (Khan *et al.*,

2009), metabolic dysregulation in obesity (Pasarica *et al.*, 2009) and is a potential diagnosis and prognosis marker of colorectal carcinoma (Qiao *et al.*, 2015). It has been shown that deficiency of the α3 subunit in mice leads to decreased muscle mass and contractile force (Pan *et al.*, 2013).

#### 1.2.2.5 RANKL

Receptor Activator of Nuclear Factor Kappa-B Ligand (RANKL) is a type ll transmembrane protein which belongs to the tumour necrosis factor (TNF) cytokine family. RANKL is also known as TNF-related activation-induced cytokine (TRANCE), osteoprotegerin ligand (OPGL) and osteoclast differentiation factor (ODF) (Fuller *et al.*, 1998; Lacey *et al.*, 1998; Takami *et al.*, 2005). RANKL is produced mainly by osteoblasts but also in other cell types such as bone marrow stromal cells, osteocytes and lymphocytes. However, recent studies have suggested that osteocytes embedded in bone express significantly higher quantities of RANKL than osteoblasts or other cell types, hence it plays a major role in inducing osteoclastogenesis i*n vitro* (Nakashima *et al.*, 2011).

RANKL is responsible for the activation and survival of mature osteoclasts (Fuller *et al.*, 1998). RANKL binds to its receptor, Receptor Activator of Nuclear Factor κ B (RANK) on the surface of osteoclasts and their precursors. The interaction between RANKL and RANK stimulates the differentiation of haematopoietic stem cells into mononuclear preosteoclast cells. These mononuclear preosteoclast cells then fuse to form multinucleated cells which are known as osteoclasts (Boyce & Xing, 2007; Lian *et al.*, 2012).

#### 1.2.2.6 Osterix

Osterix, also known as SP7, is a novel zinc finger-containing transcription factor for embryonic and postnatal osteoblast differentiation and bone formation (Liu *et al.*, 2015; Zhou *et al.*, 2010). Expression of osterix mRNA and protein is positively regulated by the RUNX2 and distal-less homeobox 5 (Dlx5) signalling pathways (bone morphogenetic protein-2 (BMP2), mitogen-activated protein kinase (MAPK) and insulin like growth factor 1 (Igf1)) and the ER-stress pathway (IRE1a/XBP1). Conversely, osterix mRNA and protein is negatively regulated by DNA methylation, p53, TNF and microRNAs (Sinha & Zhou, 2013).

Osterix shows anti-tumour activity in mouse osteosarcoma cells transfected with the osterix gene where it significantly reduced incidence and volume of tumours in both *in vitro* and *in vivo* experiments (Cao *et al.*, 2005). Osterix is also involved in the regulation of a group of miRNAs which target important genes that are involved in osteoblast differentiation and inhibition. Osterix has been shown to down-regulate the expression of miR-133a, miR-204 and miR-211 but up-regulate the expression of miR-141 and miR-200a. MiR-133a, miR-204 and miR-211 are known to target RUNX2, which is an important osteogenic transcription factor. MiR-204 and miR-211 also target sclerostin and alkaline phosphatase while miR-141 and miR-200a has been shown to target transcription factor Dlx5 (Chen *et al.*, 2013). This indicates that osterix plays an important role in controlling optimal osteoblast differentiation and function by controlling different key proteins.

### 1.2.2.7 Sclerostin

Sclerostin is an osteocyte-derived glycoprotein coded by the SOST gene that functions as a negative physiological regulator of bone formation. Sclerostin was first discovered in 2001 as the gene that responsible for causing sclerosteosis, a rare and recessively inherited disorder that is characterised by the progressive bone overgrowth. Sclerosteosis patients experience symptoms such as facial palsy, hearing loss, syndactyly and compression of the cranial nerves which can be fatal (William, 2014). Sclerosteosis is caused by the mutation in SOST gene which limits the secretion of sclerostin protein by osteocytes. Sclerostin not only inhibits bone formation by blocking the canonical Wnt signalling (Monroe *et al*., 2012) but also crucial for osteoclast formation and osteoclast bone resorption function (Wijenayaka *et al*., 2011). This means, low level of sclerostin results in higher bone formation by osteoblast and less bone resorption by osteoclast at the same time, resulting in excessive bone growth. Before this finding, it was thought that sclerosteosis is caused primarily by excessive osteoblastic bone formation rather than the defective of osteoclastic bone resorption (Hamersma *et al*., 2003). The identification of SOST gene mutation in sclerosteosis lead to the discovery of mutation that cause Van Buchem disease, a very similar disease to sclerosteosis, primarily differentiated by syndactyly and tall stature in sclerosteosis patients. Van Buchem disease is caused by deletion mutation of a 52-kb regulatory region which is 35 kb downstream of SOST gene resulting in reduced SOST expression (Balemas *et al*., 2002). These two findings show that the mutation of SOST gene which limits the SOST protein production results in the excessive bone growth, giving the first idea that the physiological role of SOST in the suppression of bone formation. Since then, many studies have been performed to investigate the role of sclerostin in bone development. A published clinical study showed that sclerostin inhibition using anti-sclerostin antibody (Scl-Ab) has been shown to efficiently prevent rapid and extensive spinal cord injury-induced cancellous and cortical bone loss (Beggs *et al*.,

2015). Other study discovered that multiple myeloma cells express high level of sclerostin, creating an environment with high sclerostin concentration which might contribute to low osteoblastic differentiation in multiple myeloma patients (Brunetti *et al*., 2011). Further investigation showed that combination of Scl-Ab with anti-myeloma drugs is effective in controlling multiple myeloma and multiple myeloma-induced bone disease in patients with active multiple myeloma (Delgado-Calle *et al*., 2017). In other study, deletion of the sclerostin gene in mice resulted in a significant increase in bone formation and bone strength. Bone densitometry analysis revealed the increase of bone mineral density of more than 50 percent. Meanwhile micro-CT analysis showed a significant increase of bone volume in both trabecular and cortical bones (Li *et al*., 2008). On the other hand, transgenic mice which overexpress sclerostin have been shown to have significantly lower bone mass and reduced bone strength (Winkler *et al*., 2003). These findings confirm the role of sclerostin as a negative regulator of bone formation and suggest that sclerostin might become a key tool for the development of therapeutic strategies for bone diseases.

Recently, there has been increasing interest in the role of microRNAs, a small non coding RNA molecule, in bone development. A few miRNAs have been identified to negatively regulate sclerostin which antagonize Wnt signalling such as miR-218 (Hassan *et al.*, 2012), miR-133a and miR-204/211 (Chen *et al.*, 2013). These miRNAs have a great potential to be used as a new method of treating bone diseases such as osteoporosis. Another finding shows that two bone-specific transcription factors, RUNX2 and osterix, activate sclerostin gene expression in a co-ordinated manner *in vitro* using human HEK-293T cells (Perez-Campo *et al.*, 2016) suggesting another approach that could be used to control bone growth.

## 1.3 Purinergic signalling and the role of Adenosine 5'-triphosphate (ATP) and Parathyroid hormone (PTH) in bone development

### 1.3.1 Purinergic signalling

Purinergic signalling is an extracellular signalling that regulates various cellular functions such as heart rate, coronary flow, liver metabolism, activation of white blood cells, nerve cells communication, renal function, and cell proliferation and function (Alan and Alexei, 2006; Junger, 2011; Mclntosh and Lasley, 2011; Oliveira *et al*., 2013, Rumney *et al*., 2012). Purinergic signalling is controlled by purine nucleotides and nucleosides which activates purinergic receptors in the cells (Praetorius and Leipziger, 2010). There are three different types of purinergic receptors, known as P1, P2X and P2Y receptors. Bone cells, osteoblasts and osteoclasts express P2X and P2Y receptors to control bone modelling and remodelling processes. P2X receptors are ligand-gated ion channel type receptors which are activated by ATP, while P2Y receptors, G protein-coupled type receptors, are activated by nucleotides such as ATP, ADP, UDP and UTP. Purinergic signalling has been shown to involve in the pathophysiology of several bone diseases such as osteoporosis. Hence, blocking nucleotides in this signalling pathway could be one of the strategy to fight osteoporosis (Rumney *et al*., 2017).

### 1.3.2 Role of adenosine 5'-triphosphate (ATP) in bone development

The role of adenosine triphosphate (ATP) in intracellular energy metabolism has long been understood. ATP is also now known as an important extracellular signalling molecule that is involved in various biological processes. The binding of ATP to the purinergic P2X receptors which function as ligand-gated $Ca^{2+}$ channel opens the cationic channels hence increase the intracellular $Ca^{2+}$ and induce

membrane depolarization. The depolarization of the membrane cell makes the membrane permeable to large molecules which assist various biological processes such as cell metabolism and function (Kumagi *et al*., 1991). ATP can be released into the extracellular environment by any cell type via several physiological mechanisms such as necrosis, following membrane damage or by exposure to different stress types such as mechanical strain. In the cytosols of cells, ATP concentration is normally between 2 and 5 mM (Orriss *et al.*, 2013). In bone cells, mechanical loading triggers the increase of ATP release by osteoblast and osteoclast cells. The released ATP and its breakdown products can activate the purinergic P2Y or P2X receptors, depending on the concentration of ATP in the environment. High concentration of ATP triggers the P2X7 receptors on the osteoclast precursors and triggers the fusion and multinucleation of osteoclasts. This will result in the increase of mature osteoclast production hence increase the bone resorption (Orriss *et al*., 2010; Rumney *et al*., 2012).

### 1.3.3 Role of parathyroid hormone (PTH) in bone development

Parathyroid hormone (PTH), also known as parathormone or parathyrin, is a hormone secreted by the parathyroid gland. Its main function is to control plasma calcium levels in the blood and to prevent osteoblast and osteocyte apoptosis. A decrease in serum calcium levels induces secretion of PTH which increases calcium levels, but conversely supresses further PTH release. Intermittent administration of low levels of PTH has been shown to have an anabolic effect which occurs by activating osteoblast surface receptors, inducing the production of growth factors such as insulin-like growth factor 1 (IGF1). This results in an increase in the number of osteoblasts, bone formation and bone mass, mainly by increased production of trabecular bone (Crockett *et al.*, 2011; Hirsch *et al.*, 2013). There are two major pathways that PTH can influence bone development; through protein-

kinase A (PKA) pathway or through the release of intracellular calcium and activation of protein-kinase C (PKC). Activation of PTH1R by PTH increases several intracellular signalling molecules such as adenylate cyclase (AC) and phospholipase C (PLC). Activation of the AC signalling cascade leads to the activation of PKA and phosphorylation of transcription factors that regulate transcription of related genes such as RANKL and osterix. Stimulation of PLC signalling leads to the accumulation of inositol trisphosphate (IP3) and diacylglycerol (DAG) which increase intracellular calcium level and activate PKC resulting in the regulation of gene transcription (Datta and Abou-Samra, 2009; Swarthout *et al*., 2002). In both osteoblastic cell lines and primary osteoblast, PTH effectively increases *c-fos* gene transcription (Bowler *et al*., 1999a). Other study revealed that stimulation of P2 receptors by ATP and PTH stimulates synergistic increase of *c-fos* gene expression, suggesting that in the presence of both ATP and PTH, bone remodelling could be increased. This could occur via different pathways depending on the cell types and which P2 receptor is activated. ATP activates P2Y type receptors (either $P2Y_1$ or $P2Y_2$) which results in the intracellular calcium level to increase. Meanwhile PTH can react independently to increase the *c-fos* expression by activating the $G_s$ subunit (Gartland *et al*., 2012).

## 1.4 microRNAs in bone development

### 1.4.1 Overview

MicroRNAs (miRNAs) are small, genetically conserved non-coding RNA molecules of only approximately 19-25 nucleotides in length (Hupkes *et al.*, 2014). miRNAs are produced by all cell types and is secreted into blood by endothelial cells, vascular smooth cells, red blood cells and platelets. The same miRNAs can be produced by different cell types for different purposes (Navickas *et al.*, 2016). Generally, miRNAs

are negative regulators of gene expression through the inhibition of target messenger RNA (mRNA) translation (Iorio *et al.*, 2010). However, some miRNAs can bind to the 5' UTR region (coding region) of mRNA and enhance protein translation (Orom *et al.*, 2008).

MiRNAs have been identified as regulating major cellular functions such as apoptosis, cell proliferation and differentiation (Brennecke *et al.*, 2003; Hupkes *et al.*, 2014; Li *et al.*, 2009; Williams *et al.*, 2009). They have also been implicated in various human diseases, such as breast cancer (Zhang *et al.*, 2014), brain tumours (Catania *et al.*, 2012), oesophageal cancer (He *et al.*, 2012), schizophrenia (Forstner *et al.*, 2013; Wang *et al.*, 2014) and osteoarthritis (Wu *et al.*, 2014). Since the first discovery of miRNA in 1993 (Lee *et. al*., 1993), more than 2000 individual miRNAs have been identified which are involved in human gene regulation and deposited in miRBase, with each miRNA predicted to control hundreds of gene transcripts (Hammond, 2015). However, their role in bone and in the aetiology of metabolic bone diseases remains to be established.

### 1.4.2 miRNA biogenesis and function

Genes encoding miRNAs can be found in various locations within the genome, both in introns and exons (Rodriguez *et al.*, 2004). However, in humans, only some of the miRNAs are encoded by exons as the majority are encoded by introns of coding or non-coding transcripts (Ha & Kim, 2014). The biogenesis of miRNA takes place firstly in the nucleus and then continues in the cell cytoplasm.

In the nucleus, RNA polymerase II/III transcribes a long, variable-length hairpin RNA known as primary miRNA (pri-miRNA) directly from the miRNA encoding gene. This pri-miRNA is processed into ~ 70- to 120-nucleotide long premature stem-loop

intermediates known as precursor miRNAs (pre-miRNAs) by the Microprocessor, a large complex that includes an RNase III enzyme known as Drosha and the RNA-binding protein DGCR8. These pre-miRNAs are then transported to the cytoplasm by Exportin 5 where the loop region of the pre-miRNAs are cleaved into double stranded miRNA by an RNase III enzyme known as Dicer. Transactivation response RNA binding protein (TRBP) facilitates the association of the Dicer-miRNA complex with RNA-induced silencing complex (RISC) that contains Argonaute 2 (Ago2), protein kinase RNA activator (PACT), trinucleotide repeat-containing gene 6A (TNRC6A) and other RNA binding proteins. Association of mature miRNA with RISC complex induces degradation of the passenger strand. The guide strand then recognizes its target site on the 3' UTR region on the target mRNA. The silencing effect of the miRNA is achieved either by degrading the mRNA (in case of perfect base complementarity) or inhibiting protein translation (in case of multiple sequence mismatch between miRNA and target mRNA) (Bhaskaran & Mohan, 2014; Lee *et al.*, 2003). Recent studies have shown that miRNAs can interact with the 5' UTR region of the target gene via complementarity yet inhibit protein translation as efficiently as an interaction in the 3' UTR region (Lytle *et al.*, 2007). The process of miRNA biogenesis is illustrated in Fig. 1.2.

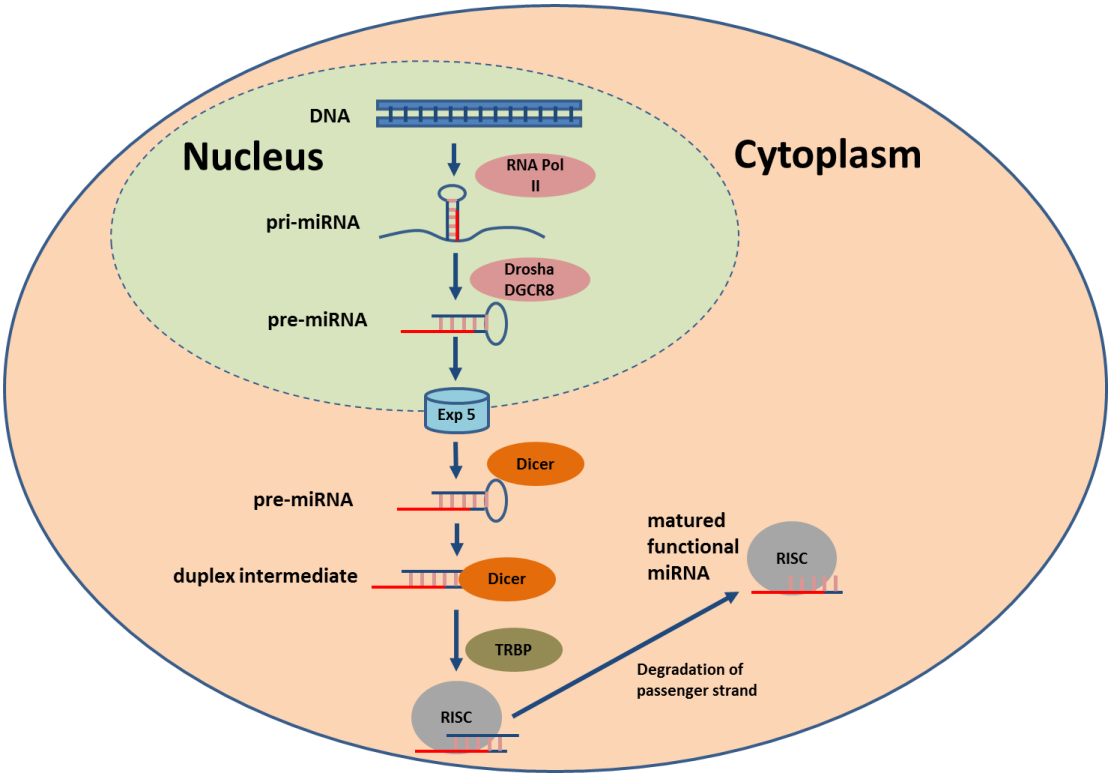


Figure 1.2: Schematic model of miRNA biogenesis which starts with miRNA transcription by RNA polymerase II (Pol II) within the nucleus.

### 1.4.3 miRNA in human diseases and disorders

As miRNAs play vital roles in many cellular functions, their dysregulation has been linked to various diseases and disorders, not surprisingly cancer in many cases (Calin & Croce, 2006; Deng *et al.*, 2016; Ha & Kim, 2014). A small change in the level of miRNA can cause major or minor cellular effects to both normal and aberrant cells. Changes in the expression of miRNAs have been detected during the progression of various human diseases, demonstrating the involvement of miRNA in human diseases (Mendell & Olson, 2012). Table 1.1 shows examples of miRNAs that are involved in human disease.

Table 1.1: List of miRNAs involved in human disease

| Locus name | Phenotype/Disease | References |
|---|---|---|
| miR-1286, miR-24-1, miR-328, miR-548a-1 | Breast cancer | (Cordero *et al.*, 2015) |
| miR-132, miR-148a, miR-18b, miR-34b, miR-34c | Prostate cancer | (Formosa *et al.*, 2013) |
| miR-1286, miR-1287, miR-432, miR-1290 | Cervical cancer | (Yao *et al.*, 2013) |
| let-7e, miR-132, miR-34b, miR-489 | Melanoma | (Mazar *et al.*, 2011) |
| miR-203 | Rheumatoid arthritis | (Stanczyk *et al.*, 2011) |
| miR-29b | Cardiovascular disease | (Chen *et al.*, 2012) |
| miR-15a, miR-21, miR-155, miR-34a, miR-125b | Lymphomagenesis | (Lawrie, 2013) |
| miR-185 | Schizophrenia | (Forstner *et al.*, 2013) |
| miR-133a | Cardiac fibrosis | (Renaud *et al.*, 2015) |
| miR-122 | Hepatitis C | (Jopling *et al.*, 2008) |

### 1.4.4 miRNAs in bone development and bone diseases

Inhibition of protein translation by miRNAs in cells has emerged as an important regulator of various cellular functions. Bone formation is a continuous and complex process which is controlled and influenced by various factors including miRNAs. MiRNAs are involved in every step of bone formation and bone repair from embryonic stage to adulthood by regulating the growth, differentiation and function of the cells that constitute bone tissue. All miRNAs that are expressed in osteoblast lineage cells that are involved in bone regulation are also known as osteomiRs (Lian *et al.*, 2012). Studies have shown that different subsets of osteomiRs are expressed during different stages of osteoblast and osteoclast maturation indicating sophisticated control of bone formation by miRNAs (Lian *et al.*, 2012; Zhang *et al.*,

2011). Several miRNAs have been identified as being involved in bone development such as miR-125 targets osterix which is required for bone mineralisation (Goettsch *et al.*, 2011) and miR-133 inhibits osteoblast differentiation by targeting Runx2 (Li *et al.*, 2008). Inhibition of osterix expression by miR-125 and suppression of osteoblast differentiation by miR-133 result in weak bone formation and could leads to osteoporosis. On the other hand, miR-378 promotes osteoblast differentiation, promoting healthy bone formation by regulating nephronectin expression, an extracellular matrix protein that plays a critical role in the development and function of various tissues (Kahai *et al.*, 2009). Other examples of miRNA involved in bone development and disease are shown in Table 1.2.

Table 1.2: List of miRNAs involve in bone development and bone diseases.

| **Locus name** | **Function** | **References** |
|---|---|---|
| miR-138 | Inhibit osteogenic differentiation | (Eskildsen *et al*., 2011) |
| miR-223 | Stimulate osteoclastogenesis | (Sugatani and Hruska, 2009) |
| miR-155 | Suppress osteoclastogenesis | (Mann *et al*., 2010) |
| miR-29 | Support osteoblastogenesis | (Kapinas *et al*., 2009) |
| miR-103a | Inhibit bone formation through targeting Runx2 | (Zuo *et al*., 2015) |
| miR-125 | Inhibit osterix production | (Goettsch *et al.*, 2011) |
| miR-133 | Inhibit osteoblast differentiation | (Li *et al.*, 2008) |
| miR-378 | Promote osteoblast differentiation | (Kahai *et al.*, 2009) |

## 1.5 Hypothesis

Our hypothesis are osteosarcoma cell lines (MG-63, TE-85 and SaOS-2) provide a useful model to study bone biology and miRNAs have promising potential to be used to control healthy bone development as well as a new treatment for various bone diseases.

## 1.6 Objectives of this thesis

- In the first experimental chapter, we wanted to prove if osteoblastic cell lines, MG-63, TE-85 and SaOS-2 represent different stages of osteoblastic differentiation. To prove this, we studied the expression of several bone markers that are known to be expressed differently at different stages of osteoblastic differentiation using these cell lines. We also studied the effects of ATP and PTH treatment on the expression of these markers to examine if these cell lines respond the same way as the primary osteoblastic cell.
- Once we were confident that these 3 cell lines do represent osteoblastic cells at different stages of osteoblastic differentiation, we then studied the differential expression of miRNAs in these cell lines to understand the differential expression of miRNA at different stages of osteoblastic differentiation.
- The next objective was to identify miRNAs that involve in the regulation of sclerostin expression, a major regulator of bone formation in these cell lines by using transient transfection method.
- The final objective was to study the effect of miR-378a-3p transfection (one of the miRNAs that we used in the transfection experiment) on bone microstructures in mice.

# CHAPTER 2:

# MATERIALS AND METHODS

## 2.1 Cell culture

MG-63, TE-85 and SaOS-2 cells were obtained from liquid nitrogen stock. Primary human osteoblasts were obtained from patients that had undergone hip replacement surgery. The experiments on the primary cells were undertaken under approval from the Liverpool Research Ethics Committee, Pathophysiological studies to understand the nature of tissue damage in Alkaptonuria (REC reference 07/Q1505/29). Resurrection of preserved cells, culture of cell lines and primary cells, their passage, enumeration and preservation were carried out according to established protocols (Gartland *et al*., 2012).

### 2.1.1 Thawing of cryo-preserved cells

Frozen vials containing MG-63, TE-85 or SaOS-2 cells were removed from liquid nitrogen storage and thawed quickly in a water bath at 37°C with gentle shaking. The thawed cell suspensions were wiped with 70% ethanol before being added into 10 cm culture dishes containing 9 mL Dulbecco's modified Eagle medium (DMEM) (D6429, Sigma-Aldrich) with 10% fetal calf serum (FCS) (FB-1001/500, Biosera) and 50 U/mL penicillin - 50 µg/mL streptomycin (P4458, Sigma-Aldrich). The cultures were incubated at 37°C in a humidified atmosphere of 95% air and 5% $CO_2$. Culture medium was replaced after overnight incubation.

### 2.1.2 Culture of osteosarcoma cell lines

Osteoblastic cell lines were cultured in DMEM with 10% FCS and 50 U/mL penicillin - 50 µg/mL streptomycin. Cells were seeded at different concentrations depending on the frequency of use. For maintaining a culture, cells were seeded at between 1 – 2 x $10^4$ cells per 10 cm culture dish. Cultures were incubated at 37°C in a

humidified atmosphere of 95% air and 5% $CO_2$. Cells were passaged when confluency reached approximately 70-80%.

### 2.1.3 Culture of primary human osteoblasts

Femoral heads obtained from patient who had undergone hip replacement were transported to the laboratory in PBS on the same day. Trabecular bone was removed from the open end of the femoral head using sterile bone rongeurs and a solid stainless steel blade with integral handle. The trabecular bone fragments were transferred to a clean Petri dish containing 3 mL of PBS and diced into pieces 3-5 mm in diameter using a scalpel blade and fine scissors. The PBS was removed slowly without disturbing the bone sediment. Bone chips were transferred to a sterile 30 mL tube containing 20 mL of PBS. The tube was vortex-mixed vigorously three times for 10 seconds and left to stand for 30 seconds to allow the bone fragments to settle. The supernatant containing haematopoietic tissue and dislodged cells was carefully removed. Another 20 mL of PBS were added to the tube and vortexed. This step was repeated at least three times until no remaining haematopoietic marrow was visible and the bone fragments appeared white. The bone fragments were cultured as explants at a density of 0.2-0.6 g of tissue/10 cm culture dish in 10 mL DMEM at 37°C in a humidified atmosphere of 95% air, 5% $CO_2$. The cultures were incubated for 7 days then the medium replaced carefully without dislodging the explants. The outgrowths of cells were checked at day 7-10. The medium was changed at day 14 and twice weekly thereafter until the desired confluency had been attained. This isolation and culture of primary human osteoblast procedures was performed by Dr. Peter Wilson, Musculuskeletal Biology Department, Institute of Ageing and Chronic Disease, University of Liverpool.

### 2.1.4 Passage of primary cells

Bone chips were removed using sterile forceps and discarded. The spent medium was removed and the cell layers were gently washed three times with 10 mL of $Ca^{2+}$ and $Mg^{2+}$-free PBS. The culture dish was incubated with 5 mL of freshly thawed trypsin-EDTA for 5 minutes at 37°C. The culture was gently rocked every 30 seconds to ensure the entire surface of the dish was exposed to the trypsin-EDTA solution. The culture was removed from the incubator and examined by light microscopy to ensure all cells had dislodged from the dish. The culture that was not fully dislodged was incubated for another 5 minutes at 37°C. When all cells had detached from the dish, the cells were transferred to an eppendorf tube containing 10 mL of complete medium. The culture dish was then washed 3 times with serum-free medium. The washings were pooled with the original cell isolate and centrifuged at 250 x g for 5 minutes at room temperature to recover the cells. The supernatant was removed carefully by inverting the tube without loosening the cell pallet. The cell pellet was then resuspended in 2 mL serum-free medium. The number of cells was determined using a Neubauer haemocytometer (section 2.1.6). The harvested cells were seeded at a cell density suitable for the required experiment at 37°C in a humidified atmosphere of 93% air and 5% $CO_2$. Generally, cells were subcultured at a concentration of 5 x $10^3$ – $10^4$ cells/$cm^2$. At this concentration, the culture was ≥70% confluent after 24 hours.

### 2.1.5 Passage of cell lines

Culture medium was removed and the cells washed twice with 5 mL of PBS. Five mL of trypsine-EDTA were added and incubated at 37°C for 5 minutes. The cells were checked by light microscopy to ensure all had detached from the culture dish. They were then transferred to an eppendorf tube containing 10 mL of complete medium. The number of cells was determined using a Neubauer haemocytometer

(section 2.1.6). The harvested cells were seeded at a density suitable for the required experiment at 37°C in a humidified atmosphere of 95% air and 5% $CO_2$. For the maintenance purposes, cells were seeded at 1 - 2 x $10^4$ cells per 10 cm culture dish.

### 2.1.6 Cell counting

Twenty µL of the harvested cell suspension were diluted with 80 µL serum free medium. One hundred µL of trypan blue solution were added and mixed well. The mixture was left for 1 minute before counting viable and nonviable cells using a Neubauer haemocytometer. The number of cells in five squares (Fig. 2.1) was determined and the cell concentration calculated using the following formula:

**Total cells/mL = Total cells counted x (dilution factor ÷ number of squares) x 10,000 cells/mL**

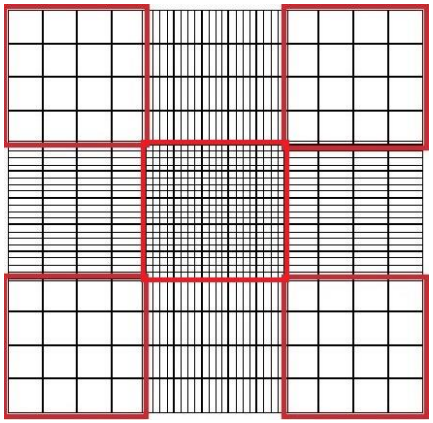

Figure 2.1: Grid layout of a Neubauer Improved haemocytometer. Cells in four corner squares and the middle squares were counted to determine cell concentration

### 2.1.7 Cryo-preservation of cells

Cultures were harvested when confluency had reached approximately 80-90% using the same procedure for routine subculture. After performing cell counting, cells were centrifuged at 250 x g for 5 minutes and the supernatant was removed. The cell pellet was resuspended in an appropriate quantity of freezing medium (0.9 mL FCS + 0.9 mL dimethyl sulfoxide (DMSO) per sample) to achieve a cell concentration of 2 - 4 x $10^6$ cells/mL per cryovial. Cryovials were closed tightly and frozen overnight in a -80°C freezer using a Mr. Frosty. Cells were then transferred into liquid nitrogen for long term storage.

## 2.2 Molecular biology

### 2.2.1 Extraction and quantification of total RNA

Total RNA was extracted from cells using an miRNeasy Mini Kit (Qiagen, Cataloque No. 217004) according to the protocol provided by the manufacturer. The purified total RNA was quantified using a NanoDrop 2000 spectrophotometer (Thermo Scientific).

### 2.2.2 Reverse transcription of RNA

Reverse transcription of RNA was carried out using a high capacity RNA-to-cDNA kit (Applied Biosystems, Catalogue No: 4387406) according to the protocol provided by the manufacturer. Reverse transcription mix per 20 µL reaction is shown in Table 2.1.

Table 2.1: Reverse transcription mix per 20 µL reaction

| **Component** | **Volume/Reaction (µL)** |
|---|---|
| 2x RT Buffer | 10.0 |
| 20x Enzyme Mix | 1.0 |
| RNA Sample | up to 9 µL (1 µg) |
| Nuclease-free $H_2O$ | quantity sufficient for 20.0 µL |
| **Total per Reaction** | **20.0** |

The reaction mix was incubated at 37°C for 60 minutes. The reaction was then halted by incubating the reaction mix at 95°C for 5 minutes and held at 4°C. The cDNA was diluted 10 times and used for real-time PCR or stored in a -20°C freezer.

### 2.2.3 Designing PCR primers

Primers for miRNA expression were ordered from Qiagen (https://www.qiagen.com/gb/geneglobe) while primers for gene expression study were designed using free online software and synthesized by Invitrogen (UK). Primer specification and the location of the free software used to design the primers were:

Primer3 (http://frodo.wi.mit.edu/primer3)

- Product size: 100-150bp
- Primer size: 18-22bp
- Primer Tm: 58-62°C
- Primer GC%: 20-50%

DNA mfold (http://mfold.bioinfo.rpi.edu/cgi-bin/dna-form1.cgi)

- Sequence type: Linear
- Folding temperature: 58-62°C
- $[Na^+]$: 50 mM, $[Mg^{2+}]$: 3mM

Beacon Designer (http://www.premierbiosoft.com/qOligo/Oligo.jsp?PID=1)

- Nucleic acid concentration: 500 nM
- Mono ion concentration: 50 mM
- Free Mg2+ concentration: 3 mM

### 2.2.4 Quantitative reverse transcription PCR (RT-qPCR) of gene expression

RT-qPCR for gene expression was performed using a CFX Connect™ Real-Time PCR Detection System (Bio-Rad). Diluted cDNA samples (1:10) were used as templates. RT-qPCR was performed according to the protocol supplied by the manufacturer for iQ™ SYBR® Green Supermix (Bio-Rad). Primer sequences are shown in Table 2.2 and the reaction mix for each reaction in Table 2.3. Reactions

were performed using 6 biological replicates and 3 technical replicates for each sample, on a 96-well plate. The reaction conditions are listed in Table 2.4. Relative normalized expression was automatically calculated by the Bio-Rad CFX Manager 3.1 software using the ΔΔCt formula.

Table 2.2: Primer sequences for gene expression

| **Primer** | **Sequence** |
|---|---|
| Col 1a2 forward | 5'- GGC ACT CCA GGT CCT CAG-3' |
| Col 1a2 reverse | 5'- CCA CAG CAC CAG CAA CAC-3' |
| OPG forward | 5'-GCA GCG GCA CAT TGG ACA TG-3' |
| OPG reverse | 5'-AGG ATC TGG TCA CTG GGT TTG C-3' |
| Col 6a3 forward | 5'-GCT GTC TCC AGC GTT TAT CC-3' |
| Col 6a3 reverse | 5'-TCA AGC AGA AAC ACC ACG TC-3' |
| SOST forward | 5'-AAG AAT GAT GCC ACG GAA AT-3' |
| SOST reverse | 5'-AGC TGT ACT CGG ACA CGT CTT T-3' |
| Osterix forward | 5'- CCC ACC TCA GGC TAT GCT AA-3' |
| Osterix reverse | 5'- CAC TGG GCA GAC AGT CAG AA-3' |
| RANKL forward | 5'- TAT GCC AAC ATT TGC TTT CG-3' |
| RANKL reverse | 5'- CTT GGG ATT TTG ATG CTG GT-3' |
| ALP forward | 5'-GCT GAA CAG GAA CAA CGT GA-3' |
| ALP reverse | 5'-TCA ATT CTG CCT CCT TCC AC-3' |
| B-actin forward | 5'-GGA CCT GAC TGA CTA CCT C-3' |
| B-actin reverse | 5'-GCC ATC TCT TGC TCG AAG-3' |

Table 2.3 Reaction mix for each reaction

| **Component** | **Volume/Reaction (µL)** |
|---|---|
| iQ™ SYBR® Green Supermix | 7.5 |
| Forward primer | 1.0 |
| Reverse primer | 1.0 |
| RNase-free water | 3.5 |
| Template cDNA | 2.0 |
| **Total per Reaction** | **15.0** |

Table 2.4: Reaction conditions for RT-qPCR of gene expression

| **Polymerase activation & DNA denaturation** | **Amplification** | | | **Melt curve analysis** |
|---|---|---|---|---|
| | **Denaturation** | **Annealing/Extension + plate read** | **Cycles** | |
| 95°C<br>3 minutes | 95°C<br>30 seconds | 60°C<br>30 seconds | 40 | 65-96°C<br>0.5°C increment<br>5 seconds/step |

### 2.2.5 Total DNA extraction and quantification

DNA extraction was carried out using a CyQUANT® Cell Proliferation Assay Kit (Life Technologies, Catalogue No. C7026) according to the manufacturer's protocol.

### 2.2.6 ATP and PTH treatments

The medium was replaced with serum free DMEM when the culture reached 80 – 85 percent confluency. Cells were incubated for a further 48 hours. Cells were then treated with ATP (final concentration: 5 µg/ml), PTH (final concentration: 10 ng/ml) or ATP + PTH (final concentration: 5 µg/ml ATP + 10 ng/ml PTH). In control cultures, cells were grown in serum-free DMEM.

## 2.3 miRNA profiling

### 2.3.1 Extraction of total RNA

RNA (including miRNA) was extracted using an miRNeasy Mini Kit (Qiagen, Catalogue No. 217004) according to protocol provided by the manufacturer.

### 2.3.2 Microarray analysis

Total RNA samples (free from genomic DNA) were quantified and the quality of RNA assessed using an Agilent 2100 Bioanalyser RNA 6000 Nano chip and small RNA chips. Samples were prepared for hybridisation onto Affymetrix miRNA 4.0 arrays. 1000 ng of total RNA was used as the initial input, and an Affymetrix Flash Tag labelling kit used to prepare samples for hybridisation according to the manufacturer's instructions. Biotin-labelled samples were hybridised onto Affymetrix GeneChip miRNA 4.0 for 17 hours at 48°C at 60 rpm in an Affymetrix hybridisation oven 640. Following hybridisation the arrays were washed using an Affymetrix Hybridisation wash and stain kit on a GeneChip Fluidics station 450 using fluidics script FS450_0002 and scanned using the Affymetrix GeneChip scanner 3000 7G. CEL files were generated using Affymetrix GeneChip Command Console Software, and Expression Console software was used to QC array performance.

### 2.3.3 Differential expression of miRNA between cell lines

Differential expression of miRNAs between all three cell lines and human primary osteoblasts was analysed using Mass Profiler Professional Version B.14.5 (Agilent Technologies). The estimated log2 fold change (logFC) for the 6 contrasts were tested in limma using a t-test. P-values associated with logFC were adjusted for multiple testing using the False Discovery Rate (FDR) approach (Benjamini and

Hochberg, 1995). Significantly differentially expressed (DE) miRNAs were defined as those with an FDR-adjusted P-value < 5%.

### 2.3.4 miRNA target prediction

From 6940 miRNAs that were differentially expressed between osteosarcoma cell lines and primary human cells, we investigated miRNAs that have the potential to inhibit sclerostin expression, a protein that inhibits new bone formation by blocking the Wnt signalling pathway. To predict miRNAs that target mRNA coding for sclerostin, we use five different online prediction tools: miRWalk (http://zmf.umm.uni-heidelberg.de/apps/zmf/mirwalk2/), miRanda (http://www.microrna.org/microrna/home.do), Pictar (http://www.pictar.org/), RNA22 (https://cm.jefferson.edu/rna22/) and Targetscan (http://www.targetscan.org/vert_71/). MiRNAs that were predicted by a majority of the prediction algorithms were chosen for further experimental validation.

### 2.3.5 Reverse transcription of miRNA

Reverse transcription for miRNAs that were predicted to target the sclerostin gene was carried out using miScript® II RT Kit (Qiagen, Catalogue No: 218161) according to the protocol provided by the manufacturer. Reverse transcription mix per 20 µL reaction is shown in Table 2.5.

Table 2.5: Reverse transcription mix per 20 µL reaction

| **Component** | **Volume/Reaction (µL)** |
|---|---|
| 5x HiSpec Buffer | 4 |
| 10x miScript Nucleic Mix | 2 |
| miScript RT Mix | 1 |
| $H_2O$ | quantity sufficient to 20.0 µL |
| RNA Sample | up to 13 µL (1 µg) |
| **Total per Reaction** | **20.0** |

The reaction mix was incubated at 37°C for 60 minutes. The reaction was then stopped by incubating the reaction mix at 95°C for 5 minutes and held at 4°C. cDNA was diluted 10 times and used for real-time PCR or stored in a -20°C freezer.

### 2.3.6 Quantitative reverse transcription PCR (RT-qPCR) for the validation of miRNA expression

RT-qPCR for gene expression was performed using a CFX Connect™ Real-Time PCR Detection System (Bio-Rad). Diluted cDNA samples (1:10) were used as templates. RT-qPCR was performed according to the protocol supplied by the manufacturer for the miScript® SYBR® Green PCR Kit (Qiagen). The primer sequences used are shown in Table 2.6, reaction mix for each reaction is shown in Table 2.7 and the reaction conditions shown in Table 2.8. Relative normalised expression was automatically calculated by the Bio-Rad CFX Manager 3.1 software using the ΔΔCt formula (Livak and Schmittgen, 2001).

Table 2.6: Primers used for miRNA expression

| **Primer Assay** | **Catalogue No. (Qiagen)** | **Sequence** |
|---|---|---|
| hsa-miR-422a | MS00004172 | 5'-ACU GGA CUU AGG GUC AGA AGG C-3’ |
| hsa-miR-1231 | MS00031290 | 5'-GUG UCU GGG CGG ACA GCU GC-3’ |
| hsa-miR-1254 | MS00042350 | 5'-AGC CUG GAA GCU GGA GCC UGC AGU-3’ |
| hsa-miR-1914-3p | MS00016548 | 5'-GGA GGG GUC CCG CAC UGG GAG G-3’ |
| hsa-miR-103a-3p | MS00031241 | 5'-AGC AGC AUU GUA CAG GGC UAU GA-3’ |
| hsa-miR-378a-3p | MS00006909 | 5'-ACU GGA CUU GGA GUC AGA AGG C-3’ |
| RNU6-2 | MS00033740 | N/A |

Table 2.7: The reaction mix for each reaction

| **Component** | **Volume/Reaction (µL)** |
|---|---|
| 2x QuantiTect SYBR Green PCR Master Mix | 7.5 |
| 10x miScript Universal Primer | 1.5 |
| 10x miScript Primer Assay | 1.5 |
| RNase-free water | 3.0 |
| Template cDNA | 1.5 |
| **Total per Reaction** | **15.0** |

Table 2.8: Reaction conditions for RT-qPCR of miRNA expression

| Polymerase activation & DNA denaturation | 3-step amplification | | | | Melt curve analysis |
|---|---|---|---|---|---|
| | Denaturation | Annealing | Extension | Cycles | |
| 95°C<br>15 minutes | 94°C<br>15 seconds | 55°C<br>30 seconds | 70°C<br>30 seconds | 40 | 65-95°C<br>0.5°C increment<br>5 seconds/step |

### 2.3.7 Validation of miRNA function - Transfection of cells with miRNA mimics and antagomirs

For miRNA transfection, only TE-85 and SaOS-2 cells were used as sclerostin expression was not detected in the MG-63 cell line. Cells were seeded into 6-well plates 24 hours before transfection at a density of 1.5 x $10^5$ cells/mL in complete DMEM. The culture medium was then removed from each well and replaced with fresh DMEM without any supplementation and incubated for 30 minutes. During this incubation period, transfection media were prepared. Cells were to be transfected with scrambled miRNA, miRNA mimics and miRNA inhibitors (antagomirs). For the control cells DMEM only was used. Two 15 mL tubes were prepared for each transfection, tube A and tube B. In tube A, 5 µL of Lipofectamine 2000 (Invitrogen) were mixed with 500 µL of DMEM for each well. In tube B, 1 µL miRNA mimic, antagomir or scrambled miRNA was mixed with 500 µL of DMEM for each well. The miRNA mimics, antagomirs and scrambled miRNAs were purchased from Qiagen (Table 2.9). Transfection tubes were incubated for 5 minutes at room temperature. The contents were then completely mixed and incubated for another 20 minutes. Cell culture medium was removed from each well of the 6 well plates and replaced with 500 µL of the contents of each of both tubes A and B for the appropriate

transfection (n=3). Cells were incubated with these transfection media for 6 hours before the transfection media were replaced with complete DMEM. After 48 hours, culture media were collected for sclerostin protein analysis and cells were harvested for total RNA extraction.

Table 2.9: miRNA mimics, antagomirs and scrambled miRNA used in transfection

| **miRNA Mimic/Inhibitor** | **Catalogue No. (Qiagen)** | **Nucleotide Sequence of miRNA** |
|---|---|---|
| hsa-miR-422a mimic | MSY0001339 | 5'-ACU GGA CUU AGG GUC AGA AGG C-3’ |
| hsa-miR-422a inhibitor | MIN0001339 | 5'-ACUGGACUUAGGGUCAGAAGGC |
| hsa-miR-1231 mimic | MSY0005586 | 5'GUGUCUGGGCGGACAGCUGC |
| hsa-miR-1231 inhibitor | MIN0005586 | 5'GUGUCUGGGCGGACAGCUGC |
| hsa-miR-1254 mimic | MSY0005905 | 5'AGCCUGGAAGCUGGAGCCUGCAGU |
| hsa-miR-1254 inhibitor | MIN0005905 | 5'AGCCUGGAAGCUGGAGCCUGCAGU |
| hsa-miR-1914-3p mimic | MSY0007890 | 5'GGAGGGGUCCCGCACUGGGAGG |
| hsa-miR-1914-3p inhibitor | MIN0007890 | 5'GGAGGGGUCCCGCACUGGGAGG |
| hsa-miR-103a-3p mimic | MSY0000101 | 5'AGCAGCAUUGUACAGGGCUAUGA |
| hsa-miR-103a-3p inhibitor | MIN0000101 | 5'AGCAGCAUUGUACAGGGCUAUGA |
| hsa-miR-378a-3p mimic | MSY0000732 | 5'ACUGGACUUGGAGUCAGAAGGC |
| hsa-miR-378a-3p inhibitor | MIN0000732 | 5'ACUGGACUUGGAGUCAGAAGGC |
| Inhibitor negative control (scrambled miRNA) | 1027271 | N/A |

### 2.3.8 Protein quantification

Media from treated cell cultures were stored at -80°C until further analysis. The quantity of SOST protein secreted into the culture media was measured using a Quantikine® Human SOST ELISA (R&D Systems) according to the protocol provided by the manufacturer with some modification. Three hundred µL of test culture medium were added to the appropriate wells of the ELISA plate and covered with an adhesive strip. Plates were incubated for two hours at room temperature on a horizontal orbital microplate shaker set at 500 ± 50 rpm. For each well medium was then discarded and replaced with another 300 µL culture medium from the same sample. Fifty µL of control and fresh media (blank) were added to the ELISA plate as controls. Plates were incubated for a further 2 hours on a horizontal orbital microplate shaker (500 ± 50 rpm) at room temperature. Each well was then aspirated and washed with 400 µL of wash buffer. The washing step was repeated three times for a total of four washes. After the last wash, any remaining wash buffer was removed by aspirating and the plates were inverted and blotted using clean paper towels. Two hundred µL of human SOST conjugate were added to each well. Plates were covered with adhesive strip and incubated at room temperature on the orbital shaker. After two hours, the washing step was repeated. Two hundred µL of substrate solution were added and plates wrapped with aluminium foil to protect the samples from light. Plates were incubated for one hour at room temperature. Fifty µL of stop solution were added to each well and the plates gently tapped to ensure thorough mixing. The colour in the wells changed from blue to yellow after positive detection of SOST protein. The optical density of each well was determined within 30 minutes using a microplate reader set to 450 nm. The readings at 450 nm were subtracted from the reading at 570 nm to correct optical imperfections in the ELISA plate.

## 2.4 Trabecular bone analysis

### 2.4.1 miR-378a-3p treatment of mice

Treatment of mice with miR-378a-3p was done by Muscle Research Group members, Department of Musculoskeletal Biology, Institute of Ageing and Chronic Diseases, University of Liverpool. Six month old adult mice and old mice aged 2 years were used to study the effect of miR-378a-3p on the properties of trabecular bone. Mice were treated with 2 mg/kg body weight of microRNA mimics or inhibitors/antagomirs through tail vein injection over 3 weeks of treatment. Mice were culled a week following the last injection and the left hind limbs were preserved in 10% phosphate buffered formal saline (PBFS) and used for micro-CT scanning. Experiments were performed in accordance with UK Home Office guidelines under the UK Animals (Scientific Procedures) Act 1986 and received ethical approval from the University of Liverpool Animal Welfare and Ethical Review Body (AWERB).

### 2.4.2 Micro-computed tomography (micro-CT) scan of trabecular bone of tibial head

Preserved samples were transferred into micro-computed tomography (micro-CT) scanning tubes and scanned using a Skyscan 1272 system in water. The scanner was set as follows: voltage = 50kV, source current = 200 µA, filter = Al 0.5 mm, resolution = 4032 x 2688, pixel size = 4.5 µm, rotation step (degree) = 0.30 and frame averaging = Off. Reconstruction of the bone scans was achieved using NRecon software with the following settings: smoothing = 1, misalignment = auto value, ring affect reduction = 5 and beam hardening correction = 38%. The reconstructed bone image files were then opened using Data Viewer software to determine the volume of interest to be used for the analysis of the trabecular bone

properties in the head of the tibia. The position of the growth plate half way between the two ends was determined as the reference point (Figure 2.2). The volume of interest was then measured as the volume of 200 slices of scanned images after the first 10 slices of scanned images from the reference point. Properties of the trabecular bone were than analysed using CTan software.

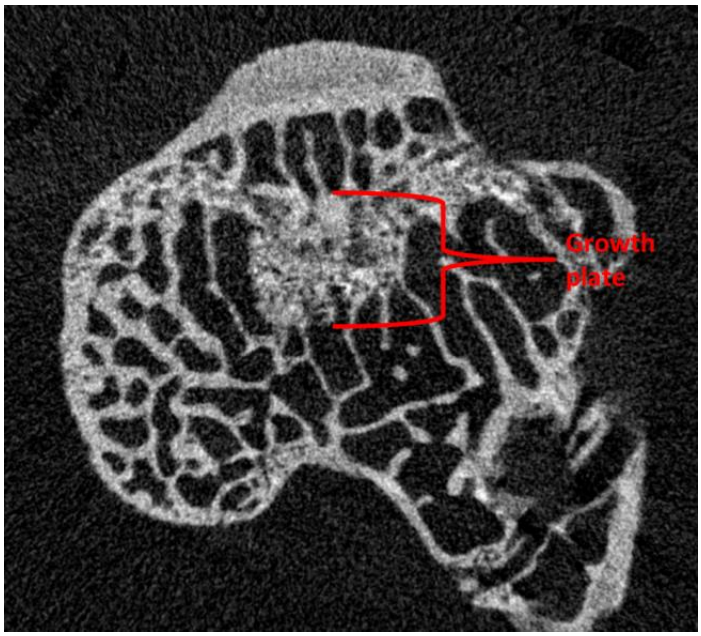


Figure 2.2: Growth plate in the head of tibia.

## 2.5 Statistical analysis

Results were analysed using One-Way Independent ANOVA. The significance level was set at *p* values less than 0.05. Results are presented as mean ± standard error of the mean (SEM).

# CHAPTER 3:

# EXPRESSION OF OSTEOBLASTIC BONE MARKERS IN HUMAN OSTEOSARCOMA CELL LINES AND THE EFFECTS OF ADENOSINE TRIPHOSPHATE (ATP) AND PARATHYROID HORMONE (PTH) ON THE EXPRESSION OF THESE MARKERS

## 3.1 Introduction

The first objective of this thesis was to study the expression of mRNA of selected bone markers in the three most commonly used osteosarcoma cell lines: MG-63, TE-85 and SaOS-2. The expression of these markers in primary human osteoblast, HOB was also studied as a comparison to the cell lines. Each cell line represents different stages of osteoblast maturation. MG-63 represents the early stage of osteoblast differentiation, TE-85 represents the intermediate stage while SaOS-2 represents the most differentiated and matured osteoblasts (Pacheco-Pantoj *et al*., 2011). We have selected seven bone markers which are alkaline phosphatase (ALP), collagen 1a2 (COL1A2), collagen 6a3 (COL6A3), osteoprotegerin (OPG), osterix (OSX), RANK ligand (RANKL) and sclerostin (SOST). Each marker plays an important role in bone modelling and remodelling processes. To understand the expression pattern of these markers, the expression of the mRNA of these markers was compared between cell lines to examine the regulation of bone markers at different stages of osteoblastic differentiation.

ATP has been shown to inhibit bone mineralisation in primary rat osteoblasts (Orriss, Key, Hajjawi, & Arnett, 2013) while the administration of PTH has been shown to increase osteoblast number and bone formation (Crockett, Rogers, Coxon, Hocking, & Helfrich, 2011). Other study showed combined treatment of ATP and PTH significantly increase bone mineral density in ovariectomized female mice by increasing bone formation and decrease bone resorption (Syberg *et al*., 2011). In this chapter, we also studied the effect of ATP and PTH treatments in MG-63, TE-85 and SaOS-2 to identify if these cells respond to the treatment similar to primary osteoblast. The findings of this study will help us to understand if MG-63, TE-85 and SaOS-2 are good cell models to be used to study bone biology.

## 3.2 Brief methods

### 3.2.1 Expression of bone markers in osteosarcoma cell lines

Osteosarcoma cell lines (MG-63, TE-85 and SaOS-2) were cultured in 10 mm cell culture dishes until 80-85% confluent (Section 2.1.2). Total RNA was extracted from cells using a miRNeasy Mini Kit and purified total RNA quantified using a NanoDrop 2000 spectrophotometer (Section 2.2.1). cDNA was synthesized using a high capacity RNA-to-cDNA Kit (Section 2.2.2). To examine the expression of the bone markers, real-time PCR was performed as described earlier (Section 2.2.4).

### 3.2.2 Effect of ATP and PTH treatments on bone marker expression

Osteosarcoma cell lines (MG-63, TE-85 and SaOS-2) were cultured in complete DMEM with 10% FCS in 10 mm cell culture dishes until 80-85% confluent (Section 2.1.2). Cells were then treated with ATP, PTH or ATP + PTH (Section 2.2.6). Cells were incubated overnight before proceeding with total RNA extraction (Bowler *et al*., 1999).

Total RNA was extracted from cells using a miRNeasy Mini Kit and purified total RNA quantified using a NanoDrop 2000 spectrophotometer (Section 2.2.1). Synthesis of the cDNA was performed using a high capacity RNA-to-cDNA Kit with a total volume of 20 µL per reaction (Section 2.2.2). The expression of the bone markers was analysed using RT-qPCR (Section 2.2.4). Result was analysed using One-Way Independent ANOVA.

## 3.3 Results

### 3.3.1 Expression of osteoblastic bone markers in human osteoblastic cells

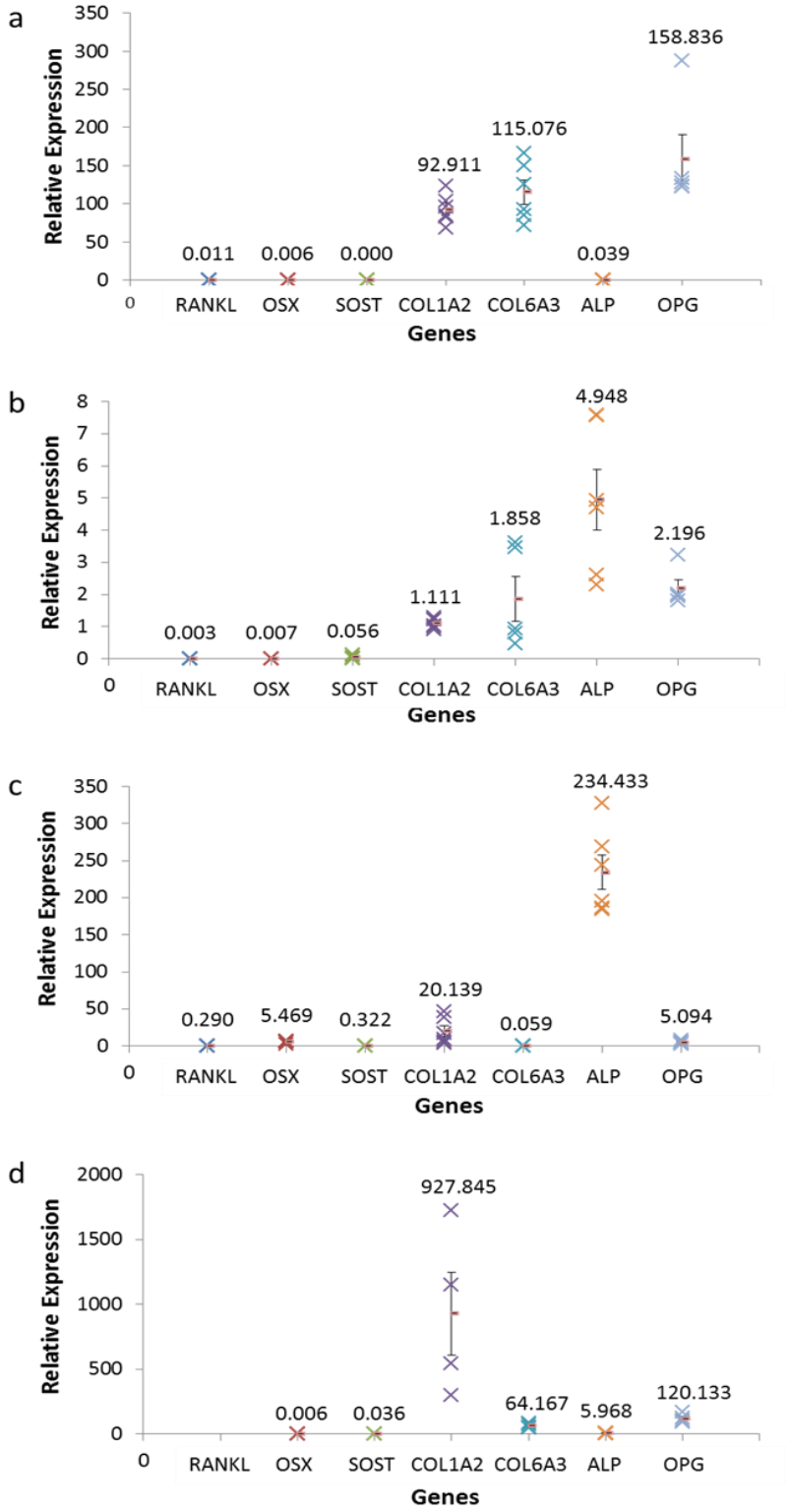


Figure 3.2: Expression of selected bone markers in a) MG-63 b) TE-85 c) SaOS-2 and d) HOB. Value of the mean expression of 5/6 biological replicates (n=5/6) are shown on top of each plot. Error bar represent standard error of the mean (SE). Data were analysed using One-Way Independent ANOVA and LSD Post-Hoc test.

The expressions of the seven selected bone markers in cell lines and HOB were analysed and compared. The expression of ALP mRNA was compared between MG-63, TE-85, SaOS-2 and HOB. ALP mRNA expression was significantly higher in SaOS-2 than MG-63, TE-85 and HOB cells ($p<0.005$). The expression of ALP was 47 times higher in SaOS-2 than TE-85, which was 120 times higher than in MG-63 ($p<0.005$). The ALP mRNA expression level was similar in MG-63 and HOB ($p>0.05$). The expression of COL1A2 mRNA was compared between the three different osteosarcoma cell lines and HOB. Among the cell lines, the highest expression was observed in MG-63 while the lowest was in TE-85. The expression of COL1A2 mRNA was 4.6 times higher in MG-63 compared to SaOS-2, which in turn was 18 times higher than in TE-85 cells ($p<0.05$). There was no significant different of COL1A2 expression between the HOB and all three cell lines due to big standard error value in HOB. The expression of COL6A3 mRNA in MG-63, TE-85 and SaOS-2 cells was compared using One-Way Independent ANOVA and LSD Post-Hoc test. It is apparent that the expression of COL6A3 mRNA was higher in MG-63 cells compared to that in the other cell lines. There was no significant different of the expression level of COL6A3 between MG-63 and HOB ($p>0.05$). COL6A3 mRNA was expressed 62 times higher in MG-63 cells than in TE-85 cells, which was 31 times higher than in SaOS-2 cells ($p<0.05$).

Expression of OPG mRNA was compared between the three osteosarcoma cell lines and HOB. The expression of OPG mRNA was very much higher in MG-63 cells than in the other cell lines, being expressed 72 times higher than in TE-85 and 31 times higher than in SaOS-2 cells ($p<0.05$). The difference between the expression of OPG mRNA in TE-85 and SaOS-2 was also significant ($p<0.05$). The expression of OSX mRNA was analysed and compared between all three osteosarcoma cell lines. No significant difference was observed between the expression of OSX mRNA in MG-63 and TE-85, but it was significantly higher in

SaOS-2 than in both MG-63 and TE-85 cells ($p<0.05$). The expression of RANKL mRNA between MG-63, TE-85 and SaOS-2 cells was compared. The expression of RANKL in HOB was not studied due to technical difficulties. The expression of RANKL mRNA was significantly higher in SaOS-2 cells than in MG-63 and TE-85 cells ($p<0.05$). The expression was 27 times higher in SaOS-2 compared to MG-63 ($p<0.05$). However, no difference was found between the expression of RANKL mRNA in MG-63 and TE-85 ($p>0.05$). The expression of SOST mRNA was compared between the osteosarcoma cell lines. SaOS-2 expressed the highest levels of SOST mRNA while it was not detected in MG-63 cells. The expression of SOST mRNA was 5.8 times higher in SaOS-2 than in TE-85 cells ($p<0.05$). The differences in SOST mRNA expression was also significant between SaOS-2 and HOB ($p<0.05$).

### 3.3.2 Effects of adenosine triphosphate (ATP) and parathyroid hormone (PTH) on the expression of bone markers

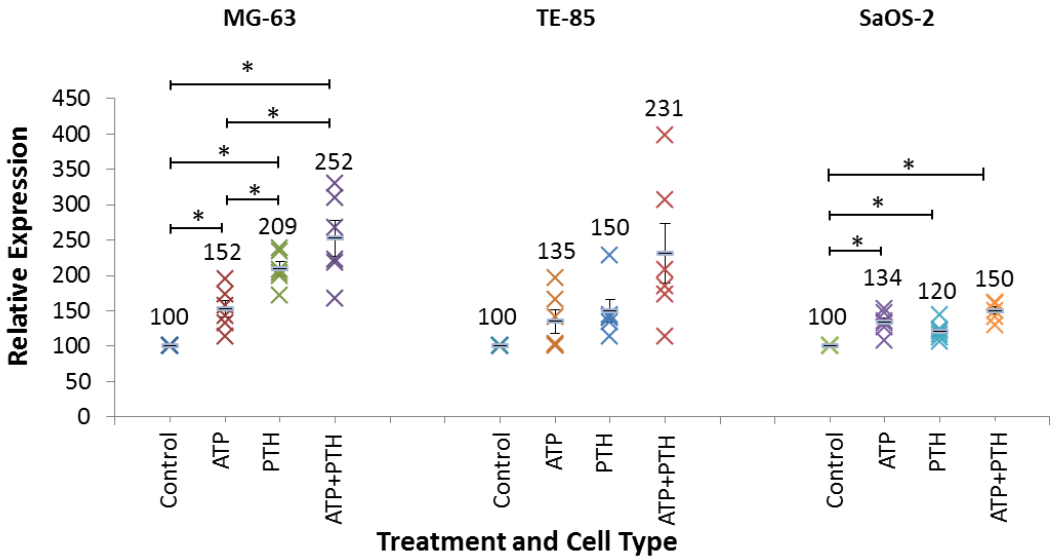


Figure 3.2: Expression of alkaline phosphatase in osteosarcoma cell lines (MG-63, TE-85 and SaOS-2) treated with Adenosine 5'-triphosphate (ATP) and parathyroid hormone (PTH). Data are normalized to β-actin. The values of the mean expression of the gene are shown on top of each plot. Error bars represent standard error of the mean (S.E.M). * indicates significant difference as analysed by One-Way Independent ANOVA and LSD Post-Hoc test, $p<0.05$.

Following treatment by ATP or PTH, the expression of ALP mRNA in all three cell lines was compared. ALP mRNA expression was normalised to the expression of β-actin mRNA. In MG-63, treatment with ATP, PTH and combination of ATP and PTH significantly increased the expression of ALP compared to the control, $p<0.05$. Expression of ALP was significantly higher in MG-63 treated with PTH compared to MG-63 treated with ATP, ($p<0.05$). Combination of ATP and PTH treatment in MG-63 enhanced the expression of ALP significantly compared to control cells and and cells treated with ATP ($p<0.05$). There was no significant difference in the expression of ALP between MG-63 treated with PTH alone and combined ATP-PTH. In TE85 cells however, there was no significant difference of ALP expression throughout the treatments. Interestingly, there were significant increases of ALP

expression in all treatments using SaOS-2 compared to the control ($p<0.05$). SaOS-2 cells treated with ATP and PTH alone equally increased the expression of ALP, $p>0.05$. Meanwhile, the combination of ATP-PTH treatment significantly increased the ALP expression compared to control and PTH, $p<0.05$ but not significantly different compared to ATP.

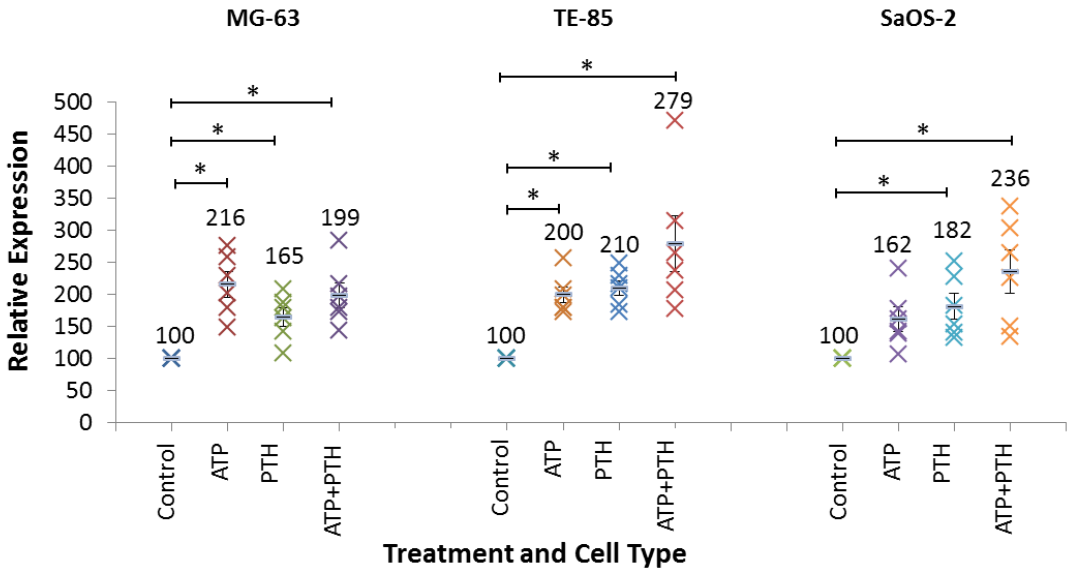


Figure 3.3: Expression of collagen 1a2 in osteosarcoma cell lines (MG-63, TE-85 and SaOS-2) treated with Adenosine 5'-triphosphate (ATP) and parathyroid hormone (PTH). Data are normalized to β-actin. The values of the mean expression of the gene are shown on top of each plot. Error bars represent standard error of the mean (S.E.M). * indicates significant difference as analysed by One-Way Independent ANOVA and LSD Post-Hoc test, $p<0.05$.

The expression of COL1A2 mRNA in MG-63, TE-85 and SaOS-2 cells treated with ATP, PTH and combined ATP-PTH was analysed and compared. Treatments with ATP, PTH and ATP + PTH significantly increased the COL1A2 mRNA in all three cell lines ($p<0.005$) compared to control except in SaOS-2 treated with ATP. However, no significant differences were found between cells treated with ATP + PTH and cells treated with ATP or PTH alone ($p>0.05$). COL1A2 mRNA expression

was normalised to β-actin mRNA expression. Data are presented as mean from 6 biological replicates (n=6). Error bars represent standard error of the mean (S.E.M).

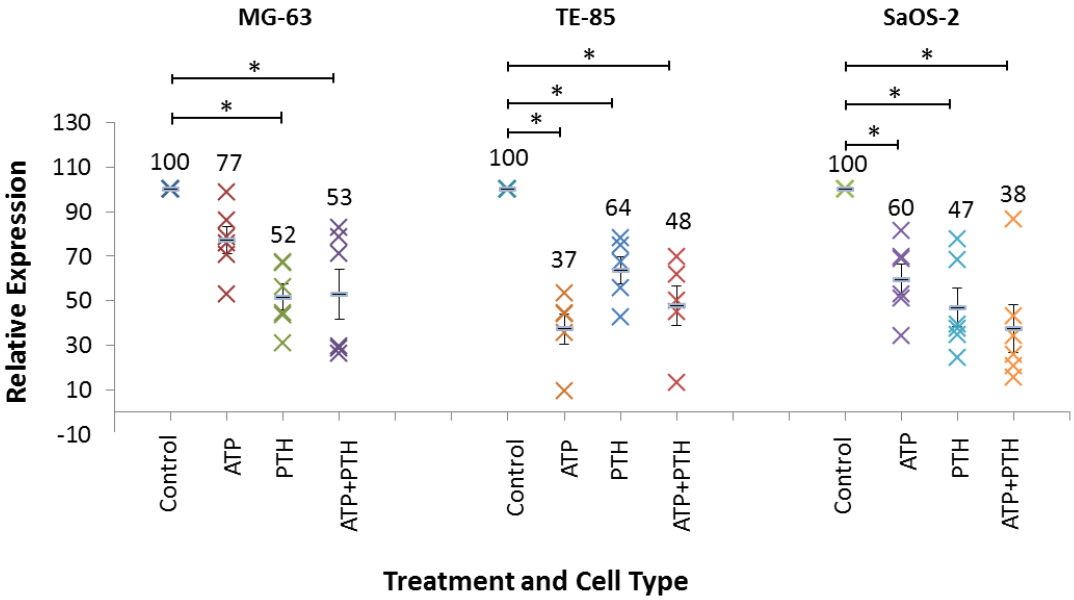


Figure 3.4: Expression of collagen 6a3 in osteosarcoma cell lines (MG-63, TE-85 and SaOS-2) treated with Adenosine 5'-triphosphate (ATP) and parathyroid hormone (PTH). Data are normalized to β-actin. The values of the mean expression of the gene are shown on top of each plot. Error bars represent standard error of the mean (S.E.M). * indicates significant difference as analysed by One-Way Independent ANOVA and LSD Post-Hoc test, $p<0.05$.

COL6A3 mRNA expression in MG-63, TE-85 and SaOS-2 cells treated with ATP, PTH and combined ATP-PTH was analysed and compared using One-Way Independent ANOVA and LSD Post-Hoc test. Data are presented as mean from 6 biological replicates (n=6). A significant decrease in the expression of COL6A3 mRNA in MG-63 was observed following treatment with PTH and combined ATP-PTH ($p<0.005$) compared to control. However, there were no significant difference between MG-63 treated with ATP + PTH and MG-63 treated with ATP or PTH individually ($p>0.05$) which shows combination of ATP and PTH does not enhance

the expression of COL6A3 in MG-63. In TE-85 and SaOS-2 cells, treatment with ATP, PTH and combined ATP-PTH decreased COL6A3 mRNA expression significantly ($p<0.005$) significantly. However, there was no significant difference in COL6A3 expression in TE-85 or SaOS-2 cells when treatment was with combined agonists compared to individual treatment ($p>0.05$).

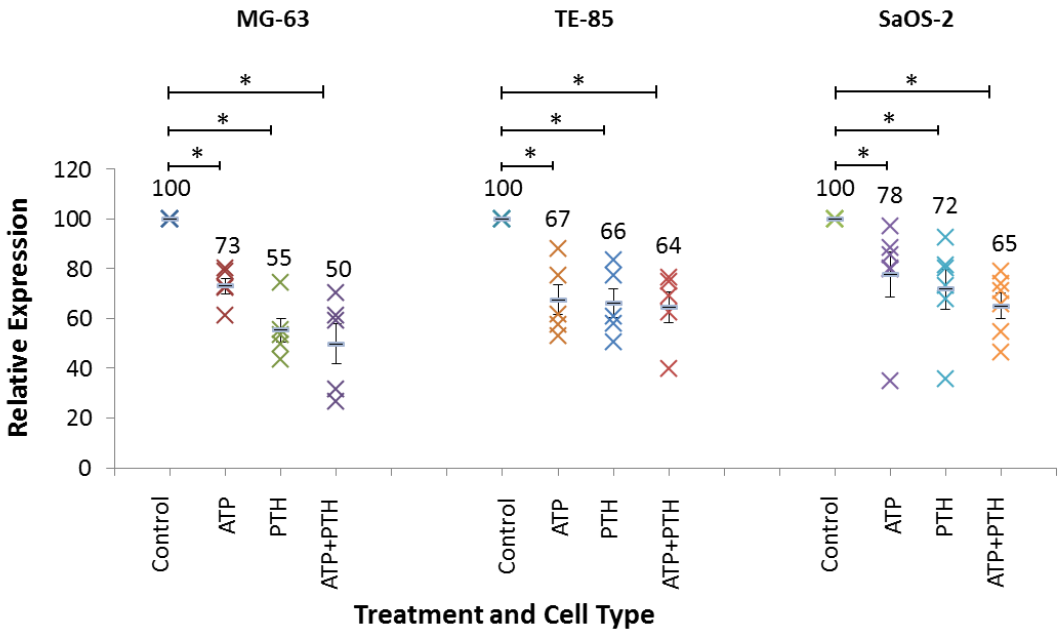


Figure 3.5: Expression of osteoprotegerin in osteosarcoma cell lines (MG-63, TE-85 and SaOS-2 cells) treated with Adenosine 5'-triphosphate (ATP) and parathyroid hormone (PTH). Data are normalized to β-actin. The values of the mean expression of the gene are shown on top of each plot. Error bars represent standard error of the mean (S.E.M). * indicates significant difference as analysed by One-Way Independent ANOVA and LSD Post-Hoc test, $p<0.05$.

The expression of OPG mRNA in all three cell lines was compared and analysed. Data are presented as mean from 5-6 biological replicates (n=5/6) ± standard error of the mean (S.E.M). Treatments with ATP, PTH and combined ATP-PTH significantly decreased OPG mRNA expressions in MG-63, TE-85 and SaOS-2 ($p<0.05$) compared to control. Further statistical tests revealed that there was no significant difference of OPG mRNA expression between cell lines treated with individual nucleotides compared to combined ATP and PTH ($p>0.05$).

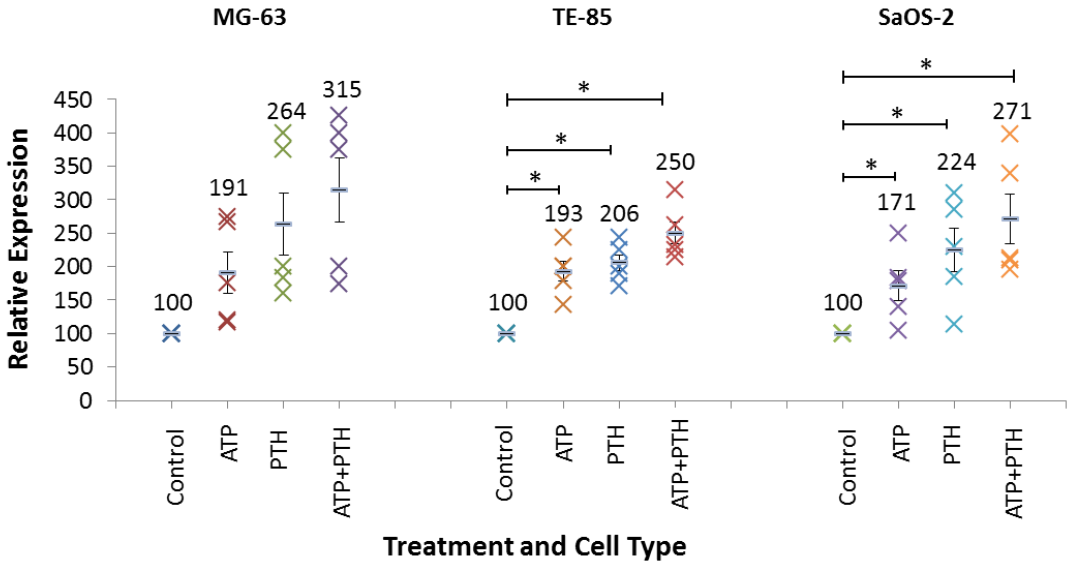


Figure 3.6: Expression of osterix in osteosarcoma cell lines (MG-63, TE-85 and SaOS-2) treated with Adenosine 5'-triphosphate (ATP) and parathyroid hormone (PTH). Data are normalized to β-actin. The values of the mean expression of the gene are shown on top of each plot. Error bars represent standard error of the mean (S.E.M). * indicates significant different as analysed by One-Way Independent ANOVA and LSD Post-Hoc test, $p<0.05$.

The expression of OSX mRNA in all three cell lines was compared. Data are presented as mean from 5-6 biological replicates (n=5/6) ± standard error of the mean (S.E.M). Treatment with ATP, PTH and ATP-PTH combined significantly increased the expression of OSX mRNA in TE-85 and SaOS-2 cells ($p<0.05$) compared to control. There was no significant increase of OSX expression in MG-63 observed throughout the treatments. Further statistical tests revealed that there were no significant difference in OSX mRNA expression in any cell line treated with individual nucleotides compared to combined ($p>0.05$).

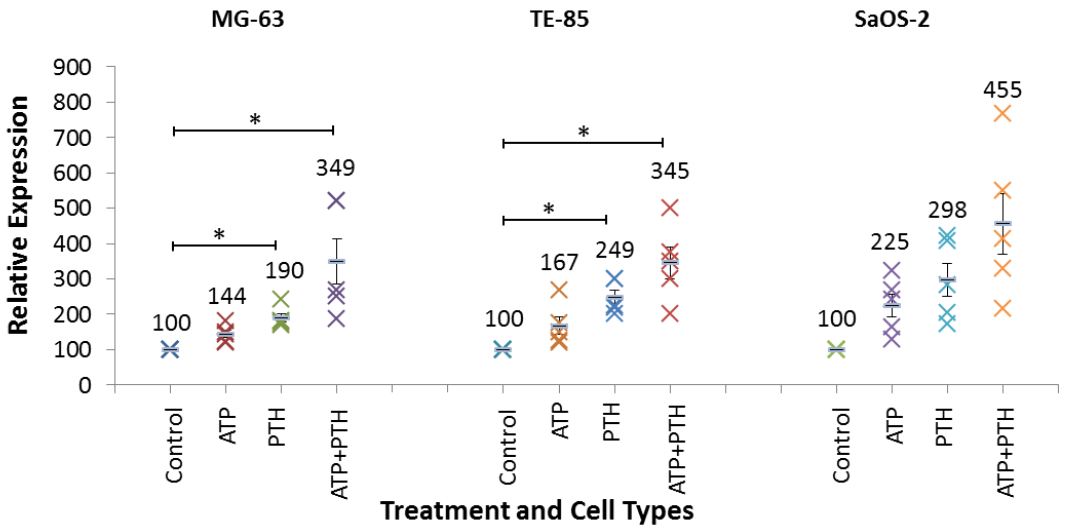


Figure 3.7: Expression of RANKL in osteosarcoma cell lines (MG-63, TE-85 and SaOS-2) treated with Adenosine 5'-triphosphate (ATP) and parathyroid hormone (PTH). Data are normalized to β-actin. The values of the mean expression of the gene are shown on top of each plot. Error bars represent standard error of the mean (S.E.M). * indicates significant difference as analysed by One-Way Independent ANOVA and LSD Post-Hoc test, $p<0.05$.

Prior to and following treatment with ATP and PTH, the expression of RANKL mRNA in all three cell lines was compared. In all cell lines, treatment with ATP, PTH and ATP-PTH combined increased the expression of RANKL mRNA. However, the significant increase of RANKL mRNA expression compared to control was only observed in MG-63 and TE-85 treated with PTH and the combination of ATP-PTH ($p<0.05$). In TE-85 cells there was no significant difference in the expression of RANKL mRNA between cells treated with ATP or PTH ($p>0.05$) and between cells treated with PTH and ATP-PTH combined ($p>0.05$). However, RANKL mRNA expression was significantly higher in TE-85 treated with combined ATP-PTH compared to TE-85 treated with ATP alone ($p<0.05$). Meanwhile no significant difference was observed in SaOS-2 cells treated with ATP, PTH or ATP-PTH ($p>0.05$). Data are presented as mean from 5 biological replicates (n=5) ± SE.

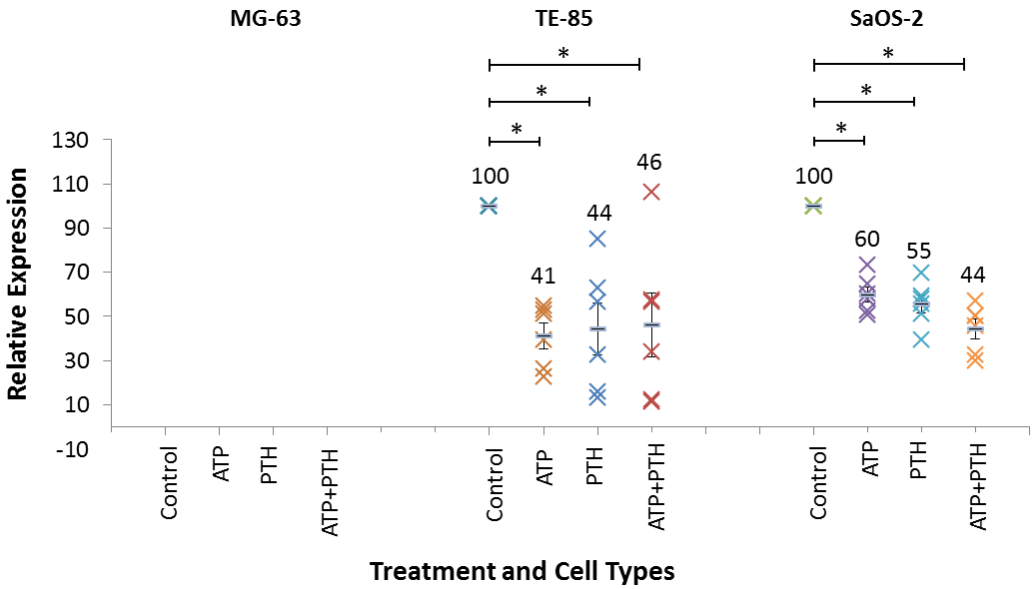


Figure 3.8: Expression of sclerostin in osteosarcoma cell lines (MG-63, TE-85 and SaOS-2) treated with Adenosine 5'-triphosphate (ATP) and parathyroid hormone (PTH). Data are normalized to β-actin. The values of the mean expression of the gene are shown on top of each plot. Error bars represent standard error of the mean (S.E.M). * indicates significant difference as analysed by One-Way Independent ANOVA and LSD Post-Hoc test, $p<0.05$.

SOST mRNA expression in TE-85 and SaOS-2 cells treated with ATP, PTH and ATP-PTH combined was analysed and compared. Data are presented as mean from 6 biological replicates (n=6). SOST mRNA expression was not detected in MG-63 cells. A significant decrease was observed in the expression of SOST mRNA in both TE-85 and SaOS-2 cells treated with ATP, PTH and combined ATP-PTH ($p<0.05$) compared to control. However, there was no significant difference in SOST mRNA expression in TE-85 and SaOS-2 cells across all treatments ($p>0.05$). There were no significant differences in SOST mRNA expression between cells treated with ATP or PTH ($p>0.05$) and between cells treated with PTH and ATP-PTH combined ($p>0.05$).

## 3.4 Discussion

In the first part of this chapter, we studied the expression of seven bone markers in three human osteosarcoma cell lines and primary osteoblast. The selected bone markers are ALP, COL1A2, COL6A3, OPG, OSX, RANKL and SOST. We selected MG-63, TE-85 and SaOS-2 cells because these cells represent different stages of osteoblast differentiation: MG-63 the least differentiated, TE-85 representing the intermediate stage and SaOS-2 as the most differentiated or matured osteoblast (Pacheco-Pantoja, *et al*., 2011). The use of these cell lines has enabled us to study the expression of proteins participating in the osteoblastic differentiation process which is crucial for normal cell development, growth and survival.

ALP has been used as a bone formation marker by many researchers due to the ease of its measurement and its potential for use as an indicator of risk of fracture and other bone complications related to disorders of bone metabolism (Havill *et al*., 2006). Osteoblasts secrete bone ALP, a non-collagenous protein which is crucial for bone mineralisation. High concentrations of ALP have been detected in menopausal women experiencing high bone turnover (Mukaiyama *et al.*, 2015) and in osteoporosis, Paget's disease and osteomalacia patients (Gomez *et al.*, 1995). In this current study, we found that the expression of ALP mRNA differed significantly between cell lines. One interesting finding was the large difference in its expression in SaOS-2 cells compared to MG-63 and TE-85 cells. This result may be explained by the fact that SaOS-2 cells represent the most differentiated and mature osteoblasts, in comparison to MG-63 and TE-85 cells. The same observation, that is, the lowest level of ALP mRNA detected at the onset of the osteoblastic differentiation in bone marrow stromal cells (BMSC) and higher concentrations at the later stages have been reported previously (Prins *et al.*, 2014).

Type 1 collagen is the most common and abundant of the collagen family of proteins. COL1A2 is especially known to be expressed abundantly in bone as the main component of the matrix. Any mutation that affects COL1A2 expression may result in genetic bone disorders such as osteogenesis imperfecta which affects bone strength (Dalgleish, 1997). It has been shown that type 1 collagens are expressed at all stages during development by osteoblastic cells (Kem *et al*., 2001). In this current study, we found that COL1A2 mRNA was expressed in all three cell lines. However, the highest expression was detected in MG-63 cells, which represent the early stage of osteoblastic differentiation, at 4.6 times higher than detected in SaOS-2 cells, the most differentiated osteoblast. This result suggests that COL1A2 mRNA expression decreases as osteoblasts differentiate further into a more mature form. Other studies have observed the same situation during *in vitro* osteogenic induction of BMSCs. After 12 days, induced BMSCs differentiated into mineralized osteoblasts and subsequently expressed very low levels of COL1A2 (Guo *et al.*, 2016).

A study in 2014 reported that COL6A3-silencing induced the expression of Sfrp2 (secreted Frizzled-related protein 2), an antagonist of Wnt signalling which efficiently suppresses 3D growth in cultured cells. This indicates that COL6A3 plays an important role in bone formation by favouring Wnt signalling (Martianov *et al.*, 2014). However, the expression pattern of COL6A3 in developing bone matrix is still not very well understood. Our findings suggest that the expression of COL6A3 mRNA was highest in MG-63 cells and decreased as the cells became more differentiated. The lowest levels of COL6A3 mRNA expression were detected in TE-85 cells. This result corroborates the finding by the other researcher in our laboratory that COL6A3 stabilises the extracellular matrix during bone development by providing the initial scaffolding at an early stage of osteoblastic differentiation upon which mineralization takes place (unpublished data).

OPG is a protein known to regulate osteoclastogenesis by inhibition of both the function and differentiation of osteoclasts (Yamaguchi, 2009). In this study, we found that the expression pattern of OPG mRNA is quite similar to COL1A2 and COL6A3, where the highest expression levels were detected in MG-63 cells. These results suggest that osteoblasts at the early stage of differentiation inhibit osteoclastogenesis via OPG. This finding however is inconsistent with previous reported study which investigated whether osteoclastogenesis depends on the stage of osteoblastic differentiation. The study reported an increase of OPG mRNA expression in murine primary osteoblast cultures after the onset of mineralization. High expression of OPG at the later stage of osteoblastic differentiation caused the mature osteoblast to have relatively decreased osteoclastogenic activity (Thomas *et al*., 2001).

OSX mRNA and RANKL mRNA were expressed at significantly higher concentrations in SaOS-2 cells compared to MG-63 or TE-85 cells, in which expression levels were very similar. OSX is an essential transcription factor for osteoblastic differentiation (Cao *et al.*, 2005) while RANKL is essential for osteoclastogenesis (Atkins *et al.*, 2003). However, the expression patterns of OSX and RANKL at different stages of osteoblastic differentiation in human osteosarcoma cell lines have not been reported. Here, we found that OSX and RANKL mRNAs were expressed at higher levels in SaOS-2 which represent the most matured osteoblastic cell. A similar observation was reported in mice where OSX and RUNX2 were reported to independently regulate osteoblastic differentiation at a later stage (Yoshida *et al.*, 2012). A further study showed that OSX and RUNX2 could activate the expression of SOST in a co-ordinated manner *in vitro* (Perez-Campo *et al.*, 2016).

SOST is a locally-derived inhibitor of bone formation which signals through the Wnt pathway and thought to be a major regulator of bone modelling and remodelling (Moyses & Schiavi, 2015). Consequently, there was much interest in SOST as a potential therapeutic target for bone disorders. Our result indicates that the SOST mRNA expression profile in the three cells lines was consistent with their reported differentiation status. SaOS-2 cells had the highest expression, 5.75 fold higher than that in TE-85 cells. Interestingly, SOST mRNA expression was barely detectable in MG-63 cells (Fig. 3.7). This result reinforces previous reports on the relative differentiation status of these commonly used osteoblastic cell models. The robust expression patterns of these bone markers suggest that these cell types do indeed represent different stages of the osteoblast / osteocyte lineage and reinforce their utility in investigating osteoblast biology.

In the second part of this chapter, we measured the mRNA expression of seven selected bone markers: ALP, COL1A2, COL6A3, OPG, OSX, RANKL and SOST, with and without ATP and PTH treatments in the three human osteosarcoma cell lines: MG-63, TE-85 and SaOS-2 cells. Each cell line was treated with ATP, PTH and ATP + PTH for 48 hours before cells were harvested for analysis.

The results of this study indicate that ATP and PTH increase the mRNA expression of ALP, COL1A2, OSX and RANKL in all cell lines. Interestingly, the individual treatment with ATP or PTH equally increased the mRNA expression of ALP, COL1A2, OSX and RANKL with no significant difference between cell lines except for ALP mRNA expression in MG-63 cells. MG-63 cells treated with PTH expressed significantly more ALP mRNA compared to treatment with ATP. The largest increase in ALP mRNA expression was observed with the combined treatment with ATP and PTH, although the increase was not significantly higher than in TE-85 cells treated only with ATP or PTH. The ability of PTH to increase ALP expression also

has been reported in early differentiating MC3TE-E1 mice cells (Rey *et al*., 2007). Similar expression profile was observed for COL1A2 and OSX mRNA in all cell lines, where combined treatment with the nucleotide agonists induced expression that was not significantly different from cells treated with individual agonists. A published study reported that HOBIT cells that were treated with 100 μM of ATP showed a significant increase of COL1A2 gene expression (Pines *et al*., 2003). Same result has been observed in a study using primary rat osteoblast which showed that OSX mRNA expression increased significantly 12 hours after treated with 500 nM of PTH (Wang *et al*., 2006). Slightly different results were observed in RANKL mRNA expression. Combined ATP and PTH treatment on MG-63 cells induced significantly higher expression of RANKL mRNA compared with treatment with individual agonists. However, RANKL mRNA expression was similar in SaOS-2 cells regardless the treatment given. The same effect of PTH treatments on RANKL mRNA expression has been reported in an *in Vivo* study using rat. This study reported that PTH treatment increased RANKL mRNA expression as much as 27 folds as early as 1 hour after treatment (Ma *et al*., 2001).

The inhibitory effect of ATP and PTH was observed on the mRNA expression of COL6A3, OPG and SOST genes (Fig. 3.4, Fig. 3.5 and Fig. 3.8 respectively). MG-63, TE-85 and SaOS-2 cells treated with ATP, PTH and the combination of ATP and PTH showed a significant decrease in the mRNA expression of COL6A3, OPG and SOST. The combination of ATP + PTH treatment did not induce any further significant reduction in COL6A3, OPG or SOST mRNA expression across the cell lines except for COL6A3 mRNA expression in MG-63 and SOST mRNA expression in SaOS-2 cells. The effect of ATP and PTH treatment in this study is consistent with the previous study which reported that PTH treatment dramatically reduces the expression of SOST mRNA and sclerostin protein in primary cultures of neonatal murine calvaria and osteocytic MLO-A5 cells (Bellido *et al*., 2005). PTH also has

been shown to inhibit OPG expression by 40% when treated with 0.1 ng/ml of PTH in murine bone marrow cultures. Complete inhibition of OPG was observed when the same cells were treated with 1 ng/ml of PTH (Lee and Lorenzo, 1999). The results of this investigation indicate that ATP and PTH increase ALP, COL1A2, OSX and RANKL mRNA gene expression and inhibit the mRNA expression of COL6A3, OPG and SOST at all stages of osteoblast differentiation.

OPG and RANKL are two critical proteins for osteoclastogenesis. RANKL induces osteoclastogenesis by binding to its receptor on the surface of osteoclast precursors. On the other hand, OPG inhibits excessive bone resorption by inhibiting osteoclast formation by blocking the binding of RANKL to its receptor (Thomas, *et al*., 2001). This finding suggest that ATP and PTH control bone resorption by increasing RANKL mRNA expression and inhibiting OPG mRNA expression at all stages of osteoblastic differentiation. ATP and PTH also play a role in inhibition of bone formation by inhibiting COL6A3 mRNA expression, a protein which creates a scaffold for bone mineralisation.

ATP and PTH also favour bone formation by increasing concentrations of proteins that are essential for new bone formation, such as ALP and COL1A2 and supressing SOST (Cutarelli *et al*., 2016; Keller and Kneissel, 2005; Pines *et al*., 2013). ALP is a protein secreted by osteoblasts which is crucial for bone mineralisation while COL1A2 is the main component of bone matrix. Higher OSX expression contributes to a higher rate of bone formation because OSX is an important transcription factor for osteoblast differentiation. This study has shown that ATP and PTH are directly involved in the regulation of proteins that are crucial for bone development. This could support the notions that they are involved in bone remodelling at all stages of osteoblastic differentiation. As ATP can be released by osteoblasts through mechanical stimulation, it would be interesting to investigate

techniques that could be used to control ATP production by osteoblasts. Identification of the factors which regulate ATP and PTH levels may also contribute to the development of new therapeutic approaches to prevent bone loss.

## 3.5 Conclusions

From the results in this chapter, we conclude that:

- ALP, OSX, RANKL and SOST mRNAs were expressed highest in SaOS-2 cells while COL1A2, COL6A3 and OPG mRNAs were expressed highest in MG-63cells;
- SOST mRNA was not detected in MG-63 cells. This is consistent with the fact that SOST is only produced by matured osteoblast;
- The effects of ATP and PTH treatment on the expression of bone markers were consistent between cell lines;
- MG-63, TE85, and SaOS-2 cells were shown to be good models to study osteoblastic cells as they express specific proteins and react to ATP or PTH treatments in a similar way to primary osteoblast.

# CHAPTER 4:

# DIFFERENTIAL EXPRESSION OF miRNAs IN HUMAN OSTEOBLASTIC CELLS

## 4.1 Introduction

As described in Chapter 1, microRNAs (miRNAs) are endogenously expressed small non-coding RNA molecules that have been demonstrated to play important roles in the post-transcriptional regulation of gene expression. To summarise, miRNAs are transcribed as a long RNA precursor known as pri-miRNA which is then cleaved to pre-miRNA. Pre-miRNA is then further processed into mature and functional miRNA that targets complementary mRNA. Mature miRNAs regulate protein translation and mRNA cleavage by binding to specific sites within the 3'-end region and rarely the 5′-end of the mRNA (Gulyaeva & Kushlinskiy, 2016; Lytle *et al.*, 2007). MiRNAs have been linked to numerous biological processes including cellular proliferation, differentiation and apoptosis. Over the past decade, studies have assessed the expression of miRNA in samples from healthy and diseased humans and demonstrated that various health issues, especially cancer (Schulte *et al.*, 2010) were the result of variation in normal gene expression as a result of changes in the expression of miRNAs. These findings revealed that the miRNA expression profile can provide an important tool for better understanding, in addition to normal cell physiology, the aetiology and potential treatment options of numerous diseases.

We aim to understand the involvement of miRNAs at different stages of osteoblastic differentiation. In bone biology, numerous miRNAs have been predicted and described as key factors for bone modelling and remodelling. To date, studies of miRNAs as regulators of bone development and miRNA as a treatment option for bone-related diseases are still scarce. In this chapter, we assessed the miRNA expression profile in normal primary human osteoblasts and three osteosarcoma cell lines which represent different stages of osteoblastic differentiation: MG-63 represents the earliest stage of osteoblast differentiation; TE-85 an intermediate stage and SaOS-2 the most differentiated or matured osteoblast. We compared

miRNA expression profiles by microarray in these cells using cluster analysis to identify differentially expressed miRNAs. Identification of miRNAs expressed differentially across these four cell lines and variations in expression patterns may give insights into the next step of finding the miRNA candidates for tackling issues affecting healthy bone maintenance and development.

## 4.2 Brief methods

### 4.2.1 Extraction of miRNA

Total RNA (including miRNA) was extracted using an miRNeasy Mini Kit (Qiagen, Catalog No. 217004) according to the protocol provided by the manufacturer.

### 4.2.2 MiRNA analysis of total RNA

Total purified RNA samples (free from genomic DNA) were sent for Affymetrix miRNA profiling using an Affymetrix GeneChip miRNA 4.0. CEL files were generated using Affymetrix GeneChip Command Console Software. Expression Console software was used for quality control of array performance. Transcriptome Analysis Console v2 (Affymetrix) was used to analyse miRNA differential expression between cell types. Detailed methods are provided in Section 2.3.2. The estimated log2 fold change (logFC) for the 6 contrasts were tested in limma using a t-test. P-values associated with logFC were adjusted for multiple testing using the False Discovery Rate (FDR) approach (Benjamini and Hochberg, 1995). Significantly differentially expressed (DE) miRNAs were defined as those with an FDR-adjusted P-value < 5%.

## 4.3 Results

Below are the results of miRNAs expression comparisons between two osteoblastic cells.

Table 4.1: Number of differentially expressed (DE) miRNA types.

| | **MG-63 vs HOB** | **MG-63 vs TE-85** | **MG-63 vs SaOS-2** | **TE-85 vs SaOS-2** | **TE-85 vs HOB** | **SaOS-2 vs HOB** |
|---|---|---|---|---|---|---|
| **DE: all** | 210 | 132 | 92 | 132 | 314 | 215 |
| **DE: up-regulated** | 174 | 51 | 49 | 76 | 263 | 174 |
| **DE: down-regulated** | 36 | 81 | 43 | 56 | 51 | 41 |

Table 4.1 shows the number of differentially expressed miRNAs in different bone cell types. Significant differential expression was defined as comparisons with a false discovery rate (FDR)-adjusted *p*-value < 0.05 and miRNA expression fold change of at least 2 fold. The highest number of differentially expressed miRNAs was observed between TE-85 and HOB with 314 miRNAs.

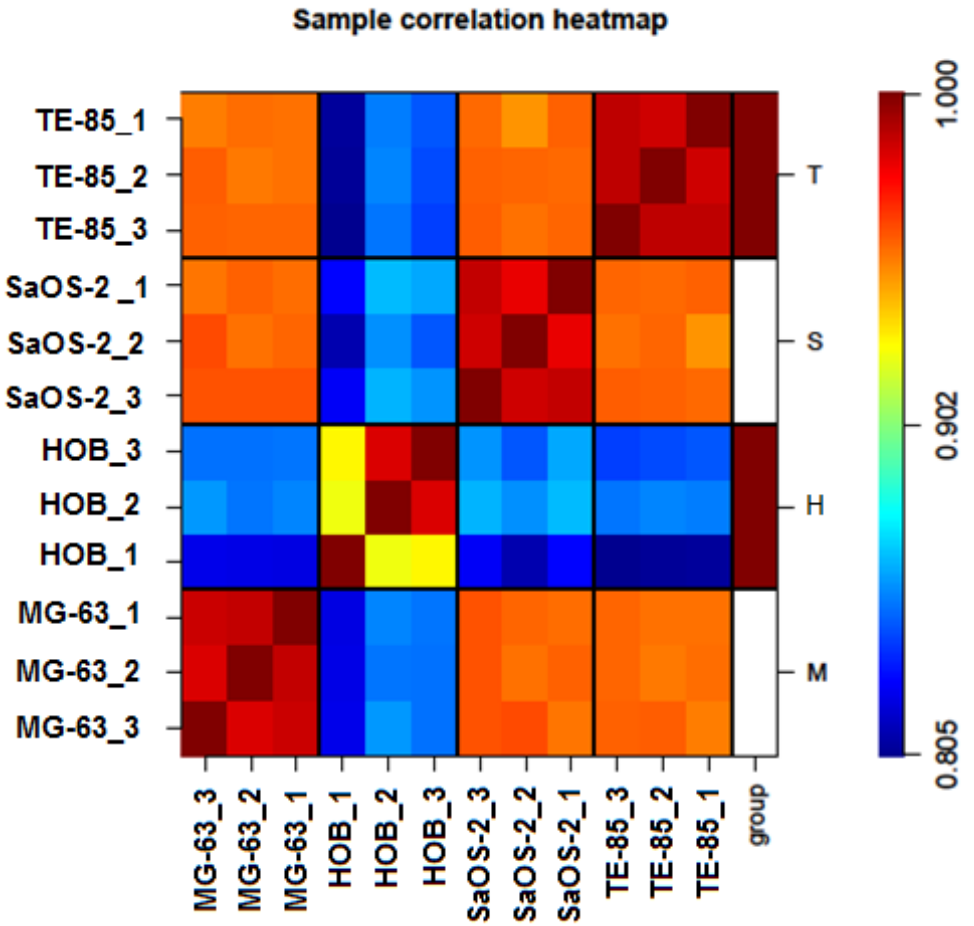


Figure 4.1: Correlation heatmap of miRNA expression in all 12 cell varieties and repeats, displaying comparative levels of miRNA expression between samples.

Figure 4.1 shows correlated total miRNA expression levels between the 4 different cell types (MG-63, TE-85, SaOS-2 and HOB) and 3 repeats over 12 arrays. There was stronger correlation between samples from the same group than between samples from different groups. This implies that the variation between groups is stronger than the technical variation or variation within the group.

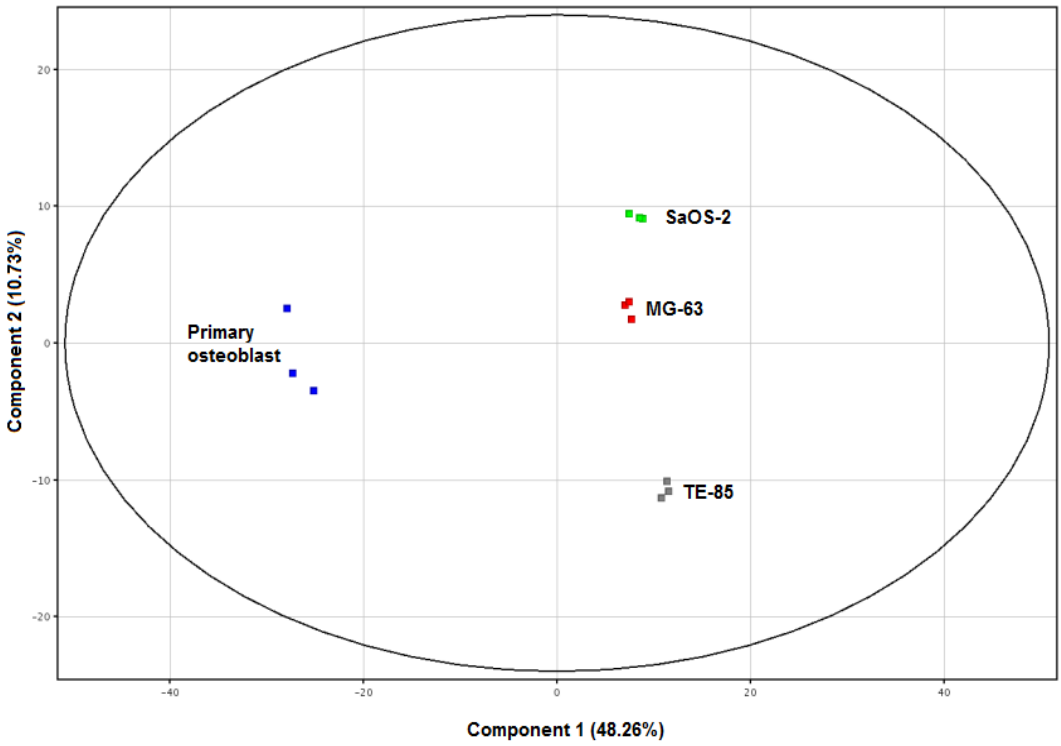


Figure 4.2: Principal Components Analysis plot of miRNA expression. PCA plot shows clear demonstration that samples from the same groups are tightly cluster together. Component 1 differentiates the cell lines from the primary cell and component 2 differentiates the cell lines from each other.

By performing principal components analysis (PCA) of these data a very clear demonstration arises that samples from the same group tightly cluster together (Fig. 4.2), and supports the finding that the difference between groups is much larger than that within any group. Thus, some miRNA molecules can be expected to be differentially expressed by different cell types.

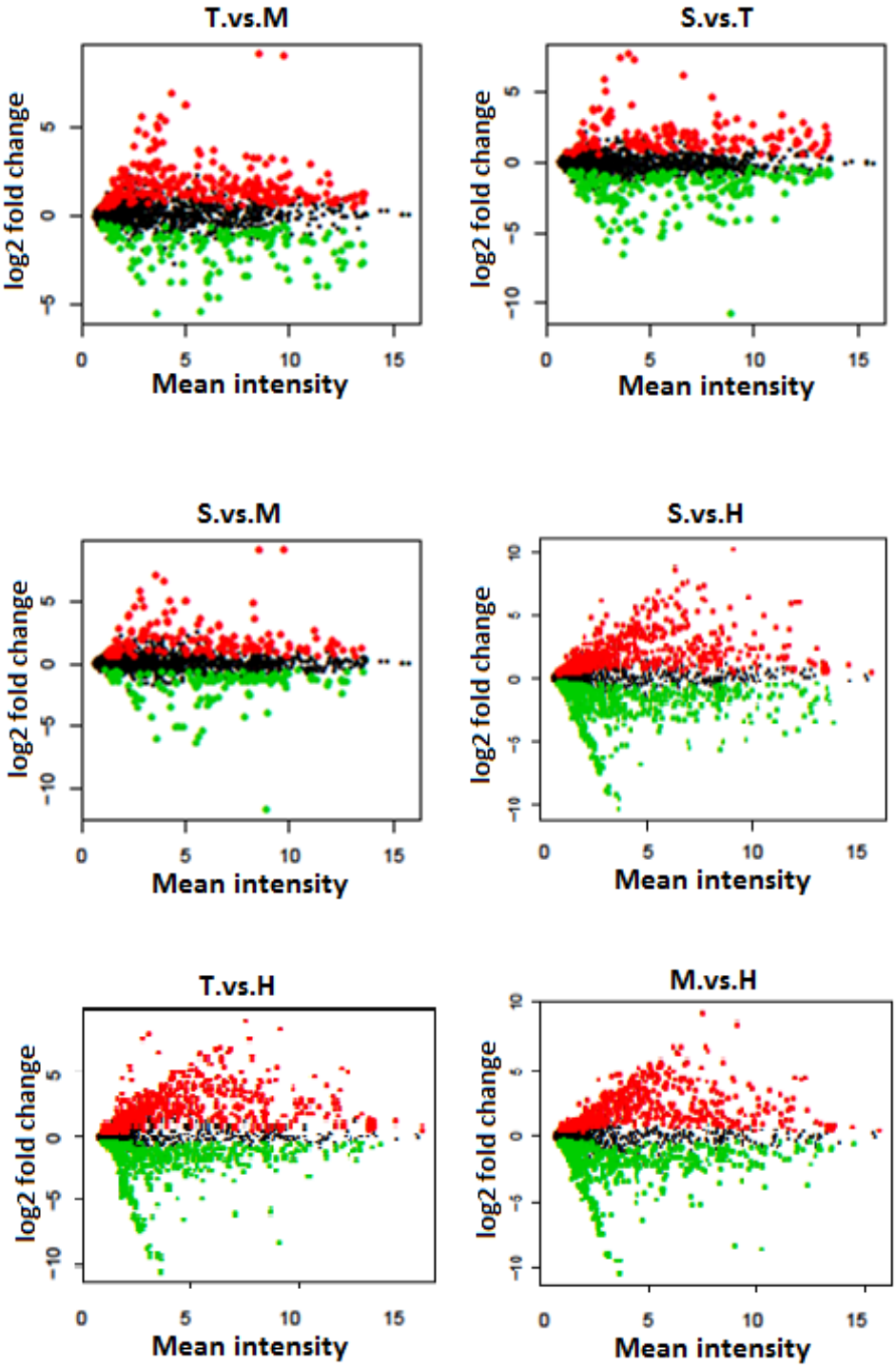


Figure 4.3: Visualisation of upregulation (red) or downregulation (green) of raw miRNA expression data (MA plots) of the six combinations of TE-85 (T), MG-63 (M), SaOS-2 (S) and HOBs (H) for *Homo sapiens* probe sets.

We analysed the comparative expression of each human miRNA across each cell type and repeat (Fig. 4.4), in which each line represents a single miRNA, the expression of which is compared across each sample in a heatmap, the colour

scale illustrating the relative expression level of an miRNA in a specific slide where red represents high relative expression and green low relative expression, and so each column therefore represents a single repeat for a distinct cell line. The miRNA-clustering tree is shown on the right and the cell line-clustering tree at the top, clustering together the most similar results.

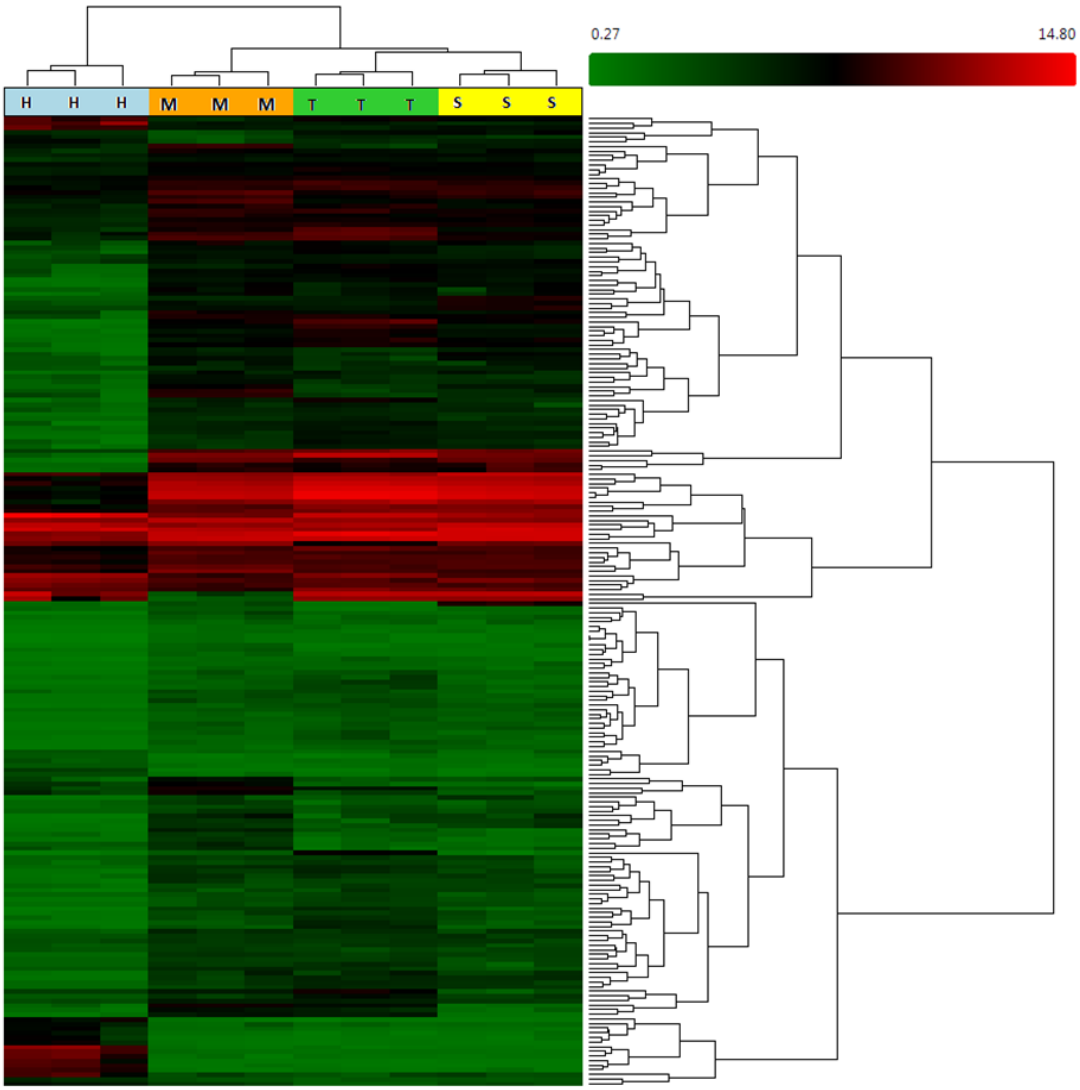


Figure 4.4: Hierarchical clustering showing all 210 differentially expressed miRNA levels between MG-63 (M) and primary human osteoblasts, HOBs (H). The expression of these same miRNAs in TE-85 (T) and SaOS-2 (S) are also included.

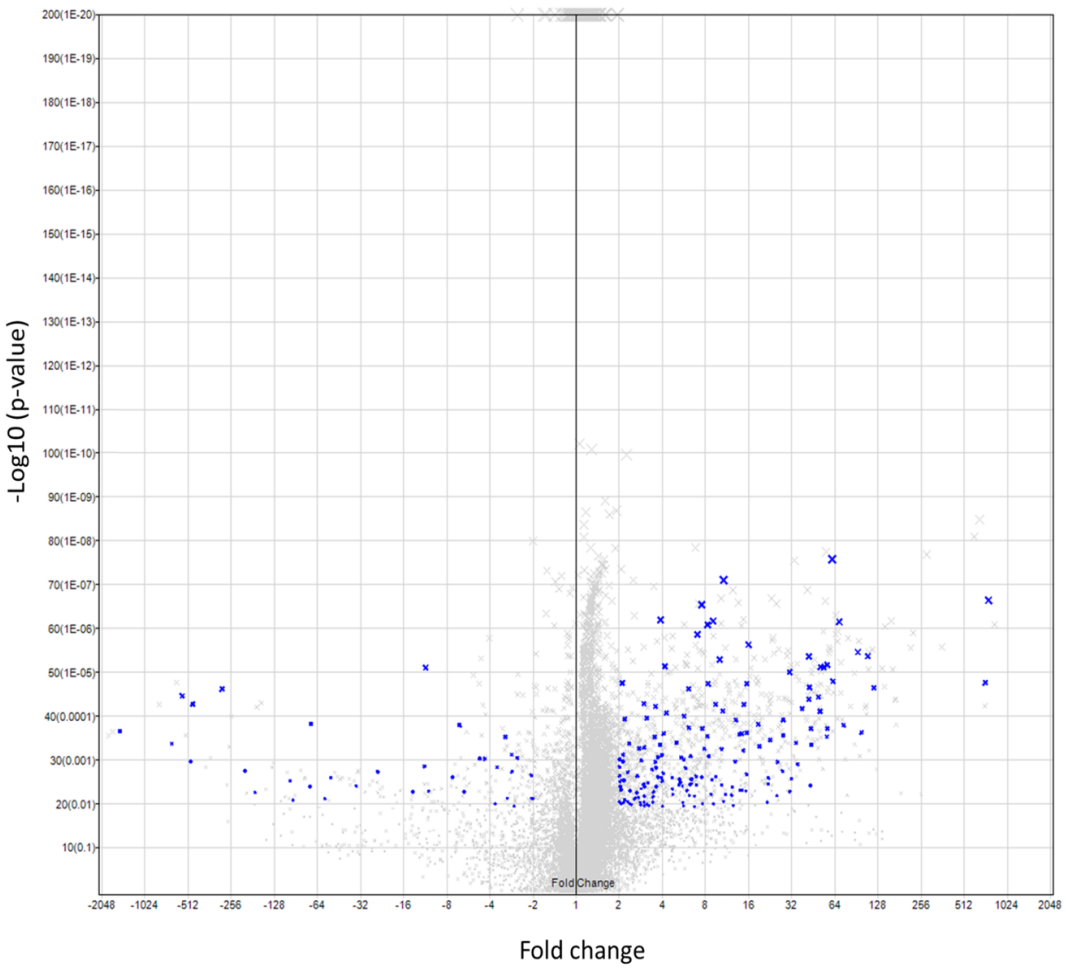


Figure 4.5: Volcano plot of the differential expression of miRNAs between MG-63 and primary human osteoblasts, HOBs. Change in expression is plotted on the x-axis, log (significance) on y-axis. Blue dots represent human miRNAs which are greater than 2 fold different and whose difference is statistically significant ($p$<0.05).

The volcano plot shows that 210 miRNAs show statistically significant difference ($p$ < 0.05) with at least 2 fold changes between the two groups and are highlighted in blue. The grey data points are either not significant, are expressed at a rate less than twice, or more than half, that of the comparative cell line.

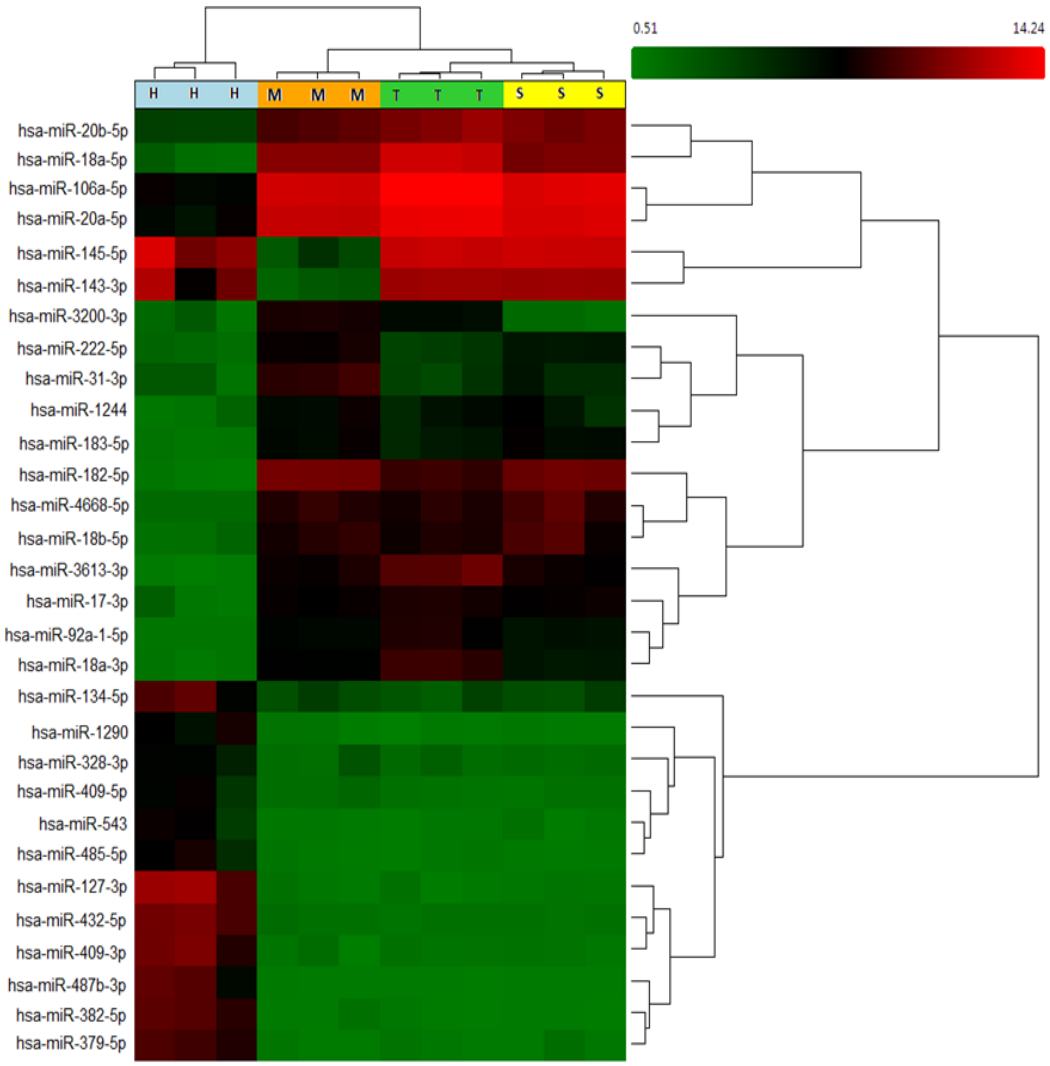


Figure 4.6: Heat map and hierarchical clustering of the 30 miRNAs with the biggest fold difference between MG-63 (M) and HOB (H) cells. The expression of these same miRNAs in TE-85 (T) and SaOS-2 (S) are also included.

Figure 4.6 shows a heat map diagram representing the clustering of the 30 miRNAs with the largest fold difference between MG-63 cells and HOBs, and in Table 4.2. Each row represents a single miRNA and each column represents a cell line. The miRNA-clustering tree is shown on the right and the cell line-clustering tree is shown at the top. The colour scale illustrates the relative expression level. Red represents a high relative expression level and a green a low relative expression.

Table 4.2: 30 miRNAs with the greatest differential expression between MG-63 and HOBs.

| Transcript ID (Array Design) | Fold Change (linear) (MG-63 vs. HOB) | FDR p-value (MG-63 vs. HOB) |
|---|---|---|
| hsa-miR-182-5p | 754.62 | 0.000023 |
| hsa-miR-18a-5p | 717.97 | 0.000606 |
| hsa-miR-3613-3p | 119.46 | 0.000740 |
| hsa-miR-18b-5p | 108.29 | 0.000194 |
| hsa-miR-17-3p | 98.43 | 0.004299 |
| hsa-miR-4668-5p | 92.60 | 0.000172 |
| hsa-miR-3200-3p | 73.42 | 0.003241 |
| hsa-miR-18a-3p | 68.80 | 0.000057 |
| hsa-miR-183-5p | 61.99 | 0.000569 |
| hsa-miR-92a-1-5p | 61.04 | 0.000003 |
| hsa-miR-1244 | 56.68 | 0.003722 |
| hsa-miR-222-5p | 56.52 | 0.000285 |
| hsa-miR-31-3p | 56.23 | 0.004969 |
| hsa-miR-106a-5p | 53.40 | 0.000312 |
| hsa-miR-20b-5p | 50.95 | 0.000308 |
| hsa-miR-20a-5p | 50.38 | 0.001856 |
| hsa-miR-328-3p | -51.58 | 0.020834 |
| hsa-miR-409-5p | -56.85 | 0.038952 |
| hsa-miR-1290 | -71.09 | 0.003074 |
| hsa-miR-134-5p | -72.06 | 0.027496 |
| hsa-miR-543 | -95.24 | 0.040835 |
| hsa-miR-485-5p | -99.44 | 0.022798 |
| hsa-miR-143-3p | -174.64 | 0.031891 |
| hsa-miR-145-5p | -204.85 | 0.017295 |
| hsa-miR-379-5p | -296.10 | 0.000768 |
| hsa-miR-382-5p | -475.46 | 0.001411 |
| hsa-miR-487b-3p | -491.07 | 0.012562 |
| hsa-miR-432-5p | -562.10 | 0.001010 |
| hsa-miR-409-3p | -665.64 | 0.006532 |
| hsa-miR-127-3p | -1534.58 | 0.004035 |

A heat map diagram showing the hierarchical clustering results from all 132 differentially expressed miRNA between MG-63 (M) and TE-85 (T) is shown in Fig 4.7, whilst a volcano plot shows the distribution of significantly different expression which is greater than double, or less than half, the expression of the comparative cell type (Fig 4.8)

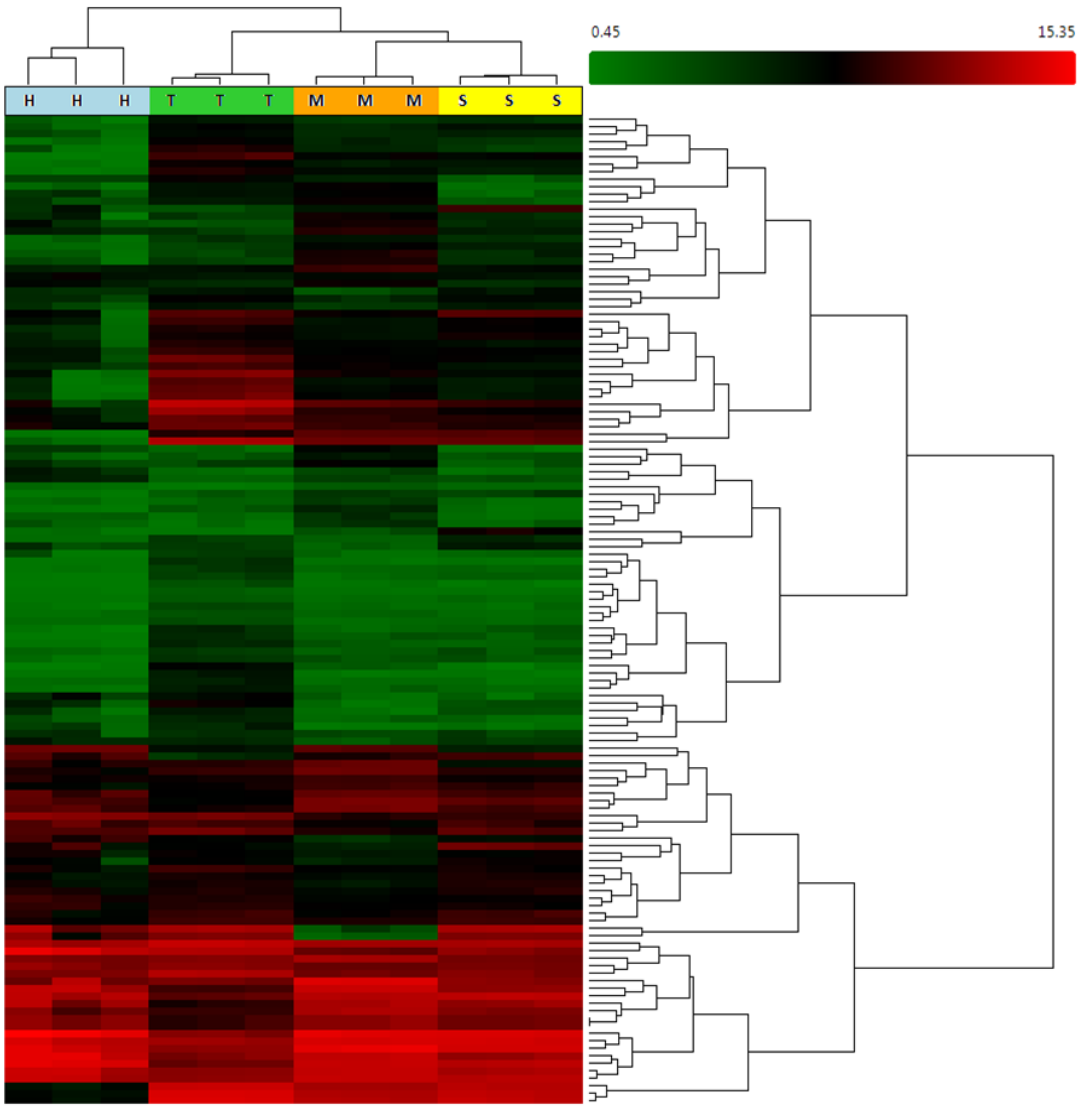


Figure 4.7: Hierarchical clustering of all 132 differentially expressed miRNAs between MG-63 (M) and TE-85 (T). The expression of these same miRNAs in SaOS-2 (S) and HOBs (H) are also included.

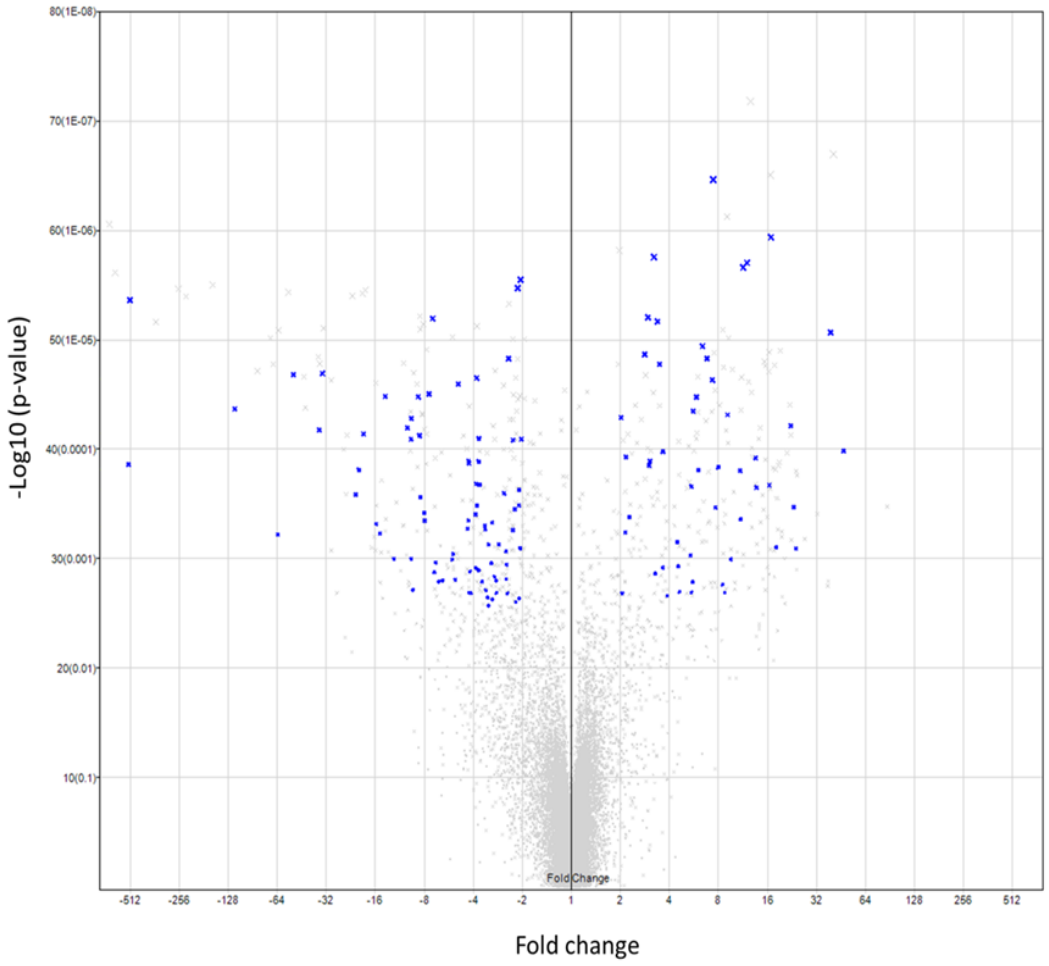


Figure 4.8: Volcano plot of the differential expression of miRNAs between MG-63 and TE-85 cells. Change in expression is plotted on the x-axis, log (significance) on y-axis. Blue dots represent human miRNAs which are greater than 2 fold different and whose difference is statistically significant ($p$<0.05).

30 miRNAs with the largest difference in expression between MG-63 cells and TE-85 are displayed in a heatmap in Fig. 4.9 and in Table 4.3.

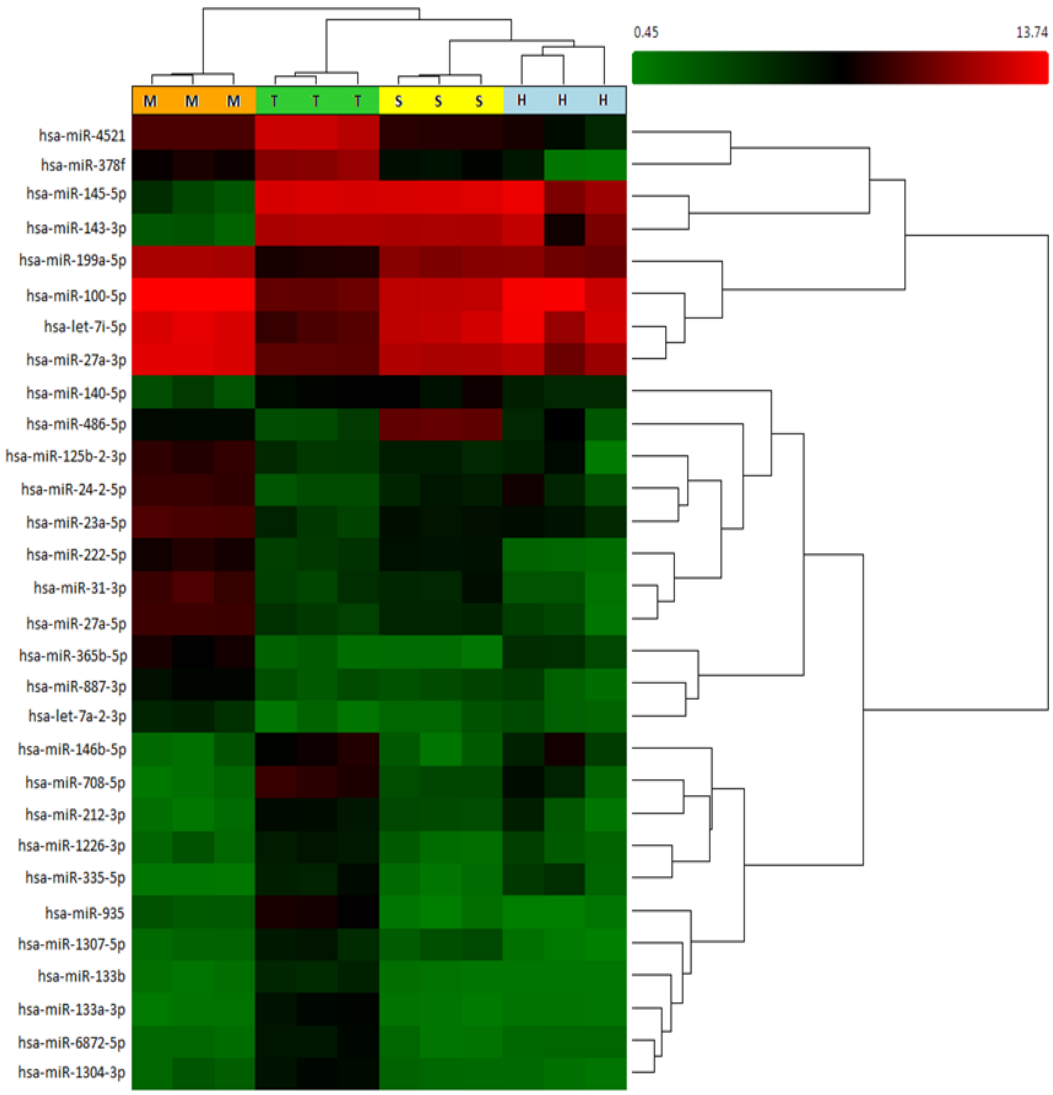


Figure 4.9: Hierarchical clustering shows 30 miRNAs with the biggest fold change between MG-63 (M) and TE-85 (T). The expression of the same miRNAs in SaOS-2 (S) and HOBs (H) are also included.

Table 4.3: 30 miRNAs with the greatest differential expression between MG-63 and TE-85.

| Transcript ID (Array Design) | Fold Change (linear) (MG-63 vs. TE-85) | FDR p-value (MG-63 vs. TE-85) |
|---|---|---|
| hsa-miR-365b-5p | 46.91 | 0.005608 |
| hsa-miR-24-2-5p | 39.02 | 0.001315 |
| hsa-miR-23a-5p | 23.90 | 0.022549 |
| hsa-miR-31-3p | 23.23 | 0.011710 |
| hsa-miR-27a-5p | 22.14 | 0.003883 |
| hsa-let-7a-2-3p | 18.07 | 0.022265 |
| hsa-miR-100-5p | 16.80 | 0.000720 |
| hsa-miR-125b-2-3p | 16.41 | 0.009027 |
| hsa-miR-887-3p | 13.67 | 0.009427 |
| hsa-let-7i-5p | 13.55 | 0.006067 |
| hsa-miR-199a-5p | 11.96 | 0.000743 |
| hsa-miR-27a-3p | 11.36 | 0.000743 |
| hsa-miR-486-5p | 10.93 | 0.014413 |
| hsa-miR-222-5p | 10.86 | 0.006952 |
| hsa-miR-378f | -9.66 | 0.004648 |
| hsa-miR-4521 | -10.16 | 0.004012 |
| hsa-miR-140-5p | -12.29 | 0.026141 |
| hsa-miR-133b | -13.93 | 0.002609 |
| hsa-miR-1307-5p | -14.96 | 0.017638 |
| hsa-miR-1226-3p | -15.77 | 0.015458 |
| hsa-miR-6872-5p | -18.84 | 0.004390 |
| hsa-miR-1304-3p | -20.16 | 0.006861 |
| hsa-miR-335-5p | -21.09 | 0.010281 |
| hsa-miR-935 | -33.68 | 0.001982 |
| hsa-miR-212-3p | -35.31 | 0.004156 |
| hsa-miR-133a-3p | -50.91 | 0.001982 |
| hsa-miR-146b-5p | -63.30 | 0.017884 |
| hsa-miR-708-5p | -116.74 | 0.003135 |
| hsa-miR-143-3p | -512.20 | 0.000962 |
| hsa-miR-145-5p | -522.54 | 0.006550 |

A heat map diagram showing the hierarchical clustering results from all 92 differentially expressed miRNA between MG-63 and SaOS-2 is shown in Fig 4.10, whilst a volcano plot shows the distribution of significantly different expression which is greater than double, or less than half, the expression of the comparative cell type (Fig 4.11).

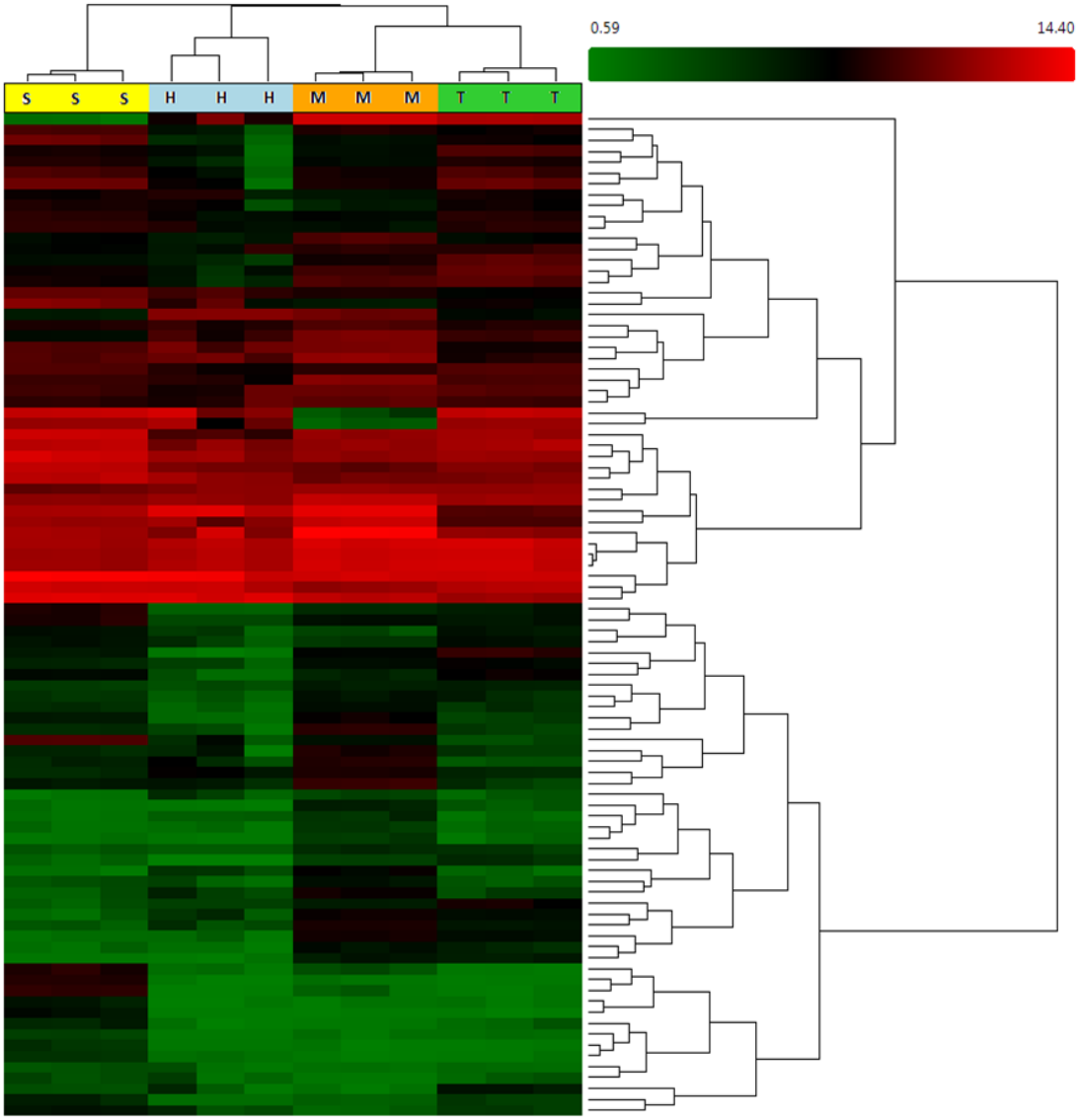


Figure 4.10: Hierarchical clustering shows all 92 differentially expressed miRNAs between MG-63 (M) and SaOS-2 (S). The expression of the same miRNAs in TE-85 (T) and HOBs (H) are also included.

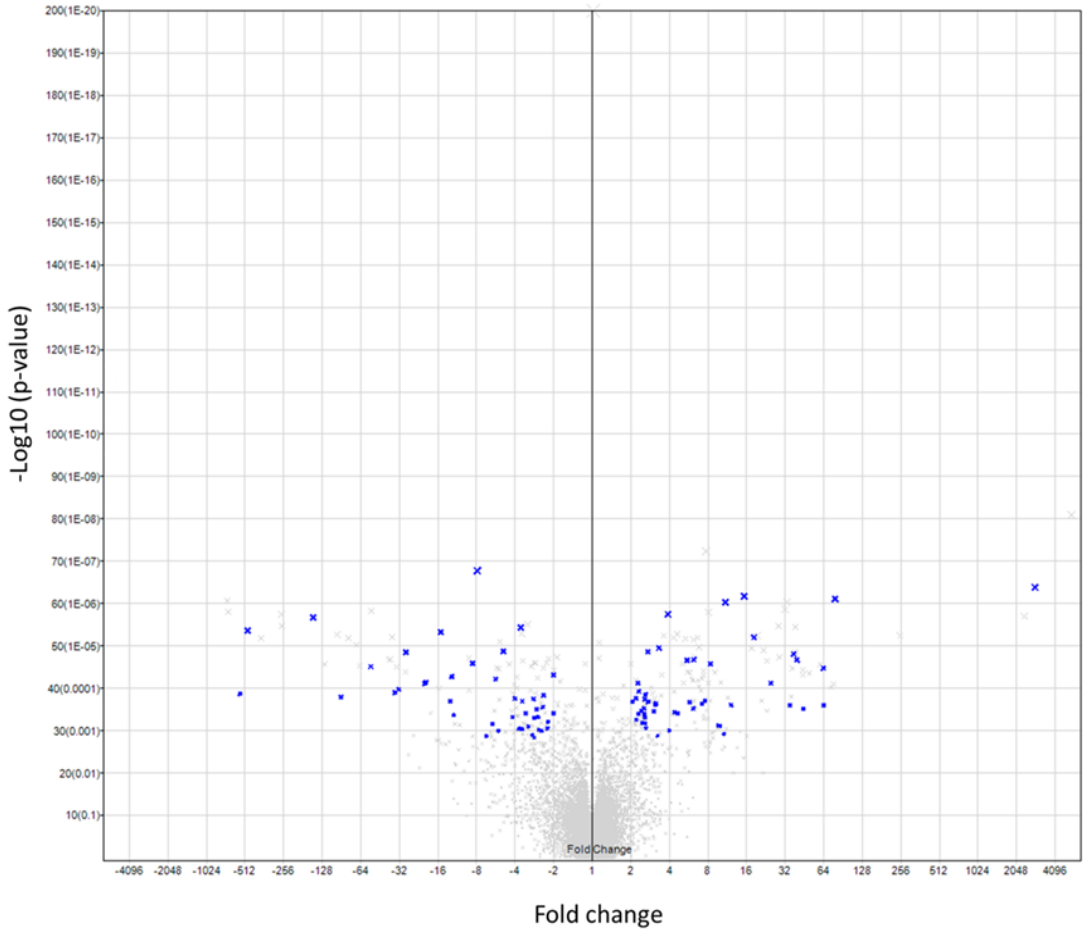


Figure 4.11: Volcano plot of the differential epression of miRNAs between MG-63 and SaOS-2 cells. Change in expression is plotted on the x-axis, log (significance) on y-axis. Blue dots represent human miRNAs which are greater than 2 fold different and whose difference is statistically significant ($p$<0.05).

30 miRNAs with the largest difference in expression between MG-63 cells and TE-85 are displayed in a heatmap in Fig. 4.12 and in Table 4.4.

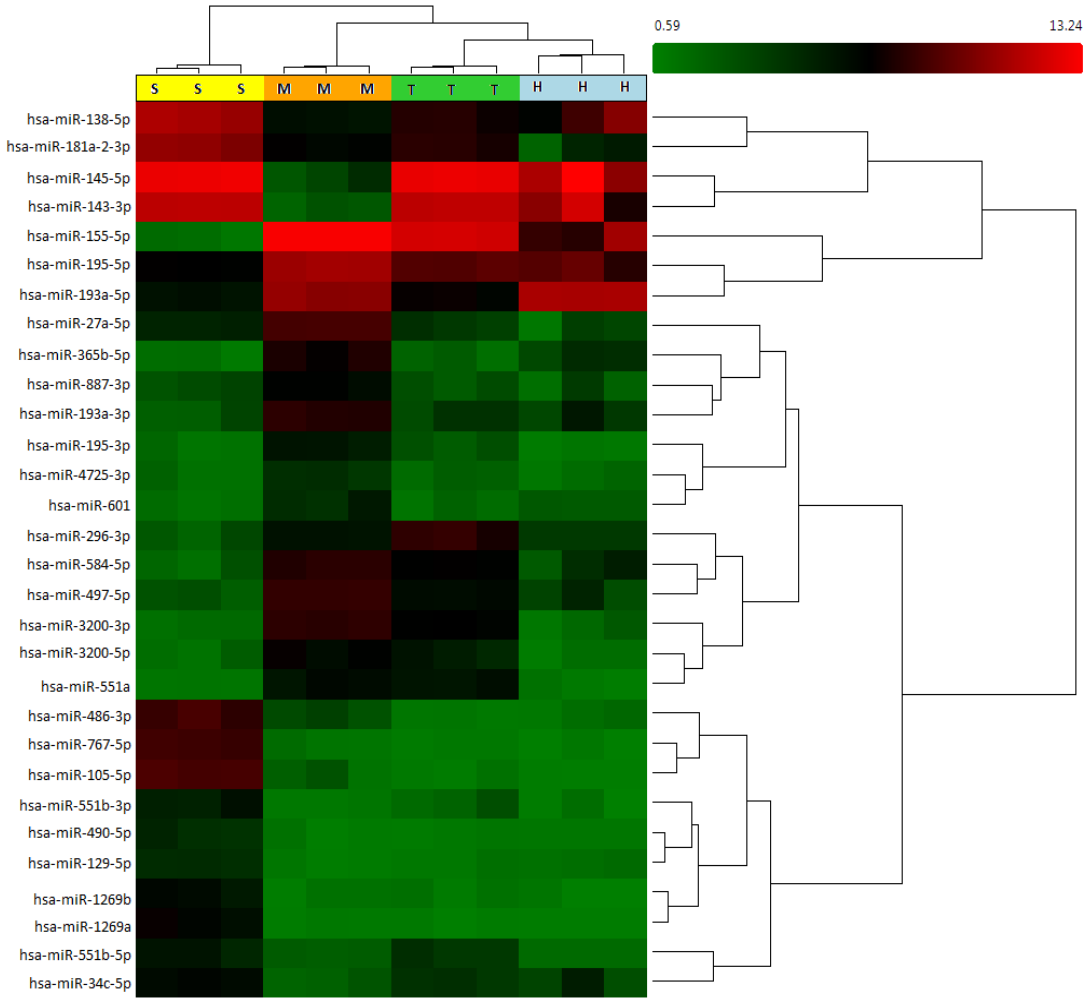


Figure 4.12: Hierarchical clustering shows 30 miRNAs with the biggest fold change between MG-63 (M) and SaOS-2 (T). The expression of the same miRNAs in TE-85 (T) and HOBs (H) are also included.

Table 4.4: 30 miRNAs with the greatest differential expression between MG-63 and SaOS-2.

| Transcript ID (Array Design) | Fold Change (linear) (MG-63 vs. SaOS-2) | FDR p-value (MG-63 vs. SaOS-2) |
|---|---|---|
| hsa-miR-155-5p | 2842.10 | 0.000675 |
| hsa-miR-3200-3p | 78.55 | 0.000701 |
| hsa-miR-584-5p | 64.08 | 0.013628 |
| hsa-miR-365b-5p | 63.51 | 0.003607 |
| hsa-miR-193a-3p | 44.47 | 0.015420 |
| hsa-miR-497-5p | 39.54 | 0.002704 |
| hsa-miR-551a | 37.38 | 0.002212 |
| hsa-miR-3200-5p | 35.02 | 0.013628 |
| hsa-miR-195-3p | 24.73 | 0.006004 |
| hsa-miR-193a-5p | 18.31 | 0.001423 |
| hsa-miR-195-5p | 15.32 | 0.000701 |
| hsa-miR-887-3p | 12.11 | 0.013506 |
| hsa-miR-27a-5p | 10.94 | 0.000701 |
| hsa-miR-296-3p | 10.65 | 0.038422 |
| hsa-miR-4725-3p | 9.92 | 0.028367 |
| hsa-miR-601 | 9.64 | 0.028235 |
| hsa-miR-551b-5p | -12.06 | 0.019384 |
| hsa-miR-181a-2-3p | -12.48 | 0.004937 |
| hsa-miR-490-5p | -12.84 | 0.012145 |
| hsa-miR-129-5p | -15.23 | 0.001289 |
| hsa-miR-34c-5p | -19.87 | 0.005956 |
| hsa-miR-551b-3p | -20.38 | 0.006004 |
| hsa-miR-138-5p | -28.55 | 0.002043 |
| hsa-miR-486-3p | -32.46 | 0.007947 |
| hsa-miR-1269b | -34.75 | 0.009184 |
| hsa-miR-1269a | -53.55 | 0.003360 |
| hsa-miR-105-5p | -91.48 | 0.010815 |
| hsa-miR-767-5p | -151.28 | 0.001057 |
| hsa-miR-143-3p | -487.53 | 0.001289 |
| hsa-miR-145-5p | -561.08 | 0.009482 |

A heat map diagram showing the hierarchical clustering results from all 132 differentially expressed miRNA between TE-85 and SaOS-2 cells is shown in Fig 4.13, whilst a volcano plot shows the distribution of significantly different expression which is greater than double, or less than half, the expression of the comparative cell type (Fig 4.14).

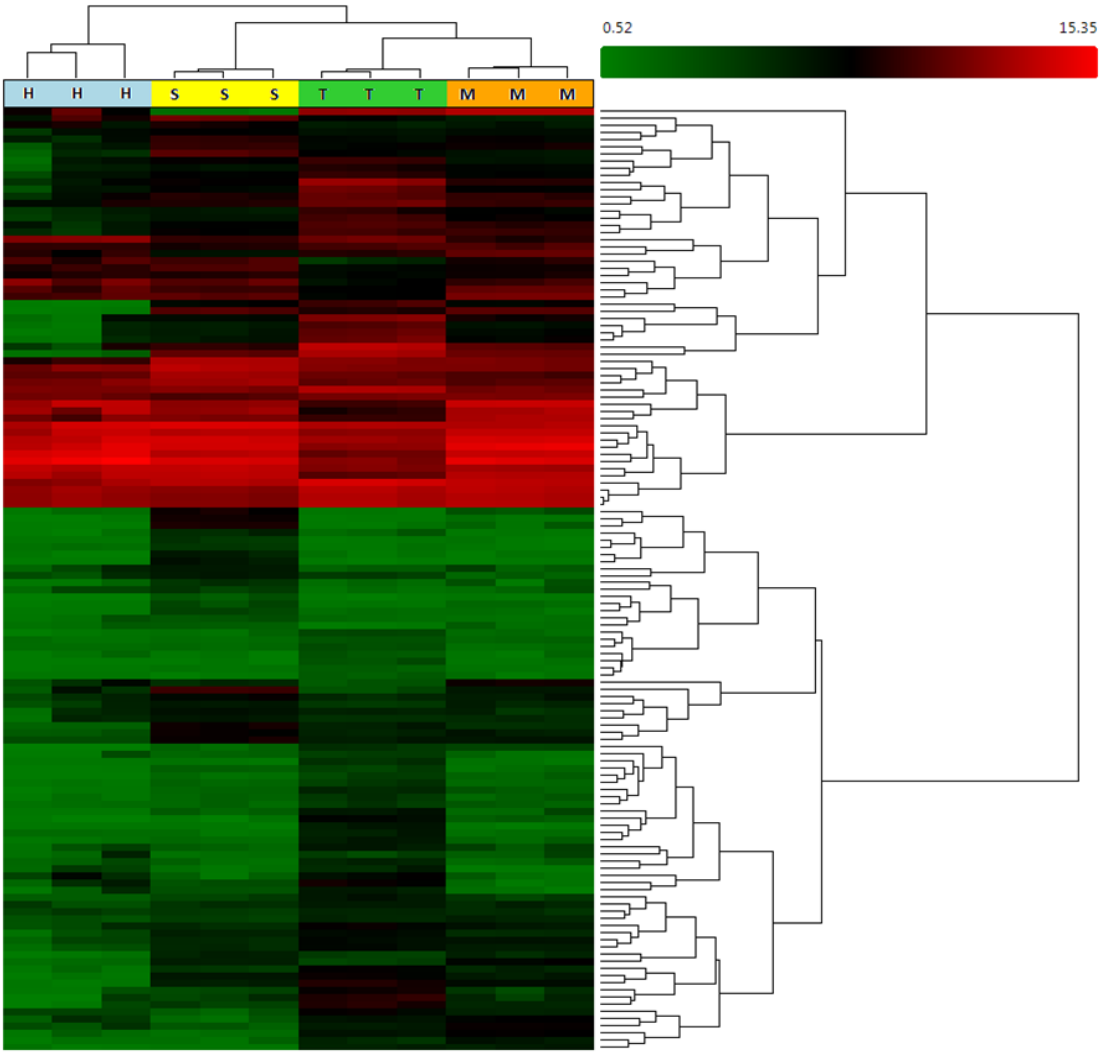


Figure 4.13: Hierarchical clustering shows all 132 differentially expressed miRNAs between TE-85 (T) and SaOS-2 (S). The expression of the same miRNAs in MG-63 (M) and HOBs (H) are also included.

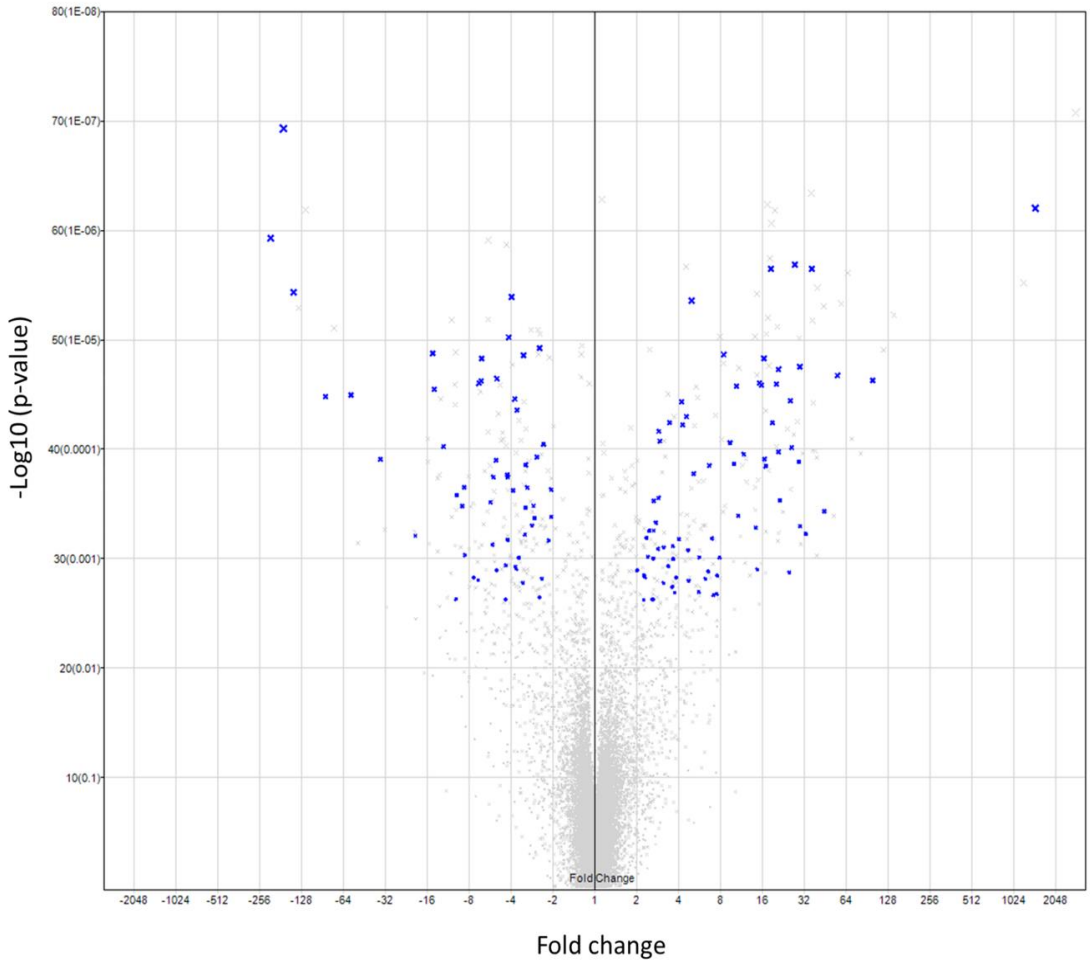


Figure 4.14: Volcano plot of the differential expression of miRNAs between TE-85 and SaOS-2 cells. Change in expression is plotted on the x-axis, log (significance) on y-axis. Blue dots represent human miRNAs which are greater than 2 fold different and whose difference is statistically significant ($p$<0.05).

30 miRNAs with the largest difference in expression between TE-85 and SaOS-2 cells are displayed in a heatmap in Fig. 4.15 and in Table 4.5.

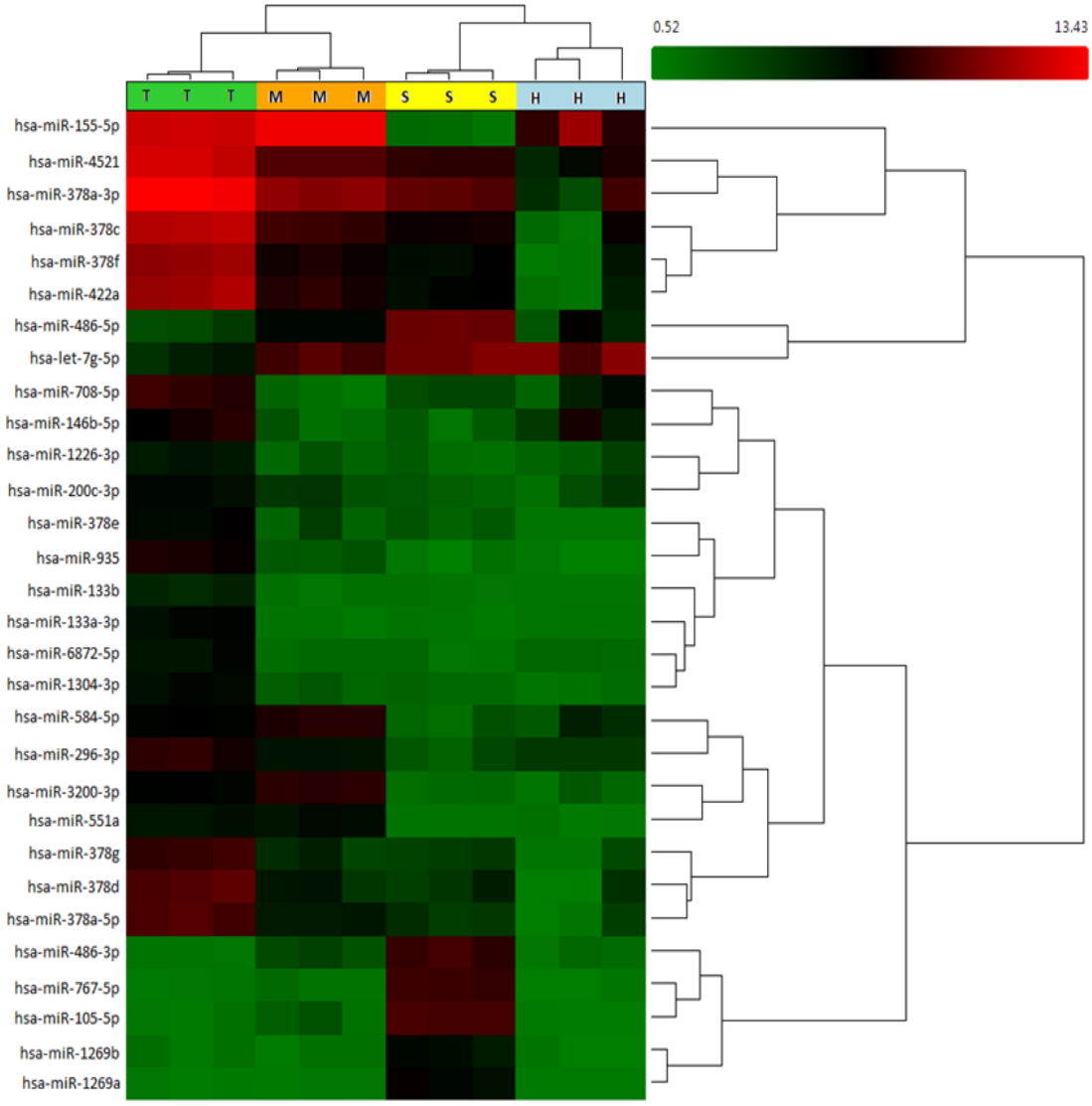


Figure 4.15: Hierarchical clustering shows 30 miRNAs with the biggest fold change between TE-85 (T) and SaOS-2 (T). The expression of the same miRNAs in MG-63 (M) and HOBs (H) are also included.

Table 4.5: 30 miRNAs with the greatest differential expression between TE-85 and SaOS-2.

| Transcript ID (Array Design) | Fold Change (linear) (TE-85 vs. SaOS-2) | FDR p-value (TE-85 vs. SaOS-2) |
|---|---|---|
| hsa-miR-155-5p | 1467.24 | 0.001030 |
| hsa-miR-935 | 99.54 | 0.002489 |
| hsa-miR-133a-3p | 55.35 | 0.002489 |
| hsa-miR-296-3p | 44.60 | 0.015201 |
| hsa-miR-3200-3p | 36.34 | 0.001175 |
| hsa-miR-146b-5p | 32.77 | 0.021155 |
| hsa-miR-584-5p | 29.91 | 0.019101 |
| hsa-miR-1304-3p | 29.74 | 0.002380 |
| hsa-miR-6872-5p | 29.27 | 0.007516 |
| hsa-miR-551a | 27.43 | 0.001175 |
| hsa-miR-378a-5p | 25.97 | 0.006137 |
| hsa-miR-708-5p | 25.43 | 0.003008 |
| hsa-miR-378d | 24.94 | 0.033087 |
| hsa-miR-1226-3p | 21.36 | 0.013405 |
| hsa-miR-200c-3p | 20.94 | 0.006605 |
| hsa-miR-378g | 20.92 | 0.002489 |
| hsa-miR-4521 | 20.18 | 0.002516 |
| hsa-miR-378f | 18.89 | 0.004322 |
| hsa-miR-378c | 18.37 | 0.001175 |
| hsa-miR-422a | 16.90 | 0.007975 |
| hsa-miR-378e | 16.58 | 0.007335 |
| hsa-miR-378a-3p | 16.41 | 0.002105 |
| hsa-miR-133b | 15.74 | 0.002516 |
| hsa-let-7g-5p | -19.53 | 0.021442 |
| hsa-miR-1269b | -34.85 | 0.007335 |
| hsa-miR-1269a | -56.69 | 0.002882 |
| hsa-miR-486-5p | -86.23 | 0.002925 |
| hsa-miR-486-3p | -146.95 | 0.001426 |
| hsa-miR-767-5p | -173.02 | 0.000707 |
| hsa-miR-105-5p | -213.34 | 0.001175 |

A heat map diagram showing the hierarchical clustering results from all 314 differentially expressed miRNA between TE-85 and HOBs is shown in Fig 4.16, whilst a volcano plot shows the distribution of significantly different expression which is greater than double, or less than half, the expression of the comparative cell type (Fig 4.17).

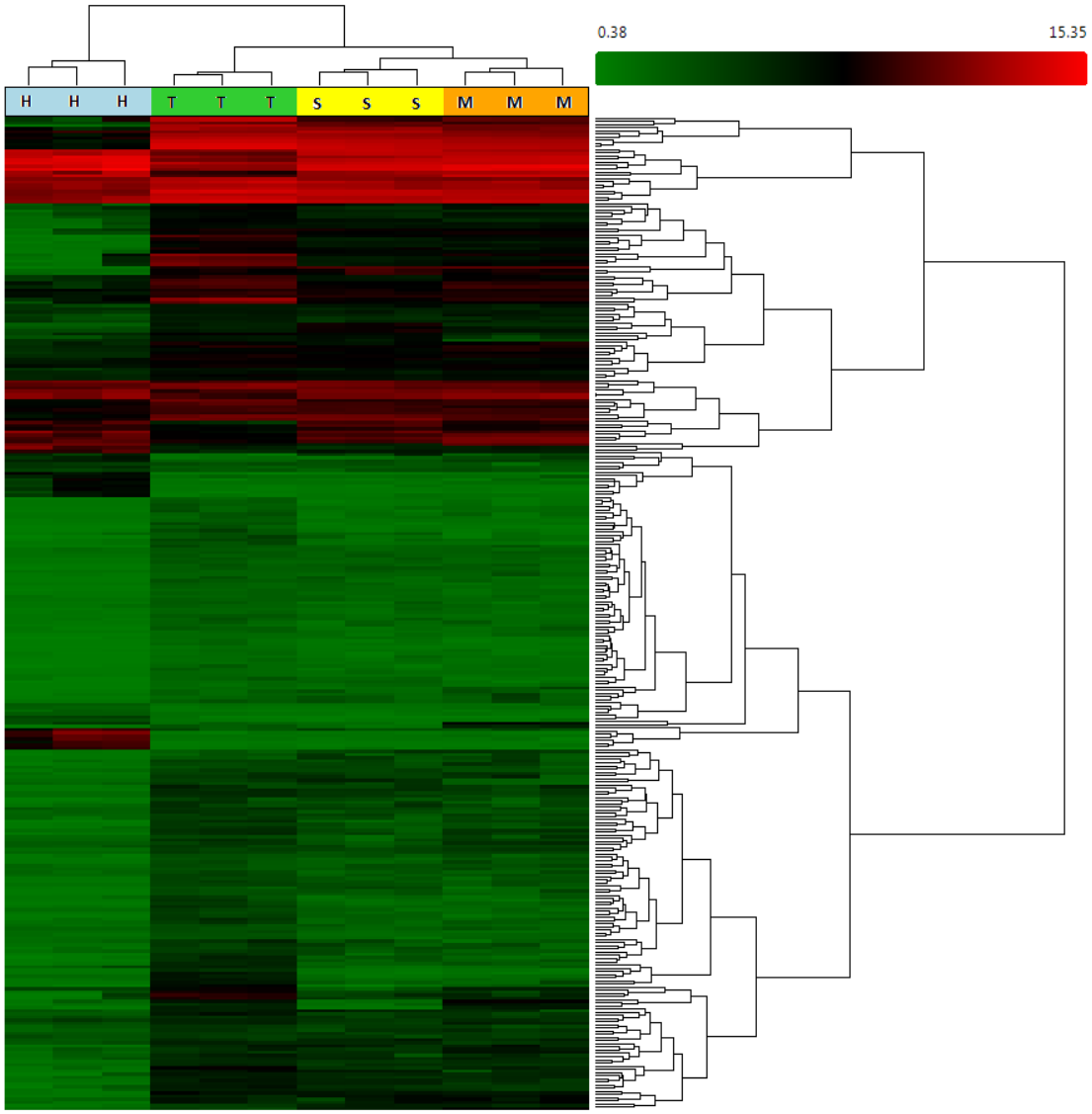


Figure 4.16: Hierarchical clustering shows all 314 differentially expressed miRNAs between TE-85 (T) and HOBs (H). The expression of the same miRNAs in SaOS-2 (S) and MG-63 (M) are also included.

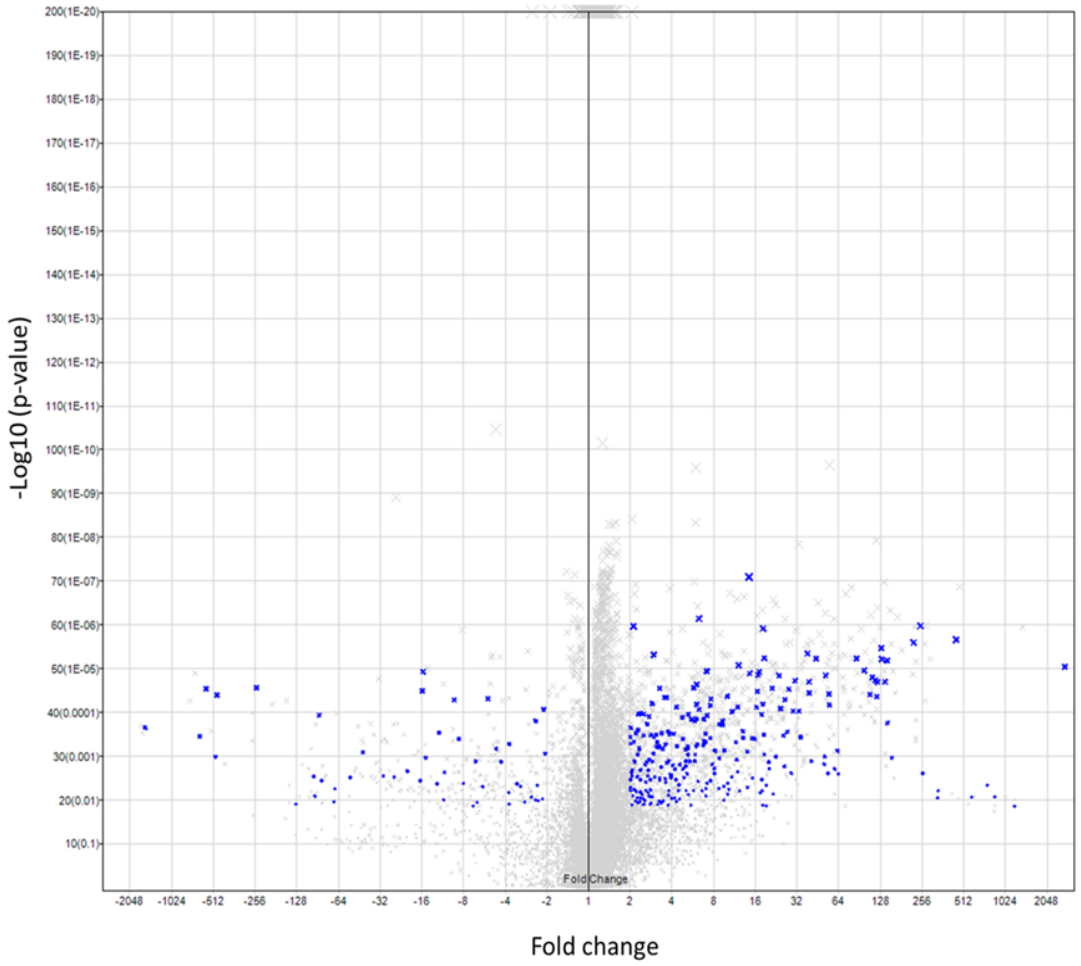


Figure 4.17: Volcano plot of the expression difference in miRNA expression between TE-85 and HOBs. Change in expression is plotted on the x-axis, log (significance) on y-axis. Blue dots represent human miRNAs which are greater than 2 fold different and whose difference is statistically significant

.

30 miRNAs with the largest difference in expression between TE-85 and HOBs are displayed in a heatmap in Fig. 4.18 and in Table 4.6.

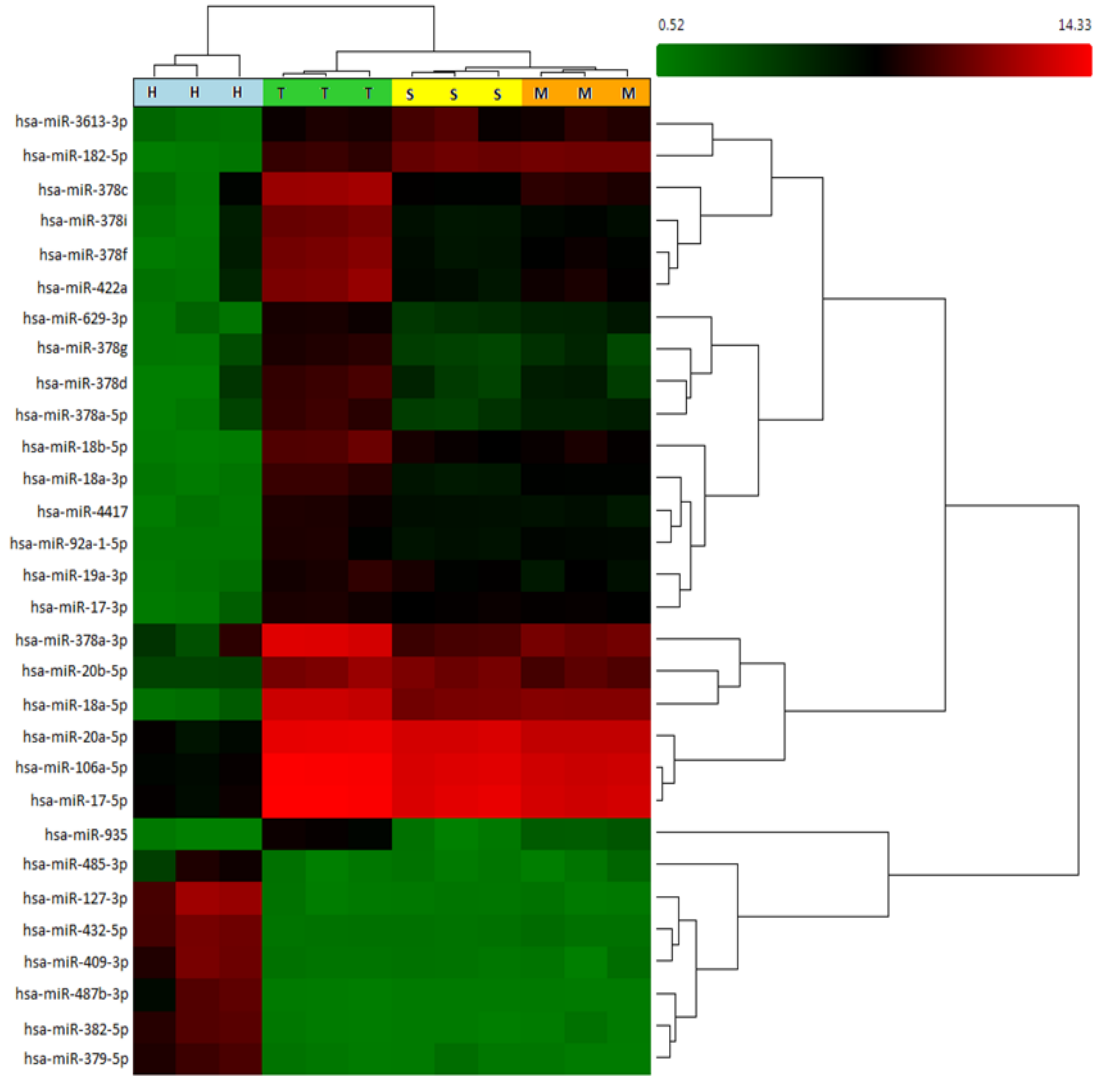


Figure 4.18: Hierarchical clustering shows the 30 miRNAs with the biggest fold change between TE-85 (T) and HOBs (H). The expression of the same miRNAs in SaOS-2 (S) and MG-63 (M) are also included.

Table 4.6: 30 miRNAs with the greatest differential expression between TE-85 and HOBs.

| Transcript ID (Array Design) | Fold Change (linear) (TE-85 vs. HOBs) | FDR p-value (TE-85 vs. HOBs) |
|---|---|---|
| hsa-miR-18a-5p | 2737.90 | 0.000324 |
| hsa-miR-378c | 1187.84 | 0.049561 |
| hsa-miR-378f | 855.26 | 0.036359 |
| hsa-miR-422a | 753.10 | 0.024589 |
| hsa-miR-378i | 583.22 | 0.036702 |
| hsa-miR-18b-5p | 448.43 | 0.000119 |
| hsa-miR-378d | 334.04 | 0.029608 |
| hsa-miR-378a-3p | 330.63 | 0.036877 |
| hsa-miR-378a-5p | 257.41 | 0.016766 |
| hsa-miR-182-5p | 248.22 | 0.000067 |
| hsa-miR-18a-3p | 221.62 | 0.000132 |
| hsa-miR-378g | 154.44 | 0.010146 |
| hsa-miR-17-3p | 143.48 | 0.002668 |
| hsa-miR-4417 | 142.75 | 0.000254 |
| hsa-miR-92a-1-5p | 138.39 | 0.000556 |
| hsa-miR-935 | 130.16 | 0.000242 |
| hsa-miR-106a-5p | 129.99 | 0.000159 |
| hsa-miR-20b-5p | 121.70 | 0.000556 |
| hsa-miR-629-3p | 120.29 | 0.000991 |
| hsa-miR-19a-3p | 117.62 | 0.000530 |
| hsa-miR-17-5p | 111.95 | 0.000474 |
| hsa-miR-20a-5p | 107.51 | 0.000917 |
| hsa-miR-3613-3p | 97.74 | 0.000375 |
| hsa-miR-485-3p | -129.63 | 0.047197 |
| hsa-miR-379-5p | -251.24 | 0.000717 |
| hsa-miR-382-5p | -482.67 | 0.000946 |
| hsa-miR-487b-3p | -494.03 | 0.009910 |
| hsa-miR-432-5p | -576.58 | 0.000741 |
| hsa-miR-409-3p | -638.88 | 0.004593 |
| hsa-miR-127-3p | -1588.00 | 0.003210 |

A heat map diagram showing the hierarchical clustering results from all 215 differentially expressed miRNA between SaOS-2 and HOBs is shown in Fig 4.19, whilst a volcano plot shows the distribution of significantly different expression which is greater than double, or less than half, the expression of the comparative cell type (Fig 4.20).

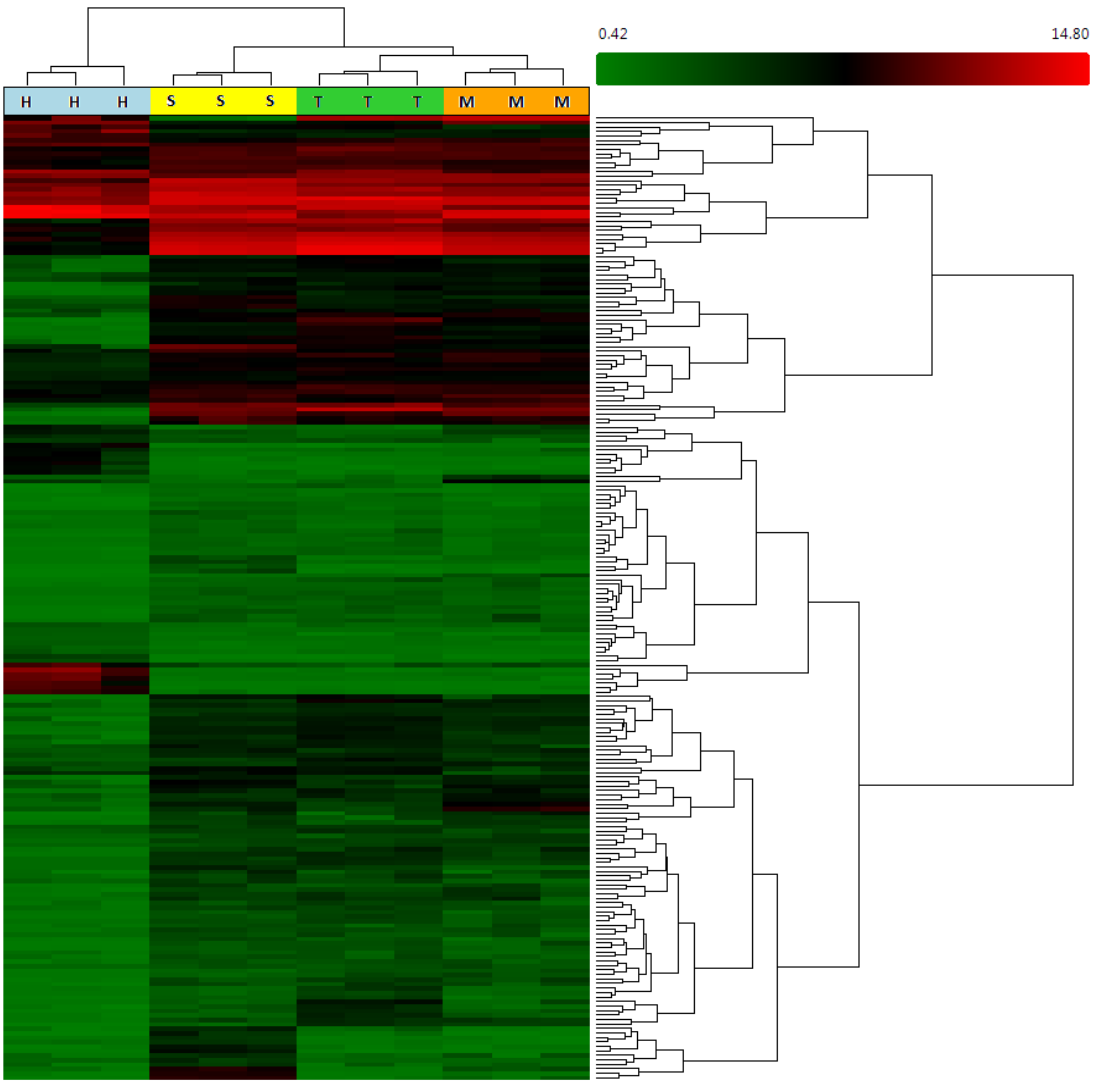


Figure 4.19: Hierarchical clustering shows all 215 differentially expressed miRNAs between SaOS-2 (S) and HOBs (H). The expression of the same miRNAs in MG-63 (M) and TE-85 (T) are also included.

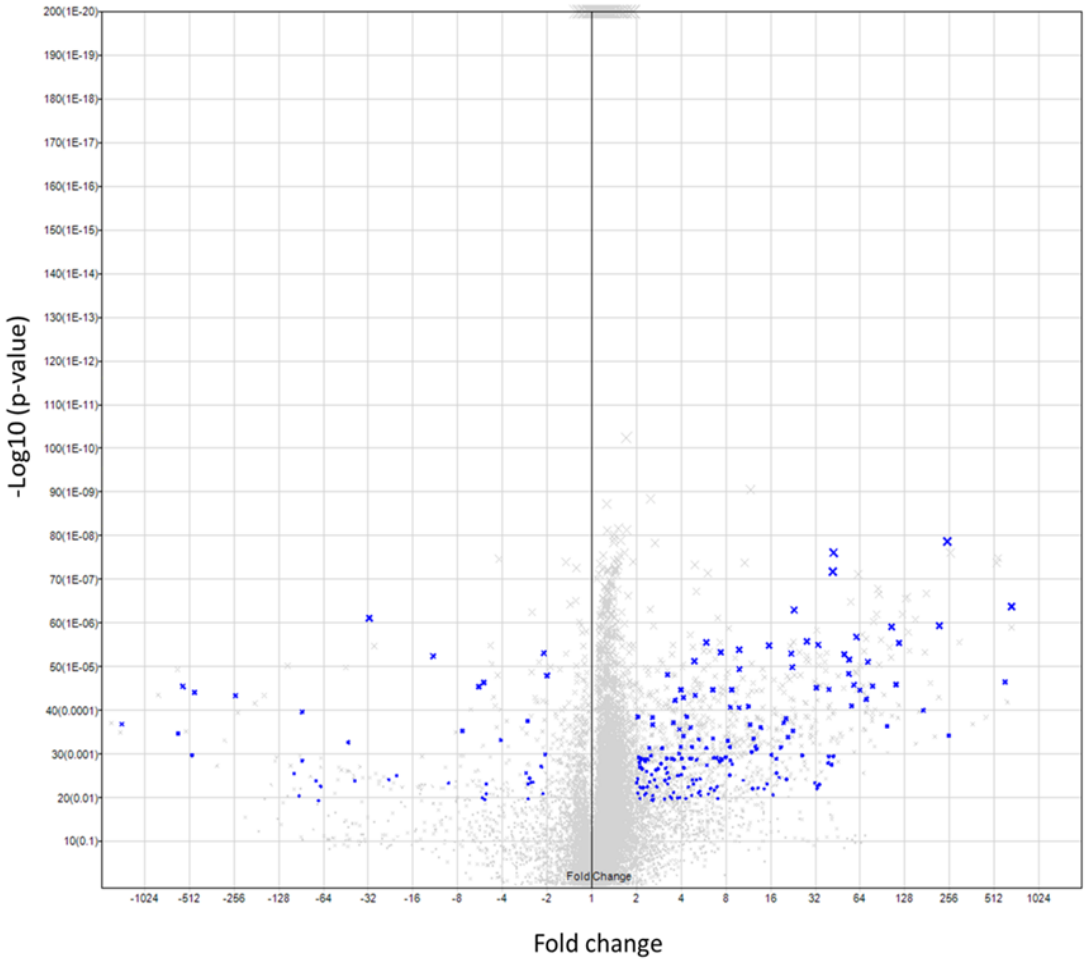


Figure 4.20: Volcano plot of the differential expression of miRNAs between SaOS-2 and HOBs. Change in expression is plotted on the x-axis, log (significance) on y-axis. Blue dots represent human miRNAs which are greater than 2 fold different and whose difference is statistically significant ($p$<0.05).

30 miRNAs with the largest difference in expression between TE-85 and HOBs are displayed in a heatmap in Fig. 4.21 and in Table 4.7.

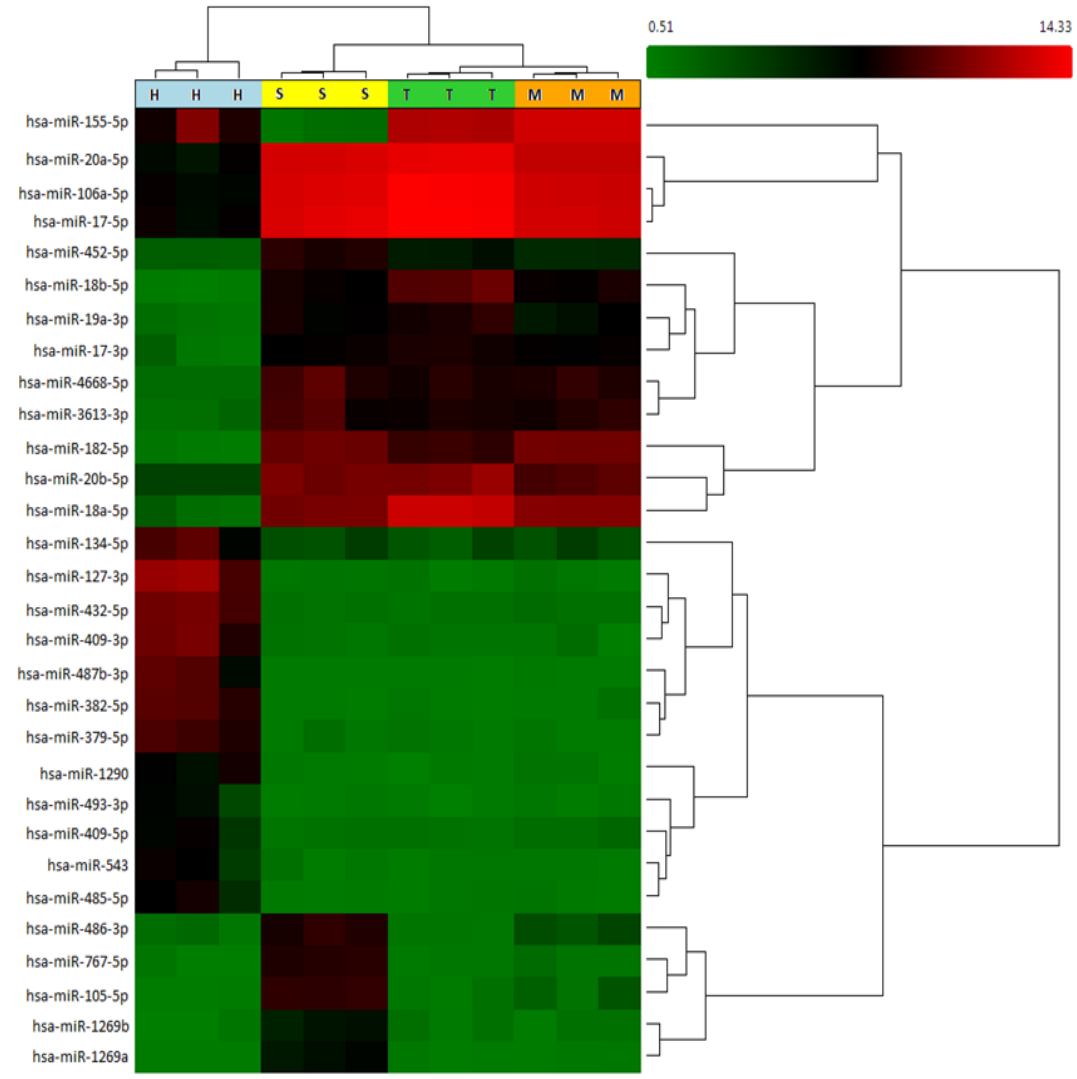


Figure 4.21: Hierarchical clustering shows the 30 miRNAs with the largest fold change between SaOS-2 (S) and HOBs (H). The expression of the same miRNAs in MG-63 (M) and TE-85 (T) are also included.

**Table 4.7:** 30 miRNAs with the greatest differential expression between SaOS-2 and HOBs.

| Transcript ID (Array Design) | Fold Change (linear) (SaOS-2 vs. HOBs) | FDR p-value (SaOS-2 vs. HOBs) |
|---|---|---|
| hsa-miR-182-5p | 669.13 | 0.000037 |
| hsa-miR-18a-5p | 603.60 | 0.000783 |
| hsa-miR-3613-3p | 253.74 | 0.005521 |
| hsa-miR-105-5p | 247.29 | 0.000002 |
| hsa-miR-767-5p | 218.69 | 0.000085 |
| hsa-miR-4668-5p | 170.22 | 0.002361 |
| hsa-miR-18b-5p | 116.88 | 0.000162 |
| hsa-miR-486-3p | 111.54 | 0.000852 |
| hsa-miR-20b-5p | 104.46 | 0.000088 |
| hsa-miR-17-3p | 97.33 | 0.003978 |
| hsa-miR-19a-3p | 77.89 | 0.000889 |
| hsa-miR-106a-5p | 72.09 | 0.000346 |
| hsa-miR-20a-5p | 70.34 | 0.001527 |
| hsa-miR-17-5p | 63.92 | 0.001053 |
| hsa-miR-452-5p | 60.53 | 0.000129 |
| hsa-miR-1269a | 58.01 | 0.000866 |
| hsa-miR-1269b | 55.91 | 0.001990 |
| hsa-miR-409-5p | -66.98 | 0.031407 |
| hsa-miR-493-3p | -69.17 | 0.049419 |
| hsa-miR-134-5p | -72.06 | 0.026629 |
| hsa-miR-1290 | -89.18 | 0.002477 |
| hsa-miR-155-5p | -89.25 | 0.013733 |
| hsa-miR-543 | -93.18 | 0.043385 |
| hsa-miR-485-5p | -101.01 | 0.020690 |
| hsa-miR-379-5p | -250.77 | 0.001349 |
| hsa-miR-382-5p | -473.02 | 0.001139 |
| hsa-miR-487b-3p | -491.07 | 0.011292 |
| hsa-miR-432-5p | -566.66 | 0.000897 |
| hsa-miR-409-3p | -612.18 | 0.005262 |
| hsa-miR-127-3p | -1459.96 | 0.003684 |

## 4.4 Discussion

In chapter 3, we found that MG-63, TE-85 and SaOS-2 are the good models for studying bone biology by studying the expression of 7 bone markers and the effect of ATP and PTH treatments on the expressions of these markers. In this chapter, we wanted to investigate the differential expression of miRNAs which are the key to the gene expression regulation in these cells. Understanding the miRNA expression in these cells is the first step toward the identification of miRNAs that can be used to control gene expression.

In this chapter, expression profiles of miRNAs were compared between groups of osteoblastic cells: primary human osteoblasts (HOBs), MG-63, TE-85 and SaOS-2 cell lines. Significant differential expression was defined as those with FDR-adjusted *p*-values < 0.05 and miRNA expression change of at least two fold. The highest number of differentially-expressed miRNAs was recorded between TE-85 and HOBs with 314 miRNAs. Of these, 263 were up-regulated in TE-85 compared to HOBs and 51 were down-regulated. The second highest number of differentially expressed miRNAs was observed between SaOS-2 and HOBs with 215 miRNAs followed by MG-63 and HOBs with 210 miRNAs. A comparison of miRNA expression between the different osteosarcoma cell lines identified fewer differentially expressed miRNAs: MG-63 and TE-85 (132 miRNAs), MG-63 and SaOS-2 (92 miRNAs) and TE-85 and SaOS-2 (132 miRNAs) (Table 4.1). The higher number between HOBs and all three human osteosarcoma cell lines might be due to cancer-related miRNAs which can play oncogenic or anti-tumour roles in the cell lines (Garzon *et al.*, 2010).

The sample correlation heatmap displays the general degree of similarity between the 12 libraries (Fig. 4.1). Primary human osteoblasts are clearly different from the osteosarcoma cell lines. However, overall miRNA expression is highly correlated

between the 12 libraries, the Spearman correlation coefficient being greater than 0.805. Principle component analysis of the differentially-expressed miRNAs showed clearer sample clustering (Fig. 4.2), corroborating the sample correlation heatmap result. When we observed the overall comparison of differentially expressed miRNAs between each cell type (Fig. 4.3) it was clear that there were a greater number of differentially-expressed miRNAs between primary cells and any of the cell lines.

Comparison of miRNA expression profiles between MG-63 and HOBs revealed 210 miRNAs that were differentially expressed (Fig. 4.4). Most of these miRNAs were expressed to a higher level in MG-63 with 174 miRNAs. Clearer visualization of the differential expression distribution with highly significant differences and greater fold change is shown in Fig. 4.5. Out of the 210 differentially-expressed miRNAs, we selected 30 that had the largest fold change between (Fig. 4.6 and Table 4.2). One miRNA which had a large differential expression was miR-127-3p, which was expressed 1530 times higher in HOBs than in MG-63 ($p$<0.005). An online search using miRWalk revealed that miR-127-3p has been validated to target 23 genes, namely: ACTR3B, ACTR3C, BCL6, BOLA1, KCNA6, LGALS8, MAPK4, MMP13, NBEA, PRDM1, RGMA, SEC31A, SEPT7, SERPINB9, SETD8, SFRP1, SKI, SLC29A1, TGM2, USP35, XBP1, ZWINT and DAGLA. Secreted frizzled related protein 1 (SFRP1) is involved in the regulation of the Wnt signalling pathway by acting as a soluble modulator. Inhibition of this gene leads to deregulated activation of the Wnt pathway (Svensson *et al.*, 2008).

Hierarchical clustering clearly shows that miRNA expression in all three cell lines was very similar and quite different to that of HOBs. Interestingly, however, we found that the expression of miR-145-5p and miR-143-3p were very similar, high in TE-85, SaOS-2 and HOBs but very low in MG-63. These miRNAs were expressed

205 and 175 times higher in HOBs than in MG-63 cells, $p<0.05$. The expression of these miRNAs appears to be low in the early stage of osteoblastic differentiation (MG-63) but very high in the later stages (represented by TE-85 and SaOS-2). This finding suggests that miR-145-5p and miR-143-3p might be actively involved in gene regulation during the later stages of osteoblastic differentiation. Down-regulation of miR-145-5p and miR-143-3p in MG-63 cells compared to HOBs was also reported in a study published in 2012 (Hu *et al.*, 2012).

Comparison of miRNA expression profiles between MG-63 and TE-85 showed that 132 miRNAs were differentially expressed. The volcano plot (Fig. 4.8) illustrates the distribution of the miRNAs based on fold change and significance of difference. We selected the 30 miRNAs with the biggest difference in fold change between MG-63 and TE-85 (Fig. 4.9, Table 4.3). The miRNA which had the largest difference in expression was miR-145-5p which was expressed in TE-85 522.54 times higher than in MG-63 cells, $p<0.05$. MiR-365b-5p was expressed highest in MG-63 compared to TE-85 cells, which was expressed 46.91 fold higher. Further investigation using miRWalk and miRTarBase show this miRNA has been validated to target more than 100 genes including Wnt family member 2B (WNT2b), a secreted signalling factor crucial for Wnt signalling. However, all of these targets were validated using only next generation sequencing, which is considered inferior to other validation methods that are considered as robust as reporter assay, western blot, ELISA and real-time PCR.

Other miRNA expression profiles we compared relating to osteosarcoma cell lines was that in MG-63 compared to SaOS-2 and between TE-85 and SaOS-2. Hierarchical clustering indicate that only 92 miRNAs were differentially expressed in MG-63 compared to SaOS-2 and 132 between TE-85 and SaOS-2. The volcano plots of significance versus relative difference in expression show almost equal

numbers of miRs were expressed higher and lower in MG-63 compared to SaOS-2 (49 and 43 miRNAs respectively). We selected the 30 miRNAs that had the largest difference in expression between cell lines. The most striking result to emerge from this data is that miR-155-5p expression was 2840 times higher in MG-63 cells than in SaOS-2 and 1470 times higher in TE-85 than in SaOS-2, $p<0.005$. The high expression of miR-155-5p in MG-63 and low expression in SaOS-2 suggests that it might target proteins that negatively regulate osteoblastic differentiation during the early stages of differentiation. Generally, miR-155 is a well-studied multifunctional miRNA involved in numerous biological processes such as hematopoiesis and associated with various types of cancer, cardiovascular diseases and viral infections (Jurkovicova *et al.*, 2014). In bone, miR-155 has been shown to indirectly regulate osteoclastogenesis by targeting several essential transcriptional factors such as MITF (microphthalmia-associated transcription factor), which is essential for osteoclast differentiation (Mann *et al.*, 2010).

Analysis of differential miRNA expression between TE-85 and HOBs identified 314 miRNAs that were expressed differentially, 263 miRNAs that were up-regulated and 51 miRNAs were down-regulated in TE-85 compared to HOBs. We selected the 30 miRNAs that had the largest difference in expression, illustrated by hierarchical clustering in Fig. 4.18 and Table 4.6. The three miRNAs with the biggest fold changes were miR-18a-5p, miR-127-3p and miR-378c. MiR-18a-5p and miR-378c were expressed 2740 and 1190 times higher in TE-85 compared to HOBs while miR-127-3p was expressed 1590 times higher in HOBs.

MiR-18a-5p has been shown to enhance vascular smooth muscle cell differentiation by inhibiting syndecan4, an inducer of Smad2 expression (Kee *et al.*, 2014). Another study showed the involvement of miR-18a-5p in idiopathic pulmonary fibrosis (IPF), a chronic progressive lung disease that normally causes respiratory

failure and death less than 5 years following diagnosis (Zhang *et al*., 2016). This study shows that inhibition of miR-18a-5p mediates sub-pleural pulmonary fibrosis which is the pathological hallmark of IPF through up-regulation its target TGF-β receptor II (TGF-βRII). Thus researchers believe that increasing the expression of miR-18a-5p might be an effective treatment (Zhang *et al.*, 2016). Using miRWalk online software, we found that miR-18a-5p has been validated to target more than 200 genes including those related to Wnt signalling such as SMAD family member 4 (SMAD4), cyclin D1 (CCND1), dishevelled associated activator of morphogenesis 2 (DAAM2) and tumour protein p53 (TP53).

Among the 30 miRNAs that are most different between TE-85 and HOBs, seven miRNAs are the family member of miR-378 which is one of the most abundant miRNA molecules in all human samples (Lee *et al.*, 2010). The family members of miR-378 are miR-378a-3p, miR-378a-5p, miR-378c, miR-378d, miR-378f, miR-378g and miR-378i. Although the occurrences of different miRNA family members are common, the functional effect and importance of the majority of miRNA variants remain to be resolved.

The final comparison of miRNA expression profiles we evaluated was between SaOS-2 and HOBs which revealed 215 differentially expressed miRNAs. The volcano plot in Fig. 4.20 indicates that 174 miRNAs were up-regulated and 41 down-regulated in SaOS-2 cells compared to HOBs. The 30 miRNAs whose expression varied most between the two cell types were again selected. Among these miRNAs, miR-127-3p had the largest fold change, 1460 fold higher in HOBs compared to SaOS-2, $p<0.005$. Expression of this miRNA was much lower in all three osteosarcoma cell lines than in HOBs, as discussed earlier, 1530 fold lower in MG-63 and 1588 fold in TE-85, $p<0.005$. Similar observations have been reported in the literature in three osteosarcoma cell lines: KHOS, U-2OS and SaOS-2 in

comparison to osteoblasts (Duan *et al.*, 2011). An interesting finding is that miR-127-3p plays a role as a tumour suppressor by inhibiting proliferation and invasion of human osteosarcoma cells by targeting the SETD8 gene, which regulates DNA replication and the cell cycle. Thus, miR-127-3p could be a potential therapeutic target in the treatment of osteosarcoma (Zhang *et al.*, 2016).

In total, there were more than 4600 miRNAs were differently expressed between all four different cells used in this study. Table 4.8 shows 10 examples of the miRNAs that were expressed with the biggest fold changes between the cells and their validated or published targets. Among these miRNAs, miR-378a-3p and miR-422a were also predicted to target sclerostin gene by the online prediction tools based on the complementary sequences and thermodynamics between these miRNAs and the SOST mRNA  These miRNAs were investigated for the regulation of sclerostin expression in chapter 5. This shows each miRNA always has more than one targets across different species.

Table 4.8: List of miRNAs with the biggest fold change between MG-63, TE-85, SaOS-2 and primary osteoblast and their targets.

| miRNA | Target genes and functions | Reference |
|---|---|---|
| hsa-miR-127-3p | **BCL6** - Regulate cell proliferation and senescence.<br>**BAG5** - Tumor suppressor in epithelial ovarian cancer.<br>**SKI** - Inhibits glioblastoma proliferation and activates TGF-β signalling. | (Chen *et al*., 2013)<br>(Bi *et al*., 2016)<br>(Jiang *et al*., 2014) |
| hsa-miR-155-5p | **NF-κB p65 –** Promotes the transition of mesenchymal stem cells to gastric cancer tissue derived MSC-like cells.<br>**ELK3** - Regulate hypoxia response. | (Zhu *et al*., 2016)<br>(Robertson *et al*., 2014) |
| hsa-miR-18a-5p | **SDC4** – Increase vascular smooth muscle cell differentiation.<br>**TGF-βRII** – Inhibit sub-pleural pulmonary fibrosis.<br>**IRF2** – As an oncogene. | (Kee *et al*., 201)<br>(Zhang *et al*., 2017)<br>(Liang *et al*., 2017) |
| hsa-miR-378a-3p | **HDAC4** – Inhibit proliferation of myoblast in skeletal muscle development.<br>**WNT10a** – Inhibit activation of hepatic stellate cell. | (Wei *et al*., 2016)<br>(Yu *et al*., 2016) |
| hsa-miR-379-5p | **FAK** – Inhibit tumor invasion and metastasis<br>**EIF4G2** – Supress the proliferation, migration and invasion of human osteosarcoma cells.<br>**MDM2** – Inhibit growth and metastasis of human bladder tumor. | (Chen *et al*., 2016)<br>(Xie *et al*., 2017)<br>(Wu *et al*., 2017) |
| hsa-miR-409-3p | **ZEB1** - regulates cell invasion and metastasis. As prognostic marker for breast cancer.<br>**E74-like factor 2** - regulates cell proliferation and tumor growth in osteosarcoma. | (Ma *et al*., 2016)<br>(Cao *et al*., 2016)<br>(Zhang *et al*., 2017) |
| hsa-miR-422a | **PIK3CA** - Tumor suppressor in glioblastoma. A potential marker for postmenopausal osteoporosis.<br>**NT53/CD73** - Promotes loco-regional recurrence in head and neck squamous cell carcinoma. | (Liang *et al*., 2016)<br>(Cao *et al*., 2014)<br>(Bonnin *et al*., 2016) |
| hsa-miR-432-5p | **E2F3** – Inhibit myogenesisthrough PI3K/AKT/mTOR signalling pathway.<br>**P53** - Inhibit the proliferation of neuroblastoma cells. | (Ma, *et al*., 2017)<br>(Rihani *et al*., 2015) |
| hsa-miR-487b-3p | **GRM3** – Inhibit colon cancer cell growth and survival. | (Yi *et al*., 2017) |
| hsa-miR-182-5p | **FOXF2, RECK, MTSS1** - Promotes cell invasion and proliferation in human prostate cancer.<br>**CASP9** – Induce apoptosis in human breast cancer. | (Hirata *et al*., 2013)<br>(Sharifi and Moridnia, 2017) |

## 4.5 Conclusions

From the results in chapter 4, we conclude that;

- MicroRNAs are expressed differentially during osteoblastic differentiation;
- MicroRNAs that induced the largest fold change between the cells we studied were: miR-127-3, miR-155-5p and miR-18a-5p. Each of these miRNAs is predicted to target hundreds of different genes which are still need to be studied;
- MicroRNA differential expression profiles provide the first step for the identification of specific miRNAs that target our gene of interest.

# CHAPTER 5:

# IDENTIFICATION OF miRNAs INVOLVED IN THE REGULATION OF SCLEROSTIN EXPRESSION

## 5.1 Introduction

Important regulators of protein production by cells are miRNAs. MiRNA molecules inhibit the expression of many genes by binding within the 3'UTR of the targeted mRNA and therefore block translation and/or induce the degradation of mRNA molecules, thereby reducing protein levels. miRNAs has been used as a therapeutic approach to treat various human diseases, especially cancer, as they play a vital role in the regulation of tumour cell differentiation, proliferation, cell cycle progression, invasion and metastasis (Rothschild, 2013). In chapter 4, we studied the differential expression of miRNAs between the osteosarcoma cell lines and primary osteoblast. We found that miRNA expression level of certain miRNAs changed greatly between cells to suit the biological and physiological function of the cells. Then, in this chapter, we focused on the miRNAs that are involved in the regulation of the protein of our interest, sclerostin (SOST). We studied this protein because SOST plays a key role in limiting bone formation by blocking Wnt signalling pathway. Hence, inhibiting or limiting the overexpression of SOST by osteoblastic cells could help to control or limit the inhibitory effect of SOST against new bone formation. This method could be another approach to treat bone diseases. In the first part of this chapter, we have utilised online prediction tools to predict the potential miRNAs which could target SOST. Many miRNA targets that have been predicted using prediction software based mainly on nucleotide sequences and thermodynamics of the miRNA-mRNA interaction have been experimentally validated in very limited numbers.

Thus we have selected multiple putative miRNAs that might target SOST, and have transfected TE-85 and SaoS-2 cells with the selected miRNA mimics, antagomirs and scrambled miRNA using Lipofectamine 2000. Theoretically, when an miRNA mimic is transfected into a cell, it mimics natural miRNA by binding target mRNA and inhibits or reduces protein translation (Kuhn *et al.*, 2008). On the other hand,

antagomir binds to its related miRNA and inhibits the binding to its target mRNA therefore blocking its inhibitory effect (Stenvang *et al.*, 2012). To verify the function of the selected miRNAs, quantitative analysis of SOST mRNA and protein levels by ELISA was performed.

## 5.2 Brief methods

### 5.2.1 miRNA target prediction – Bioinformatic analysis

To identify potential miRNAs that target sclerostin mRNA, we used five different online prediction tools: miRWalk, miRanda, Pictar, RNA22 and Targetscan. The six miRNAs that were predicted by the majority of the prediction algorithms were chosen for further experimental validation (section 2.3.4).

### 5.2.2 Transient transfection of cells with miRNA mimics and inhibitors

TE-85 and SaOS-2 cells were transfected with scrambled miRNA as a negative control, miRNA mimics and anti-miRNA/antagomir using Lipofectamine 2000 in medium free of serum and antibiotics. After 6 hours of incubation, culture medium was replaced with medium containing 10% FCS. Cells were incubated at 37°C for a further 48 hours before being harvested for total DNA and RNA extraction and the culture medium collected for sclerostin protein quantification. The detailed procedure is described in section 2.3.7.

### 5.2.3 Total RNA extraction and protein quantification

Total RNA (including miRNA) was extracted using an miRNeasy Mini Kit (Qiagen, Catalogue No. 217004) according to the protocol provided by the manufacturer. Culture medium from treated cells was stored at -80°C until further analysis. Protein secreted into the culture medium was quantified using a Quantikine® human SOST ELISA (R&D Systems) according to the protocol provided by the manufacturer with some modifications (section 2.3.8).

### 5.2.4 Total DNA extraction for sclerostin protein normalisation

DNA extraction was carried out using a CyQUANT® cell proliferation assay kit (Life Technologies, Catalogue No.C7026) according to the manufacturer's protocol. The total quantity of DNA was used to normalise the SOST protein secreted by TE-85 and SaOS-2 cells.

## 5.3 Results

### 5.3.1 miRNA target prediction – Bioinformatic analysis

We used five different online prediction algorithms (miRWalk, miRanda, Pictar, RNA22 and Targetscan) to identify miRNA candidates that might target the protein of our interest, sclerostin. Based on the predictions, six miRNAs (hsa-miR-1231, hsa-miR-103a-3p, hsa-miR-1914, hsa-miR-1254, hsa-miR-378a-3p and hsa-miR-422a) were selected for further investigation. Table 5.1 shows the prediction of the miRNAs by all five prediction algorithms. The expression of these sclerostin targeting miRNAs was not investigated in MG-63 due to undetectable level of sclerostin mRNA in MG-63 as we reported in chapter 3.

Table 5.1: miRNAs expressed in TE-85 and SaOS-2 cells that are predicted to target sclerostin mRNA using different prediction tools (miRWalk, miRanda, Pictar, RNA22 and Targetscan). 1 denotes predicted, 0 denotes not predicted.

| miRNA | miRWalk | miRanda | Pictar | RNA22 | Targetscan | SUM |
|---|---|---|---|---|---|---|
| hsa-miR-1231 | 1 | 1 | 1 | 1 | 1 | 5 |
| hsa-miR-103a-3p | 1 | 1 | 0 | 1 | 1 | 4 |
| hsa-miR-1914 | 1 | 1 | 0 | 1 | 1 | 4 |
| hsa-miR-1254 | 1 | 1 | 0 | 1 | 1 | 4 |
| hsa-miR-378a-3p | 0 | 1 | 0 | 1 | 1 | 3 |
| hsa-miR-422a | 0 | 1 | 0 | 1 | 1 | 3 |

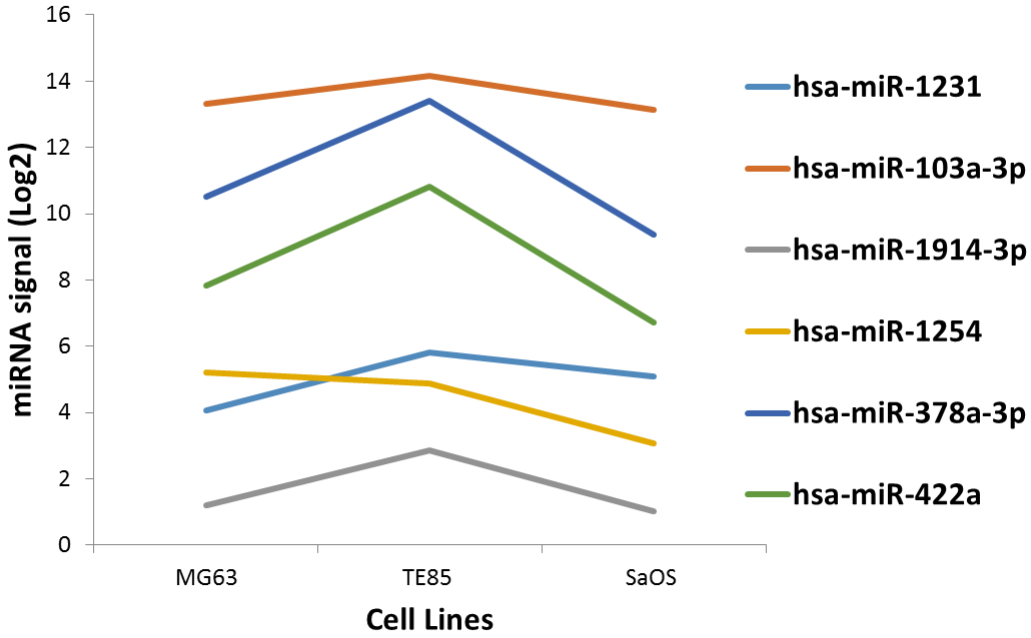


Figure 5.1: Expression of the selected miRNAs that were predicted to target sclerostin in osteosarcoma cell lines.

The expression of the selected miRNAs in the cell lines clearly shows that all of these miRNAs were expressed higher in TE-85 compared to MG-63 and SaOS-2. High expression of these miRNAs could result in lower expression of one of the target genes, SOST. This result is consistent with the result from chapter 3 where SOST expression was significantly lower in TE-85 compared to SaOS-2. We were unable to compare the expression of SOST in MG-63 because SOST is not expressed in MG-63 as shown in chapter 3.The expression of these selected miRNAs that are predicted to target SOST in MG-63 is because each miRNA may involve in the regulation of many genes as its targets and one gene may be controlled by many miRNAs (Hashimoto *et al.*, 2013). Hence, we believe that the expression of these miRNAs in MG-63 is to regulate the expression of other genes.

Table 5.2: Putative miRNA binding sites on SOST mRNA predicted by the chosen algorithms.

| | **Predicted consequential pairing of target region (top) and miRNA (bottom)** |
|---|---|
| Position 355-361 of SOST 3' UTR<br><br>**hsa-miR-378a-3p** | 5' ...GUGUGGGAGUGGGAAAGUCCAGG...<br>3' CGGAAGACUGAGGUUCAGGUCA |
| Position 1567-1574 of SOST 3' UTR<br><br>**hsa-miR-378a-3p** | 5' ...AGUCUGUUCUUCCAGAGUCCAGA...<br>3' CGGAAGACUGAGGUUCAGGUCA |
| Position 355-361 of SOST 3' UTR<br><br>**hsa-miR-422a** | 5' ...GUGUGGGAGUGGGAAAGUCCAGG...<br>3' CGGAAGACUGGGAUUCAGGUCA |
| Position 1567-1574 of SOST 3' UTR<br><br>**hsa-miR-422a** | 5' ...AGUCUGUUCUUCCAGAGUCCAGA...<br>3' CGGAAGACUGGGAUUCAGGUCA |
| Position 826-832 of SOST 3' UTR<br><br>**hsa-miR-103a-3p** | 5' ...CUCCUGGAAGAAGCUAUGCUGCU...<br>3' AGUAUCGGGACAUGUUACGACGA |
| Position 1299-1306 of SOST 3' UTR<br><br>**hsa-miR-1231** | 5' ...UUUUGAAAAUCAUUUCCAGACAA...<br>3' CGUCGACAGGCGGGUCUGUG |
| Position 137-143 of SOST 3' UTR<br><br>**hsa-miR-1254** | 5' ...AGGGGGCUGAGACCUUCCAGGCC...<br>3' UGACGUCCGAGGUCGA-AGGUCCGA |
| Position 870-876 of SOST 3' UTR<br><br>**hsa-miR-1914** | 5' ...UGUUUGGCUACCUCCACCCCUCC...<br>3' GGAGGGUCACGCCCUGGGGAGG |

Table 5.2 shows the putative binding sites of the miRNAs on the sclerostin mRNAs. Two of the miRNAs, miR-378a-3p and miR-422a were predicted to bind to two different sites. The binding site or the nucleotide sequence where the binding of miRNA and mRNA occurs is also known as seed region.

### 5.3.2 Transient transfection of cells with miRNA mimics and inhibitors and sclerostin protein secretion

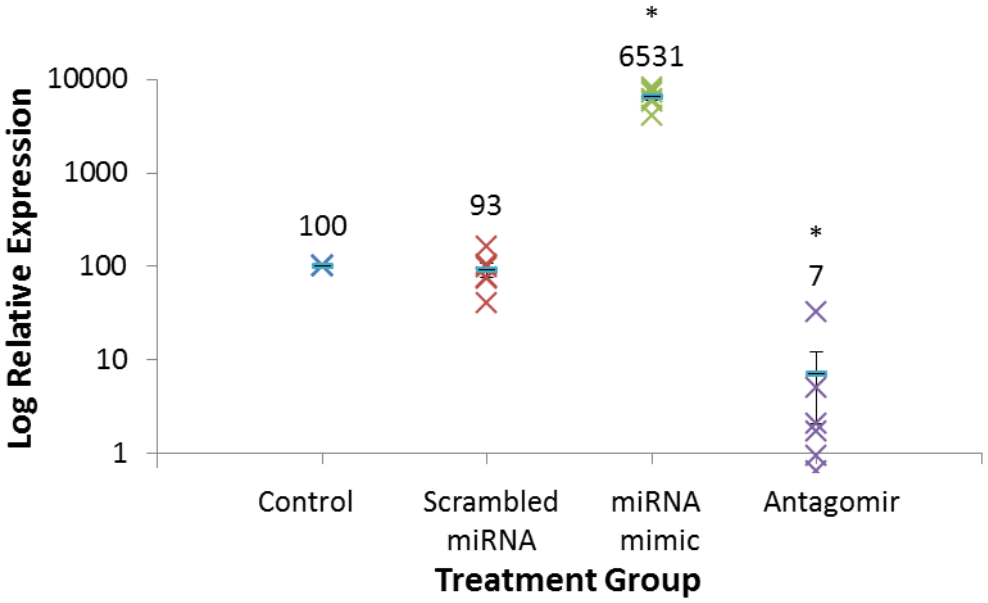


Figure 5.2: Expression of miR-103a-3p in SaOS-2 transfected with scrambled miRNA, miR-103a-3p mimic and antagomir. The expression of miR-103a-3p was normalised to the expression of RNU6-2. Data is presented as mean expression of 6 biological replicates (n=6) ± SE. * indicates a significant difference compared to the negative control as analysed by One-Way Independent ANOVA and LSD Post-Hoc test ($p<0.05$).


Figure 5.3: Expression of miR-103a-3p in TE-85 transfected with scrambled miRNA, miR-103a-3p mimic and antagomir. The expression of miR-103a-3p was normalised to the expression of RNU6-2. Data is presented as mean expression of 6 biological replicates (n=6) ± SE. * indicates a significant difference compared to the negative control as analysed by One-Way ANOVA and LSD Post-Hoc test ($p<0.05$).

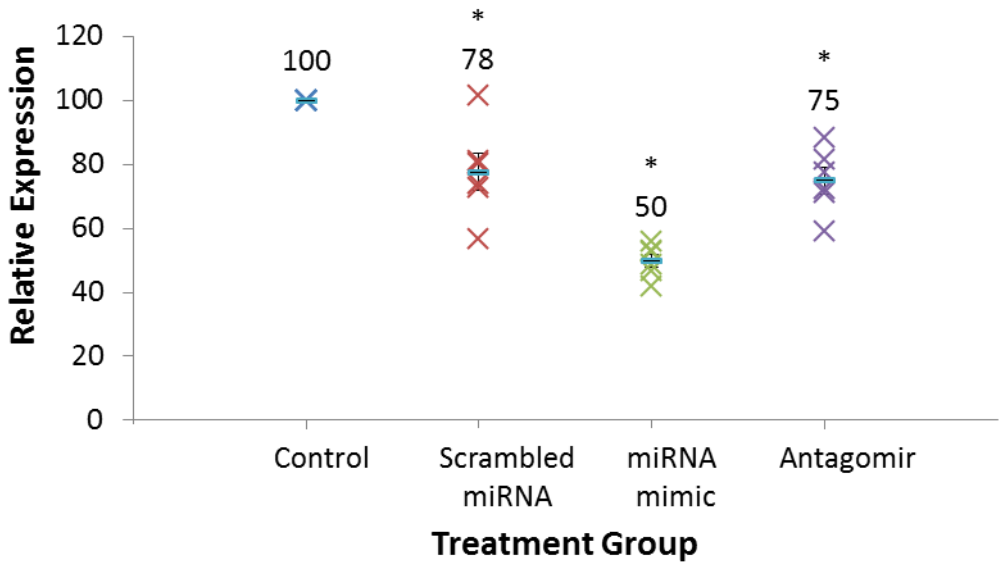


Figure 5.4: Expression of sclerostin gene in SaOS-2 transfected with scrambled miRNA, miR-103a-3p mimic and antagomir. The expression of sclerostin was normalised to the expression of ß-actin. Data is presented as mean expression of 6 biological replicates (n=6) ± SE. * indicates a significant difference compared to the negative control as analysed by One-Way Independent ANOVA and LSD Post-Hoc test ($p<0.05$).

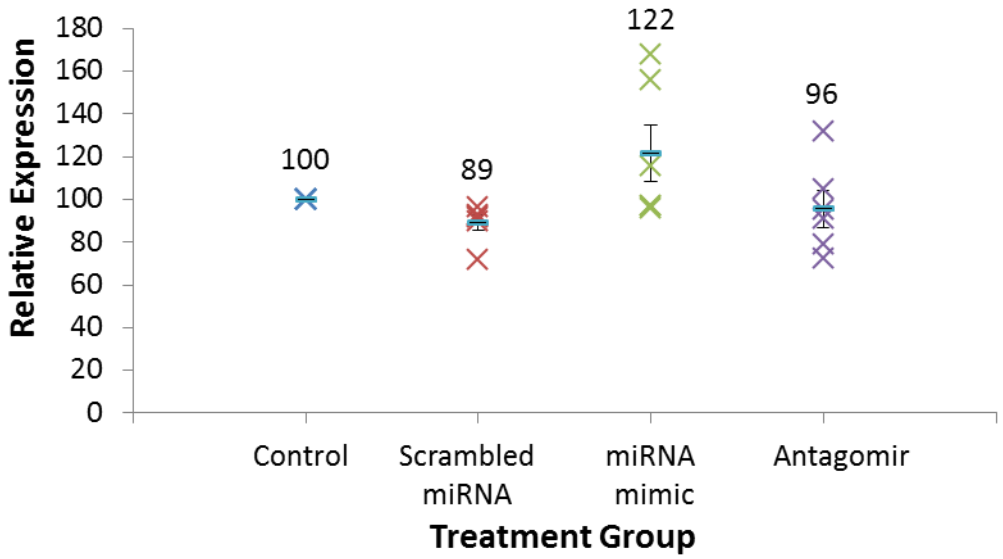


Figure 5.5: Expression of sclerostin gene in TE-85 transfected with scrambled miRNA, miR-103a-3p mimic and antagomir. The expression of sclerostin was normalised to the expression of ß-actin. Data is presented as mean expression of 6 biological replicates (n=6) ± SE. * indicates a significant difference compared to the negative control as analysed by One-Way Independent ANOVA and LSD Post-Hoc test ($p<0.05$).

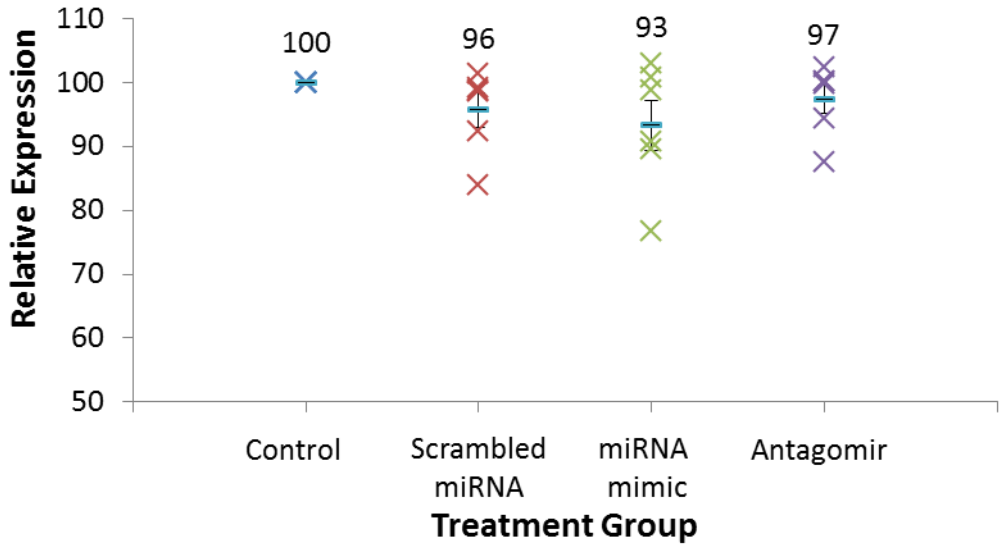


Figure 5.6: Expression of sclerostin in media from SaOS-2 transfected with scrambled miRNA, miR-103a-3p mimic and antagomir. The expression of sclerostin was normalised to the total DNA content. Data is presented as mean expression of 6 biological replicates (n=6) ± SE. * indicates a significant difference compared to the negative control as analysed by One-Way Independent ANOVA and LSD Post-Hoc test ($p<0.05$).

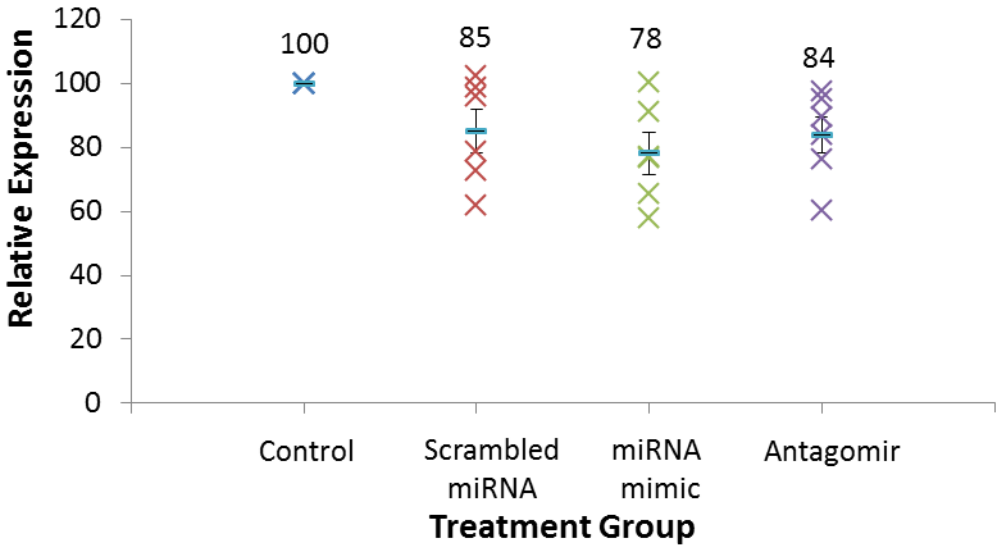


Figure 5.7: Expression of sclerostin in media from TE-85 transfected with scrambled miRNA, miR-103a-3p mimic and antagomir. The expression of sclerostin was normalised to the total DNA content. Data is presented as mean expression of 6 biological replicates (n=6) ± SE. * indicates a significant difference compared to the negative control as analysed by One-Way Independent ANOVA and LSD Post-Hoc test ($p<0.05$).

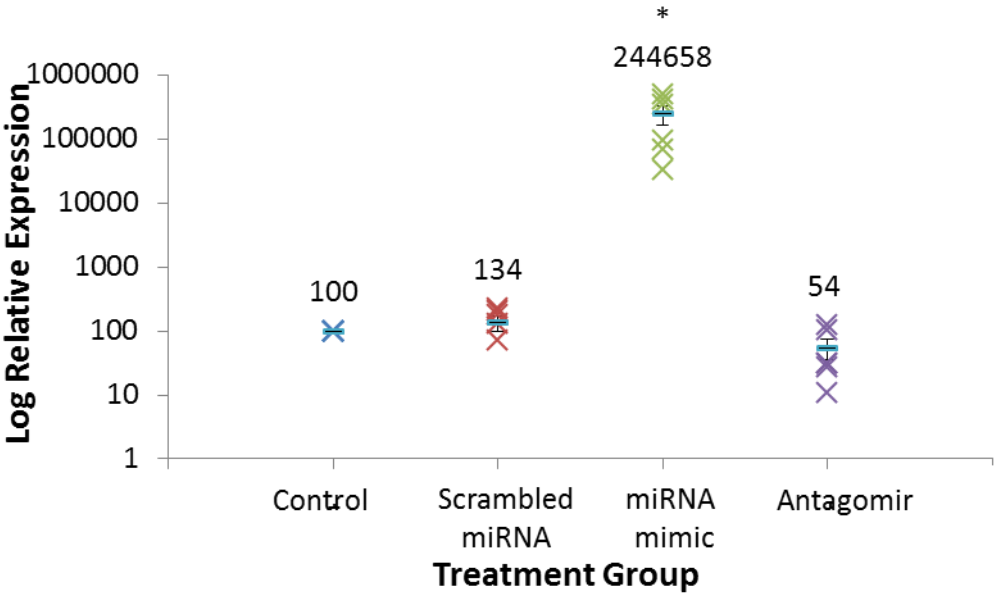


Figure 5.8 Expression of miR-378a-3p in SaOS-2 transfected with scrambled miRNA, miR-378a-3p mimic and antagomir. The expression of miR-378a-3p was normalised to the expression of RNU6-2. Data is presented as mean expression of 6 biological replicates (n=6) ± SE. * indicates a significant difference compared to the negative control as analysed by One-Way Independent ANOVA and LSD Post-Hoc test ($p<0.05$).

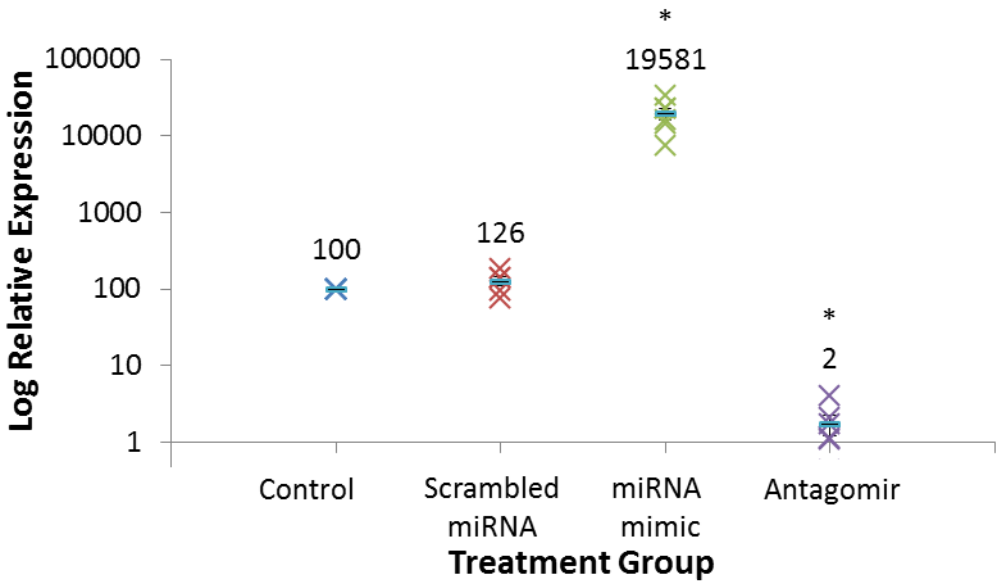


Figure 5.9 Expression of miR-378a-3p in TE-85 transfected with scrambled miRNA, miR-378a-3p mimic and antagomir. The expression of miR-378a-3p was normalised to the expression of RNU6-2. Data is presented as mean expression of 6 biological replicates (n=6) ± SE. * indicates a significant difference compared to the negative control as analysed by One-Way Independent ANOVA and LSD Post-Hoc test ($p<0.05$).

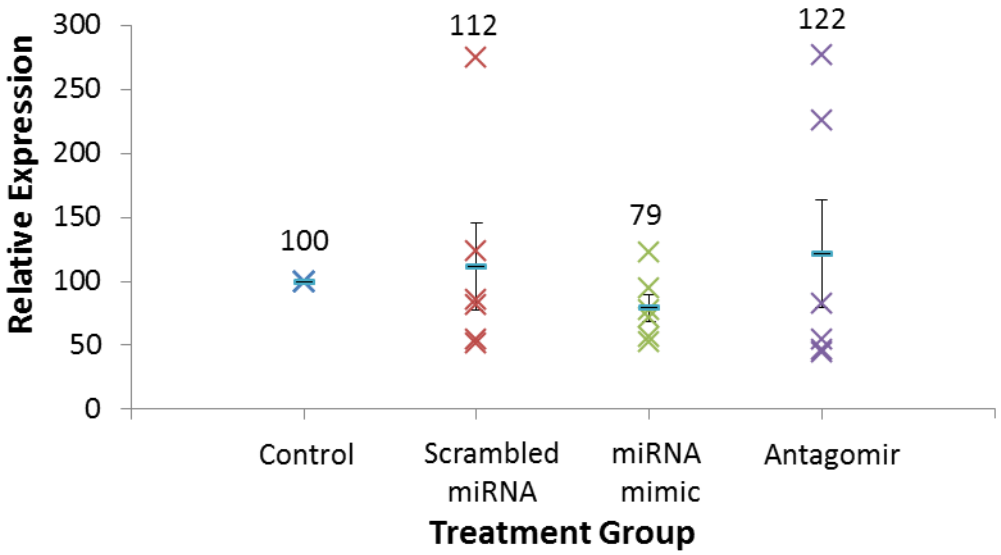


Figure 5.10: Expression of sclerostin gene in SaOS-2 transfected with scrambled miRNA, miR-378a-3p mimic and antagomir. The expression of sclerostin was normalised to the expression of ß-actin. Data is presented as mean expression of 6 biological replicates (n=6) ± SE. * indicates a significant difference compared to the negative control as analysed by One-Way Independent ANOVA and LSD Post-Hoc test ($p<0.05$).

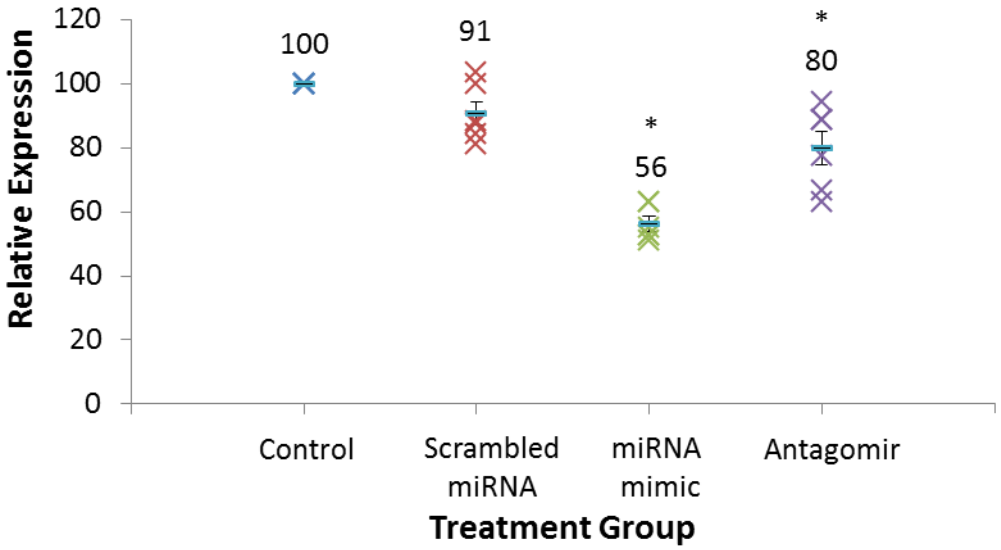


Figure 5.11 Expression of sclerostin gene in TE-85 transfected with scrambled miRNA, miR-378a-3p mimic and antagomir. The expression of sclerostin was normalised to the expression of ß-actin. Data is presented as mean expression of 6 biological replicates (n=6) ± SE. * indicates a significant difference compared to the negative control as analysed by One-Way Independent ANOVA and LSD Post-Hoc test ($p<0.05$).

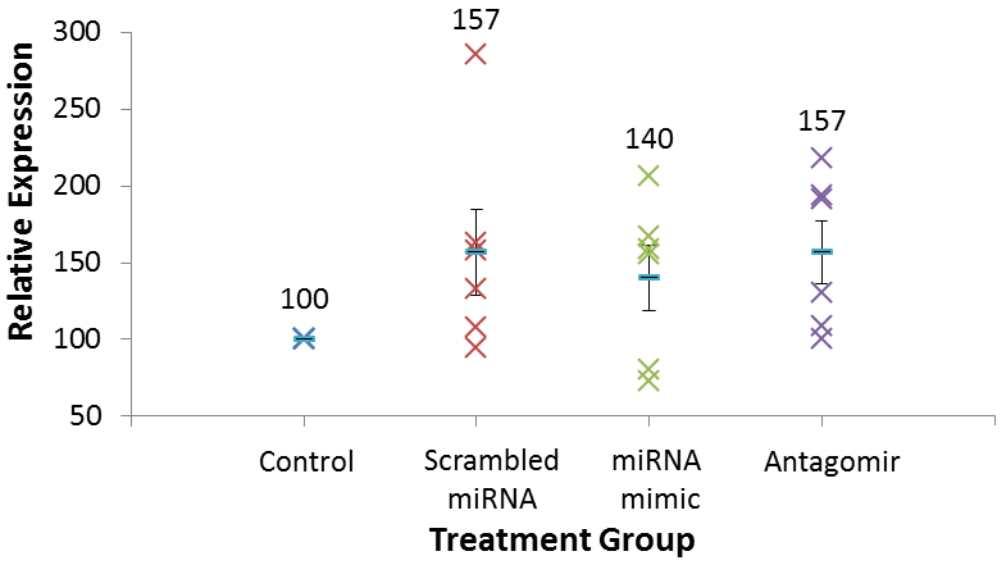


Figure 5.12: Expression of sclerostin in media from SaOS-2 transfected with scrambled miRNA, miR-378a-3p mimic and antagomir. The expression of sclerostin was normalised to the total DNA content. Data is presented as mean expression of 6 biological replicates (n=6) ± SE. * indicates a significant difference compared to the negative control as analysed by One-Way Independent ANOVA and LSD Post-Hoc test ($p<0.05$).

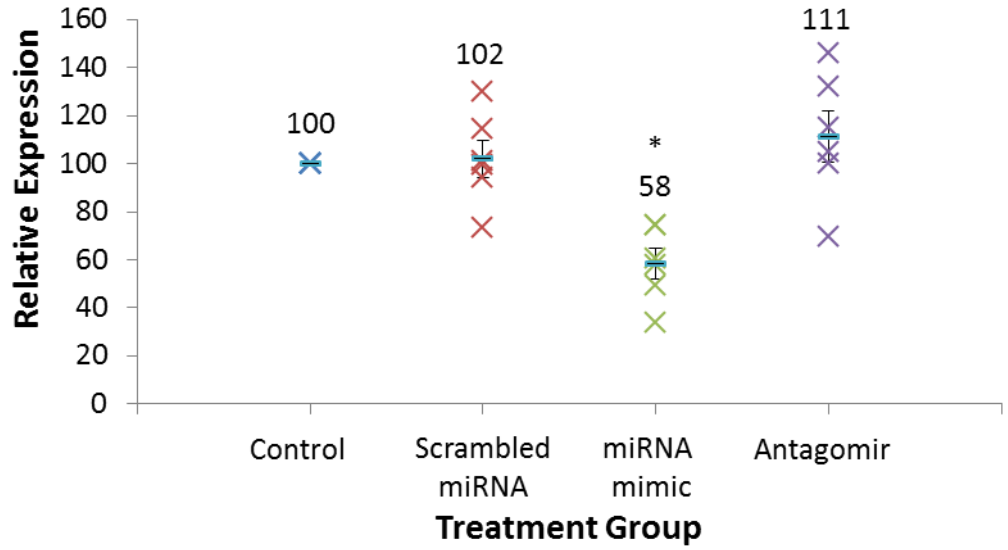


Figure 5.13: Expression of sclerostin in media from TE-85 transfected with scrambled miRNA, miR-378a-3p mimic and antagomir. The expression of sclerostin was normalised to the total DNA content. Data is presented as mean expression of 6 biological replicates (n=6) ± SE. * indicates a significant difference compared to the negative control as analysed by One-Way Independent ANOVA and LSD Post-Hoc test ($p<0.05$).

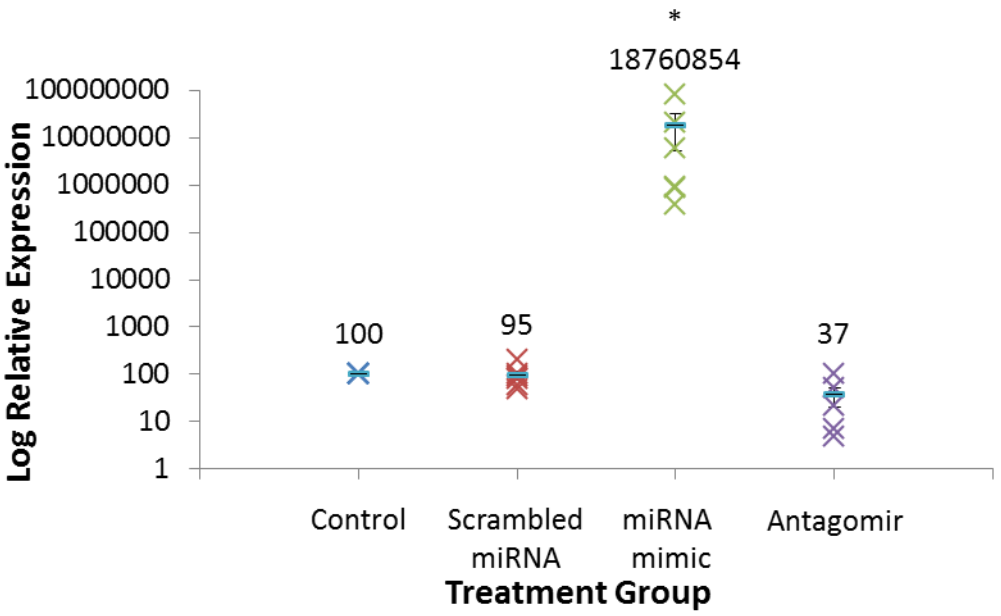


Figure 5.14: Expression of miR-422a in SaOS-2 transfected with scrambled miRNA, miR-422a mimic and antagomir. The expression of miR-422a was normalised to the expression of RNU6-2. Data is presented as mean expression of 6 biological replicates (n=6) ± SE. * indicates a significant difference compared to the negative control as analysed by One-Way Independent ANOVA and LSD Post-Hoc test ($p<0.05$).

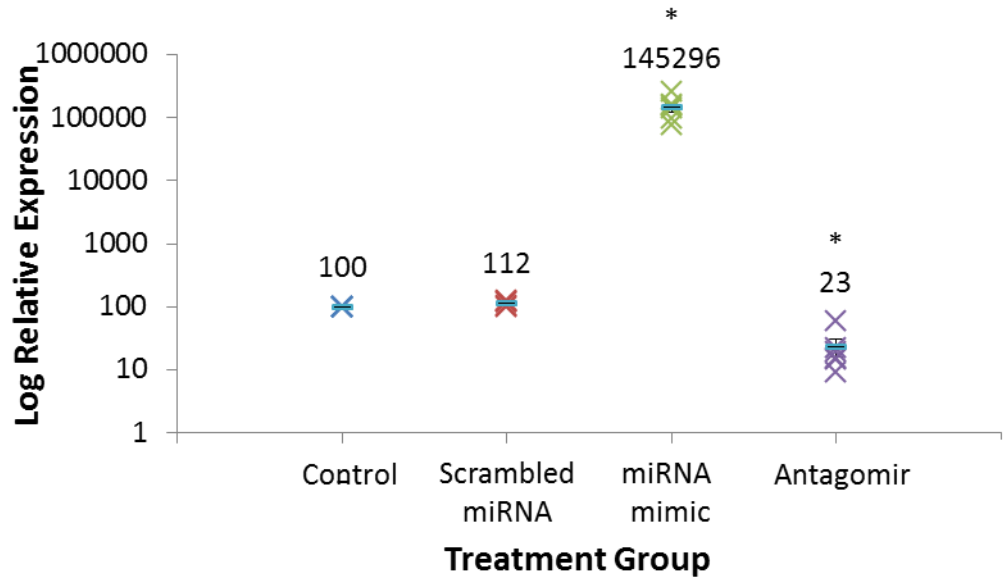


Figure 5.15: Expression of miR-422a in TE-85 transfected with scrambled miRNA, miR-422a mimic and antagomir. The expression of miR-422a was normalised to the expression of RNU6-2. Data is presented as mean expression of 6 biological replicates (n=6) ± SE. * indicates a significant difference compared to the negative control as analysed by One-Way Independent ANOVA and LSD Post-Hoc test ($p<0.05$).

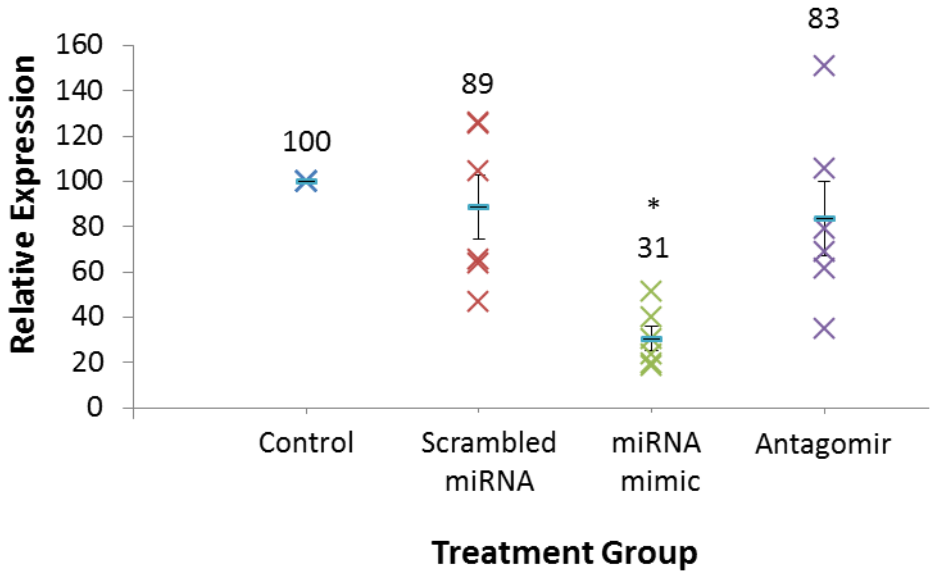


Figure 5.16: Expression of sclerostin gene in SaOS-2 transfected with scrambled miRNA, miR-422a mimic and antagomir. The expression of sclerostin was normalised to the expression of ß-actin. Data is presented as mean expression of 6 biological replicates (n=6) ± SE. * indicates a significant difference compared to the negative control as analysed by One-Way Independent ANOVA and LSD Post-Hoc test ($p<0.05$).

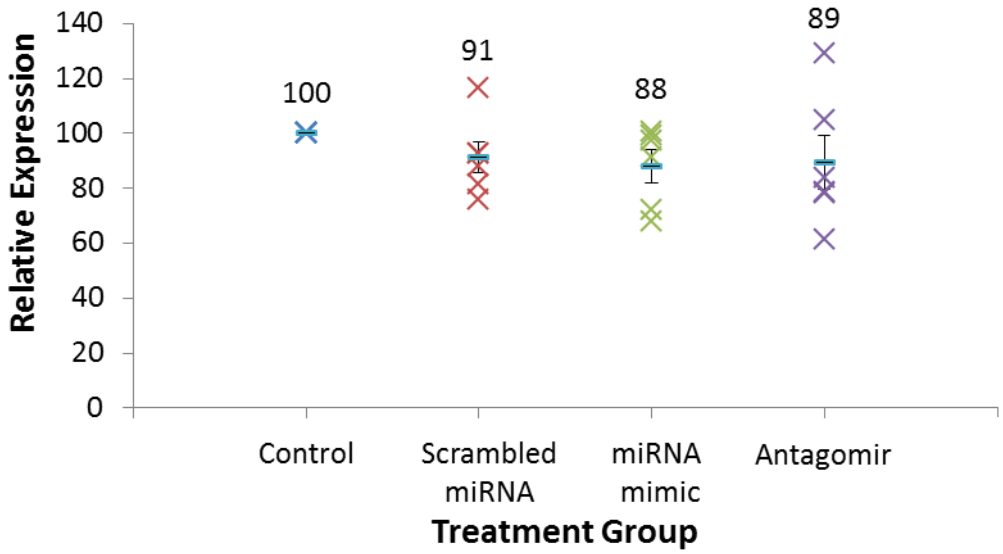


Figure 5.17: Expression of sclerostin gene in TE-85 transfected with scrambled miRNA, miR-422a mimic and antagomir. The expression of sclerostin was normalised to the expression of ß-actin. Data is presented as mean expression of 6 biological replicates (n=6) ± SE. * indicates a significant difference compared to the negative control as analysed by One-Way Independent ANOVA and LSD Post-Hoc test ($p<0.05$).

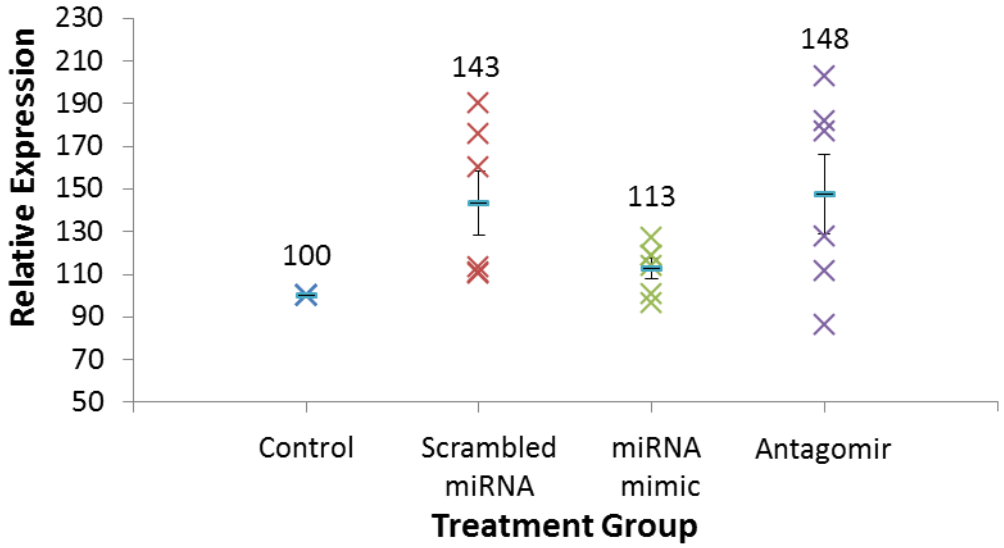


Figure 5.18: Expression of sclerostin in media from SaOS-2 transfected with scrambled miRNA, miR-422a mimic and antagomir. The expression of sclerostin was normalised to the total DNA content. Data is presented as mean expression of 6 biological replicates (n=5-6) ± SE. * indicates a significant difference compared to the negative control as analysed by One-Way Independent ANOVA and LSD Post-Hoc test ($p<0.05$).

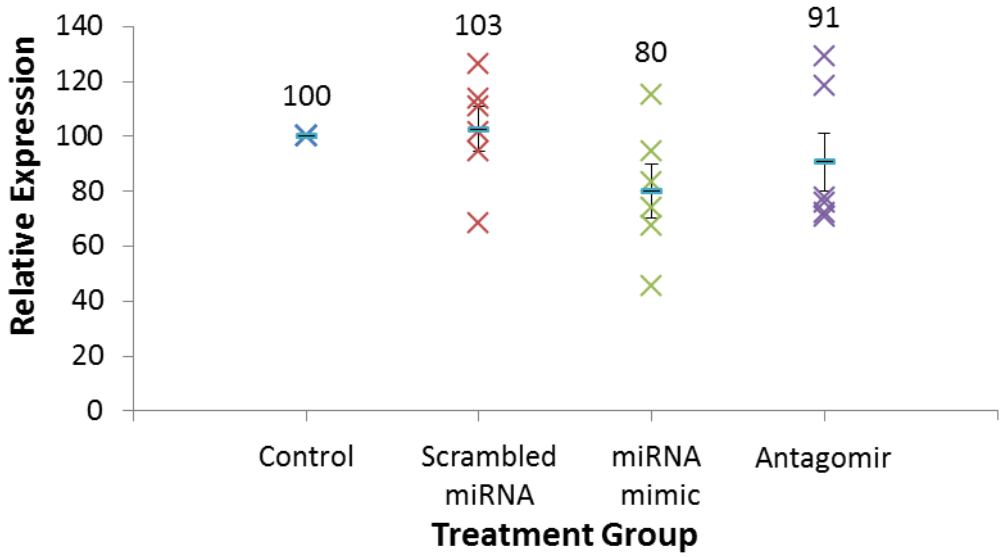


Figure 5.19: Expression of sclerostin in media from TE-85 transfected with scrambled miRNA, miR-422a mimic and antagomir. The expression of sclerostin was normalised to the total DNA content. Data is presented as mean expression of 6 biological replicates (n=6) ± SE. * indicates a significant difference compared to the negative control as analysed by One-Way Independent ANOVA and LSD Post-Hoc test ($p<0.05$).

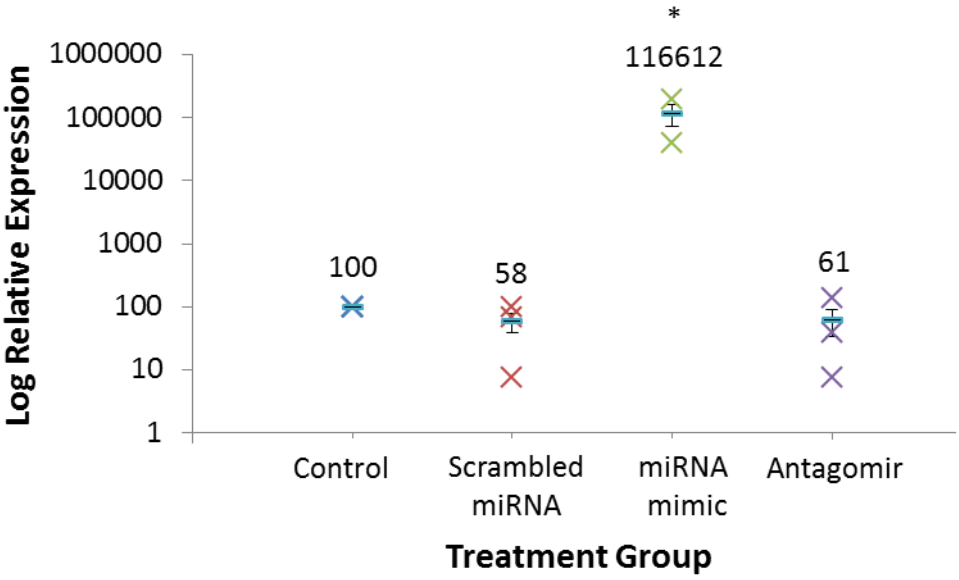


Figure 5.20: Expression of miR-1231 in SaOS-2 transfected with scrambled miRNA, miR-1231 mimic and antagomir. The expression of miR-1231 was normalised to the expression of RNU6-2. Data is presented as mean expression of 6 biological replicates (n=6) ± SE. * indicates a significant difference compared to the negative control as analysed by One-Way Independent ANOVA and LSD Post-Hoc test ($p<0.05$).

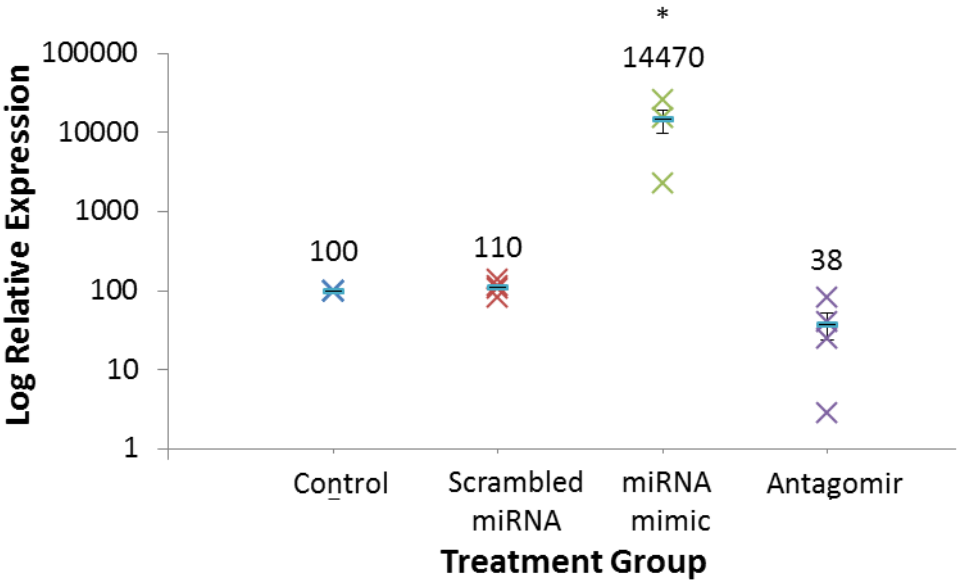


Figure 5.21: Expression of miR-1231 in TE-85 transfected with scrambled miRNA, miR-1231 mimic and antagomir. The expression of miR-1231 was normalised to the expression of RNU6-2. Data is presented as mean expression of 6 biological replicates (n=3-6) ± SE. * indicates a significant difference compared to the negative control as analysed by One-Way Independent ANOVA and LSD Post-Hoc test ($p<0.05$).

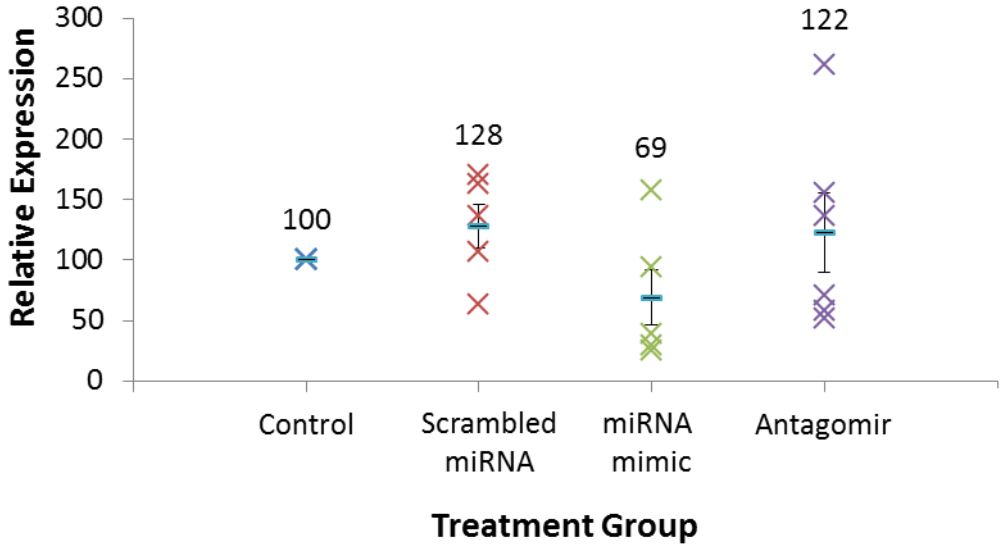


Figure 5.22: Expression of sclerostin gene in SaOS-2 transfected with scrambled miRNA, miR-1231 mimic and antagomir. The expression of sclerostin was normalised to the expression of ß-actin. Data is presented as mean expression of 6 biological replicates (n=5-6) ± SE. * indicates a significant difference compared to the negative control as analysed by One-Way Independent ANOVA and LSD Post-Hoc test ($p<0.05$).

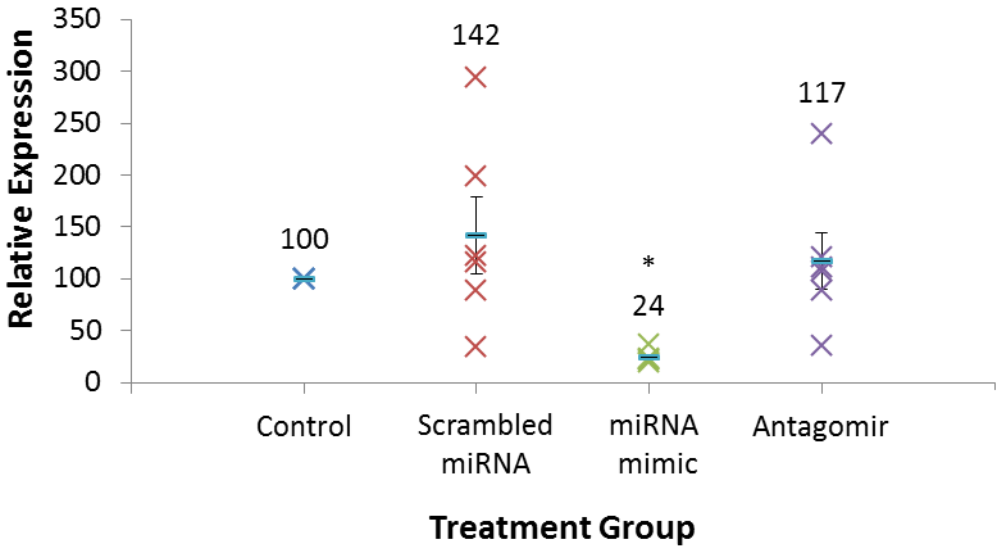


Figure 5.23: Expression of sclerostin gene in TE-85 transfected with scrambled miRNA, miR-1231 mimic and antagomir. The expression of sclerostin was normalised to the expression of ß-actin. Data is presented as mean expression of 6 biological replicates (n=6) ± SE. * indicates a significant difference compared to the negative control as analysed by One-Way Independent ANOVA and LSD Post-Hoc test ($p<0.05$).

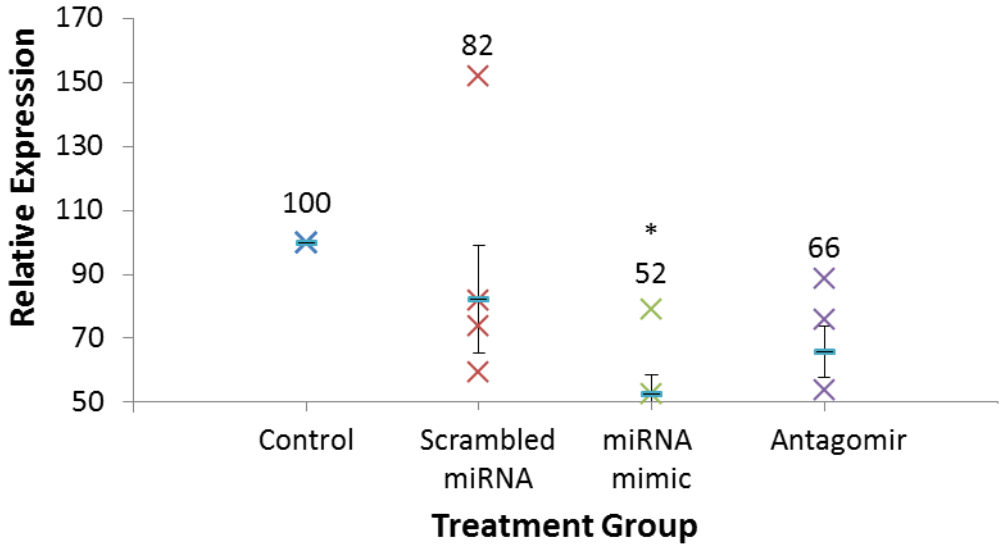


Figure 5.24: Expression of sclerostin in media from SaOS-2 transfected with scrambled miRNA, miR-1231 mimic and antagomir. The expression of sclerostin was normalised to the total DNA content. Data is presented as mean expression of 6 biological replicates (n=6) ± SE. * indicates a significant difference compared to the negative control as analysed by One-Way Independent ANOVA and LSD Post-Hoc test ($p<0.05$).

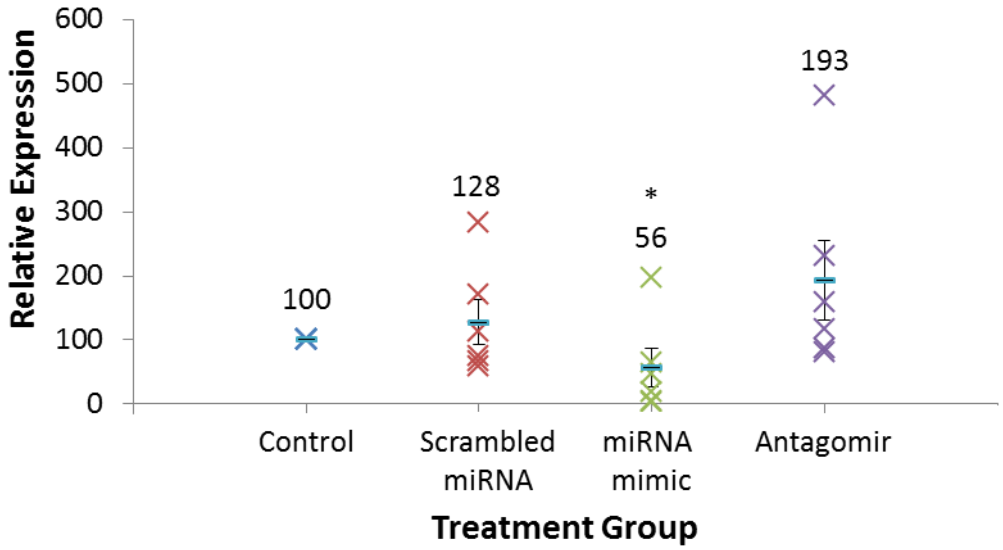


Figure 5.25: Expression of sclerostin in media from TE-85 transfected with scrambled miRNA, miR-1231 mimic and antagomir. The expression of sclerostin was normalised to the total DNA content. Data is presented as mean expression of 6 biological replicates (n=6) ± SE. * indicates a significant difference compared to the negative control as analysed by One-Way Independent ANOVA and LSD Post-Hoc test ($p<0.05$).

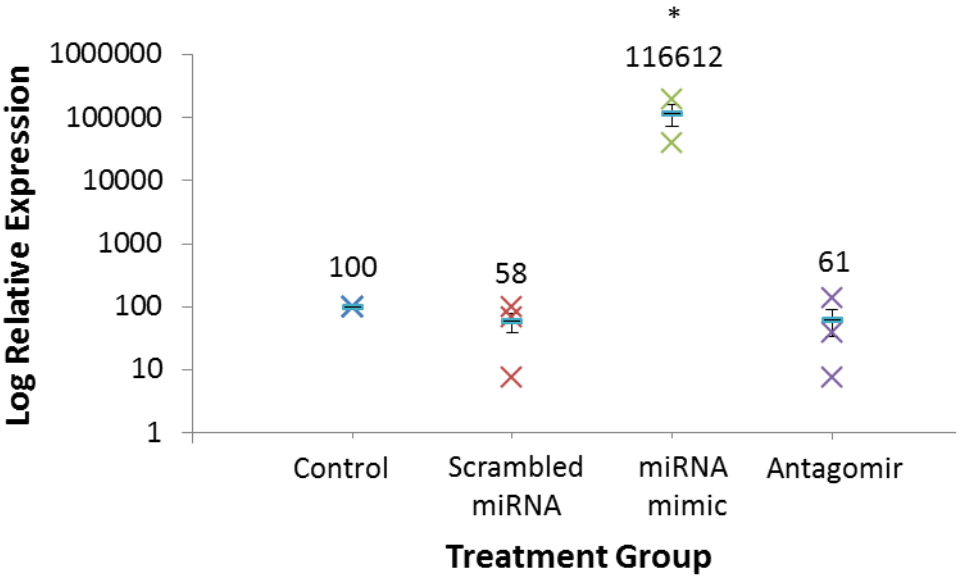


Figure 5.26: Expression of miR-1254 in SaOS-2 transfected with scrambled miRNA, miR-1254 mimic and antagomir. The expression of miR-1254 was normalised to the expression of RNU6-2. Data is presented as mean expression of 6 biological replicates (n=5-6) ± SE. * indicates a significant difference compared to the negative control as analysed by One-Way Independent ANOVA and LSD Post-Hoc test ($p<0.05$).

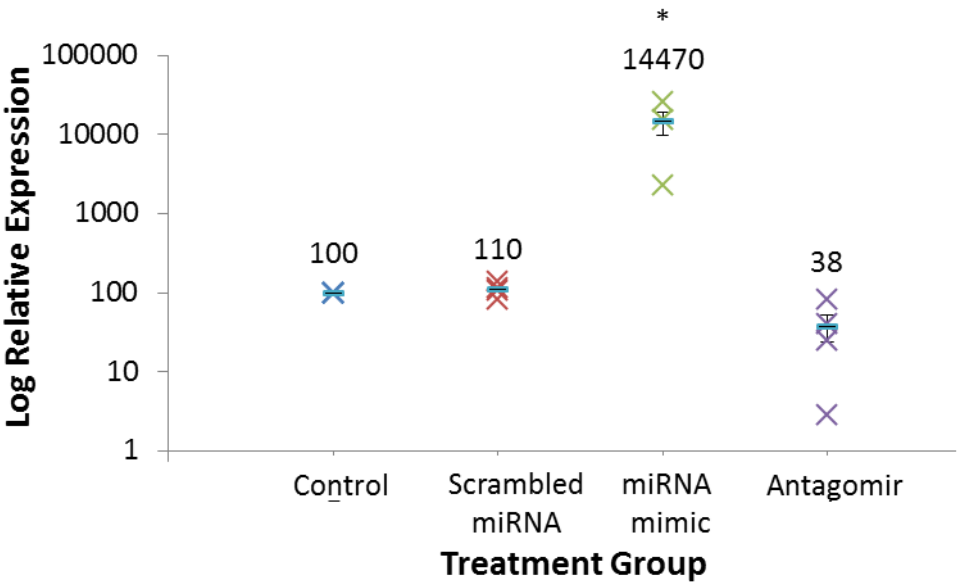


Figure 5.27: Expression of miR-1254 in TE-85 transfected with scrambled miRNA, miR-1254 mimic and antagomir. The expression of miR-1254 was normalised to the expression of RNU6-2. Data is presented as mean expression of 6 biological replicates (n=5-6) ± SE. * indicates a significant difference compared to the negative control as analysed by One-Way Independent ANOVA and LSD Post-Hoc test ($p<0.05$).

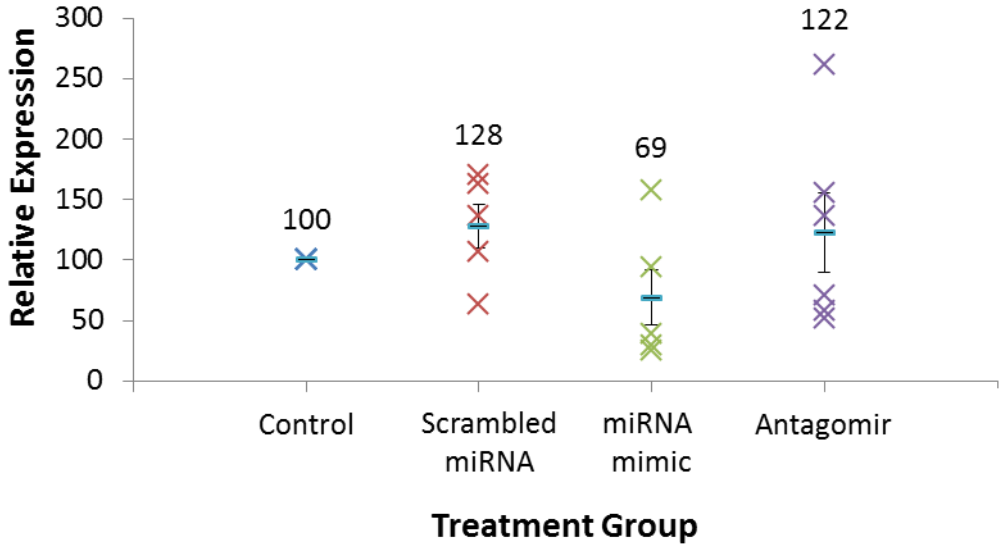


Figure 5.28: Expression of sclerostin gene in SaOS-2 transfected with scrambled miRNA, miR-1254 mimic and antagomir. The expression of sclerostin was normalised to the expression of ß-actin. Data is presented as mean expression of 6 biological replicates (n=5-6) ± SE. * indicates a significant difference compared to the negative control as analysed by One-Way Independent ANOVA and LSD Post-Hoc test ($p<0.05$).

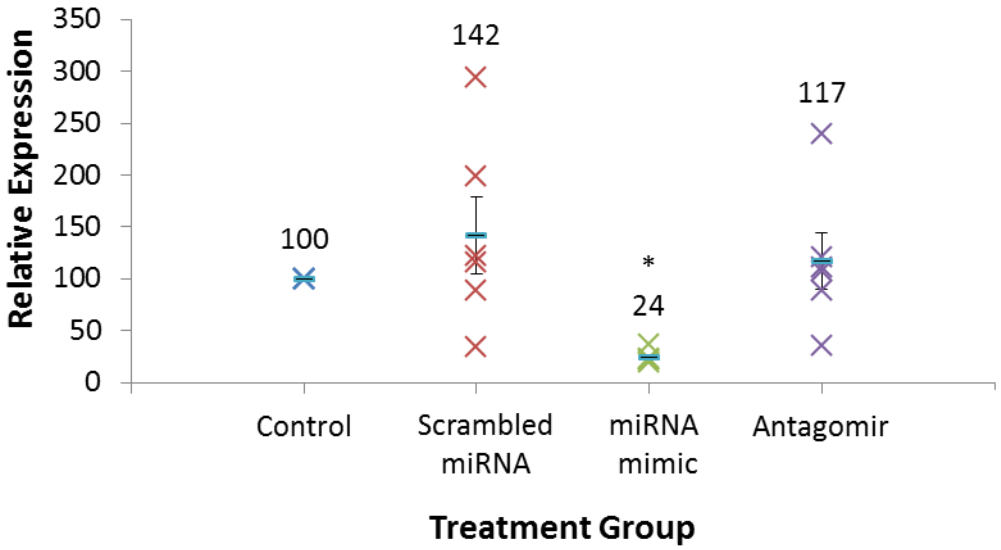


Figure 5.29: Expression of sclerostin gene in TE-85 transfected with scrambled miRNA, miR-1254 mimic and antagomir. The expression of sclerostin was normalised to the expression of ß-actin. Data is presented as mean expression of 6 biological replicates (n=6) ± SE. * indicates a significant difference compared to the negative control as analysed by One-Way Independent ANOVA and LSD Post-Hoc test ($p<0.05$).

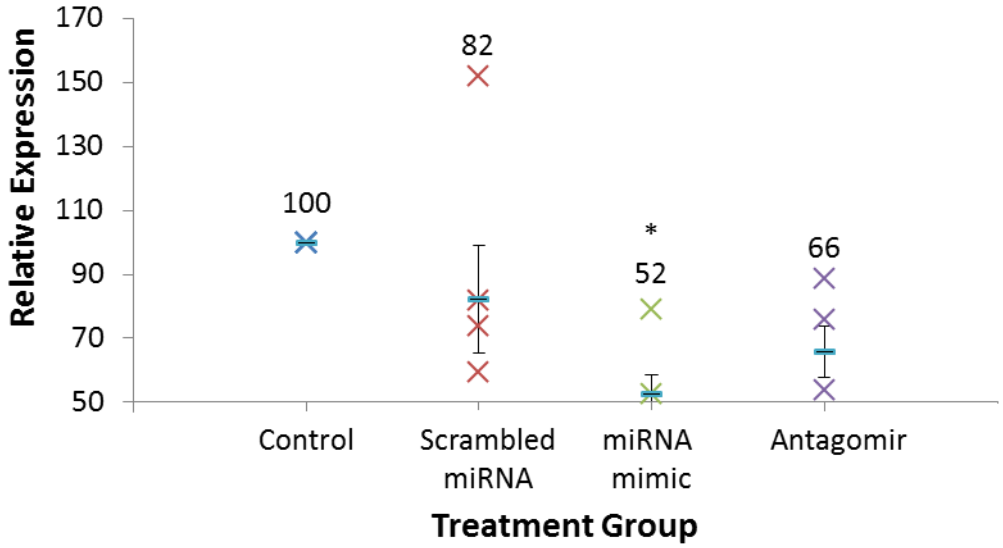


Figure 5.30: Expression of sclerostin in media from SaOS-2 transfected with scrambled miRNA, miR-1254 mimic and antagomir. The expression of sclerostin was normalised to the total DNA content. Data is presented as mean expression of 6 biological replicates (n=5-6) ± SE. * indicates a significant difference compared to the negative control as analysed by One-Way Independent ANOVA and LSD Post-Hoc test ($p<0.05$).

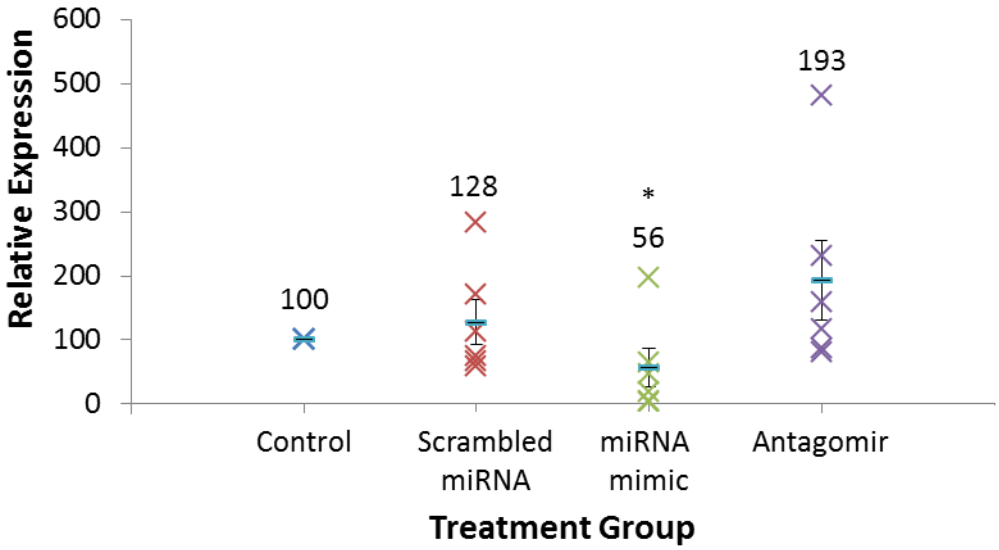


Figure 5.31: Expression of sclerostin in media from TE-85 transfected with scrambled miRNA, miR-1254 mimic and antagomir. The expression of sclerostin was normalised to the total DNA content. Data is presented as mean expression of 6 biological replicates (n=6) ± SE. * indicates a significant difference compared to the negative control as analysed by One-Way Independent ANOVA and LSD Post-Hoc test ($p<0.05$).

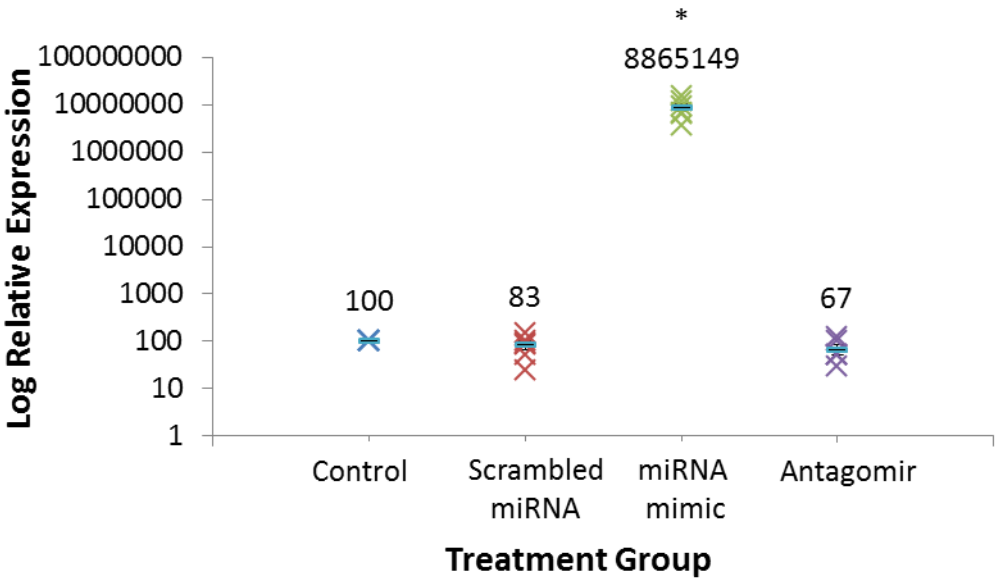


Figure 5.32: Expression of miR-1914 in SaOS-2 transfected with scrambled miRNA, miR-1914 mimic and antagomir. The expression of miR-1914 was normalised to the expression of RNU6-2. Data is presented as mean expression of 6 biological replicates (n=6) ± SE. * indicates a significant difference compared to the negative control as analysed by One-Way Independent ANOVA and LSD Post-Hoc test ($p<0.05$).

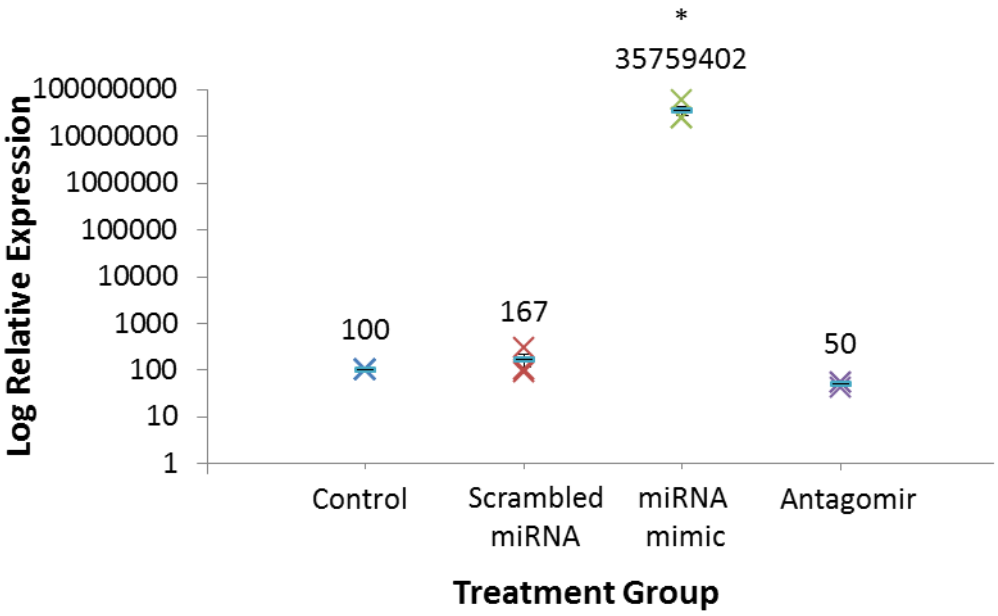


Figure 5.33: Expression of miR-1914 in TE-85 transfected with scrambled miRNA, miR-1914 mimic and antagomir. The expression of miR-1914 was normalised to the expression of RNU6-2. Data is presented as mean expression of 6 biological replicates (n=3) ± SE. * indicates a significant difference compared to the negative control as analysed by One-Way Independent ANOVA and LSD Post-Hoc test ($p<0.05$).

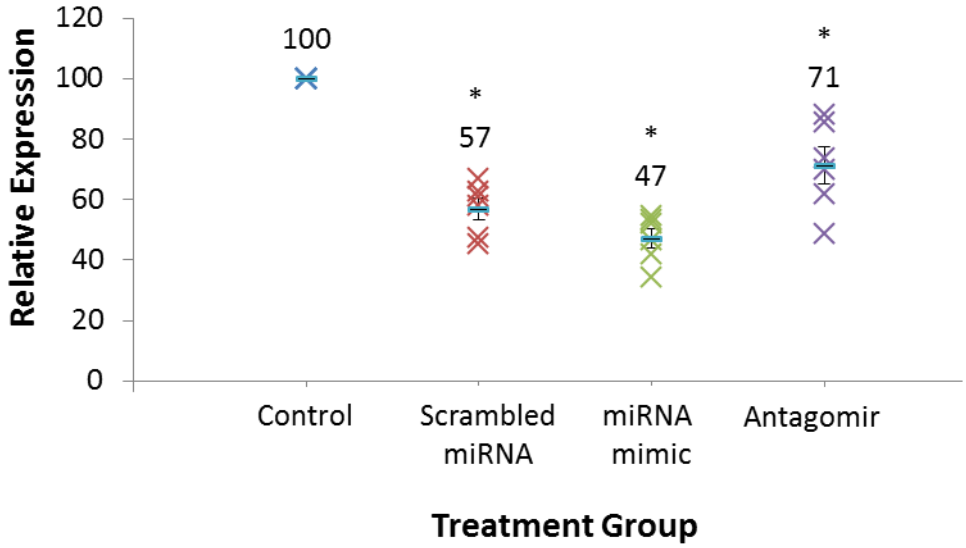


Figure 5.34: Expression of sclerostin gene in SaOS-2 transfected with scrambled miRNA, miR-1914 mimic and antagomir. The expression of sclerostin was normalised to the expression of ß-actin. Data is presented as mean expression of 6 biological replicates (n=6) ± SE. * indicates a significant difference compared to the negative control as analysed by One-Way Independent ANOVA and LSD Post-Hoc test ($p<0.05$).

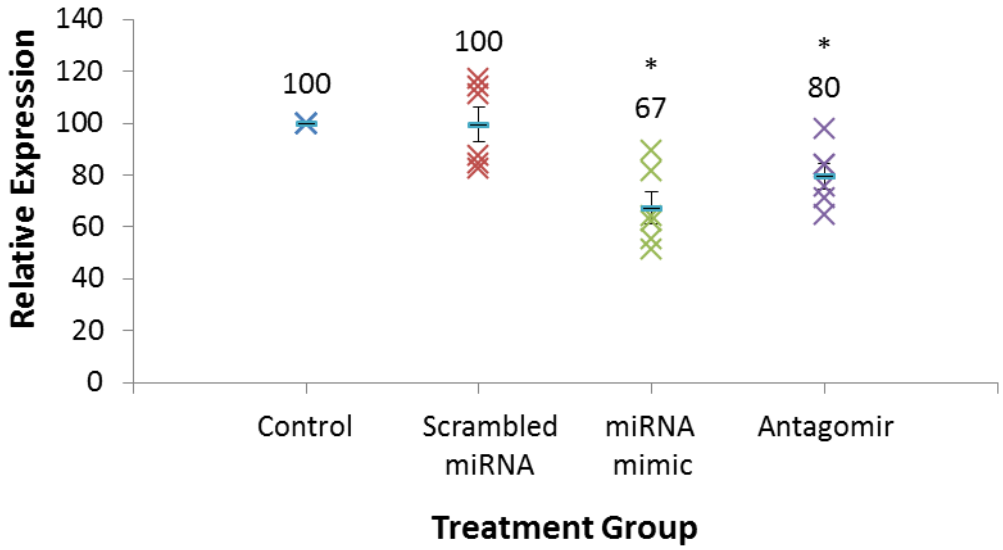


Figure 5.35: Expression of sclerostin gene in TE-85 transfected with scrambled miRNA, miR-1914 mimic and antagomir. The expression of sclerostin was normalised to the expression of ß-actin. Data is presented as mean expression of 6 biological replicates (n=6) ± SE. * indicates a significant difference compared to the negative control as analysed by One-Way Independent ANOVA and LSD Post-Hoc test ($p<0.05$).

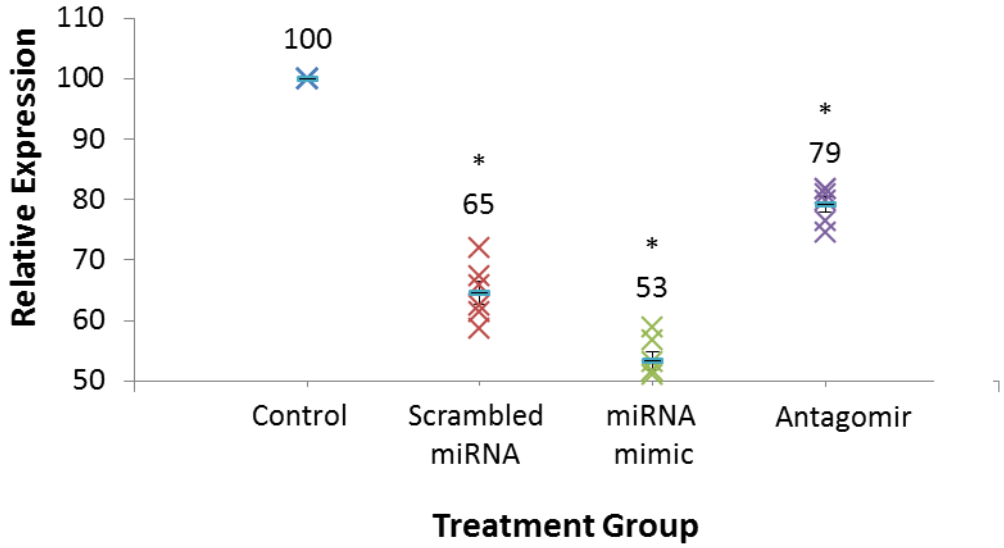


Figure 5.36: Expression of sclerostin in media from SaOS-2 transfected with scrambled miRNA, miR-1914 mimic and antagomir. The expression of sclerostin was normalised to the total DNA content. Data is presented as mean expression of 6 biological replicates (n=6) ± SE. * indicates a significant difference compared to the negative control as analysed by One-Way Independent ANOVA and LSD Post-Hoc test ($p<0.05$).

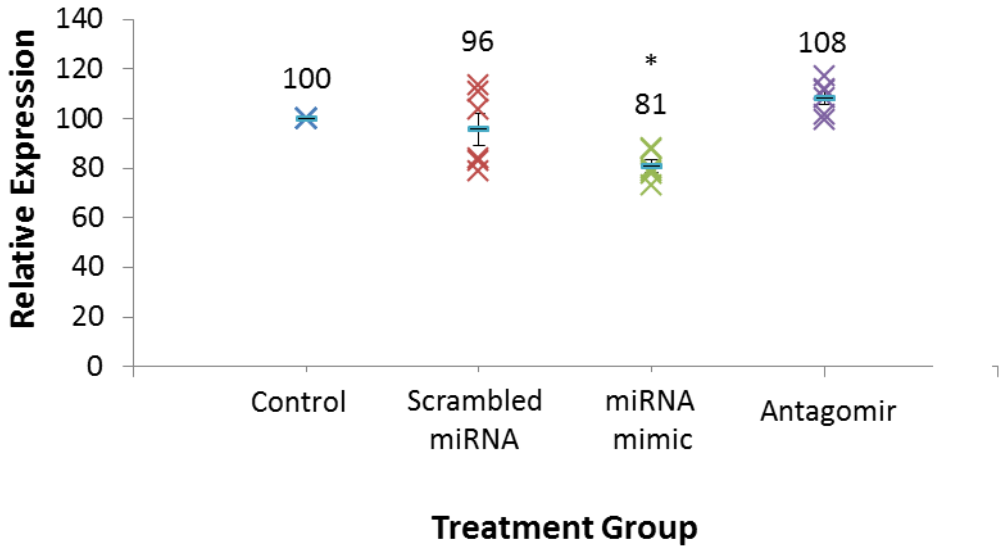


Figure 5.37: Expression of sclerostin in media from TE-85 transfected with scrambled miRNA, miR-1914 mimic and antagomir. The expression of sclerostin was normalised to the total DNA content. Data is presented as mean expression of 6 biological replicates (n=6) ± SE. * indicates a significant difference compared to the negative control as analysed by One-Way Independent ANOVA and LSD Post-Hoc test ($p<0.05$).

## 5.4 Discussion

### 5.4.1 miRNA target prediction – Bioinformatic analysis

In order to identify potential miRNAs that target sclerostin mRNA, we used five different miRNA target prediction tools: miRWalk, miRanda, Pictar, RNA22 and Targetscan. Each tool uses different characteristics of the interaction between miRNAs and target genes to predict miRNA targets: (1) miRWalk searches for perfect complementarities in the seed region of the miRNA-mRNA interaction and then extends it until a mismatch is found; (2) miRanda predict miRNA targets by using nucleotide sequence matching, miRNA and mRNA duplex stability and conservation of the target site; (3) Pictar is an abbreviation of "probabilistic identification of combination of target sites". Pictar predicts miRNA targets based on complementarity of the seed region, conservation of the sequence between species and the thermodynamics of the entire miRNA-mRNA duplex; (4) RNA22 creates a prediction based mainly on complementarities in the seed region and thermodynamics of the miRNA-mRNA duplex. RNA22 does not consider cross-species sequence conservation which are parameters utilised by miRanda, Pictar and Targetscan; (5) Targetscan predicts mammalian miRNA targets based on seed region complementarities and thermodynamics to predict conserved miRNA binding sites among different species (John *et al.*, 2004; Tabas-Madrid *et al.*, 2014; Xia *et al.*, 2009). We used all these miRNA prediction algorithms to increase the chance of finding an miRNA that very effectively targets sclerostin mRNA. MiRNAs that were predicted by the majority of the tools were thus chosen for further experimental analysis.

In this study, we identified several miRNAs which were predicted to interact with sclerostin mRNA. Six of these miRNAs were chosen for further analysis for verification of their functionality: hsa-miR-1231, hsa-miR-103a-3p, hsa-miR-1914,

hsa-miR-1254, hsa-miR-378a-3p and hsa-miR-422a (Table 5.1). Two of these miRNAs, miR-378a-3p and miR-422a were predicted to bind to sclerostin mRNA at two different sites each while miR-1914, miR-103a-3p, miR-1231 and miR-1254 were predicted to have only one binding site, all binding sites being 7-8 nucleotides long (Table 5.2). Mimics and inhibitors of these miRNAs were then transfected into TE-85 and SaOS-2 cells to evaluate the involvement of these miRNA in the regulation of sclerostin synthesis.

### 5.4.2 Validation of miRNA function

In this chapter, the expression of each miRNA in transfected TE-85 and SaOS2 cells was analysed using real-time PCR to evaluate whether miRNA transfection was successful. Theoretically, miRNA levels increase in cells transfected with miRNA mimics and decrease in cells transfected with miRNA inhibitor/antagomirs. To validate the function of selected miRNAs as negative sclerostin regulators, sclerostin gene expression was measured using real-time PCR and the sclerostin protein secreted into culture medium was measured using ELISA. It is anticipated that sclerostin gene expression and protein secretion would decrease in cells transfected with miRNA mimics and increase in cells transfected with antagomirs.

#### 5.4.2.1 miR-103a-3p transfection in SaOS-2 and TE-85 cells

The expression of miR-103a-3p level in SaOS-2 cells transfected with miRNA mimic was significantly higher and in cells transfected with antagomir it was significantly lower compared to the negative control and cells with scrambled miRNA. The results for TE-85 cells broadly mirrored those for SaOS-2 cells, where miR-103a-3p expression in cells transfected with miRNA mimic was significantly higher compared to negative control and scrambled miRNA, and significantly lower when transfected

with antagomir compared to the negative control and scrambled miRNA. This result demonstrates that the miRNA transfections were successful, entering the cells and exerting their function.

Sclerostin gene expression and protein secretion was also measured. In SaOS-2, sclerostin gene expression was significantly decreased in cells transfected with scrambled miRNA, miRNA mimic and antagomir compared to the negative control. However, there was no significant difference in the quantity of sclerostin protein secreted into the culture medium in any treatment group compared to the negative control. In TE-85 cells, there was no significant difference in sclerostin gene expression and amount of sclerostin protein secreted into culture media in all treatments compared to the negative control.

As scrambled miRNA does not bind to any known mammalian mRNA, we did not expect to see any significant difference in sclerostin gene or protein expression and in cells transfected with it compared to the negative control. However, in this experiment sclerostin gene expression in both SaOS-2 transfected with scrambled miRNA were significantly lower compared to negative control, $p<0.05$. It can therefore be assumed that miR-103a-3p alone might not efficiently inhibit sclerostin production by osteosarcoma cell lines.

#### 5.4.2.2 miR-378a-3p transfection in SaOS-2 and TE-85 cells

Transfection of miR-378a-3p mimic significantly increased its expression in both SaOS-2 and TE-85 cells compared to the negative control and scrambled miRNA. Cells transfected with miR-378a-3p antagomir demonstrated a significant decrease in miR-378a-3p expression in SaOS-2 and TE-85 cells compared to the negative

control and scrambled miRNA. These results show that the transfection process was efficient and thus we proceeded with gene expression analysis.

Sclerostin gene expression was not significantly reduced in SaOS-2 transfected with miRNA mimic compared to negative control and scrambled miRNA. There was a small, but not significant increase in sclerostin gene expression in SaOS-2 transfected with antagomir. However, miRNA mimic transfection in TE-85 showed a significant decrease in sclerostin gene expression compared to the negative control and scrambled miRNA. A significant decrease in sclerostin gene expression was also detected in TE-85 transfected with antagomir compared to negative control and scrambled miRNA.

Sclerostin protein quantification using ELISA showed that there was no significant difference in the quantity of sclerostin secreted into culture media by SaOS-2 cells between treatment groups and the negative control. What is interesting about this finding is that in TE-85, there was a significant reduction in sclerostin protein expression in cells transfected with miRNA mimic compared to the negative control and scrambled miRNA. This demonstrates that miR-378a-3p binds to sclerostin mRNA and is able to inhibit sclerostin protein translation. In TE-85 transfected with antagomir, there was an increase, although not significant, in sclerostin protein detected. This might be due to the nature of the antagomir which has moderate affinity to the related miRNA sequence and has to be used in relatively high concentrations compared to the miRNA mimic. Hence, we believe that by increasing the concentration of antagomir, its inhibitory effect would be significant.

#### 5.4.2.3 miR-422a transfection in SaOS-2 and TE-85 cells

SaOS-2 cells transfected with miR-422a mimic showed a significant increase of miR-422a expression compared to the control. Similar results were observed in TE-85 cells where a significant increase in miR-422a levels were detected in cells transfected with mimic and a significant decrease in cells transfected with antagomir, indicating successful miRNA transfection.

Transfection of miR-422a significantly reduced sclerostin gene expression in SaOS-2 compared to the control. Transfection of antagomir did not increase or decrease sclerostin expression level in SaOS-2. Meanwhile in TE-85, there was no change in sclerostin expression in all treatment groups compared to the control.

ELISA analysis showed that there was no significant different between the amount of sclerostin protein secreted into culture media by SaOS-2 transfected with miRNA mimic and antagomir compared to control. Same observation was recorded in TE-85 cells.

#### 5.4.2.4 miR-1231 transfection in SaOS-2 and TE-85 cells

The expression of miR-1231 and its antagomir in SaOS-2 and TE-85 cells demonstrated successful transfection, indicated by a significant increase in miR-1231 in cells transfected with miRNA mimic and significant decrease in antagomir transfection compared to the control.

There was no significant difference in the expression of sclerostin gene in SaOS-2 transfected with scrambled miRNA, miR-1231 mimic and antagomir compared to control. However, sclerostin gene expression in TE-85 was significantly lower in TE-85 transfected with miRNA mimic. Surprisingly, there was no significant different in sclerostin gene expression in SaOS-2 and TE-85 transfected with antagomir

compared to control. Theoretically, the expression of the sclerostin gene in cells transfected with antagomir should increase compared to the negative control. However, our findings again show that it was significantly decreased in both SaOS-2 and TE-85 transfected with antagomir compared to the negative control. As discussed previously, this could be due to the lower affinity of the antagomir to its miRNA target compared to that of the miRNA mimic.

Interestingly, the amount of sclerostin protein secreted into the culture media was significantly lower in both SaOS-2 and TE-85 transfected with miR-1231 mimic compared to control. This result suggests that miR-1231 could reduce the sclerostin protein translation by blocking the mRNA transcript for sclerostin.

#### 5.4.2.5 miR-1254 transfection in SaOS-2 and TE-85 cells

A significant increase in miR-1254 expression was detected in SaOS-2 and TE-85 transfected with miRNA mimic compared to the negative control, indicating that transfection was achieved efficiently.

In SaOS-2 cells, transfection with miRNA mimic did not significantly reduce sclerostin gene expression. Meanwhile, in TE-85 transfected with miRNA mimic a significant decrease of sclerostin gene expression was observed compared to the negative control.

Analysis by ELISA showed that there was a significant decrease in sclerostin protein secretion by both SaOS-2 and TE-85. However, transfection with antagomir did not increase sclerostin protein secretion in both cells. This result indicates that miR-1254 mimic was able to inhibit sclerostin production by osteosarcoma cell lines by inhibition of the translation of sclerostin mRNA.

#### 5.4.2.6 miR-1914 transfection in SaOS-2 and TE-85 cells

In SaOS-2 cells transfected with miRNA mimic, the expression of miR-1914 was significantly higher compared to the negative control, while that in cells transfected with antagomir was lower compared to the negative control but not significantly so. Those observations were mirrored in TE-85 cells transfected with miRNA mimic and antagomir compared to negative control.

Sclerostin gene expression was significantly lower than the negative control in SaOS-2 cells transfected with scrambled miRNA, miRNA mimic and antagomir. As scrambled miRNA does not bind to any known mammalian mRNA, gene expression in cells transfected with it should not be significantly different from the negative control. While in TE-85 cells, there was no significant difference in expression when transfected with scrambled miRNA compared to the negative control. A significant decrease in sclerostin gene expression was observed in TE-85 transfected with miRNA mimic and antagomir.

Analysis by ELISA showed a significant decrease in sclerostin protein secreted into the culture medium in SaOS-2 transfected with scrambled miRNA, miRNA mimic and antagomir. The quantity of sclerostin protein secreted by TE-85 cells transfected with miRNA mimic was also significantly lower compared to the control. This result demonstrates that miR-1914 has the potential to inhibit sclerostin protein production in SaOS-2 and TE-85 cells. To further validate SOST as the target of these miRNAs, *in vivo* test using mice is a most popular approach used by researchers. However, due to budget and time constrains, we only had the opportunity to study in vivo effect of miR-37a-3p on trabecular bone in mice which is reported in chapter 6.

## 5.5 Conclusions

In this chapter, the aim was to identify miRNAs involved in the regulation of SOST using well-characterised osteosarcoma cell lines. The main research findings are:

- miR-378a-3p decreased SOST protein expression in TE-85. miR-1231, miR-1254 and miR-1914 decrease SOST protein expression in both SaOS-2 and TE-85.
- surprisingly, transfection of antagomirs of all selected miRNAs, did not significantly increase SOST mRNA in either TE-85 or SaOS-2 cells. This might be due to the fact that antagomir has lower affinity to its target compared to miRNA mimic. Hence, increasing antagomir concentration used for the treatment might enhance the effect of antagomir.

Based on our results, the use of antagomirs appears to be less effective compared to miR mimics which have higher affinity to bind to their mRNA targets. The findings of this study suggest that miR-378a-3p, miR-1231, miR-1254 and miR-1914 mimics might be used for limiting the over-production of SOST protein in patients suffering low bone mass density. Although a great deal further *in vivo* validation and stringent clinical assessment would need to be performed before these miRNAs could be used as potential therapies, we are optimistic that miRNA has promising potential in the future. The inhibition of SOST expression by ATP and PTH as shown in chapter 3 could be combined with miRNA treatment to increase the efficiency of the regulation of SOST expression. However, further study is needed to investigate any potential unwanted effect as too much SOST inhibition could lead to other issue such as bone overgrowth.

# CHAPTER 6:

# EFFECTS OF miRNA-378a-3p TRANSFECTION ON BONE MICROSTRUCTURE IN MICE

## 6.1 Introduction

In chapter 5, using online prediction tools, we selected several miRNAs that were predicted to target sclerostin for *in vitro* validation using miRNA mimics and miRNA antagomirs. One miRNAs that we selected for the *in vitro* validation was miR-378a-3p. From a separate series of experiments conducted by Muscle Research Group members, Department of Musculoskeletal Biology, Institute of Ageing and Chronic Diseases, University of Liverpool, we had access to the hind legs of both aged and adult mice that had been treated with miR-378a-3p mimic and antagomir.

We used microcomputed tomography (micro-CT), to study the effect of miR-378a-3p treatment on trabecular bone properties in mice. Micro-CT, is a high-resolution imaging technique widely used to measure bone mass and architecture in animal and human models. It's key advantage is the non-destructive nature of this scanning technique and following analysis, samples then can be investigated by techniques such as histology or immunostaining (Bouxsein *et al.*, 2010). Bone researchers have used micro-CT for more than a decade to study bone structure-function relationships and disease progression.

## 6.2 Brief methods

### 6.2.1 miR-378a-3p treatment via tail vein injection

Treatment of mice with miR-378a-3p was done by Muscle Research Group members, Department of Musculoskeletal Biology, Institute of Ageing and Chronic Diseases, University of Liverpool. Adult (6 months old) and elderly (2 year old) mice were treated with miR-378a-3p mimics or inhibitors/antagomirs through tail vein injection. Mice were sacrificed 3 weeks after the treatment and the left hind limbs removed, preserved in 10% PBFS and used for micro-CT scanning, histology and fibre type analysis (Section 2.4.1).

### 6.2.2 Micro-computed tomography (micro-CT) scan of trabecular bone of tibial head of treated mice

Samples were transferred into micro-computed tomography (micro-CT) scanning tubes and scanned using a Skyscan 1272 system in water. The cross-section reconstruction was performed using NRecon software. Volumes of interest were determined using Data Viewer software and the properties of the trabecular bone were analysed using CTan software (Section 2.4.2).

## 6.3 Results

### 6.3.1 Micro-computed tomography (micro-CT) scan of trabecular bone of tibial head

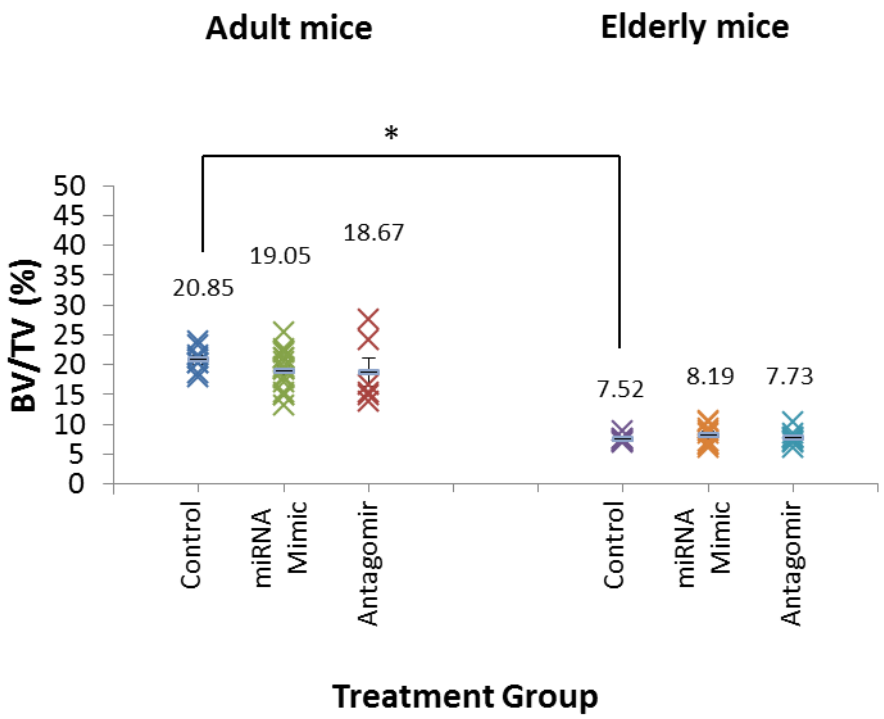


Figure 6.1: Micro-CT analysis of the trabecular bone of tibial head of six month old adult mice and two year old elderly mice. Graph shows trabecular bone volume/tissue volume (BV/TV) in adult and elderly mice, untreated, treated with miR-378a-3p mimic and treated with anti-miR-378a-3p/antagomir. Data are expressed as mean ± SE. * indicates significant different compared to control. Data was analysed using One-Way Independent ANOVA and LSD Post-Hoc test. Adult control, n=8; adult miRNA mimic, n=18; adult antagomir, n=6; elderly control, n=7; elderly miRNA mimic, n=9; elderly antagomir, n=8.

Fig. 6.1 shows the bone volume/tissue volume (BV/TV) ratio in adult and elderly mice, untreated, treated with miR-378a-3p mimic and with antagomir at a dose of 2 mg/kg body weight through tail vein injection. Three weeks after treatment there was no significantly change in the BV/TV ratio in treated compared to control mice for both adult and elderly animals, $p>0.05$. However, bone volume in untreated adults was 2.7 times higher than in untreated elderly mice, $p<0.05$.

Treatment with miR-378a-3p mimic or its antagomir also did not significantly affect trabecular thickness in either adult or elderly mice compared to untreated animals, $p>0.05$ (Fig. 6.2). Surprisingly, there was no significant difference in trabecular thickness between untreated adult and untreated elderly mice either, $p>0.05$.

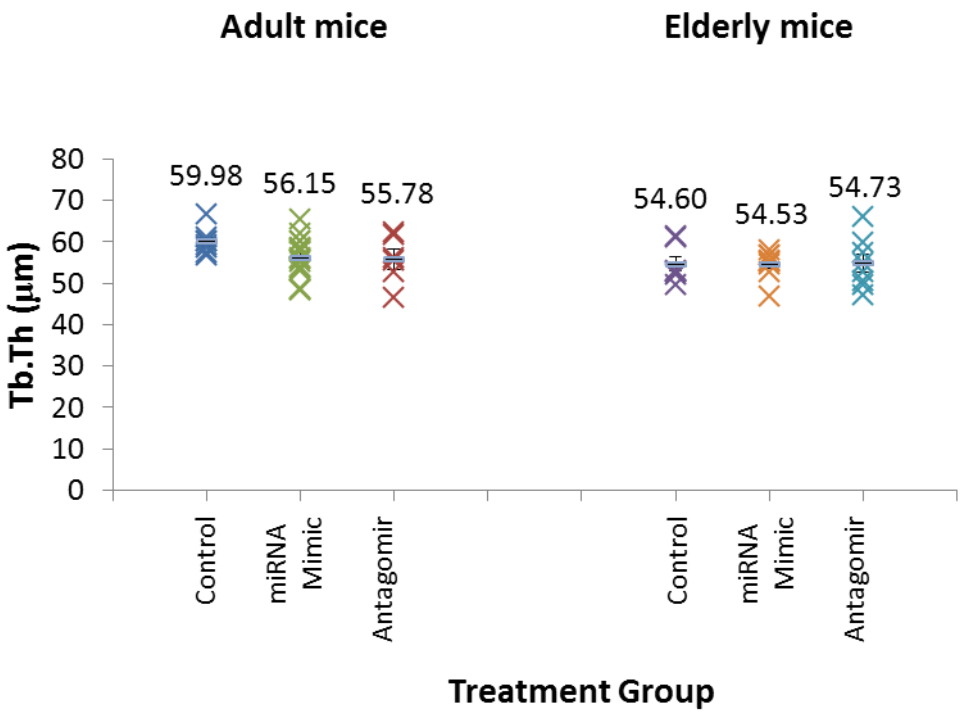


Figure 6.2: Micro-CT analysis of the trabecular bone of tibial head of six month old adult mice and two year old elderly mice. Graph shows trabecular thickness (Tb.Th) in adult and elderly mice treated with miR-378a-3p mimic and anti-miR-378a-3p/antagomir. Data are expressed as mean ± SE. Data was analysed using One-Way Independent ANOVA and LSD Post-Hoc test. Adult control, n=8; adult miRNA mimic, n=18; adult antagomir, n=6; elderly control, n=7; elderly miRNA mimic, n=9; elderly antagomir, n=8.

Treatment of adult and elderly mice with miR-378a-3p mimic and its antagomir does not significantly change total bone porosity compared to control mice for both adult and elderly animals, $p>0.05$ (Fig. 6.3). As expected, total bone porosity in untreated elderly mice is significantly higher than that in untreated adult mice, $p<0.05$.

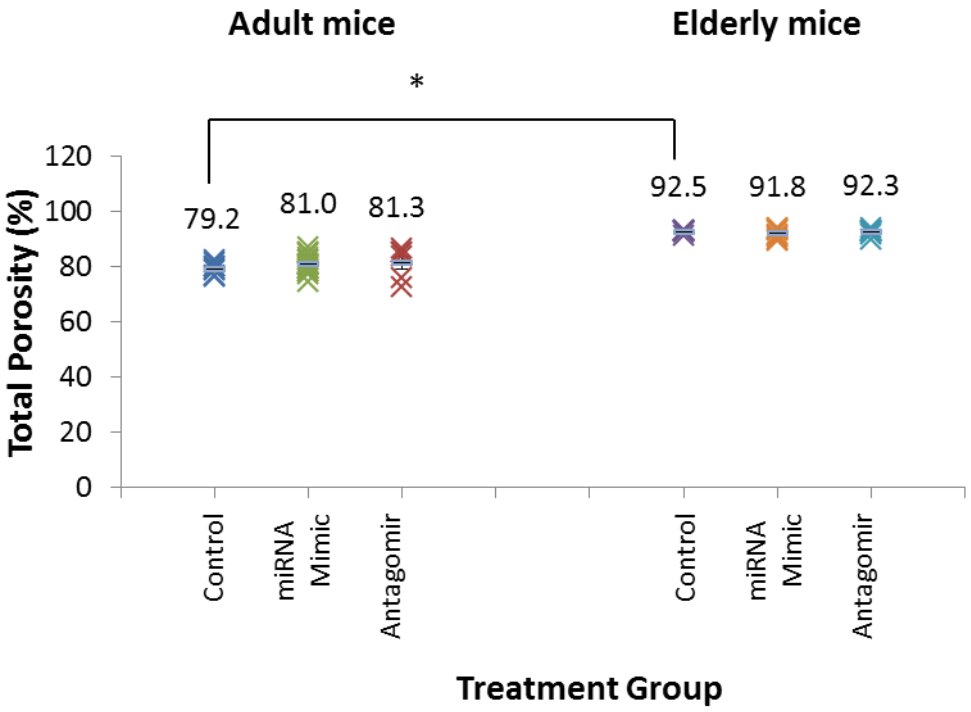


Figure 6.3: Micro-CT analysis of the trabecular bone of tibial head of six month old adult mice and two year old elderly mice. Graph shows total bone porosity (%) in untreated mice, mice treated with miR-378a-3p mimic and with anti-miR-378a-3p/antagomir. Data are expressed as mean ± SE. * indicates significant different compared to control. Data was analysed using One-Way Independent ANOVA and LSD Post-Hoc test. Adult control, n=8; adult miRNA mimic, n=18; adult antagomir, n=6; elderly control, n=7; elderly miRNA mimic, n=9; elderly antagomir, n=8.

There was no significant difference in the mean number of trabeculae per millimetre (trabecular number) of bone in the tibial head of adult and elderly mice treated miR-378a-3p mimic and its antagomir compared to untreated animals (Fig. 6.4), $p>0.05$. Untreated adult mice had 2.5 times more trabecular bone compared to elderly mice, $p<0.05$.

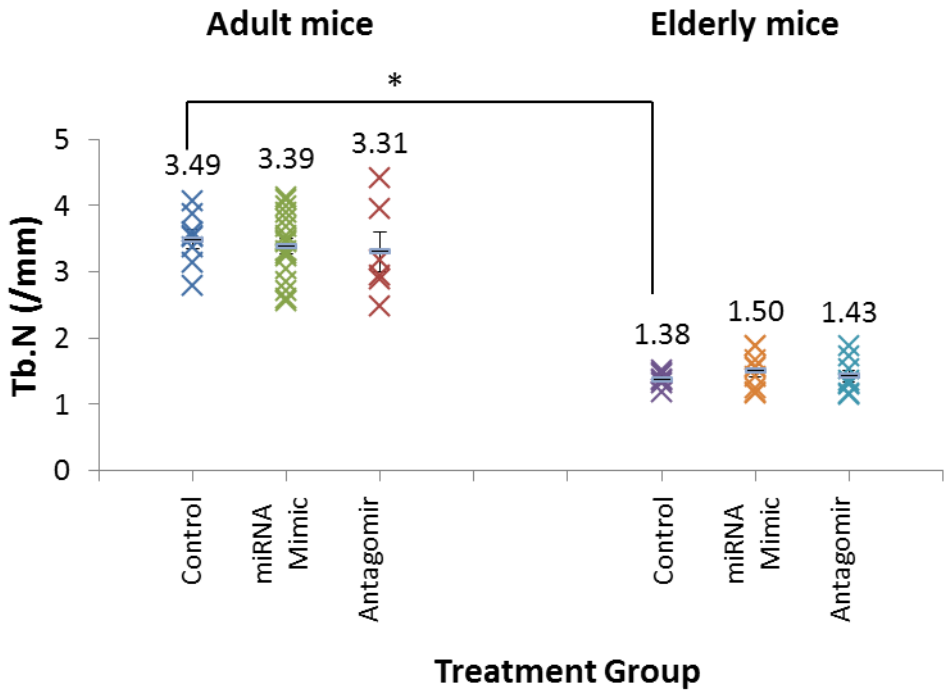


Figure 6.4: Micro-CT analysis of the trabecular bone of tibial head of six month old adult mice and two year old elderly mice. Graph shows the number of trabeculae per mm in adult and elderly mice, untreated, treated with miR-378a-3p mimic and treated with anti-miR-378a-3p/antagomir. Data are expressed as mean ± SE. * indicates significant different compared to control. Data was analysed using One-Way Independent ANOVA and LSD Post-Hoc test. Adult control, n=8; adult miRNA mimic, n=18; adult antagomir, n=6; elderly control, n=7; elderly miRNA mimic, n=9; elderly antagomir, n=8.

There was no significant difference in trabecular pattern factor in adult mice treated with miR-378a-3p mimic or anti-miR-378a-3p/antagomir compared to untreated mice, $p>0.05$ (Fig. 6.5). However, the trabecular pattern factor in old mice treated with miRNA mimic was significantly higher compared to the control, $p<0.05$. Generally, trabecular pattern factor is 54% higher in untreated elderly mice compared to untreated adult mice, $p<0.05$, indicating poor connectedness of the trabecular bone in elderly mice, contributing to weakening of the bone.

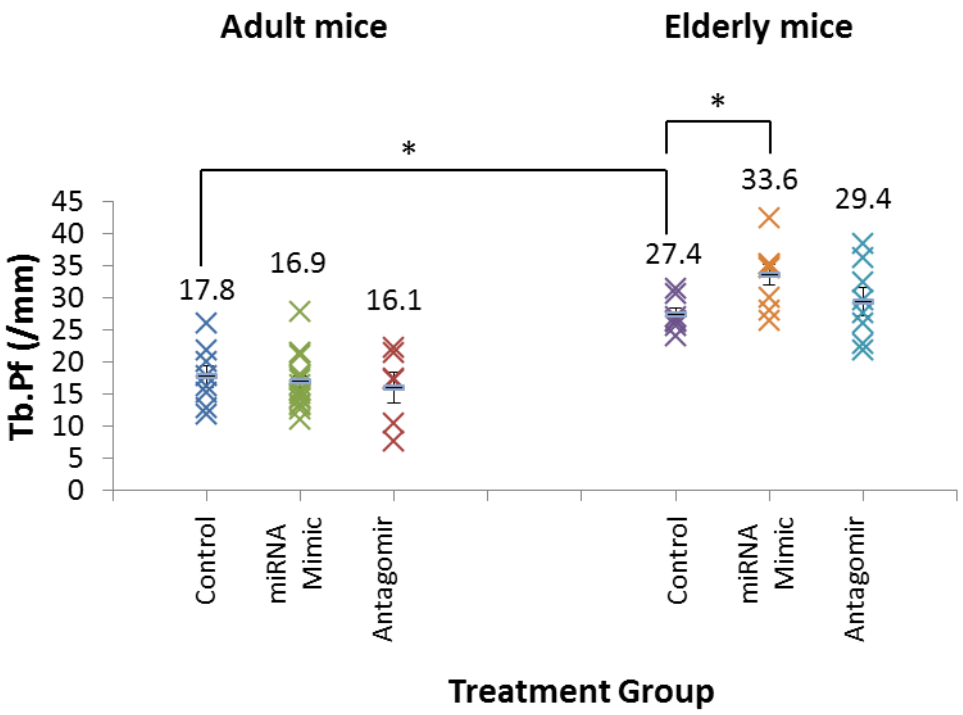


Figure 6.5: Micro-CT analysis of the trabecular bone of tibial head of six month old adult mice and two year old elderly mice. Graph shows trabecular pattern factor (/mm) in adult and elderly mice, untreated, treated with miR-378a-3p mimic and with anti-miR-378a-3p/antagomir. Data are expressed as mean ± SE. * indicates significant different compared to control. Data was analysed using One-Way Independent ANOVA and LSD Post-Hoc test. Adult control, n=8; adult miRNA mimic, n=18; adult antagomir, n=6; elderly control, n=7; elderly miRNA mimic, n=9; elderly antagomir, n=8.

The was no significant change to trabecular separation in adult mice treated with miR-378a-3p mimic and it's antagomir. Compared to untreated mice, $p>0.05$ (Fig. 6.6). There was no significant difference in trabecular separation between elderly mice treated with miR-378a-3p mimic and antagomir compared to untreated mice. In general, trabecular separation in elderly mice was 1.8 times higher than that of adult mice, $p<0.05$.

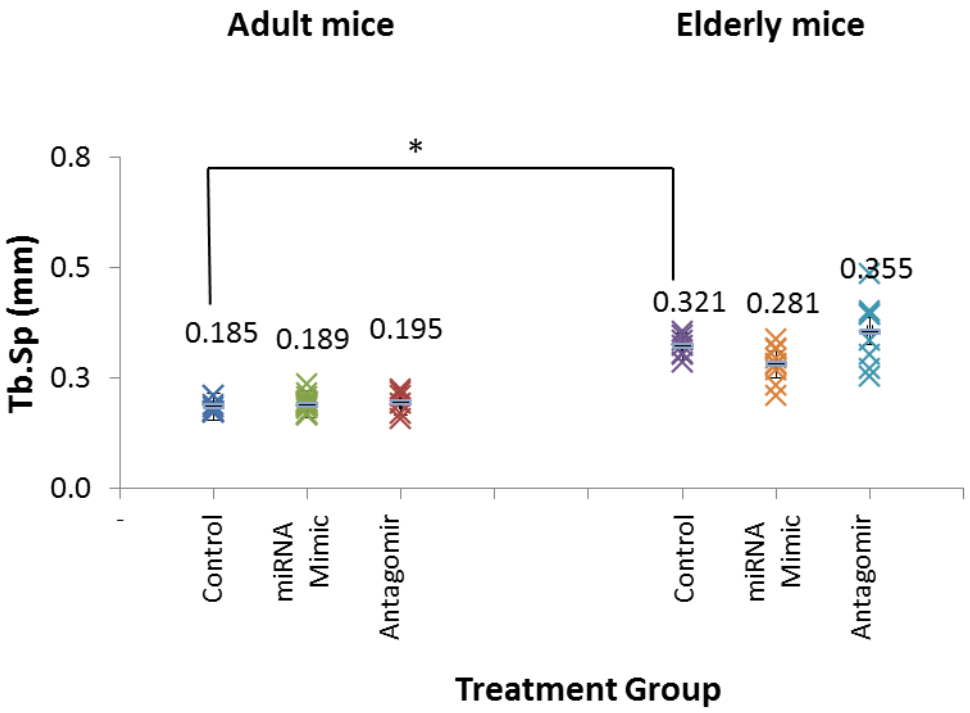


Figure 6.6: Micro-CT analysis of the trabecular bone of tibial head of six month old adult mice and two year old elderly mice. Graph shows trabecular separation (mm) in adult and elderly mice, untreated, treated with miR-378a-3p mimic and with anti-miR-378a-3p/antagomir. Data are expressed as mean ± SE. * indicates significant different compared to control. Data was analysed using One-Way Independent ANOVA and LSD Post-Hoc test. Adult control, n=8; adult miRNA mimic, n=18; adult antagomir, n=6; elderly control, n=7; elderly miRNA mimic, n=9; elderly antagomir, n=8.

Figure 6.7 shows images from the micro-CT scan of the tibial head of adult and elderly mice treated with miR-378a-3p mimic and its antagomir. Bones were scanned at a high resolution of 4.5 µm. There is a clear difference between the trabecular bones of adult (Fig. 6.7a-c) and elderly (Fig. 6.7d-f) mice. Adult mice had significantly higher trabecular bone volume and trabecular number compared to elderly mice, $p<0.05$ (Fig. 6.1 and Fig. 6.4). From these images also we can see clearly that elderly mice have higher trabecular separation and bone porosity compared to adult mice.

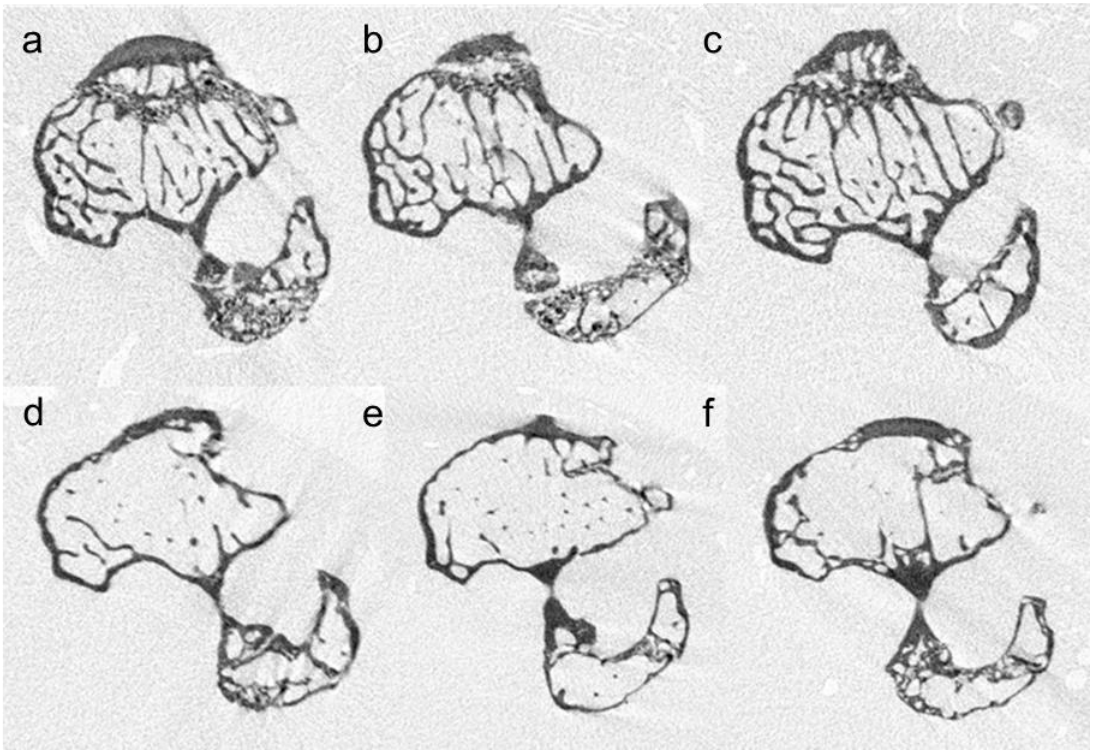


Figure 6.7: micro-CT scan images of the proximal tibia and fibula of the mice hind limb. (a) Adult mice, untreated control; (b) Adult mice, treated with miR-378a-3p mimic; (c) Adult mice, treated with antagomir; (d) Elderly mice, untreated control; (e) Elderly mice, treated with miR-378a-3p mimic; (f) Elderly mice, treated with antagomir.

## 6.4 Discussion

In the first part of this chapter, we analysed the effect of miR-378a-3p mimic and its antagomir treatment on trabecular bone in adult and elderly mice. Parameters of trabecular bone such as bone volume fraction,r bone volume density (BV/TV), bone thickness (Tb.Th), total porosity, trabecular number (Tb.N), trabecular pattern factor (Tb.Pf) and trabecular separation (Tb.Sp) were measured to evaluate the effect of the treatment on the condition of the bone. The values of these parameters depend on the species, type of bone, location within it and the health status of the subject.

BV/TV is the ratio of segmented bone volume to the total volume of the region of interest and is normally presented as percentage. Tb.Th is the mean thickness of the trabeculae which is a key measure for characterising the three-dimensional (3D) structure of trabecular bone. It can be used to compare the thickness of a trabecular structure but it is unable to describe all structural changes. For example, if one sample were composed of struts of uniform thickness and another sample had thicker vertical struts but interconnected with much thinner horizontal trabeculae, the two samples could have similar Tb.Th but with very different bone strength. Total porosity is the volume of all open and closed pores presented as a percentage of the total volume of interest.

Another parameter of trabecular bone we measured was Tb.N which conveys the mean number of trabeculae per unit length (normally per mm) within the selected volumetric region of interest. Assessed using a direct 3D method, Tb.Sp is the mean distance between trabeculae. Tb.Th and Tb.Sp can be used as a powerful parameter to characterize the shape of a complex trabecular structure. The last parameter of trabecular bone we studied was Tb.Pf which describes the connectedness of the bone based on the relationship between convex and concave surfaces. When there are many convex surfaces present, trabecular bone is

considered badly connected whereas if there are more concave structures, the bone becomes more connected. Briefly, a lower Tb.Pf signifies better connectivity while a higher value indicates poor connectivity between the trabeculae (Chen *et al.*, 2013; Hahn *et al.*, 1992; Legrand *et al.*, 2000).

Our result indicate that three weeks after treatment with miR-378a-3p mimic or its antagomir the anatomy of adult mice were not affected in terms of BV/TV, Tb.Th, total porosity, Tb.N, Tb.Pf or Tb.Sp. In elderly mice, similar results were recorded for BV/TV, Tb.Th, total porosity and Tb.N. However, there were a significant change in Tb.Pf and Tb.Sp following treated with miR-378a-3p mimic compared to the control, $p<0.05$. Tb.Pf was significantly higher (33.59±1.60) compared to the control (27.36±1.02), $p<0.05$. This result suggests that, miR-378a-3p significantly reduces the connectivity of trabecular bone in elderly mice but not in adult mice. A higher value of Tb.Pf indicates that there are more convex than concave surfaces in the trabeculae, reducing the connectivity of the trabecular bone. Lower connectivity contributes to the weakening of the bone structure.

In parallel with this result, Tb.Sp was significantly lower in adult mice treated with miR-378a-3p mimic (0.28±0.01) compared to the control (0.32±0.01), $p<0.05$. In general, Tb.Sp continuously increases with ageing. This result suggests that treatment with miR-378a-3p mimic has the potential for use in reducing the rate of increasing Tb.Sp as we age. The inhibitory effect of miR-378a-3p on bone formation might be less clear in adult mice due to a higher natural bone formation rate compared to elderly mice. Comparison between untreated adult and elderly mice showed that BV/TV and Tb.N significantly decreases with ageing while total porosity, Tb.Pf and Tb.Sp significantly increases. However, there was no significant difference in Tb.Th between adult and elderly mice. Tb.Th does not have a big impact on bone strength compared to Tb.N and Tb.Sp (Chen *et al.*, 2013).

The age of the mice is an important factor in an experimental design as it could increase the experimental variability if the choice of age is inconsistent. In this study, we used 2 age groups of mice, six months old adult male mice and two years old elderly male mice. At the age of six months, mice are fully grown and their bone mass is at the peak while two years old mice are considered as aged mice and their bone mass is decreasing (Brodt *et al*., 1999, Halloran, *et al*., 2002). Since this treatment was performed by our fellow researchers from Muscle group, mice were treated with miR-378a-3p for three weeks at this period of time is enough to see any change in muscle prior to the treatment. However, in term of trabecular bone, a study have shown that four weeks of treatment was enough to cause significant increase in trabecular bone volume, trabecular number, and trabecular separation (Eom *et al*., 2013). Mice model was chosen to study human bone because their genome is easy to manipulate and their skeleton is similar to human which exhibit trabecular cortical bone loss as they aged that is caused by inadequate new bone formation by osteoblast. Furthermore, mice models of atherosclerosis also experience loss of bone which is common in osteoporotic individuals. This suggests that atherosclerosis and osteoporosis share the same pathophysiological pathways. However unlike human skeleton, after puberty the mice murine skeleton continues to grow slowly and lacks osteonal remodelling of cortical bone (Robert, 2013).

It should be noted that there are limitations to our study. We studied the effect of the inhibition and introduction of selected miRNAs (miR-1231, miR-103a-3p, miR-1914-3p, miR-1254, miR-378a-3p and miR-422a) on the gene and protein expression in osteosarcoma cell lines (MG-63, TE-85 and SaOS-2) *in vitro*. However, the *in vivo* effects, were not examined except only for one miRNA, miR-378a-3p. Another limitation was the concentration of the miRNA mimics and miRNA inhibitors/antagomir used was only one concentration. Using a few different concentrations or a series of concentration could give us more interesting finding to

understand the optimum concentration for both miRNA mimics and antagomirs. Also, for the *in vivo* study, miR-378a-3p transfection was conducted for three weeks. Extending this treatment period might reveal the actual effect of miRNA treatment on the trabecular bone.

In general, there are two different approaches of miRNA therapeutics; miRNA mimic and miRNA inhibitor/antagomir. The use of miRNA mimic is also known as 'miRNA replacement therapy' where the specific miRNA is introduced into unhealthy or diseased cells that are normally expressed in healthy cells. The reintroduction of this miRNA into the cells helps to reactivate the pathways that are important for normal cell function and prevent those that cause the disease. On the other hand, antagomir acts by blocking the inhibition of protein translation by miRNAs. Hence, antagomir could be used to enhance the expression of proteins that are crucial for normal cell survival and functions. Compared to anti-sclerostin antibodies, the use of miRNA therapeutics to treat human diseases is still relatively new. In osteoporosis treatment by using anti-sclerostin antibody, the antibody specifically binds to sclerostin and prevents the binding of sclerostin to LRP5/6 and co-receptor frizzled. Therefore, Wnt is able to bind to LRP5/6 and co-receptor frizzled and activates the Wnt signalling pathway which is important for bone formation (Suen and Qin, 2016). The use of miRNA therapeutics however, might have unwanted side effect as each miRNA could have many different target genes. Hence, efficient delivery of miRNA to the desired target is still the biggest challenge in miRNA therapeutic research. However, a few miRNAs have entered the preclinical and clinical stage and are expected to be available in the market in the next few years (Christopher *et al*., 2016).

## 6.5 Conclusions

The main findings of chapter 6 are:

- Treatment using miR-378a-3p mimic and its antagomir did not have an effect on bone volume, trabecular thickness, total porosity or trabecular number in either adult or elderly mice;
- MiR-378a-3p mimic increased the trabecular pattern factor in elderly mice. It has no effect in adult mice;

# CHAPTER 7:

# GENERAL DISCUSSION

## 7.1 Summary of findings

In chapter 3, the principal objective was to identify the mRNA expression patterns of several bone markers at different stages of osteoblastic differentiation using the osteosarcoma cell lines MG-63, TE-85 and SaOS-2. The behaviour of these cell lines has been shown to reflect their stage of osteoblastic differentiation, MG-63 cells representing osteoblasts at an early stage, TE-85 an intermediate stage and SaOS-2 the most matured or differentiated osteoblast (Pacheco-Pantoja *et al.*, 2011). Our results showed that ALP, OSX and SOST mRNAs were expressed highest in SaOS-2, which is the most differentiated cell line. ALP, OSX and SOST are regarded as important bone markers and are highly expressed in mature osteoblasts. A study has shown that clonal bone marrow stromal cells (BMSCs) with *in vivo* bone forming capacity express their lowest level of ALP during the early stages of osteoblastic differentiation and a level more than 8.2 times higher at later stages (Prins *et al.*, 2014). OSX and SOST have also been reported to be involved in regulation at a later stage of osteoblastic differentiation in murine and human bone (Poole *et al.*, 2005; van Bezooijen *et al.*, 2004; Yoshida *et al.*, 2012). Interestingly, the expression of SOST mRNA was not detected in MG-63 cells, the least differentiated cells. This result corroborates the finding that SOST is secreted by osteocytes, a matured cell, to inhibit or limit new bone formation (Winkler *et al.*, 2003).

The results provide an overview of differential expression of crucial bone markers at different stages of osteoblast maturation. Identification of the factors which regulate the induction or inhibition of these bone markers will help us to better understand the complex process of osteoblast development. The expression pattern of mRNAs of the selected bone markers in different cell lines also provide further evidence that MG-63, TE-85 and SaOS-2 cells are good models for the study of osteoblastic cell biology.

The effect of treating these cell lines with ATP, PTH and ATP combined with PTH for 48 hours on the expression of bone marker mRNA was investigated. It was found that treatment with ATP, PTH and ATP and PTH combined, significantly increased the expression of ALP, COL1A2, OSX and RANKL in all three cell lines. Conversely, these treatments significantly decreased the expression of COL6A3, OPG and SOST in all cell lines. Our findings indicate that these treatments exerted the same inhibitory or inductive effect on osteoblastic cells at all stages of differentiation or maturation.

The expression of bone markers is controlled by various factors. Researchers have found that control of the expression of these markers by small non-coding RNA molecules, miRNAs, makes a very important contribution to overall expression. The discovery of miRNAs altered our understanding of gene regulation in various diseases. Over the preceding ten years, the study of miRNAs in various animal and plant species has steadily accelerated so that thousands of mature functional miRNAs and their targets have now been identified. In chapter 4, by studying MG-63, TE-85, SaOS-2 cells and HOBs, the identity of individual miRNA molecules that were differentially expressed were ascertained in order to provide a better understanding of miRNA expression patterns at different stages of osteoblastic differentiation. Our investigation also provided data that identified miRNA candidates that are specific to osteosarcoma cell survival and function. Because of the capacity of miRNA molecules to simultaneously target multiple genes, I am optimistic that further investigations of these miRNAs will help to facilitate the identification of promising and novel early diagnostic/prognostic markers that may be potentially powerful therapeutic agents/targets. However, to fully exploit miRNAs in diagnostic or therapeutic practice, many more studies will need to be performed, in particular to identify every gene that a single miRNA can target, and to create

efficient methods of delivery of miRNAs to their target cells and tissues to avoid potentially unwanted side effects.

In chapter 5, several miRNAs were identified which are predicted to regulate SOST expression in osteoblastic cells by use of an online prediction tool. From hundreds of miRNAs that were predicted to target the SOST gene, six miRNAs were selected for further experimental validation: miR-1231, miR-103a-3p, miR-1914, miR-1254, miR-378a-3p and miR-422a. To validate the roles of these miRNAs in SOST regulation, we transfected miRNA mimics and antagomirs of these miRNAs into TE-85 and SaOS-2 cells. MG-63 cells were not used in this transfection assay as our findings in chapter 3 demonstrated that SOST is not expressed in this cell line. In this miRNA transfection experiment, SOST gene expression and protein secretion into the culture media were measured. From these results it was found that miR-378a-3p, miR-1231, miR-1254 and miR-1914 significantly reduced the amount of SOST protein secreted into the culture media.

Theoretically, antagomirs bind to their complementary miRNA hence blocking its binding to the specific mRNA target. Thus antagomirs increase the expression of that protein as the mRNA molecule is free to proceed with protein translation. However, surprisingly, transfection of antagomirs of all the selected miRNAs did not significantly increase SOST mRNA in TE-85 or SaOS-2 cells. This could be due to the low affinity of the antagomirs to their respective miRNAs. Increasing the concentration of antagomir used in the transfection experiment might be required to illicit the expected effect. Thus, miR-378a-3p, miR-1231, miR-1254 and miR-1914 mimics may be promising therapeutic options for controlling the over-production of SOST.

Subsequently, the trabecular bone properties of tibial heads from adult and elderly mice treated with miR-378a-3p mimic and its antagomir were analysed. Anatomical observation of the mice 3 weeks after treatment did not provide evidence for an effect on bone volume, trabecular thickness, total porosity, trabecular number, trabecular pattern factor or trabecular separation in adult mice. In elderly mice, the only effects that were observed due to these treatments were in trabecular pattern factor in mice treated with miR-378a-3p mimic. An observation of increased trabecular pattern factor indicates a reduction in trabecular bone connectivity which results in a reduction in the strength of the bone. Overall bone strength will have been influenced by these contradictory effects. Comparison of untreated adult and elderly mice clearly showed that adult mice had significantly higher bone volume and trabecular number and significantly lower bone porosity, trabecular pattern factor and trabecular separation than did elderly mice. All these parameters suggest that the trabecular bones in adult mice are generally much stronger than in elderly mice. Trabecular thickness however was not significantly different in adult and elderly mice.

## 7.2 Discussion of research findings

The expression pattern of selected bone markers throughout the osteoblastic differentiation process in this study corroborate previous reports on the utility of human osteosarcoma cell lines in studying osteoblastic cells (Pacheco-Pantoja *et al*., 2011). MG-63 cells are widely used to study osteoblastic cells because they retain many osteoblastic properties such as the synthesis of bone-specific proteins (osteocalcin and alkaline phosphatase) as a response to 1,25-dihydroxyvitamin D3 (1,25-$(OH)_2D_3$) and PTH treatments (Lajeunesse *et al.*, 1990). Various studies also show that the osteoblastic phenotypes of SaOS-2 cells have high levels of alkaline phosphatase activity and respond to PTH and 1α,25-dihydroxyvitamin $D_3$ to induce the synthesis of osteonectin (Franceschi *et al.*, 1985; Murray *et al.,* 1987). Effects of ATP and PTH treatments on the expression of bone markers in MG-63, TE-85 and SaOS-2 cells were consistent in all cell lines. A significant increase in ALP, RANKL and COL1A2 expression and a decrease in OPG and SOST expression following ATP and PTH treatments have also been reported in various studies using different cell types (Bellido, 2006; Huang *et al*., 2004; Keller & Kneissel, 2005; Orriss *et al.*, 2013; Pines *et al*., 2003).

The expression of these bone markers are not only controlled by direct factors such as ATP and PTH but also by indirect factors. An interesting study has reported that osteoblastic cells release ATP as a response to induced mechanical stress (Romanello *et al.*, 2001) and ATP has been shown to affect the expression of vital proteins for bone development. This shows that bone development is a very complex continuous process, involving various factors which have synergistic effects.

Another important factor that has an important role in controlling bone formation is the regulation of protein expression by miRNAs. Over the preceding decade,

miRNAs have been very popular with researchers studying the regulatory aspects of human health and disease. Hundreds of miRNAs that were differentially expressed between MG-63, TE-85, SaOS-2 cells and HOBs were identified. The differential expression of miRNAs between these cells provides a platform to further investigate other miRNAs that target proteins of interest that may be involved in enhancing osteoblastic differentiation and growth. In this study, six miRNAs were selected that were predicted to target the protein of interest, SOST, a protein that negatively regulates bone formation via inhibition of Wnt signalling (Poole *et al*., 2005). The online database (miRWalk) indicates that, as of now, three human miRNAs have been validated to target SOST: miR-335-5p, miR-218-5p and miR-204-5p.

Our transient transfection experiment of miRNA mimics and their antagomirs suggests that miR-378a-3p, miR-1231, miR-1254 and miR-1914 mimics have potential for use as negative regulators of SOST expression in osteoblastic cells. We found that the use of antagomirs was less effective in the inhibition of miRNAs as they have lower affinity to their target miRNAs compared to the affinity of miRNA mimics with their mRNA targets. In this study, a final concentration of mimics and antagomirs of 100 nM was used. Increasing the concentration of antagomirs might increase their effectiveness. One study showed that antagomirs at a concentration of 0.125 to 1 µM significantly inhibited their target miRNA in primary B and T lymphocytes by up to 99.5% without affecting cell viability (Haftmann *et al*., 2015).

Treatment of adult and elderly mice with miR-378a-3p did not affect trabecular bone volume. The treatment only affected trabecular pattern factor in elderly mice using miR-378a-3p mimic. One can speculate that the poor effects of miRNA treatment in our mice samples might be due to the low concentration of mimic and antagomir used in the treatment, which was 2 mg/kg of body weight. Increasing the

concentration of mimic and antagomir might increase the effects of miR-378a-3p treatment on bone. A study showed that the use of a much higher antagomir concentration, 80 mg/kg of body weight, via three tail vein infusions efficiently silenced miR-16 in mice (Krutzfeldt *et al*., 2005). A major challenge in miRNA research is the efficient delivery of the oligonucleotides to specific cells or tissues of interest. Thus efficient delivery is a determining factor in the development of miRNA-based therapeutics. One miRNA molecule always has more than one target. Inefficient delivery might result in unwanted alteration of the expression of other genes leading to serious side effects. One of the best approaches for efficient nucleotide delivery appears to be through chemical modification of mimic and antagomir oligonucleotides which show good pharmacokinetic properties, good tissue uptake and high stability *in vivo*.

### 7.3 Limitations in this study and future investigations

Following the results of the expression pattern of bone markers at different stages of osteoblastic differentiation and the effect of ATP and PTH on their expression, identification of other factors such as hormones or stimulants, might help to better understand the complex process of bone formation. Identification of these factors might enable us to control bone formation by manipulating these factors. In this study, only one concentration of ATP and PTH was used to treat the cells. Using a range of concentration of ATP and PTH might give us a clearer idea of the optimum concentration of ATP and PTH to exert their effect on the cells.

Identification of miRNAs that control the protein of interest is an interesting research project. However, the short sequence of the seed region of miRNAs enables one miRNA to bind to many different targets. For example, an online validated miRNA database (miRTarBase) shows that miR-155-5p has been validated to target

hundreds of different genes in different species. This also means that one target gene can be controlled by several different miRNAs. In this study only one miRNA was transfected at a time to determine the individual role of miRNA molecule has towards the regulation of SOST protein. It would be interesting to investigate whether transfection of more than one miRNA mimic or antagomir into the same cell line might have greater effects on SOST gene expression. The use of higher concentrations of antagomirs might also show a stronger effect in miRNA silencing. Identification of miRNAs that control SOST expression could become a novel therapy for low or excessive bone mass-related disease. However, the biggest challenge is still to avoid off-target effects of miRNA therapeutics by developing efficient delivery of the miRNAs to the desired specific target.

## 7.4 Conclusions

Overall it can be concluded that:

- The effects of ATP and PTH treatment on the expression of bone markers are consistent at different stages of osteoblastic differentiation;
- SOST expression was not detected in the least differentiated osteoblastic cell, MG-63;
- MG-63, TE-85 and SaOS-2 cells are good models for studying osteoblastic cell biology;
- Hundreds of miRNAs were differentially expressed at different stages of osteoblastic differentiation;
- MiR-378a-3p, miR-1231, miR-1254 and miR-1914 mimics might be promising therapeutic options for limiting the over-production of SOST protein;
- The effect of transient transfection of miRNA mimics and antagomirs was greater in TE-85 cells than in SaOS-2 cells;
- Treatment with miR-378a-3p mimic and antagomir did not have any effect on bone volume, trabecular thickness, total porosity or trabecular number in either adult or elderly mice. However, it did increase trabecular pattern factor in elderly mice treated with miR-378a-3p mimic.

## REFERENCES


Akagi, R., Takai, Y., Ohta, M., Kanehisa, H., Kawakami, Y., & Fukunaga, T. (2009). Muscle volume compared to cross-sectional area is more appropriate for evaluating muscle strength in young and elderly individuals. *Age Ageing, 38*(5), 564-569. doi: 10.1093/ageing/afp122.

Alan, N. R. and Alexei, V. (2006). Purinergic transmission in the central nervous system. *European Journal of Physiology*, 452 (5), 479–485.

Arvidson, K., Abdallah, B. M., Applegate, L. A., Baldini, N., Cenni, E., Gomez-Barrena, E., Finne-Wistrand, A. (2011). Bone regeneration and stem cells. *J Cell Mol Med, 15*(4), 718-746. doi: 10.1111/j.1582-4934.2010.01224.x.

Atkins, G. J., Kostakis, P., Pan, B., Farrugia, A., Gronthos, S., Evdokiou, A., Zannettino, A. C. (2003). RANKL expression is related to the differentiation state of human osteoblasts. *J Bone Miner Res, 18*(6), 1088-1098. doi: 10.1359/jbmr.2003.18.6.1088.

Balemans, W., Patel, N., Ebeling, M., et al. (2002). Identification of a 52kb deletion downstream of the SOST gene in patients with van Buchem disease. *J Med Genet*. 39:91–97.

Beggs, L. A., Ye, F., Ghosh, P., Beck, D. T., Conover, C. F., Balaez, A., Yarrow, J. F. (2015). Sclerostin inhibition prevents spinal cord injury-induced cancellous bone loss. *J Bone Miner Res, 30*(4), 681-689. doi: 10.1002/jbmr.2396.

Bellido, T. (2006). Downregulation of SOST/sclerostin by PTH: a novel mechanism of hormonal control of bone formation mediated by osteocytes. *J Musculoskelet Neuronal Interact, 6*(4), 358-359.

Bellido, T., Ali, A. A., Gubrij, I., Plotkin, L. I., Fu, Q., O'Brien, C.A., Manolagas, S. C. and Jilka, R. L. (2005). Chronic Elevation of Parathyroid Hormone in Mice Reduces Expression of Sclerostin by Osteocytes: A Novel Mechanism for Hormonal Control of Osteoblastogenesis, Endocrinology, 146(11): 4577–4583. https://doi.org/10.1210/en.2005-0239.

Bhaskaran, M., & Mohan, M. (2014). MicroRNAs: history, biogenesis, and their evolving role in animal development and disease. *Vet Pathol, 51*(4), 759-774. doi: 10.1177/0300985813502820.

Bi, L., Yang, Q., Yuan, J., Miao, Q., Duan, L., Li, F. and Wang, S. (2016). MicroRNA-127-3p acts as a tumor suppressor in epithelial ovarian cancer by regulating the BAG5 gene. *Oncology Reports*, 36(5), 2563-2570. doi: 10.3892/or.2016.5055.

Bielby, R., Jones, E., & McGonagle, D. (2007). The role of mesenchymal stem cells in maintenance and repair of bone. [Review]. *Injury, 38 Suppl 1*, S26-32. doi: 10.1016/j.injury.2007.02.007.

Blade, J., de Larrea, C. F. and Rosinol, L. (2012). Extramedullary involvement in multiple myeloma. *Haematologica*. 97(11), 1618–1619.

Blume, S. W., & Curtis, J. R. (2011). Medical costs of osteoporosis in the elderly Medicare population. *Osteoporos Int, 22*(6), 1835-1844. doi: 10.1007/s00198-010-1419-7.

Bock, O. and Felsenberg, Dieter. (2008). Bisphosphonates in the management of postmenopausal osteoporosis – optimizing efficacy in clinical practice. *Clinical interventions in ageing,* 3(2), 279-297.

Bonewald, L. F. (2011). The amazing osteocyte. *J Bone Miner Res, 26*(2), 229-238. doi: 10.1002/jbmr.320.

Bonnin, N., Armandy, E., Carras, J., Ferrandon, S., Aubry, M., Guihard, S., Meyronet, D., Foy, J. P., Saintingy, P., Ledrappier, S. and Poncet, D. (2016). *Oncotarget*, 7, 44023-44038. doi: 10.18632/oncotarget.9829.

Bouxsein, M. L., Boyd, S. K., Christiansen, B. A., Guldberg, R. E., Jepsen, K. J., & Muller, R. (2010). Guidelines for assessment of bone microstructure in rodents using micro-computed tomography. [Review]. *J Bone Miner Res, 25*(7), 1468-1486. doi: 10.1002/jbmr.141.

Bowler, W. B., Dixon, C. J., Halleux, C., Maier, R., Bilbe, G., Fraser, W. D., Gallagher, J. A. and Hipskind, R. A. (1999). Signaling in human osteoblasts by extracellular nucleotides. *Journal Biol. Chem*, 274(20), 14315-14324.

Bowler, W.B., Dixon, C.J., Halleux, C., et al. (1999a). Signaling in human osteoblasts by extracellular nucleotides. Their weak induction of the c-fos proto-

oncogene via Ca2+ mobilization is strongly potentiated by a parathyroid hormone/cAMP-dependent protein kinase pathway independently of mitogen-activated p. *J Biol Chem*, 274:14315–14324. doi: 10.1074/jbc.274.20.14315.

Boyce, B. F. (2013). Advances in the regulation of osteoclasts and osteoclast functions. *J Dent Res, 92*(10), 860-867. doi: 10.1177/0022034513500306.

Boyce, B. F., & Xing, L. (2007). The RANKL/RANK/OPG pathway. *Curr Osteoporos Rep, 5*(3), 98-104.

Brandi, M. L. (2009). Microarchitecture, the key to bone quality. *Rheumatology (Oxford), 48 Suppl 4*, iv3-8. doi: 10.1093/rheumatology/kep273.

Brennecke, J., Hipfner, D. R., Stark, A., Russell, R. B., & Cohen, S. M. (2003). bantam encodes a developmentally regulated microRNA that controls cell proliferation and regulates the proapoptotic gene hid in Drosophila. *Cell, 113*(1), 25-36.

Brodt, M. D., Ellis, C. B. and Silva, M. J. (1999). Growing C57BL/6 mice increase whole bone mechanical properties by increasing geometric and material properties. *Journal of Bone and Mineral Reseach*, 14, 2159–2166.

Brunetti, G., Oranger, A., Mori, G., et al. (2001). Sclerostin is overexpressed by plasma cells from multiple myeloma patients. *Ann N Y Acad Sci*. 1237:19-23.

Brunkow, M. E., Gardner, J. C., Van Ness, J., Paeper, B. W., Kovacevich, B. R., Proll, S., Mulligan, J. (2001). Bone dysplasia sclerosteosis results from loss of the SOST gene product, a novel cystine knot-containing protein. *Am J Hum Genet, 68*(3), 577-589.

Calin, G. A., & Croce, C. M. (2006). MicroRNA-cancer connection: the beginning of a new tale. *Cancer Res, 66*(15), 7390-7394. doi: 10.1158/0008-5472.CAN-06-0800.

Calvo, M. S., Eyre, D. R., & Gundberg, C. M. (1996). Molecular basis and clinical application of biological markers of bone turnover. *Endocr Rev, 17*(4), 333-368. doi: 10.1210/edrv-17-4-333.

Cao, G. H., Sun, X. L., Wu, F., Chen, W. F., Li, J. Q. and Hu, W. C. (2016). *European review for medical and pharmacological sciences.* 20(18), 3825-3829.

Cao, G., Moore, B. T., Wang, W., Peng, X. H., Lappe, J. M., Recker, R. R. and Xiao, P. (2014). MiR-422a as a potential cellular microrna marker for postmenopausal osteoporosis. *PLoS One*, 9(5), e97098. doi: 10.1371/ journal.pone.0097098.

Cao, Y., Zhou, Z., de Crombrugghe, B., Nakashima, K., Guan, H., Duan, X., Kleinerman, E. S. (2005). Osterix, a transcription factor for osteoblast differentiation, mediates antitumor activity in murine osteosarcoma. *Cancer Res, 65*(4), 1124-1128. doi: 10.1158/0008-5472.CAN-04-2128.

Catania, A., Maira, F., Skarmoutsou, E., D'Amico, F., Abounader, R., & Mazzarino, M. C. (2012). Insight into the role of microRNAs in brain tumors. *Int J Oncol, 40*(3), 605-624. doi: 10.3892/ijo.2011.1305.

Chan, G. K., & Duque, G. (2002). Age-related bone loss: old bone, new facts. *Gerontology, 48*(2), 62-71. doi: 48929.

Chen, H., Zhou, X., Fujita, H., Onozuka, M., & Kubo, K. Y. (2013). Age-related changes in trabecular and cortical bone microstructure. *Int J Endocrinol, 2013*, 213234. doi: 10.1155/2013/213234.

Chen, J., Wang, M., Guo, M., Xie, Y. and Cong, Y. S. (2013). mir-127 regulates cell proliferation and senescence by targeting BCL6. *PLoS ONE,* 8(11), e80266. doi:10.1371/journal.pone.0080266.

Chen, J. S., Li, H. S., Huang, J. Q., Dong, S. H., Huang, Z. J., Yi, W., Zhan, G. F., Feng, J. T., Sun, J, C. and Huang, X. H. (2016). MicroRNA-379-5p inhibits tumor invasion and metastasis by targeting FAK/AKT signaling in hepatocellular carcinoma. *Cancer letters.* 375(1), 73-83. doi: 10.1016/j.canlet.2016.02.043.

Chen, K. C., Liao, Y. C., Hsieh, I. C., Wang, Y. S., Hu, C. Y., & Juo, S. H. (2012). OxLDL causes both epigenetic modification and signaling regulation on the microRNA-29b gene: novel mechanisms for cardiovascular diseases. *J Mol Cell Cardiol, 52*(3), 587-595. doi: 10.1016/j.yjmcc.2011.12.005.

Chen, Q., Liu, W., Sinha, K. M., Yasuda, H., & de Crombrugghe, B. (2013). Identification and characterization of microRNAs controlled by the osteoblast-specific transcription factor Osterix. *PLoS One, 8*(3), e58104. doi: 10.1371/journal.pone.0058104.

Cheung, M. S., Glorieux, F. H., & Rauch, F. (2009). Large osteoclasts in pediatric osteogenesis imperfecta patients receiving intravenous pamidronate. *J Bone Miner Res, 24*(4), 669-674. doi: 10.1359/jbmr.081225.

Christopher, A. F., Kaur, R. P., Kaur, G., Kaur, A., Gupta, V., & Bansal, P. (2016). MicroRNA therapeutics: Discovering novel targets and developing specific therapy. *Perspectives in Clinical Research*, 7(2), 68–74. http://doi.org/10.4103/2229-3485.179431

Cordero, F., Ferrero, G., Polidoro, S., Fiorito, G., Campanella, G., Sacerdote, C., Naccarati, A. (2015). Differentially methylated microRNAs in prediagnostic samples of subjects who developed breast cancer in the European Prospective Investigation into Nutrition and Cancer (EPIC-Italy) cohort. *Carcinogenesis, 36*(10), 1144-1153. doi: 10.1093/carcin/bgv102.

Crockett, J. C., Rogers, M. J., Coxon, F. P., Hocking, L. J., & Helfrich, M. H. (2011). Bone remodelling at a glance. *J Cell Sci, 124*(Pt 7), 991-998. doi: 10.1242/jcs.063032.

Cundy, T. (2012). Recent advances in osteogenesis imperfecta. *Calcified Tissue International*, 90(6), 439–449.

Cutarelli, A., Marini, M., Tancredi, V., D'Arcangelo, G., Murdocca, M., Frank, C. and Tarantino, U. (2016). Adenosine Triphosphate stimulates differentiation and mineralization in human osteoblast-like Saos-2 cells. *Dev Growth Differ*, 58(4):400-8. doi: 10.1111/dgd.12288.

Delgado-Calle, J., Anderson, J., Cregor, M. D., Condon, K. W., Kuhstoss, S. A., Plotkin, L. I., Bellido, T. and Roodman, G. D. (2017). Genetic deletion of Sost or pharmacological inhibition of sclerostin prevent multiple myeloma-induced bone disease without affecting tumor growth. *Leukemia*, doi: 10.1038/leu.2017.152.

D'Ippolito, G., Schiller, P. C., Ricordi, C., Roos, B. A., & Howard, G. A. (1999). Age-related osteogenic potential of mesenchymal stromal stem cells from human vertebral bone marrow. *J Bone Miner Res, 14*(7), 1115-1122. doi: 10.1359/jbmr.1999.14.7.1115.

Dalgleish, R. (1997). The human type I collagen mutation database. *Nucleic Acids Res, 25*(1), 181-187.

Dallas, S. L., & Bonewald, L. F. (2010). Dynamics of the transition from osteoblast to osteocyte. *Ann N Y Acad Sci, 1192*, 437-443. doi: 10.1111/j.1749-6632.2009.05246.x.

Dallas, S. L., Prideaux, M., & Bonewald, L. F. (2013). The osteocyte: an endocrine cell ... and more. *Endocr Rev, 34*(5), 658-690. doi: 10.1210/er.2012-1026.

Datta, N. S. and Abou-Samra, A. B. (2009). PTH and PTHrP signalling in osteoblast. *Cell signal,* 21(8),12445-1254.

David Zieve, David R. Eltz, Stephanie Slon, & Wang, N. (2013, 22 March 2013). Osteoporosis - overview, from http://www.nlm.nih.gov/medlineplus/ency/article/000360.htm

Deng, Z., Hao, J., Lei, D., He, Y., Lu, L., & He, L. (2016). Pivotal MicroRNAs in Melanoma: A Mini-Review. *Mol Diagn Ther, 20*(5), 449-455. doi: 10.1007/s40291-016-0219-y.

Drexler, H. G., Dirks, W. G., Matsuo, Y. (2003). False leukemia–lymphoma cell lines: an update on over 500 cell lines. *Leukemia*, 172, 416–426.

Duan, Z., Choy, E., Harmon, D., Liu, X., Susa, M., Mankin, H., & Hornicek, F. (2011). MicroRNA-199a-3p is downregulated in human osteosarcoma and regulates cell proliferation and migration. *Mol Cancer Ther, 10*(8), 1337-1345. doi: 10.1158/1535-7163.MCT-11-0096.

Duce, S. M., Londale; Schmidt, Katy; Cunningham, Craig; Liu, Guoqing; Barker, Simon; Tennant, Gordon; Tickle, Cheryll; Chudek, Sandy; Miedzybrodzka, Zosia. (2010). Micro-magnetic resonance imaging and embryological analysis of wild-type and pma mutant mice with clubfoot. *Journal of Anatomy, 216*(1), 108-120. doi: 10.1111/j.1469-7580.2009.01163.x.

Edwards, J. R., & Mundy, G. R. (2011). Advances in osteoclast biology: old findings and new insights from mouse models. *Nat Rev Rheumatol, 7*(4), 235-243. doi: 10.1038/nrrheum.2011.23.

Eom, S., Ko, C. Y., Park, J. H., Seo, D. H., Jung, Y. J. and Kim, H. S. (2013). Improvement in morphological properties of trabecular bones and longitudinal growth in tibia for growing rats through an impact stimulation. *Bone Abstracts,* 2, 65 | DOI:10.1530/boneabs.

Eskildsen, T., Taipaleenmaki, H., Stenvang, J., Abdallah, B. M., Ditzel, N., Nossent, A. Y., Bak, M., Kauppinen, S. and Kassem, M. (2011). MicroRNA-138 regulates osteogenic differentiation of human stromal (mesenchymal) stem cells in vivo. *PNAS*, 108(15), 6139-6144.

Everts, V., Delaisse, J. M., Korper, W., Jansen, D. C., Tigchelaar-Gutter, W., Saftig, P., & Beertsen, W. (2002). The bone lining cell: its role in cleaning Howship's lacunae and initiating bone formation. *J Bone Miner Res, 17*(1), 77-90. doi: 10.1359/jbmr.2002.17.1.77.

Fleisch, H., & Bisaz, S. (1962). Mechanism of calcification: inhibitory role of pyrophosphate. *Nature, 195*, 911.

Forlino, A., & Marini, J. C. (2016). Osteogenesis imperfecta. *Lancet, 387*(10028), 1657-1671. doi: 10.1016/S0140-6736(15)00728-X.

Formosa, A., Lena, A. M., Markert, E. K., Cortelli, S., Miano, R., Mauriello, A., Candi, E. (2013). DNA methylation silences miR-132 in prostate cancer. *Oncogene, 32*(1), 127-134. doi: 10.1038/onc.2012.14.

Forstner, A. J., Degenhardt, F., Schratt, G., & Nothen, M. M. (2013). MicroRNAs as the cause of schizophrenia in 22q11.2 deletion carriers, and possible implications for idiopathic disease: a mini-review. *Front Mol Neurosci, 6*, 47. doi: 10.3389/fnmol.2013.00047.

Franceschi, R. T., James, W. M., & Zerlauth, G. (1985). 1 alpha, 25-dihydroxyvitamin D3 specific regulation of growth, morphology, and fibronectin in a human osteosarcoma cell line. *J Cell Physiol, 123*(3), 401-409. doi: 10.1002/jcp.1041230316.

Fuller, K., Wong, B., Fox, S., Choi, Y., & Chambers, T. J. (1998). TRANCE is necessary and sufficient for osteoblast-mediated activation of bone resorption in osteoclasts. *J Exp Med, 188*(5), 997-1001.

Gartland, A., Rumney, R. M., Dillon, J. P., Gallagher, J. A.. (2012). Isolation and Culture of Human Osteoblasts. *Methods Mol Biol*. 806: 337-355.

Gartland, A., Orriss, I.R., Rumney, R.M., Bond, A.P., Arnett, T. and Gallagher, J. A. (2012). Purinergic signalling in osteoblasts. *Front Biosci (Landmark Ed)*, 1(17):16-29.

Garzon, R., Marcucci, G., & Croce, C. M. (2010). Targeting microRNAs in cancer: rationale, strategies and challenges. *Nat Rev Drug Discov, 9*(10), 775-789. doi: 10.1038/nrd3179.

Gerstenfeld, L. C., Cullinane, D. M., Barnes, G. L., Graves, D.T. and Einhorn, T. A. (2003). Fracture healing as a post-natal developmental process: molecular, spatial, and temporal aspects of its regulation. *Journal of Cellular Biochemistry*, 88,873–84.

Goettsch, C., Rauner, M., Pacyna, N., Hempel, U., Bornstein, S. R., & Hofbauer, L. C. (2011). miR-125b regulates calcification of vascular smooth muscle cells. *Am J Pathol, 179*(4), 1594-1600. doi: 10.1016/j.ajpath.2011.06.016.

Golub, E. E., & Boesze-Battaglia, K. (2007). The role of alkaline phosphatase in mineralization. *Current Opinion in Orthopaedics, 18*, 444-448.

Gomez, B., Jr., Ardakani, S., Ju, J., Jenkins, D., Cerelli, M. J., Daniloff, G. Y., & Kung, V. T. (1995). Monoclonal antibody assay for measuring bone-specific alkaline phosphatase activity in serum. *Clin Chem, 41*(11), 1560-1566.

Gulyaeva, L. F., & Kushlinskiy, N. E. (2016). Regulatory mechanisms of microRNA expression. *J Transl Med, 14*(1), 143. doi: 10.1186/s12967-016-0893-x.

Guo, Y., Tang, C. Y., Man, X. F., Tang, H. N., Tang, J., Wang, F., Zhou, H. D. (2016). Insulin receptor substrate-1 time-dependently regulates bone formation by controlling collagen Ialpha2 expression via miR-342. *FASEB J*. doi: 10.1096/fj.201600445RR.

Ha, M., & Kim, V. N. (2014). Regulation of microRNA biogenesis. *Nat Rev Mol Cell Biol, 15*(8), 509-524. doi: 10.1038/nrm3838.

Haftmann, C., Riedel, R., Porstner, M., Wittmann, J., Chang, H. D., Radbruch, A., & Mashreghi, M. F. (2015). Direct uptake of Antagomirs and efficient knockdown of miRNA in primary B and T lymphocytes. *J Immunol Methods, 426*, 128-133. doi: 10.1016/j.jim.2015.07.006.

Hahn, M., Vogel, M., Pompesius-Kempa, M., & Delling, G. (1992). Trabecular bone pattern factor--a new parameter for simple quantification of bone microarchitecture. *Bone, 13*(4), 327-330.

Halloran, B. P., Ferguson, V. L., Simske, S. J., Burghardt, A., Venton, L. L. and Majumdar, S. (2002). Changes in bone structure and mass with advancing age in the male C57BL/6J mouse. *Journal of Bone and Mineral Research*, 17, 1044–1050.

Hamersma, H., Gardner, J. and Beighton, P. (2003). The natural history of sclerosteosis. *Clin Genet*, 63:192–197.

Hammond, S. M. (2015). An overview of microRNAs. *Adv Drug Deliv Rev, 87*, 3-14. doi: 10.1016/j.addr.2015.05.001.

Harada, S., & Rodan, G. A. (2003). Control of osteoblast function and regulation of bone mass. *Nature, 423*(6937), 349-355. doi: 10.1038/nature01660.

Hashimoto, Y., Akiyama, Y., & Yuasa, Y. (2013). Multiple-to-Multiple Relationships between MicroRNAs and Target Genes in Gastric Cancer. PLoS ONE, 8(5), e62589. http://doi.org/10.1371/journal.pone.0062589

Hassan, M. Q., Maeda, Y., Taipaleenmaki, H., Zhang, W., Jafferji, M., Gordon, J. A., Lian, J. B. (2012). miR-218 directs a Wnt signaling circuit to promote differentiation of osteoblasts and osteomimicry of metastatic cancer cells. *J Biol Chem, 287*(50), 42084-42092. doi: 10.1074/jbc.M112.377515.

Havill, L. M., Hale, L. G., Newman, D. E., Witte, S. M., & Mahaney, M. C. (2006). Bone ALP and OC reference standards in adult baboons (Papio hamadryas) by sex and age. *J Med Primatol, 35*(2), 97-105. doi: 10.1111/j.1600-0684.2006.00150.x.

He, B., Yin, B., Wang, B., Xia, Z., Chen, C., & Tang, J. (2012). MicroRNAs in esophageal cancer (review). *Mol Med Rep, 6*(3), 459-465. doi: 10.3892/mmr.2012.975.

Henriksen, K., Bollerslev, J., Everts, V., & Karsdal, M. A. (2011). Osteoclast activity and subtypes as a function of physiology and pathology--implications for future treatments of osteoporosis. *Endocr Rev, 32*(1), 31-63. doi: 10.1210/er.2010-0006.

Hirata, H., Ueno, K., Shahryari, V., Deng, G., Tanaka, Y., Tabatabai, Z. L., Dahiya, R. (2013). MicroRNA-182-5p promotes cell invasion and proliferation by down regulating FOXF2, RECK and MTSS1 genes in human prostate cancer. *PLoS ONE*, *8*(1), e55502. http://doi.org/10.1371/journal.pone.0055502.

Hirsch, B. P., Unnanuntana, A., Cunningham, M. E., & Lane, J. M. (2013). The effect of therapies for osteoporosis on spine fusion: a systematic review. *Spine J, 13*(2), 190-199. doi: 10.1016/j.spinee.2012.03.035.

Horowitz, M. C., Xi, Y., Wilson, K., & Kacena, M. A. (2001). Control of osteoclastogenesis and bone resorption by members of the TNF family of receptors and ligands. *Cytokine Growth Factor Rev, 12*(1), 9-18.

Hu, H., Zhang, Y., Cai, X. H., Huang, J. F., & Cai, L. (2012). Changes in microRNA expression in the MG-63 osteosarcoma cell line compared with osteoblasts. *Oncol Lett, 4*(5), 1037-1042. doi: 10.3892/ol.2012.866.

Huang, J. C., Sakata, T., Pfleger, L. L., Bencsik, M., Halloran, B. P., Bikle, D. D., & Nissenson, R. A. (2004). PTH differentially regulates expression of RANKL and OPG. *J Bone Miner Res, 19*(2), 235-244. doi: 10.1359/JBMR.0301226.

Huijing P. A. and Baan G. C. (2003). Myofascial force transmission: muscle relative position and length determine agonist and synergist muscle force. *J Appl Physiol, 94*.

Hupkes, M., Sotoca, A. M., Hendriks, J. M., van Zoelen, E. J., & Dechering, K. J. (2014). MicroRNA miR-378 promotes BMP2-induced osteogenic differentiation of mesenchymal progenitor cells. *BMC Mol Biol, 15*, 1. doi: 10.1186/1471-2199-15-1.

Iorio, M. V., Piovan, C., & Croce, C. M. (2010). Interplay between microRNAs and the epigenetic machinery: an intricate network. *Biochim Biophys Acta, 1799*(10-12), 694-701. doi: 10.1016/j.bbagrm.2010.05.005.

Jiang, H., Jin, C., Liu, J., Hua, D., Zhou, F., Lou, X., Zhao, N., Lan, Q., Huang, Q., Yoon, J. G., Zheng, S. and Lin, B. (2014). Next generation sequencing analysis of miRNAs: MiR-127-3p inhibits glioblastoma proliferation and activates TGF-β signaling by targeting SKI. *Omics : a journal of integrative biology*, 18(3), 196-206. doi: 10.1089/omi.2013.0122.

Jilka, R. L. (2013). The relevance of mouse models for investigating age-related bone loss in humans. *The Journals of Gerontology Series A: Biological Sciences and Medical Sciences*, 68(10), 1209–1217. http://doi.org/10.1093/gerona/glt046.

Jilka, R. L., Weinstein, R. S., Bellido, T., Roberson, P., Parfitt, A. M., & Manolagas, S. C. (1999). Increased bone formation by prevention of osteoblast apoptosis with parathyroid hormone. *J Clin Invest, 104*(4), 439-446. doi: 10.1172/JCI6610.

John, B., Enright, A. J., Aravin, A., Tuschl, T., Sander, C., & Marks, D. S. (2004). Human MicroRNA targets. *PLoS Biol, 2*(11), e363. doi: 10.1371/journal.pbio.0020363.

Jopling, C. L., Schutz, S., & Sarnow, P. (2008). Position-dependent function for a tandem microRNA miR-122-binding site located in the hepatitis C virus RNA genome. *Cell Host Microbe, 4*(1), 77-85. doi: 10.1016/j.chom.2008.05.013.

Junger, W. G. (2011). Immune cell regulation by autocrine purinergic signalling. *Nature Reviews Immunology*, 11 (3), 201–212.

Jurkovicova, D., Magyerkova, M., Kulcsar, L., Krivjanska, M., Krivjansky, V., Gibadulinova, A., Chovanec, M. (2014). miR-155 as a diagnostic and prognostic marker in hematological and solid malignancies. *Neoplasma, 61*(3), 241-251. doi: 10.4149/neo_2014_032.

Kahai, S., Lee, S. C., Lee, D. Y., Yang, J., Li, M., Wang, C. H., Yang, B. B. (2009). MicroRNA miR-378 regulates nephronectin expression modulating osteoblast differentiation by targeting GalNT-7. *PLoS One, 4*(10), e7535. doi: 10.1371/journal.pone.0007535.

Kapinas, K., Kessler, C. B. and Delany, A. M. (2009). miR-29 suppression of osteonectin in osteoblasts: regulation during differentiation and by canonical Wnt signaling. *J Cell Biochem*, 108, 216–224.

Kee, H. J., Kim, G. R., Cho, S. N., Kwon, J. S., Ahn, Y., Kook, H., & Jeong, M. H. (2014). miR-18a-5p MicroRNA Increases Vascular Smooth Muscle Cell Differentiation by Downregulating Syndecan4. *Korean Circulation Journal, 44*(4), 255-263. doi: 10.4070/kcj.2014.44.4.255.

Keller, H., & Kneissel, M. (2005). SOST is a target gene for PTH in bone. *Bone, 37*(2), 148-158. doi: 10.1016/j.bone.2005.03.018.

Kern, B., Shen, J., Starbuck, M., & Karsenty, G. (2001). Cbfa1 contributes to the osteoblast-specific expression of type I collagen genes. *J Biol Chem, 276*(10), 7101-7107. doi: 10.1074/jbc.M006215200.

Khan, T., Muise, E. S., Iyengar, P., Wang, Z. V., Chandalia, M., Abate, N., Scherer, P. E. (2009). Metabolic dysregulation and adipose tissue fibrosis: role of collagen VI. *Mol Cell Biol, 29*(6), 1575-1591. doi: 10.1128/MCB.01300-08.

Khan, Y., Mansour, Iyad., Ong, E. Shrestha, M. (2015). Obstructive jaundice as initial presentation of multiple myeloma: case presentation and literature review. *Case Reports in Medicine.* doi.org/10.1155/2015/686210.

Kikuta, J., & Ishii, M. (2013). Osteoclast migration, differentiation and function: novel therapeutic targets for rheumatic diseases. *Rheumatology (Oxford), 52*(2), 226-234. doi: 10.1093/rheumatology/kes259.

Kini, U., & Nandeesh, B. N. (2012). Physiology of Bone Formation, Remodeling, and Metabolism. In I. Fogelman, G. Gnanasegaran & H. Wall (Eds.), *Radionuclide and Hybrid Bone Imaging* (pp. 29-57): Springer Berlin Heidelberg.

Krampera, M., Pizzolo, G., Aprili, G., & Franchini, M. (2006). Mesenchymal stem cells for bone, cartilage, tendon and skeletal muscle repair. *Bone, 39*(4), 678-683. doi: 10.1016/j.bone.2006.04.020.

Krutzfeldt, J., Rajewsky, N., Braich, R., Rajeev, K. G., Tuschl, T., Manoharan, M., & Stoffel, M. (2005). Silencing of microRNAs in vivo with 'antagomirs'. *Nature, 438*(7068), 685-689. doi: 10.1038/nature04303.

Kuhn, D. E., Martin, M. M., Feldman, D. S., Terry, A. V., Jr., Nuovo, G. J., & Elton, T. S. (2008). Experimental validation of miRNA targets. [Review]. *Methods, 44*(1), 47-54. doi: 10.1016/j.ymeth.2007.09.005.

Kumagai, H., Sacktor, B., and Filburn, C. R. (1991). Purinergic regulation of cytosolic calcium and phosphoinositide metabolism in rat osteoblast-like osteosarcoma cells. *J. Bone Miner. Res*. 6, 697–708.

Kwon, B. S., Wang, S., Udagawa, N., Haridas, V., Lee, Z. H., Kim, K. K., Ni, J. (1998). TR1, a new member of the tumor necrosis factor receptor superfamily, induces fibroblast proliferation and inhibits osteoclastogenesis and bone resorption. *FASEB J, 12*(10), 845-854.

Lacey, D. L., Timms, E., Tan, H. L., Kelley, M. J., Dunstan, C. R., Burgess, T., Boyle, W. J. (1998). Osteoprotegerin ligand is a cytokine that regulates osteoclast differentiation and activation. *Cell, 93*(2), 165-176.

Lajeunesse, D., Frondoza, C., Schoffield, B., & Sacktor, B. (1990). Osteocalcin secretion by the human osteosarcoma cell line MG-63. *J Bone Miner Res, 5*(9), 915-922. doi: 10.1002/jbmr.5650050904.

Lamande, S. R., Morgelin, M., Adams, N. E., Selan, C., & Allen, J. M. (2006). The C5 domain of the collagen VI alpha3(VI) chain is critical for extracellular microfibril formation and is present in the extracellular matrix of cultured cells. *J Biol Chem, 281*(24), 16607-16614. doi: 10.1074/jbc.M510192200.

Lawrie, C. H. (2013). MicroRNAs and lymphomagenesis: a functional review. *Br J Haematol, 160*(5), 571-581. doi: 10.1111/bjh.12157.

Lee, L. W., Zhang, S., Etheridge, A., Ma, L., Martin, D., Galas, D., & Wang, K. (2010). Complexity of the microRNA repertoire revealed by next-generation sequencing. *RNA,* 16(11), 2170-2180. doi: 10.1261/rna.2225110.

Lee, R. C., Feinbaum, R. L. and Ambros, V. (1993). The *C. elegans* heterochronic gene lin-4 encodes small RNAs with antisense complementarity to lin-14. Cell, 75(5), 843-854.

Lee, S. K. and Lorenzo, J. A. (1999). Parathyroid Hormone Stimulates TRANCE and Inhibits Osteoprotegerin Messenger Ribonucleic Acid Expression in Murine Bone Marrow Cultures: Correlation with Osteoclast-Like Cell Formation. *Endocrinology*, 140:3552–3561.

Lee, Y., Ahn, C., Han, J., Choi, H., Kim, J., Yim, J., Kim, V. N. (2003). The nuclear RNase III Drosha initiates microRNA processing. *Nature, 425*(6956), 415-419. doi: 10.1038/nature01957.

Legrand, E., Chappard, D., Pascaretti, C., Duquenne, M., Krebs, S., Rohmer, V., Audran, M. (2000). Trabecular bone microarchitecture, bone mineral density, and vertebral fractures in male osteoporosis. *J Bone Miner Res, 15*(1), 13-19. doi: 10.1359/jbmr.2000.15.1.13.

Leibbrandt, A., & Penninger, J. M. (2008). RANK/RANKL: Regulators of Immune Responses and Bone Physiology. *Year in Immunology 2008, 1143*, 123-150. doi: DOI 10.1196/annals.1443.016.

Li, N., Jiang, Y., Wooley, P. H., Xu, Z., & Yang, S. Y. (2013). Naringin promotes osteoblast differentiation and effectively reverses ovariectomy-associated osteoporosis. *J Orthop Sci, 18*(3), 478-485. doi: 10.1007/s00776-013-0362-9.

Li, X., Ominsky, M. S., Niu, Q. T., Sun, N., Daugherty, B., D'Agostin, D., Paszty, C. (2008). Targeted deletion of the sclerostin gene in mice results in increased bone formation and bone strength. *J Bone Miner Res, 23*(6), 860-869. doi: 10.1359/jbmr.080216.

Li, Z., Hassan, M. Q., Jafferji, M., Aqeilan, R. I., Garzon, R., Croce, C. M., Lian, J. B. (2009). Biological functions of miR-29b contribute to positive regulation of osteoblast differentiation. *J Biol Chem, 284*(23), 15676-15684. doi: 10.1074/jbc.M809787200.

Li, Z., Hassan, M. Q., Volinia, S., van Wijnen, A. J., Stein, J. L., Croce, C. M., Stein, G. S. (2008). A microRNA signature for a BMP2-induced osteoblast lineage commitment program. *Proc Natl Acad Sci U S A, 105*(37), 13906-13911. doi: 10.1073/pnas.0804438105.

Lian, J. B., Stein, G. S., van Wijnen, A. J., Stein, J. L., Hassan, M. Q., Gaur, T., & Zhang, Y. (2012). MicroRNA control of bone formation and homeostasis. *Nat Rev Endocrinol, 8*(4), 212-227. doi: 10.1038/nrendo.2011.234.

Liang, C., Zhang, X., Wang, M. H., Liu, X, M., Zhang, X. J., Zheng, B., Qian, G. R. and Ma, Z. L. (2017). MicroRNA-18a-5p functions as an oncogene by directly targeting IRF2 in lung cancer. *Cell death and disease*, 8, e2764; doi:10.1038/cddis.2017.145.

Liang, H., Wang, R., Jin, Y., Li, J. and Zhang, S. (2016). MiR-422a acts as a tumor suppressor in glioblastoma by targeting PIK3CA. *American journal of cancer research. 6(8), 1695–1707.*

Lindsay, R., Krege, J. H., Marin, F., Jin, L. and Stepan, J. J. (2016). Teriparatide for osteoporosis: important of the full course. *Osteoporosis international*, 27, 2395-2410.

Liu, B., Wu, S., Han, L., & Zhang, C. (2015). beta-catenin signaling induces the osteoblastogenic differentiation of human pre-osteoblastic and bone marrow stromal cells mainly through the upregulation of osterix expression. *Int J Mol Med, 36*(6), 1572-1582. doi: 10.3892/ijmm.2015.2382.

Livak, K, J. and Schmittgen, T. D. (2001). Analysis of relative gene expression data using real-time quantitative PCR and the 2(-Delta Delta C(T)) Method. *Methods*, 25(4), 402-408.

Logan, C. Y., & Nusse, R. (2004). The Wnt signaling pathway in development and disease. *Annu Rev Cell Dev Biol, 20*, 781-810. doi: 10.1146/annurev.cellbio.20.010403.113126.

Longhi, A., Errani, C., De Paolis, M., Mercuri, M. and Bacci, G. (2006). Primary bone osteosarcoma in the pediatric age: state of the art. *Cancer Treatment Review*, 32(6), 423–36. [PubMed: 16860938]

Lytle, J. R., Yario, T. A., & Steitz, J. A. (2007). Target mRNAs are repressed as efficiently by microRNA-binding sites in the 5' UTR as in the 3' UTR. *Proc Natl Acad Sci U S A, 104*(23), 9667-9672. doi: 10.1073/pnas.0703820104.

Ma, Z., Li, Y., Xu, J., Ren, Q., Yao, J. and Tian, X. (2016). MicroRNA-409-3p regulates cell invasion and metastasis by targeting ZEB1 in breast cancer. *IUMB life,* 68(5), 394-402. doi: 10.1002/iub.1494.

Ma, M., Wang, X., Chen, X., Cai, R., Chen, F., Dong, W., Yang, G. and Pang, W. (2017). MicroRNA-432 targeting E2F3 and P55PIK inhibits myogenesis through PI3K/AKT/mTOR signaling pathway. *RNA biology,* 14(3), 347-360.

Ma, Y. L ., Cain, R. L., Hallady, D. L., Yang, X., Zeng, Q., Miles, R . R., Martin, T. J. and Onyia, J. E. (2001). Catabolic Effects of Continuous Human PTH (1–38) in Vivo Is Associated with Sustained Stimulation of RANKL and Inhibition of Osteoprotegerin and Gene-Associated Bone Formation. *Endocrinology*, 142(9); 4047–4054, https://doi.org/10.1210/endo.142.9.8356.

Mackie, E. J. (2003). Osteoblasts: novel roles in orchestration of skeletal architecture. [Review]. *Int J Biochem Cell Biol, 35*(9), 1301-1305.

Madyastha, P. R., Yang, S., Ries, W. L., & Key, L. L., Jr. (2000). IFN-gamma enhances osteoclast generation in cultures of peripheral blood from osteopetrotic patients and normalizes superoxide production. *J Interferon Cytokine Res, 20*(7), 645-652. doi: 10.1089/107999000414826.

Mann, M., Barad, O., Agami, R., Geiger, B., & Hornstein, E. (2010). miRNA-based mechanism for the commitment of multipotent progenitors to a single cellular fate. *Proc Natl Acad Sci U S A, 107*(36), 15804-15809. doi: 10.1073/pnas.0915022107.

Manolagas, S. C. (2000). Birth and death of bone cells: basic regulatory mechanisms and implications for the pathogenesis and treatment of osteoporosis. *Endocr Rev, 21*(2), 115-137.

Martianov, I., Cler, E., Duluc, I., Vicaire, S., Philipps, M., Freund, J. N., & Davidson, I. (2014). TAF4 inactivation reveals the 3 dimensional growth promoting activities of collagen 6A3. *PLoS One, 9*(2), e87365. doi: 10.1371/journal.pone.0087365.

Martin, T. J., & Seeman, E. (2008). Bone remodelling: its local regulation and the emergence of bone fragility. *Best Pract Res Clin Endocrinol Metab, 22*(5), 701-722. doi: 10.1016/j.beem.2008.07.006.

Matsuo, K., & Irie, N. (2008). Osteoclast-osteoblast communication. *Arch Biochem Biophys, 473*(2), 201-209. doi: 10.1016/j.abb.2008.03.027.

Mazar, J., Khaitan, D., DeBlasio, D., Zhong, C., Govindarajan, S. S., Kopanathi, S., Perera, R. J. (2011). Epigenetic regulation of microRNA genes and the role of miR-34b in cell invasion and motility in human melanoma. *PLoS One, 6*(9), e24922. doi: 10.1371/journal.pone.0024922.

McClung, M. R. (2017). Denosumab for the treatment of osteoporosis. *Osteoporosis and Sarcopenia*, 3, 8-17.

McIntosh, V. J. and Lasley, R. D. (2011). Adenosine Receptor-Mediated Cardioprotection: Are all 4 subtypes required or redundant?. *Journal of Cardiovascular Pharmacology and Therapeutics,* 17(1): 21–33.

Mendell, J. T., & Olson, E. N. (2012). MicroRNAs in stress signaling and human disease. *Cell, 148*(6), 1172-1187. doi: 10.1016/j.cell.2012.02.005.

Mikami, T., Miake, Y., Bologna-Molina, R., & Takeda, Y. (2016). Ultrastructural Analyses of Alveolar Bone in a Patient With Osteomyelitis Secondary to Osteopetrosis: A Review of the Literature. *J Oral Maxillofac Surg, 74*(8), 1584-1595. doi: 10.1016/j.joms.2016.02.016.

Monroe, D. G., McGee-Lawrence, M. E., Oursler, M. J., & Westendorf, J. J. (2012). Update on Wnt signaling in bone cell biology and bone disease. *Gene, 492*(1), 1-18. doi: 10.1016/j.gene.2011.10.044.

Morrison, M. S., Turin, L., King, B. F., Burnstock, G., & Arnett, T. R. (1998). ATP is a potent stimulator of the activation and formation of rodent osteoclasts. *J Physiol, 511 ( Pt 2)*, 495-500.

Moyses, R. M., & Schiavi, S. C. (2015). Sclerostin, Osteocytes, and Chronic Kidney Disease - Mineral Bone Disorder. *Semin Dial, 28*(6), 578-586. doi: 10.1111/sdi.12415.

Mukaiyama, K., Kamimura, M., Uchiyama, S., Ikegami, S., Nakamura, Y., & Kato, H. (2015). Elevation of serum alkaline phosphatase (ALP) level in postmenopausal women is caused by high bone turnover. *Aging Clin Exp Res, 27*(4), 413-418. doi: 10.1007/s40520-014-0296-x.

Mulari, M. T., Qu, Q., Härkönen, P. L. and Väänänen, H. K. (2004). Osteoblast-like cells complete osteoclastic bone resorption and form new mineralized bone matrix in vitro. *Calcified Tissue International,* 75:253–61.

Murray, E., Provvedini, D., Curran, D., Catherwood, B., Sussman, H., & Manolagas, S. (1987). Characterization of a human osteoblastic osteosarcoma cell line (SAOS-2) with high bone alkaline phosphatase activity. *J Bone Miner Res, 2*(3), 231-238. doi: 10.1002/jbmr.5650020310.

Nagalingam, R. S., Sundaresan, N. R., Noor, M., Gupta, M. P., Solaro, R. J., & Gupta, M. (2014). Deficiency of Cardiomyocyte-specific MicroRNA-378 Contributes to the Development of Cardiac Fibrosis Involving a Transforming Growth Factor beta (TGF beta 1)-dependent Paracrine Mechanism. *Journal of Biological Chemistry, 289*(39), 27199-27214. doi: 10.1074/jbc.M114.580977.

Nakamura, H. (2007). Morphology, Function, and Differentiation of Bone Cells. *Journal of Hard Tissue Biology, 16*(1), 15-22.

Nakashima, T., Hayashi, M., Fukunaga, T., Kurata, K., Oh-Hora, M., Feng, J. Q., Takayanagi, H. (2011). Evidence for osteocyte regulation of bone homeostasis through RANKL expression. *Nat Med, 17*(10), 1231-1234. doi: 10.1038/nm.2452.

Navickas, R., Gal, D., Laucevicius, A., Taparauskaite, A., Zdanyte, M., & Holvoet, P. (2016). Identifying circulating microRNAs as markers of cardiovascular disease: a systematic review. *Cardiovasc Res, 111*(4), 322-337. doi: 10.1093/cvr/cvw174.

Neilsen, C. T., Goodall, G. J., & Bracken, C. P. (2012). IsomiRs - the overlooked repertoire in the dynamic microRNAome. *Trends in Genetics, 28*(11), 544-549. doi: 10.1016/j.tig.2012.07.005.

Oliveira, A. G., Marques, P. E., Amaral, S. S., Quintão, J. L. D., Cogliati, B., Dagli, M. L. Z., Rogiers, V., Vanhaecke, T., Vinken, M., Menezes, G. B. (2013). Purinergic signalling during sterile liver injury. *Liver International*, 33 (3), 353–361.

Orom, U. A., Nielsen, F. C., & Lund, A. H. (2008). MicroRNA-10a binds the 5'UTR of ribosomal protein mRNAs and enhances their translation. *Mol Cell, 30*(4), 460-471. doi: 10.1016/j.molcel.2008.05.001.

Orriss, I. R., Burnstock, G., and Arnett, T. R. (2010). Purinergic signalling and bone remodelling. [Review]. *Current Opinion in Pharmacology, 10*(3), 322-330. doi: 10.1016/j.coph.2010.01.003.

Orriss, I. R., Key, M. L., Hajjawi, M. O., & Arnett, T. R. (2013). Extracellular ATP released by osteoblasts is a key local inhibitor of bone mineralisation. *PLoS One, 8*(7), e69057. doi: 10.1371/journal.pone.0069057.

Pacheco-Pantoja, E. L., Ranganath, L. R., Gallagher, J. A., Wilson, P. J., & Fraser, W. D. (2011). Receptors and effects of gut hormones in three osteoblastic cell lines. *BMC Physiol, 11*, 12. doi: 10.1186/1472-6793-11-12.

Pajevic, P. (2013). Recent progress in osteocyte research. *Endocrinol Metab (Seoul), 28*(4), 255-261. doi: 10.3803/EnM.2013.28.4.255.

Palagano, E., Blair, H. C., Pangrazio, A., Tourkova, I., Strina, D., Angius, A., Sobacchi, C. (2015). Buried in the Middle but Guilty: Intronic Mutations in the TCIRG1 Gene Cause Human Autosomal Recessive Osteopetrosis. *J Bone Miner Res, 30*(10), 1814-1821. doi: 10.1002/jbmr.2517.

Paley, C. A., Bennett, M. I . and Johnson, M. I. (2011). Acupuncture for cancer-induced bone pain?. *Evidence-Based Complementary and Alternative Medicine.* doi:10.1093/ecam/neq020.

Palumbo, A. and Anderson, K. (2011). Multiple myeloma. *The New. England Journal of Medicine*. 364(11), 1046–1060.

Pan, T. C., Zhang, R. Z., Markova, D., Arita, M., Zhang, Y., Bogdanovich, S., Chu, M. L. (2013). COL6A3 protein deficiency in mice leads to muscle and tendon defects similar to human collagen VI congenital muscular dystrophy. *J Biol Chem, 288*(20), 14320-14331. doi: 10.1074/jbc.M112.433078.

Pasarica, M., Gowronska-Kozak, B., Burk, D., Remedios, I., Hymel, D., Gimble, J., Smith, S. R. (2009). Adipose tissue collagen VI in obesity. *J Clin Endocrinol Metab, 94*(12), 5155-5162. doi: 10.1210/jc.2009-0947.

Perez-Campo, F. M., Santurtun, A., Garcia-Ibarbia, C., Pascual, M. A., Valero, C., Garces, C., Riancho, J. A. (2016). Osterix and RUNX2 are Transcriptional Regulators of Sclerostin in Human Bone. *Calcif Tissue Int, 99*(3), 302-309. doi: 10.1007/s00223-016-0144-4.

Perlot, T., & Penninger, J. M. (2012). Development and function of murine B cells lacking RANK. *J Immunol, 188*(3), 1201-1205. doi: 10.4049/jimmunol.1102063.

Pesce, V., Speciale, D., Sammarco, G., Patella, S., Spinarelli, A., & Patella, V. (2009). Surgical approach to bone healing in osteoporosis. *Clin Cases Miner Bone Metab, 6*(2), 131-135.

Phillips, C. L., Bradley, D. A., Schlotzhauer, C. L., Bergfeld, M., Libreros-Minotta, C., Gawenis, L. R., Hillman, L. S. (2000). Oim mice exhibit altered femur and incisor mineral composition and decreased bone mineral density. *Bone, 27*(2), 219-226.

Pillion, J. P., Vernick, D. and Shapiro, J. (2011). Hearing loss in osteogenesis imperfecta: characteristics and treatment considerations. *Genetics Research International.* doi:10.4061/2011/983942.

Pines, A., Romanello, M., Cesaratto, L., Damante, G., Moro, L., D'Andrea, P., & Tell, G. (2003). Extracellular ATP stimulates the early growth response protein 1 (Egr-1) via a protein kinase C-dependent pathway in the human osteoblastic HOBIT cell line. *Biochem J, 373*(Pt 3), 815-824. doi: 10.1042/BJ20030208.

Poole, K. E. S., van Bezooijen, R. L., Loveridge, N., Hamersma, H., Papapoulos, S. E., Lowik, C. W., & Reeve, J. (2005). Sclerostin is a delayed secreted product of osteocytes that inhibits bone formation. *Faseb Journal, 19*(10), 1842-+. doi: 10.1096/fj.05-4221fje.

Praetorius, H. A. and Leipziger, L. (2010). Intrarenal purinergic signaling in the control of renal tubular transport. *Annual review of physiology*, 72, 377-393.

Prins, H. J., Braat, A. K., Gawlitta, D., Dhert, W. J., Egan, D. A., Tijssen-Slump, E., Martens, A. C. (2014). In vitro induction of alkaline phosphatase levels predicts in vivo bone forming capacity of human bone marrow stromal cells. *Stem Cell Res, 12*(2), 428-440. doi: 10.1016/j.scr.2013.12.001.

Qian Zhang, Hong Ye, Fei Xiang, Lin-Jie Song, Li-Ling Zhou, Peng-Cheng Cai, Ma, W.-L. (2016). miR-18a-5p Inhibits Sub-Pleural Pulmonary Fibrosis by Targeting TGF-β Receptor II. *Molecular Therapy*. doi: 10.1016/j.ymthe.2016.12.017.

Qiao, J., Fang, C. Y., Chen, S. X., Wang, X. Q., Cui, S. J., Liu, X. H., Liu, F. (2015). Stroma derived COL6A3 is a potential prognosis marker of colorectal carcinoma revealed by quantitative proteomics. *Oncotarget, 6*(30), 29929-29946. doi: 10.18632/oncotarget.4966.

Raisz, L. G. (1999). Physiology and pathophysiology of bone remodeling. *Clin Chem, 45*(8 Pt 2), 1353-1358.

Reginster, J. Y. (2002). Strontium ranelate in osteoporosis. *Current pharmaceutical design*, 8(21),1907-1916.

Renaud, L., Harris, L. G., Mani, S. K., Kasiganesan, H., Chou, J. C., Baicu, C. F., Menick, D. R. (2015). HDACs Regulate miR-133a Expression in Pressure Overload-Induced Cardiac Fibrosis. *Circ Heart Fail, 8*(6), 1094-1104. doi: 10.1161/CIRCHEARTFAILURE.114.001781.

Rey, A., Manen, D., Rizzoli, R., Ferrari, S. L., & Caverzasio, J. (2007). Evidences for a role of p38 MAP kinase in the stimulation of alkaline phosphatase and matrix mineralization induced by parathyroid hormone in osteoblastic cells. *Bone, 41*(1), 59-67. doi: 10.1016/j.bone.2007.02.031.

Rihani, A., Van Goethem, A., Ongenaert, M., De Brouwer, S., Volders, P.-J., Agarwal, S. Van Maerken, T. (2015). Genome wide expression profiling of p53 regulated miRNAs in neuroblastoma. *Scientific Reports*, 5, 9027. http://doi.org/10.1038/srep09027

Ritter, J. and Bielack, S. S. (2010). Osteosarcoma. *Annals of Oncology*, 21(7), 320-325. doi:10.1093/annonc/mdq276

Robertson, E. D., Wasylyk, C., Ye, T., Jung, A. C. and Wasylyk, B. (2014). The oncogenic MicroRNA Hsa-miR-155-5p targets the transcription factor ELK3 and links it to the hypoxia response. *PLoS One*. 9(11), e113050. doi: 10.1371/journal.pone.0113050.

Rodan, G. A., & Fleisch, H. A. (1996). Bisphosphonates: mechanisms of action. *J Clin Invest, 97*(12), 2692-2696. doi: 10.1172/JCI118722.

Rodriguez, A., Griffiths-Jones, S., Ashurst, J. L., & Bradley, A. (2004). Identification of mammalian microRNA host genes and transcription units. *Genome Res, 14*(10A), 1902-1910. doi: 10.1101/gr.2722704.

Romanello, M., Pani, B., Bicego, M., & D'Andrea, P. (2001). Mechanically induced ATP release from human osteoblastic cells. *Biochem Biophys Res Commun, 289*(5), 1275-1281. doi: 10.1006/bbrc.2001.6124.

Roodman, G. D. (1991). Osteoclast differentiation. *Crit Rev Oral Biol Med, 2*(3), 389-409.

Rothschild, S. I. (2013). Epigenetic Therapy in Lung Cancer - Role of microRNAs. *Front Oncol, 3*, 158. doi: 10.3389/fonc.2013.00158.

Rumney, R. M. H., Wang, N., Agrawal, A. and Gartland, A. (2012). Purinergic signalling in bone. *Frontiers in Endocrinology*. 3. doi:10.3389/fendo.2012.00116.

Schulte, J. H., Marschall, T., Martin, M., Rosenstiel, P., Mestdagh, P., Schlierf, S., Schramm, A. (2010). Deep sequencing reveals differential expression of microRNAs in favorable versus unfavorable neuroblastoma. *Nucleic Acids Res, 38*(17), 5919-5928. doi: 10.1093/nar/gkq342.

Sharifi, . and Moridnia, A. (2017). Apoptosis-inducing and antiproliferative effect by inhibition of miR-182-5p through the regulation of CASP9 expression in human breast cancer. *Cancer Gene Therapy*, 24, 75-82| doi:10.1038/cgt.2016.79.

Sheng, M. H. C., Lau, K. H. W. and Baylink, D. J. (2014). Role of osteocyte-derived insulin-like growth factor I in developmental growth, modeling, remodeling, and regeneration of the bone. *J Bone Metab*, 21, 41-54.

Shulman, L. P. (2008). Transdermal hormone therapy and bone health. *Clinical interventions in ageing*, 3(1), 51-54.

Silva-Fernandez, L., Rosario, M. P., Martinez-Lopez, J. A., Carmona, L., & Loza, E. (2013). Denosumab for the treatment of osteoporosis: a systematic literature review. *Reumatol Clin, 9*(1), 42-52. doi: 10.1016/j.reuma.2012.06.007.

Sinha, K. M., & Zhou, X. (2013). Genetic and molecular control of osterix in skeletal formation. *J Cell Biochem, 114*(5), 975-984. doi: 10.1002/jcb.24439.

Spungen, A. M., Wang, J., Pierson, R. N., Jr., & Bauman, W. A. (2000). Soft tissue body composition differences in monozygotic twins discordant for spinal cord injury. *J Appl Physiol (1985), 88*(4), 1310-1315.

Stanczyk, J., Ospelt, C., Karouzakis, E., Filer, A., Raza, K., Kolling, C., Kyburz, D. (2011). Altered expression of microRNA-203 in rheumatoid arthritis synovial fibroblasts and its role in fibroblast activation. *Arthritis Rheum, 63*(2), 373-381. doi: 10.1002/art.30115.

Stenvang, J., Petri, A., Lindow, M., Obad, S., & Kauppinen, S. (2012). Inhibition of microRNA function by antimiR oligonucleotides. *Silence, 3*(1), 1. doi: 10.1186/1758-907X-3-1.

Stromsoe, K. (2004). Fracture fixation problems in osteoporosis. *Injury-International Journal of the Care of the Injured, 35*(2), 107-113. doi: DOI 10.1016/j.injury.2003.08.019.

Styrkarsdottir, U., Thorleifsson, G., Eiriksdottir, B., Gudjonsson, S. A., Ingvarsson, T., Center, J. R., Stefansson, K. (2016). Two Rare Mutations in the COL1A2 Gene Associate With Low Bone Mineral Density and Fractures in Iceland. *J Bone Miner Res, 31*(1), 173-179. doi: 10.1002/jbmr.2604.

Suen, P. K. and Qin, L. (2016). Sclerostin, an emerging therapeutic target for treating osteoporosis and osteoporotic fracture: A general review. *Journal of Orthopedic Translation*, 4, 1-13.

Sugatani, T. and Hruska, K. A. (2009). Impaired micro-RNA pathways diminish osteoclast differentiation and function. *J Biol Chem*, 284, 4667–4678.

Suominen, H. (2006). Muscle training for bone strength. *Aging Clin Exp Res, 18*(2), 85-93.

Svensson, A., Norrby, M., Libelius, R., & Tagerud, S. (2008). Secreted frizzled related protein 1 (Sfrp1) and Wnt signaling in innervated and denervated skeletal muscle. *J Mol Histol, 39*(3), 329-337. doi: 10.1007/s10735-008-9169-y.

Swarthout, J. T., Doggett, T. A., Lemker, J. L. and Paetridge, N. C. (2001). Stimulation of extracellular signal-regulated kinases and proliferation in rat osteoblastic cells by parathyroid hormone is protein kinase C-dependent. *The journal of biological chemistry*, 276(10), 7586–7592.

Syberg, S., Petersen, S., Schwarz, P. and Jorgensen, N. R. (2011). ATP treatment potentiates the positive effect of PTH on ovariectomy-induced bone loss in mice *Bone*, 48: S231 - S232.

Tabas-Madrid, D., Muniategui, A., Sanchez-Caballero, I., Martinez-Herrera, D. J., Sorzano, C. O., Rubio, A., & Pascual-Montano, A. (2014). Improving miRNA-mRNA interaction predictions. *BMC Genomics, 15 Suppl 10*, S2. doi: 10.1186/1471-2164-15-S10-S2.

Takami, M., Cho, E. S., Lee, S. Y., Kamijo, R., & Yim, M. (2005). Phosphodiesterase inhibitors stimulate osteoclast formation via TRANCE/RANKL expression in osteoblasts: possible involvement of ERK and p38 MAPK pathways. *FEBS Lett, 579*(3), 832-838. doi: 10.1016/j.febslet.2004.12.066.

Terpos, E., Dimopoulos, M. A., Sezer, O., Roodman, D., Abildgaard, N., Vescio, R., .International Myeloma Working, G. (2010). The use of biochemical markers of bone remodeling in multiple myeloma: a report of the International Myeloma Working Group. *Leukemia, 24*(10), 1700-1712. doi: 10.1038/leu.2010.173.

Thomas, G. P., Baker, S. U., Eisman, J. A., & Gardiner, E. M. (2001). Changing RANKL/OPG mRNA expression in differentiating murine primary osteoblasts. *J Endocrinol, 170*(2), 451-460.

van Bezooijen, R. L., Roelen, B. A. J., Visser, A., van der Wee-Pals, L., de Wilt, E., Karperien, M., Lowik, C. W. G. M. (2004). Sclerostin is an osteocyte-expressed negative regulator of bone formation, but not a classical BMP antagonist. *Journal of Experimental Medicine, 199*(6), 805-814. doi: 10.1084/jem.20031454.

Wada, T., Nakashima, T., Hiroshi, N., & Penninger, J. M. (2006). RANKL-RANK signaling in osteoclastogenesis and bone disease. *Trends Mol Med, 12*(1), 17-25. doi: 10.1016/j.molmed.2005.11.007.

Wang, J., Wang, Y., Yang, J., & Huang, Y. (2014). microRNAs as novel markers of schizophrenia (Review). *Exp Ther Med, 8*(6), 1671-1676. doi: 10.3892/etm.2014.2014.

Wei, X., Li, H., Zhang, B., Li, C., Dong, D. and Lan, X. (2016). miR-378a-3p promotes differentiation and inhibits proliferation of myoblasts by targeting HDAC4 in skeletal muscle development. *RNA Biology*, 13(12).

Wheater, G., Elshahaly, M., Tuck, S. P., Datta, H. K., & van Laar, J. M. (2013). The clinical utility of bone marker measurements in osteoporosis. [Review]. *J Transl Med, 11*, 201. doi: 10.1186/1479-5876-11-201.

Wijenayaka, A. R., Kogawa, M., Lim, H. P., Bonewald, L. F., Findlay, D. M. and Atkins, G.J. (2011). Sclerostin stimulates osteocyte support of osteoclast activity by a RANKL-dependent pathway. *PLoS One*, 6(10): e25900. doi: 10.1371/journal.pone.0025900.

Williams, A. H., Liu, N., van Rooij, E., & Olson, E. N. (2009). MicroRNA control of muscle development and disease. *Curr Opin Cell Biol,* 21(3), 461-469. doi: 10.1016/j.ceb.2009.01.029.

Williams, B,O. (2014). Insights into the mechanisms of sclerostin action in regulating bone mass accrual. *J Bone Miner Res,* 29 (1), 24-28. doi: 10.1002/jbmr.2154.

Winkler, D. G., Sutherland, M. K., Geoghegan, J. C., Yu, C., Hayes, T., Skonier, J. E., Latham, J. A. (2003). Osteocyte control of bone formation via sclerostin, a novel BMP antagonist. *EMBO J, 22*(23), 6267-6276. doi: 10.1093/emboj/cdg599.

Wong, F. L., Boice, J.D., Abramson, D.H., Tarone, R.E., Kleinerman, R.A., Stovall M, Goldman, M.B., Seddon, J.M., Tarbell, N., Fraumeni, J.F. and Li, F.P. (1997). Cancer incidence after retinoblastoma. Radiation dose and sarcoma risk. *JAMA*. 278(15):1262–1267.

Wong, R. K. S. and Wiffen, P. J. (2002). Bisphosphonates for the relief of pain secondary to bone metastases. *Cochrane Database of Systematic Reviews* 2002. doi: 10.1002/14651858.

Wu, C., Tian, B., Qu, X., Liu, F., Tang, T., Qin, A., Dai, K. (2014). MicroRNAs play a role in chondrogenesis and osteoarthritis (review). *Int J Mol Med, 34*(1), 13-23. doi: 10.3892/ijmm.2014.1743.

Wu, D., Niu, X., Tao, J., Li, P., Lu, Q., Xu, A., Chen, W. and Wang, Z. (2017). MicroRNA-379-5p plays a tumor-suppressive role in human bladder cancer growth and metastasis by directly targeting MDM2. *Oncology reports*, 37(6), 3502-3508. doi: 10.3892/or.2017.5607.

Xie, L., Ding, F., Jiao, J., Kan, W., & Wang, J. (2015). Total Hip and Knee arthroplasty in a patient with osteopetrosis: a case report and review of the literature. *BMC Musculoskelet Disord, 16*, 259. doi: 10.1186/s12891-015-0716-x.

Xia, W., Cao, G., & Shao, N. (2009). Progress in miRNA target prediction and identification. *Sci China C Life Sci, 52*(12), 1123-1130. doi: 10.1007/s11427-009-0159-4.

Xie, X., Li, Y. S., Xiao, W. F., Deng, Z. H., He, H. B., Liu, Q. and Luo, W. (2017). MicroRNA-379 inhibits the proliferation, migration and invasion of human osteosarcoma cells by targetting EIF4G2. *Bioscience reports*, 37(3). pii: BSR20160542. doi: 10.1042/BSR20160542.

Yamaguchi, M. (2009). RANK/RANKL/OPG during orthodontic tooth movement. *Orthod Craniofac Res*, 12(2):113–9.

Yao, T., Rao, Q., Liu, L., Zheng, C., Xie, Q., Liang, J., & Lin, Z. (2013). Exploration of tumor-suppressive microRNAs silenced by DNA hypermethylation in cervical cancer. *Virol J, 10*, 175. doi: 10.1186/1743-422X-10-175.

Ye, L., Morse, L. R., & Battaglino, R. A. (2013). Snx10: a newly identified locus associated with human osteopetrosis. *IBMS Bonekey, 2013*(10). doi: 10.1038/bonekey.2013.155.

Yi, H., Geng, L., Black, A., Talmon, G., Berim, L. and Wang, J. (2017). The miR-487b-3p/GRM3/TGFβ signaling axis is an important regulator of colon cancer tumorigenesis. *Oncogene,* DOI: 10.1038/onc.2016.499.

Yoshida, C. A., Komori, H., Maruyama, Z., Miyazaki, T., Kawasaki, K., Furuichi, T., Komori, T. (2012). SP7 inhibits osteoblast differentiation at a late stage in mice. *PLoS One, 7*(3), e32364. doi: 10.1371/journal.pone.0032364.

Yu, F., Fan, X., Chen, B., Dong, P. and Zheng, J. (2016). Activation of Hepatic Stellate Cells is Inhibited by microRNA-378a-3p via Wnt10a. *Cellular physiology and biochemistry: international journal of experimental cellular physiology, biochemistry, and pharmacology*. 39(6), 2409-2420.

Zhang, J., Hou, W., Chai, M., Zhao, H., Jia, J., Sun, X., Wang, R. (2016). MicroRNA-127-3p inhibits proliferation and invasion by targeting SETD8 in human osteosarcoma cells. *Biochem Biophys Res Commun, 469*(4), 1006-1011. doi: 10.1016/j.bbrc.2015.12.067.

Zhang, J., Hou, W., Jia, J., Zhao, Y. and Zhao, B. (2017). MiR-409-3p regulates cell proliferation and tumor growth by targeting E74-like factor 2 in osteosarcoma. *FEBS open bio, 7(3), 348-357. doi: 10.1002/2211-5463.12177.*

Zhang, K., Zhang, Y., Liu, C., Xiong, Y., & Zhang, J. (2014). MicroRNAs in the diagnosis and prognosis of breast cancer and their therapeutic potential (review). *Int J Oncol, 45*(3), 950-958. doi: 10.3892/ijo.2014.2487.

Zhang, Q., Ye, H., Xiang, F., Song, L. J., Zhou, L. L., Cai, P. C. Zhang, J. C., Xin, J. B. and Ma, W. L. (2017). miR-18a-5p inhibits sub-pleural pulmonary fibrosis by targeting tgf-β receptor II. *Molecular Therapy*, 3, 728-738.

Zhang, Y., Xie, R. L., Croce, C. M., Stein, J. L., Lian, J. B., van Wijnen, A. J., & Stein, G. S. (2011). A program of microRNAs controls osteogenic lineage progression by targeting transcription factor Runx2. *Proc Natl Acad Sci U S A, 108*(24), 9863-9868. doi: 10.1073/pnas.1018493108.

Zhu, M., Wang, M., Yang, F., Tian, Y., Cai, J., Yang, H., Fu, H., Mao, F., Zhu, W., Qian, H. and Xu, W. (2016). miR-155-5p inhibition promotes the transition of bone marrow mesenchymal stem cells to gastric cancer tissue derived MSC-like cells via NF-κB p65 activation. *Oncotarget*, 7(1), 16567-16580. doi: 10.18632 /oncotarget.7767.

Zhou, X., Zhang, Z., Feng, J. Q., Dusevich, V. M., Sinha, K., Zhang, H., de Crombrugghe, B. (2010). Multiple functions of Osterix are required for bone growth and homeostasis in postnatal mice. *Proc Natl Acad Sci U S A, 107*(29), 12919-12924. doi: 10.1073/pnas.0912855107.

Zuo, B., Zhu, J., Li, J., Wang, C., Zhao, X., Cai, G., Li, Z., Peng, J., Wang, P., Shen, C., Huang, Y., Xu, J., Zhang, X. and Chen, X. (2015). microRNA-103a functions as

a mechanosensitive microRNA to inhibit bone formation through targeting Runx2. *J Bone Miner Res,* 30(2), 330-45.